POLITECNICO DI TORINO
Repository ISTITUZIONALE

A review on computational tools for analytical visualisation and molecular interactions of sncRNAs: prospects in NDDs

Original
A review on computational tools for analytical visualisation and molecular interactions of sncRNAs: prospects in NDDs / Panagiotopoulos, K., Ibanibo, L., Perrone, B., Marchetti, C., Tumsich, M., Traetta, G., Theofilatos, K., Deriu, M.A.. - ELETTRONICO. - (2022), pp. 100-118. (1st International Workshop in Neurodevelopmental Impairments in Preterm Children - Computational Advancements (DETERMINED 2022) Ljubljana, Slovenia 26 August 2022).

Availability:
This version is available at: 11583/2982876 since: 2023-10-09T15:42:28Z

Publisher:
CEUR

Published
DOI:

Terms of use:

This article is made available under terms and conditions as specified in the corresponding bibliographic description in the repository

Publisher copyright

(Article begins on next page)

29 November 2026

Neurodevelopmental Impairments in Preterm Children – Computational Advancements

1st International Workshop on Neurodevelopmental Impairments in Preterm Children – Computational Advancements, DETERMINED 2022

Ljubljana, Slovenia, 26 August 2022

CEUR-WS.org/Vol-3363/cover.pdf

Editors:
Vida Groznik
Aleksander Sadikov
Umberto Michelucci
Marco A. Deriu





The PARENT project has received funding from the European Union's Horizon 2020 research and innovation programme under the Marie Sklodowska-Curie-Innovative Training Network 2020, Grant Agreement N° 956394.

DETERMINED 2022: Neurodevelopmental Impairments in Preterm Children — Computational Advancements
Preface

Vida Groznik[1,2,3,*,†], Aleksander Sadikov[1,3,†], Umberto Michelucci[4,5,†] and Marco A. Deriu[6,†]

[1]University of Ljubljana, Faculty of Computer and Information Science, Večna pot 113, 1000 Ljubljana, Slovenia
[2]University of Primorska, Faculty of Mathematics, Natural Sciences and Information Technologies, Glagoljaška 8, 6000 Koper, Slovenia
[3]NEUS Diagnostics d.o.o., Ziherlova 40E, 1000 Ljubljana, Slovenia
[4]TOELT llc, Machine Learning Research and Development, Birchlenstr. 25, 8600 Duebendorf, Switzerland
[5]Computer Science Department, Lucerne University of Applied Sciences and Arts, 6002 Lucerne
[6]PolitoBIOMed Lab, Department of Mechanical and Aerospace Engineering, Politecnico di Torino, 10129 Turin, Italy

Abstract

This volume contains the papers presented at the International Workshop *DETERMINED 2022: Neurodevelopmental Impairments in Preterm Children — Computational Advancements* that was held at the University of Ljubljana, Faculty of Computer and Information Science in Ljubljana, Slovenia on 26 August, 2022. The workshop, held in a hybrid mode, consisted of fourteen contributions: a keynote speech given by Marinka Žitnik from Harvard Medical School and thirteen oral presentations based on as many submissions accepted after a single-blind peer-review process. Each oral presentation was complemented by a poster displayed throughout the workshop. The workshop organisers thank all authors, contributors, and attendees to DETERMINED 2022.

Keywords

Preterm Children, Neurodevelopmental Impairments, Computational Advancements, Machine Learning, PARENT project, scientific event, MSCA-ITN, Horizon2020, Workshop

1. Introduction

The first instalment of the DETERMINED 2022 international workshop was held at the University of Ljubljana, Faculty of Computer and Information Science in Ljubljana, Slovenia on 26 August 2022. The workshop was held in conjunction with the machine learning training school that has been organised in the framework of the PARENT project funded by the European Union's

DETERMINED 2022: Neurodevelopmental Impairments in Preterm Children — Computational Advancements, August 26, 2022, Ljubljana, Slovenia
*Corresponding author.
†These authors contributed equally.
vida.groznik@fri.uni-lj.si (V. Groznik); aleksander.sadikov@fri.uni-lj.si (A. Sadikov); umberto.michelucci@toelt.ai (U. Michelucci); marco.deriu@polito.it (M. A. Deriu)
© 2022 Copyright for this paper by its authors. Use permitted under Creative Commons License Attribution 4.0 International (CC BY 4.0).
CEUR Workshop Proceedings (CEUR-WS.org)

CEUR-WS.org/Vol-3363/preface.pdf

Horizon 2020 research and innovation program under the Marie Sklodowska-Curie-Innovative Training Network 2020, Grant Agreement N° 956394 (https://parenth2020.com/). The goal of the DETERMINED 2022 workshop was to provide a unique forum for graduates, post-docs, and other scientists to present and exchange new research and ideas for the advancement of early diagnosis of motor and cognitive impairments in preterm children. This year the workshop hosted an exciting keynote talk, oral presentations, poster exhibitions, and a networking event to discuss such advancements.

DETERMINED 2022 was held in person with around fifty attendees. The whole workshop was also streamed live via ZOOM.

2. Call for papers, submission, and peer-review process

The call for papers was published on the workshop website[1] and distributed to the researchers via e-mails. The invitation to participate in the workshop aimed to gather contributions in terms of research ideas, research results, or literature reviews exploring technological innovations related to neurodevelopmental disorders, focusing primarily on preterm infants. Contributions targeted the following areas but not limited to:

- Machine Learning for Preterm Neonatal Care Applications;
- Big Data Analytics;
- Medical Image Processing and Signal Processing;
- Clinical Decision Support Systems (CDSSs);
- Precision Medicine;
- Biology and Bioinformatics;
- Neuroscience and Computational Neuroscience;
- IoT for Healthcare;
- Computational Modelling in Biological Systems and Medicine.

Authors submitted the papers to the workshop via EasyChair[2] conference management system. The system was used also for gathering the reports from reviewers selected by the scientific committee.

Each paper was reviewed by at least three independent reviewers through a single-blind review process. Thirteen papers (out of 15 submitted) were accepted for an oral presentation at the workshop.

3. Scientific Programme

DETERMINED 2022 opened with a keynote “Enabling scientific discovery using artificial intelligence” given by Marinka Žitnik, an Assistant Professor of Biomedical Informatics at Harvard Medical School. The keynote lecture was followed by the oral presentations given by the authors of the accepted submissions. The presentations were organised in two sessions.

[1] https://parenth2020.com/2022-determined/
[2] https://easychair.org/

The oral presentations were supported by posters that were displayed during a co-located training event of the PARENT project and during the workshop.

3.1. Keynote speaker

Marinka Žitnik is an Assistant Professor at Harvard University with appointments in the Department of Biomedical Informatics, Broad Institute of MIT and Harvard, and Harvard Data Science. She studies applied machine learning with a focus on challenges in scientific discovery and medicine. Her methods leverage biomedical data at the scale of billions of interactions among millions of entities, blend machine learning with statistics and data science, and infuse biomedical knowledge into deep learning. Problems she investigates are motivated by network biology and medicine, genomics, drug discovery, and health.

Before joining Harvard, she was a postdoctoral scholar in Computer Science at Stanford University. She was also a member of the Chan Zuckerberg Biohub at Stanford. She received her bachelor's degree, double majoring in computer science and mathematics, and her Ph.D. in Computer Science from the University of Ljubljana. During her Ph.D. studies she was also researching at Imperial College London, University of Toronto, Baylor College of Medicine, and Stanford University.

4. Organisation

Scientific Committee Chairs

- Marco A. Deriu, Politecnico di Torino, Italy
- Vida Groznik, University of Primorska; University of Ljubljana; NEUS Diagnostics d.o.o., Slovenia
- Umberto Michelucci, TOELT llc; Lucerne University of Applied Sciences and Arts, Switzerland
- Aleksander Sadikov, University of Ljubljana; NEUS Diagnostics d.o.o., Slovenia

Programme Committee Members

- Marco A. Deriu, Politecnico di Torino, Italy
- Dejan Georgiev, University of Ljubljana
- Vida Groznik, University of Primorska; University of Ljubljana; NEUS Diagnostics d.o.o., Slovenia
- Umberto Michelucci, TOELT llc; Lucerne University of Applied Sciences and Arts, Switzerland
- Ángel Ruiz Zafra, University of Granada, Spain
- Aleksander Sadikov, University of Ljubljana; NEUS Diagnostics d.o.o., Slovenia
- Ignacio Turias, University of Cádiz, Spain
- Daniel Urda Muñoz, University of Burgos, Spain

Session Chair

- Monica Crotti, KU Leuven, Belgium

Web Chairs

- Arnaud Gucciardi, TOELT llc, Switzerland
- Pablo Romero Diaz, 7hc, Italy

Design Chair

- Marta Malavolta, University of Ljubljana, Slovenia

Proceedings Chairs

- Janet Pigueiras del Real, University of Cádiz, Spain
- Jaime Simarro Viana, icometrix, Belgium

Organisation Committee

- Arantxa Ortega-Leon, University of Cádiz, Spain
- Roa'a Khaled, University of Cádiz, Spain
- Lolia Ibanibo, Puerta del Mar University Hospital, Spain
- Konstantinos Panagiotopoulos, Politecnico di Torino, Italy
- Enrico Piccinelli, Ospedale Pediatrico Bambino Gesu, Italy
- Syed Adil Hussain Shah, GPI SpA, Italy
- Syed Taimoor Hussain Shah, Politecnico di Torino, Italy

Local Arrangements Committee

- Andrea De Gobbis, NEUS Diagnostics d.o.o., Slovenia
- Marta Malavolta, University of Ljubljana, Slovenia
- Emiliano Trimarco, Puerta del Mar University Hospital, Spain

A new median filter application to deal with large windows of missing data in eye-gaze measurements

Arnaud Gucciardi[1,2,*], Monica Crotti[3], Nofar Ben Itzhak[3], Lisa Mailleux[4], Els Ortibus[3], Umberto Michelucci[1,5], Vida Groznik[2,6,7] and Aleksander Sadikov[2,6]

[1]TOELT llc, Machine Learning Research and Development, Birchlenstr. 25, 8600 Duebendorf, Switzerland
[2]Faculty of Computer and Information Science, University of Ljubljana, Ljubljana, Slovenia
[3]Katholieke Universiteit Leuven, Department of Development and Regeneration, Leuven, Belgium
[4]Katholieke Universiteit Leuven, Department of Rehabilitation Sciences, Leuven, Belgium
[5]Computer Science Department, Lucerne University of Applied Sciences and Arts, 6002 Lucerne
[6]NEUS Diagnostics d.o.o., Ljubljana, Slovenia
[7]Faculty of Mathematics, Natural Sciences and Information Technologies, University of Primorska, Koper, Slovenia

Abstract

Eye-hand coordination is a challenging skill to measure objectively, especially in children with motor disabilities such as Cerebral Palsy (CP). The recent development of robotic technology provides non-invasive tools for the simultaneous acquisition of eye and hand movement data. One such technology is the remote eye-tracking and virtual-reality systems namely the Kinarm Gaze-Tracker™ installed in the Kinarm Exoskeleton™. Unfortunately, no standard software interface exists to extract the data contained in the Kinarm proprietary files for an efficient further analysis in common programming languages such as Python. Additionally, in the standard Kinarm reports only hand movements parameters are available, while eye movements are only stored as raw data files. These limitations lead to difficulties in performing a complete analysis of eye-hand coordination in research settings. Additional problems can arise in the case of missing data (due to loss of tracking). The software described in this paper allows the extraction of the hands and eye-gaze time series for efficient further analysis directly from the raw data. Furthermore, a study of the distribution of missing data is presented. Finally, this paper describes a revised median filter application to deal with large windows of missing data.

Keywords

Eye-Gaze, Software, Median Filter, Unilateral Cerebral Palsy, Kinarm

1. Introduction

Cerebral Palsy (CP) describes, based on an international consensus, *"a group of permanent disorders of movement and posture, causing activity limitations, that are attributed to non-*

DETERMINED 2022: Neurodevelopmental Impairments in Preterm Children — Computational Advancements, August 26, 2022, Ljubljana, Slovenia
*Corresponding author.
arnaud.gucciardi@toelt.ai (A. Gucciardi); monica.crotti@kuleuven.be (M. Crotti); nofar.benitzhak@kuleuven.be (N. Ben Itzhak); lisa.mailleux@kuleuven.be (L. Mailleux); els.ortibus@uzleuven.be (E. Ortibus); umberto.michelucci@toelt.ai (U. Michelucci); vida@neus-diagnostics.com (V. Groznik); aleksander.sadikov@fri.uni-lj.si (A. Sadikov)
https://github.com/toelt-llc/KiPy (A. Gucciardi)
© 2022 Copyright for this paper by its authors. Use permitted under Creative Commons License Attribution 4.0 International (CC BY 4.0).
CEUR Workshop Proceedings (CEUR-WS.org)

CEUR-WS.org/Vol-3363/paper01.pdf

progressive disturbances that occurred in the developing foetal or immature brain. The motor disorders of CP are often accompanied by disturbances of sensation, perception, cognition, communication, and behavior, by epilepsy, and by secondary musculoskeletal problems" [1]. The development of movement capacity in addition to muscle tone and posture [1, 2] is affected by brain injury in the prenatal, perinatal, and postnatal phase up to the age of two years [3]. CP is a neurological disorder recognized as the leading cause of childhood motor disability and its appearance is estimated from 1 to nearly 4 per 1,000 live births [1]. Children with CP develop a wide range of conditions that may affect their functional abilities [4]. The clinical variability of children with CP can be explained by the heterogeneity of the underlying brain injury [5], which also affects the nonmotor pathways of the developing brain. Among these, the visual network is often affected in children with CP [6]. This leads to impairments in visual function [7] which is a prerequisite for typical eye-hand coordination [8] since it is crucial for planning and performing movements [9, 10]. Therefore, children with CP also suffer from difficulty in grasping objects [11].

Accurate reaching develops in children between 5 to 13 months of age [12] and is fine-tuned over a longer period of several years (often more than 8) [12, 13]. In this process, eye-hand coordination plays a fundamental role. Despite a large amount of research in this area, several aspects of the development of eye-hand coordination remain unsolved in children with CP. In addition to motor problems, 60 to 75% of children with CP also have visual deficits [14, 7]. Eye-tracker systems, which allow quantification of looking behaviour, nowadays are considered a valid tool for investigating visuomotor coordination in CP children [15, 16]. Furthermore, their implementation with robotic technology can provide an in-depth quantification of eye-hand movement impairments in the pediatric neurological population. Previous studies [15, 16, 17] attempted to quantify eye-hand coordination in children with CP using different methodologies. Results showed that children with CP have increased visual attention towards the impaired limb during object grasping and reaching [18, 17] and impaired anticipatory visual control in eye-hand coordination when compared to typically developing children [15, 19].

One novel application is the use of the Kinarm Exoskeleton [20] which allows an in-depth quantification of bimanual motor control during symmetrical and asymmetrical tasks and the simultaneously recording of eye movements via the Kinarm Gaze-Tracker [21]. With this technology, both motor and gaze measures can be seamlessly integrated for effective experimental control and data analysis. To our knowledge, no previous work fully evaluated eye-hand coordination in children with CP with the use of such a technology, although investigating this relationship would provide a better understanding of the complex function of the visual motor system. In addition, such results would provide useful information for clinicians and researchers to be applied in diagnosis and possible rehabilitation settings.

The first step for such an analysis is the extraction of information, such as gaze and hands parameters over the time course of a movement, from the Kinarm saved files. This is not a trivial task as the data is stored in proprietary file formats, making the desired analysis very difficult. This work addresses this problem and describes a possible solution. The contributions of this paper are fourfold. First, it describes a software framework able to extract hands and eye-gaze coordinates with time from the Kinarm Exoskeleton files as time series (a time series is, in its most common occurrence, a sequence of points taken at successive equally spaced points in time). Secondly, this work describes and discusses a variation of the median filter for data with

large windows of missing values. Thirdly, this paper analyses missing data windows in terms of distributions of width and frequency of the gaps in the data in two separate cases. Finally, it demonstrates the median filter variation described in this paper applied to two different examples with very different distributions of missing data windows.

The paper is organised as follows. In Section 2, the Kinarm Exoskeleton and the eye-gaze module are briefly described. The data and the median filter are also discussed and defined respectively. In Section 2.4, the different tasks possible with the Kinarm exoskeleton are described. In Section 2.6, the monitored parameters are listed. In Section 3, the Software is described. In Section 4, the results are presented and in Section 5, the conclusions are discussed.

2. Methodology and Data

2.1. The Kinarm Exoskeleton

Data collection was carried out with the Kinarm Exoskeleton Lab (BKIN Technologies, Kingston, ON, Canada) [20] combined with an integrated EyeLink 1000 Plus eye tracking system (SR Research, Ottawa, ON, Canada) [21]. The Kinarm Exoskeleton can be seen in Figure 1. The Kinarm Exoskeleton Lab (BKIN Technologies, Kingston, ON, Canada) allows movement of the arm in the horizontal plane such as flexion and extension of the shoulder and elbow joints [20]. The hands are free to interact with objects in the environment surrounding the subject. Patterns of joint motion are recorded and the system computes muscular torques, allowing the study of upper limb movement and coordination. The use of Kinarm Lab's operating system and its control software, Dexterit-E^{TM} [20], allows data collection in a user-friendly way. At the end of each experimental task, reports can be extracted from the Dexterit-E^{TM} software in a Comma-Separated Values format (CSV) where a division in LEFT and RIGHT-hand parameters is available.

2.2. Eye-Gaze tracking system and parameters

Eye tracking and gaze estimation systems are well-established techniques used to study eye movements and position, both in clinical and research settings [22]. In eye tracking systems, the eye position is calculated through different sequential steps (detection of the eyes, interpretation of eye positions, and frame-to-frame tracking) with the help of the pupil or the iris centre [23]. Gaze estimation, that is, the process made to estimate and track the 3D line of sight, is calculated from the analysis of eye movements through a device called gaze tracker [23]. A gaze tracker simultaneously records the location of the eye position and its motion to determine the direction of the gaze [24]. The EyeLink 1000 Plus system (SR Research, Ottawa, ON, Canada) integrated into the Kinarm Exoskeleton Lab (BKIN Technologies, Kingston, ON, Canada) allows recording binocular eye movements at up to 2000 frames per second. Camera images are processed using a real-time operating system from which gaze data is recorded. More information on the eye gaze estimation system can be found in the work of A. Kar et al. [25]. Eye tracking systems allow the quantification of different types of eye movements such as fixations, saccades, and smooth pursuit.



Figure 1: Kinarm Exoskeleton Lab (BKIN Technologies, Kingston, ON, Canada) [20] with integrated EyeLink 1000 Plus system (SR Research, Ottawa, ON, Canada) [21].

This paper will specifically focus on the data used to estimate fixations and saccades [26]. A visual fixation is the maintenance of gaze in a single location or area [27]. Fixations phases are defined as moments where the eyes are stationary between movements while the visual input occurs. A saccade is a quick and simultaneous movement of the eyes between phases of fixation in the same direction [27]. Saccades are mainly used for orienting the gaze towards an object of interest. They can be triggered voluntarily or involuntarily, with both eyes moving in the same direction.

Fixations and saccades can be quantified in terms of different parameters which can be used for further analysis (i.e., eye-hand coordination). The mathematical algorithms to compute them are not discussed in the present paper. For further information, the interested reader can refer to the following papers [28, 25].

The data output from Kinarm software includes gaze position (x and y positions), gaze direction, pupil position (x, y and z positions) and area, time stamps, and events such as start and end of fixations and saccades. The Kinarm software automatically saves these features in stored files, making them available to researchers. If necessary, averages and other statistical analyses of the available metrics are then possible. Additionally, by adding the formerly listed features, the parameters mentioned below can be calculated.

Fixations and saccade parameters include:

- *Fixation Duration* - total duration of a fixation in seconds.
- *Fixation Area* - position where the fixation is recorded in meters.
- *Saccadic Peak velocity* - the highest velocity recorded during the saccade in metres per second.
- *Saccadic amplitude* - the horizontal displacement during eye movement in meters.
- *Saccade Duration* - total duration of a saccade in seconds.
- *Gaze latency* - time taken from the appearance of a target to the beginning of a saccade in response to that target in seconds.
- *Gaze Accuracy* - the average distance between the target and the participant's eye position in meters.

2.3. Data

In the present paper, data from two subjects, namely A and B, are discussed. Both participants have been diagnosed with unilateral CP (mean age: 11y4m). Test subjects are chosen only if they have minimal ability to actively grasp and hold an object and sufficient cooperation to perform the assessments. None of the participants received botulinum toxin injections six months before testing or had a history of arm surgery two years prior to the assessment. Each experimental session lasted about one hour. After the experimental session, the data were anonymised and extracted from Dexterit-E^{TM} software in a Comma Separated Values (CSV) format where a division in the left and right upper limbs and the left and right eye gaze parameters is available.

The available records for this study consist of two separate file groups: group A is defined as the group that contains the first cohort of experiments, and group B is the second group. Both groups contain eight files for the three different tasks studied: *Ball On Bar* task (2 files), *Object Hit* task (2 files), and *Visually Guided Reaching* task (4 files). The files of the second group contain incomplete and damaged data: missing values are detected for the Gaze X and Gaze Y positions. In addition, the remaining values translate into a different gaze behaviour.

A comparative view of the gaze behavior in the three tasks can be seen in Figure 4. Due to the individual differences in the task protocol and the numerous rows that make up the experiment dataframes, the CSV files are of various sizes. In Table 1, the average total lines and the size of the CSV files related to subjects A and B are reported.

Size differences are directly correlated with the duration of recorded trials (number of attempts) on tasks (i.e., exercise type).

Table 1
Time series length from groups A and B. The *Average file size* is the total length of the CSV file, the *Average total lines* represents the average line count of a type of task, and the *Maximum size* is the maximum line count.

Exercise type	Average file size	Average total lines	Maximum size
Ball On Bar	81 032	79 918	130 621
Object Hit	15 274	10 427	28 080
Visually Guided Reach.	49 787	46 002	107 427

2.4. Experiment tasks and datasets differences

In this paper, the focus is on three custom experimental tasks (i.e., Kinarm standard test-KST), namely, the *Ball On Bar*, *Object Hit*, and *Visually Guided Reaching* task. Each task is standardised and performed with the Kinarm Exoskeleton, allowing the assessment of upper limbs' motor control and the simultaneous acquisition of eye-movements data [29]. A description of the KST taken from the Kinarm manual is provided below.

Ball On Bar The Ball on Bar task assesses the ability of subjects to perform a motor activity that requires coordination of the two arms. [30] A virtual bar is presented between the subject's hands, and a virtual ball is placed on the bar. The objective of the task is to move the virtual ball on the bar to successively presented targets as quickly and accurately as possible.

Object Hit The Object Hit task [31] assesses rapid motor skills throughout the workspace. It is developed to assess the ability of a subject to select and engage in motor actions with both hands over a range of speeds and a large workspace. Good performance requires the ability to generate a goal-directed motor action on a moving target, bimanual planning to select which arm to use to hit each object, and spatial awareness across the workspace.

Visually Guided Reaching The purpose of the Visually Guided Reaching task is to quantify voluntary control directed toward the goal [32]. This task assesses visuomotor response time and arm motor coordination. During this task, a central target is presented, and the subject must move a cursor (white circle) representing hand position to this target.

For each task, the Kinarm software can automatically compute a standard report (SR), as well as a CSV file [33]. CSV files contain a metadata header with calibration and experimental set-up information such as the Kinarm experiment instructions, the accessories used and the calibration values. The file header also includes the definition of all recorded channels that measure features with their unit of measurement. For each task, a different number of trials are presented, namely an attempt to accomplish the exercise. Note that the number of trials varies depending on the task exercise in both groups (A and B). For the *Object Hit* task, there is a single trial in each file. A total of 1 to 3 trials are presented for the *Ball On Bar*, and 1 to 24 for the *Visually Guided Reaching* task. In the trial information, the different time series are provided in terms of a dataframe where each row contains the data measured at a given time in

milliseconds. Rows are separated by 1 ms intervals. The individual trials also include a trial header with several lines regarding metadata that needs to be removed in pre-processing.

2.5. Files processing

The experiment files are presented as CSV files containing dataframes. In this case, the columns are the measured kinematics features, and the rows are the individual values of each frame saved. The extraction process allows the reading of the dataframes contained as raw content. Furthermore, the goal is to obtain the experiment data as time series. In the files, each trial is represented as a separate dataframe. The pre-processing algorithm allows us to extract these dataframes by splicing the CSV files and removing the general metadata header and the individual trial headers. This is done for each of the four possible tasks. The methods involved can be used for new experiment files to automate the analysis.

Table 2
Parameters of interest selected from the list of features.

Parameter (measurement unit)	Definition
Sample duration (s)	Interval between each data sample taken
Sample count	Total number of data points for each measurement
Frame number	Individual identifier of each row in the dataframe
Frame time(s)	Unique timestamp to each row. Starts at 0 for each trial
Event name	Name of the event, automatically given by Kinarm
Event time (s)	Frame time of the detected event
Right and left hand position (m)	Position of each hand, X and Y component
Gaze position (m)	Gaze position in global coordinates, X and Y component
Right and left hand speed (m/s)	Individual speed of each hand
Right and left hand acceleration (m/s^2)	Individual acceleration of each hand
Ball position (m)	Only for *Ball-On-Bar* exercises, ball X and Y position on screen
Ball relative position (m)	Only for *Ball-On-Bar* exercises, ball relative position on the bar

2.6. Monitored parameters

The features of interest used for visualisation and analysis are listed in Table 2. Note: the total real time of each trial is equal to *sample count* multiplied by *sample duration*. It can also be retrieved by looking at *frame time* in the last row of the selected trial. All tasks from both file groups are saved in a single trial (that is, in one dataframe). Some files contain more than one

trial: in the first group of files, the two *Ball-On-Bar* tasks include, respectively, 3 and 2 trials, and the two *Visually Guided* tasks include 3 (for the child practise set) and 24 (for the complete exercise) trials. And in the second group, two out of four *Visually Guided* tasks contain 9 trials.

2.7. Analysis of Missing Data in the Eye-Gaze Measurements

As mentioned in Section 2.3, some of the experiment data lines contained in the CSV files of the second group of files appear incomplete. The features presented previously require continuous data to study the detailed actions of gaze and hands. In practise, the missing values detected in the files make a complete analysis and visualisations impossible; since both gaze and hands position data in multiple time windows are missing. Indeed, events like fixations and saccades cannot be entirely detected and understood when positions are only partially saved during a given time window. As a first step, the number of extended regions of continuous missing data, or *gaps*, are counted and their respective lengths measured. Depending on the type of trial, the complete length of recorded experimental data changes, but it is possible to estimate the percentage of missing data for each trial to quickly quantify the impact on the final analysis. And this is possible for each experiment regardless of the length. This result is represented in Table 3.

Table 3
List of the nine trials contained in the CSV report file of a *Visually Guided Reaching* task for group B. The *Average gap size* column shows the rounded averages over all the detected gap sizes of size 1 and more. The amount of gaps detected in a trial is noted in the *Gaps count* column. *Max gap size* contains the size of the largest gap in the trial. *Not a Number values* (NaN values) column contains the total amount of NaN values in each trial, the *Total length* column contains the time series entire length.

Trial ID	Average gap size	Gaps count	Max gap size	NaNs values	Total length	**NaNs** %
0	181	3	281	543	3353	16.2
1	98	10	318	980	8414	11.7
2	60	9	192	539	5857	9.2
3	126	9	576	1132	4838	23.4
4	41	32	228	1299	8258	15.7
5	65	10	222	654	6665	9.8
6	65	36	1051	2355	8880	26.5
7	200	1	200	200	1269	15.8
8	210	1	210	210	2586	8.1
Mean	116	12.3	364.2	879.1	5569	**15.2**
Std Dev	62	12.1	267.7	633.9	2591	6.0

The selected example file from a task of *Visually Guided Reaching* in group B contains 9 separate trials, all of which are made of a large amount of NaN values. The minimum value of missing values is 8.1% (in trial 8) of the total data points, while the maximum is 26.5% (in trial 6). The mean proportion of missing values over the 9 trials is 15.2%. The example is representative of group B, where each file contains randomly placed NaNs gaps of various sizes.

Table 4
List of trials containing gaps from a CSV report file of a *Visually Guided Reaching* task from group A. The file contains 24 trials, of which only 4 contain NaN values represented in the table. The remaining 20 trials do not contain gaps or a single NaN value. The *Average gap size* column shows the rounded averages over all the detected gap sizes of size 1 and more. The amount of gaps detected in a trial is noted in the *Gaps count* column. *Max gap size* contains the size of the largest gap in the trial. *NaNs values* column contains the total number of NaN values in each trial, the *Total length* column contains the time series entire length.

Trial ID	Average gap size	Gaps count	Max gap size	NaNs values	Total length	**NaNs** %
4	24	1	24	24	5559	0.4
10	104	1	104	104	4941	2.1
20	144	1	144	144	5303	2.7
21	83	1	83	83	4312	1.9
Mean	14.8	1	14.8	88.7	4177	**1.8**
Std Dev	43.3	0	43.3	43.3	1340	0.8

2.8. Median Filter

To preserve the recorded data saved in the incomplete files and to reduce noise, a median filtering technique is applied. The method is compatible with missing data. Due to the noise reduction obtained, the local trend can be preserved by replacing incorrect data. The median filter eliminates extreme or empty values without having to do a mean averaging of the neighbour values, which would heavily impact the correct values. Although typically used for image pre-processing [34], the algorithm can be applied to one-dimensional signals [35] as is the case here. When used on one-dimensional input, the process is simplified : the neighbourhood includes values before and after the index.

Definition 1. *Given an array of M values* $(X_1, ..., X_M)$*, the median filter (MF) of size Q (in this paper Q is taken to be odd for simplicity of notation) is a mapping* $\mathbb{R}^M \rightarrow \mathbb{R}^M$*. By defining* $Q = 2n + 1$*, the output of the MF will be an array with elements* X_i^f *given by*

$$X_i^f = median(\{X_i - n, ..., X_i + n\}) \tag{1}$$

The median filter algorithm replaces each individual value X_i *(starting from* $i = n$*) of the original array by the median of the following and previous n values. The* ***window*** *or* ***filter size*** *of total size Q defines the amount of neighbour values considered to compute the new filtered signal* X^f*. Since there are no values preceding the first and last elements of the signal, the first and last values are repeated until enough values are reached to fill the window.*

Figure 2 shows an example of the median filter applied to a hypothetical data set with some quantity (x_i) measured at specific time points t_n. In Step 1, a time window is selected (in Figure 2 the selected time window includes the time points t_2 to t_6). In Step 2, the values are sorted, and the median value is selected (Step 3). The time window then moves along the entire data set.

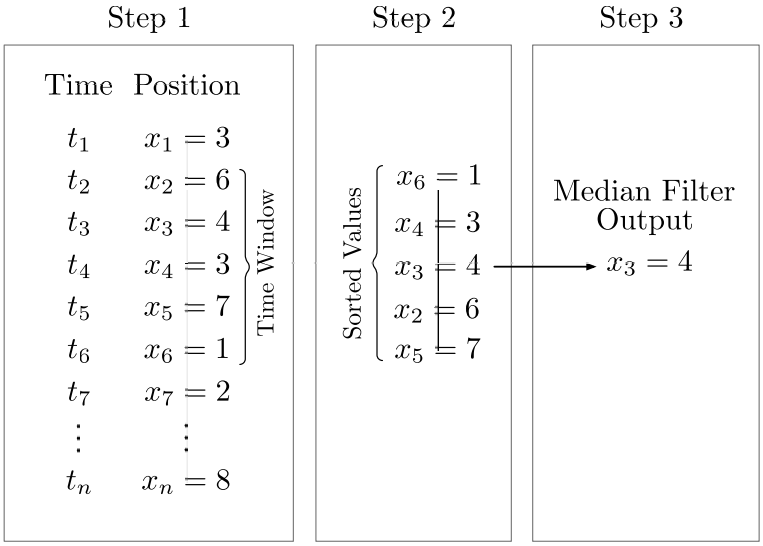

Figure 2: Diagram of an example application of the median filter to a hypothetical dataset. A hypothetical dataset with some quantity (x_i) measured at specific time points t_n is considered. In Step 1, a time window is selected (in this example the selected time window includes the time points t_2 until t_6). In Step 2, the values are ordered, and the median value is selected in Step 3.

The median filtering is applied to the experimental data in Figure 5, with two filter sizes presented. Fixations and saccades rely on specific windows of gaze position. It is important to note, as a downside, the risk of losing short movement detections as the filter size selected gets larger. Movements shorter than the filter window might be lost. This is a risk in the time series containing gaze positions if the filter is longer than some of the actual events happening within the task. The window size choice is an important parameter further developed in the article.

2.9. The Median Filter for Large Windows of Missing Data (MFLWMD)

A statistical analysis of the features of saccades and fixations is made difficult, if not impossible, when large windows of missing data are present. The most appropriate solution is to split the time series each time a gap larger than a specific size is encountered. As a possible solution to the presence of large windows of missing data, the following median filter application is presented. Given a certain measurement of a generic quantity x_i (for example, the x coordinate of the eye-gaze) at various t_i time points (for $i = 1, ..., M$). A median filter of size n can be applied by sliding a window of size n on the measured data. Let us also suppose that $M \in \mathbb{N}$ windows of missing data, in which gaps of size s_i are present at various positions along the array x_i. If a missing data window is encountered, there are two possible scenarios. Let us indicate with $g \in \mathbb{N}$ an integer that can be called *threshold*.

1. $s_i \geq g$: the array x_i is split at that point and every calculation of the statistical estimators is stopped. The two parts are considered for all purposes as separate files.
2. $s_i < g$: the median filter can be applied simply by removing the missing data and considering only the available values.

The best choice of g is, of course, related to the median filter window size. g should be larger than n to make this proposed variation of the median filter meaningful. From the available missing values files and experiments, and since the filters span across windows of size n, the authors propose that a good choice is $g \gtrsim 2n$ to $3n$. If the threshold is less than n, complete missing value gaps are never considered since the filter size will cover all possible cases. On the other hand, if the threshold is greater than $3n$ the starting and end points are considered too far apart for the filter to sufficiently fill the gap considered.

3. Software Functionalities

The *KinarmPython* extraction library presented in this article, called KiPy, can read CSV files generated from the Kinarm Dexterit-E^{TM} software [33] and support their analysis. The software provides the user with the ability to parse all accessible kinematics logs. Concerning the research questions previously mentioned in Section 2.3, the software extracts relevant information and can create visualisations which can also be easily changed by the user. The tool currently uses command-line scripts and Python functions; the goal is to keep it simple, configurable, and performant. The application is written in Python 3.8 and requires the additional Pandas, NumPy, Pickle, and Matplotlib libraries. It is open source and is available on GitHub [36]. Once the files are read, all metadata are excluded, and the remaining data are read as a Pandas DataFrame. The Pandas DataFrame is an efficient data structure to store structured data and provides powerful functions to filter and search for specific rows of columns.

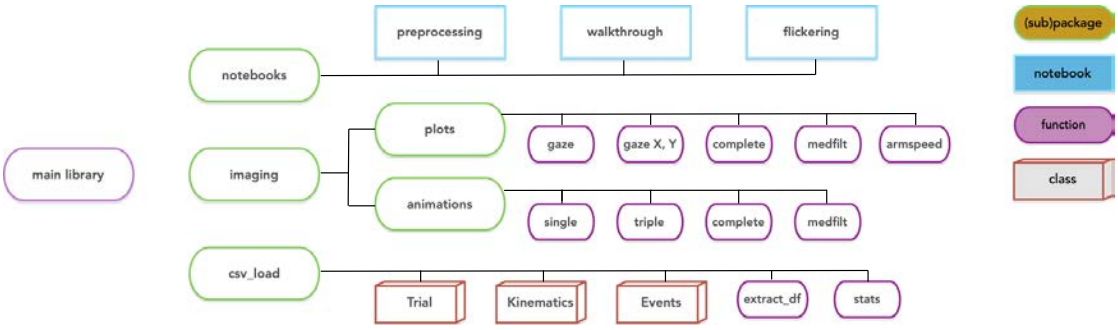

Figure 3: Software Component Diagram. The main components of the software package KiPy are depicted in this Figure. The different parts (sub-packages, notebooks, functions and classes) are represented with different colors explained in the legend. Further documentation is available online [36].

From the extracted dataframes, the algorithm accesses the visual data events. For each trial, the duration and count of all the events are given. This information can be further used to

analyse the frequency of the events over a single trial, a complete experiment, or a group of experiments (e.g., the events statistics for a given type of experimental task).

4. Results

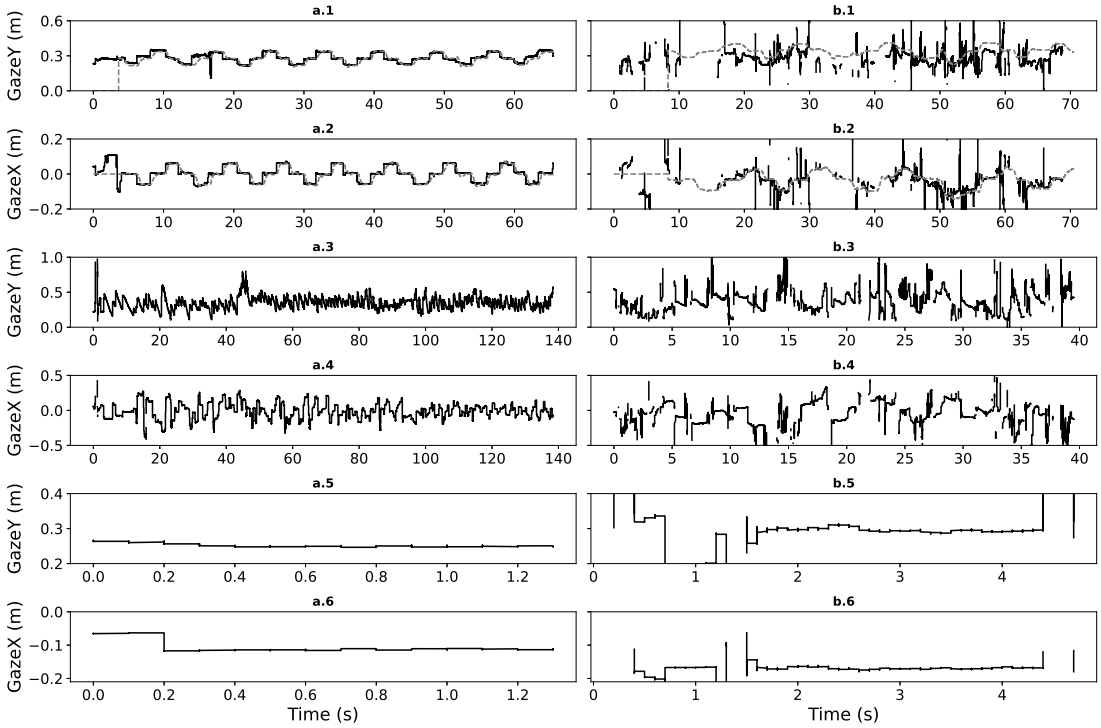

Figure 4: Gaze comparison: group A and B. Group A and group B tasks are represented on the left and right sides, respectively. Numbers 1 to 2 represent X and Y movements of the gaze on the *Ball On Bar* tasks. The ball position is shown in dotted grey lines. Numbers 3 to 4 correspond to an *Object Hit* task, and numbers 5 to 6 correspond to the *Visually Guided Reaching* task.

4.1. Eye-gaze and Hand Position Data

The central idea behind the software tool is to give the user the ability to read the CSV files and visualise and analyse the Kinarm experiments. The software makes it possible to first, given any task input, visualise the movements of the gaze and hands. The visualisation can be done with both static plots and animations. Animations are short videos that the user can produce at a chosen speed. Examples of visualisations can be seen in Figure 4 for gaze movements and in Figure 6 for hands movements over the duration of the task in the three different tasks. The figures display the differences between the two groups of files. One can identify gaps of missing values, saved as NaNs in files, and numerous peaks, hence the name of noisy *flickering* data.

4.2. Median Filter Application

Examples of the distribution of NaN gaps in gaze time series are presented in Tables 3 and 4. The examples selected are described with a precise description of the impact of the missing values. The difference is comparably significant over all the tasks and trials. In group A of the files, only 17 of 65 total trials contain missing values, and the average proportion of missing values within the 17 affected trials is 2.8%. However, 29 of the 29 trials in group B have missing values, which represent 18.8% of the total trial values on average. Due to the high variation rates and missing values in group B, the median filter technique was developed and applied to gaze X and Y time series of this group. An example of a median filter application is shown in Figure 5. In each of the three panels, missing data points are not replaced by the median filter.

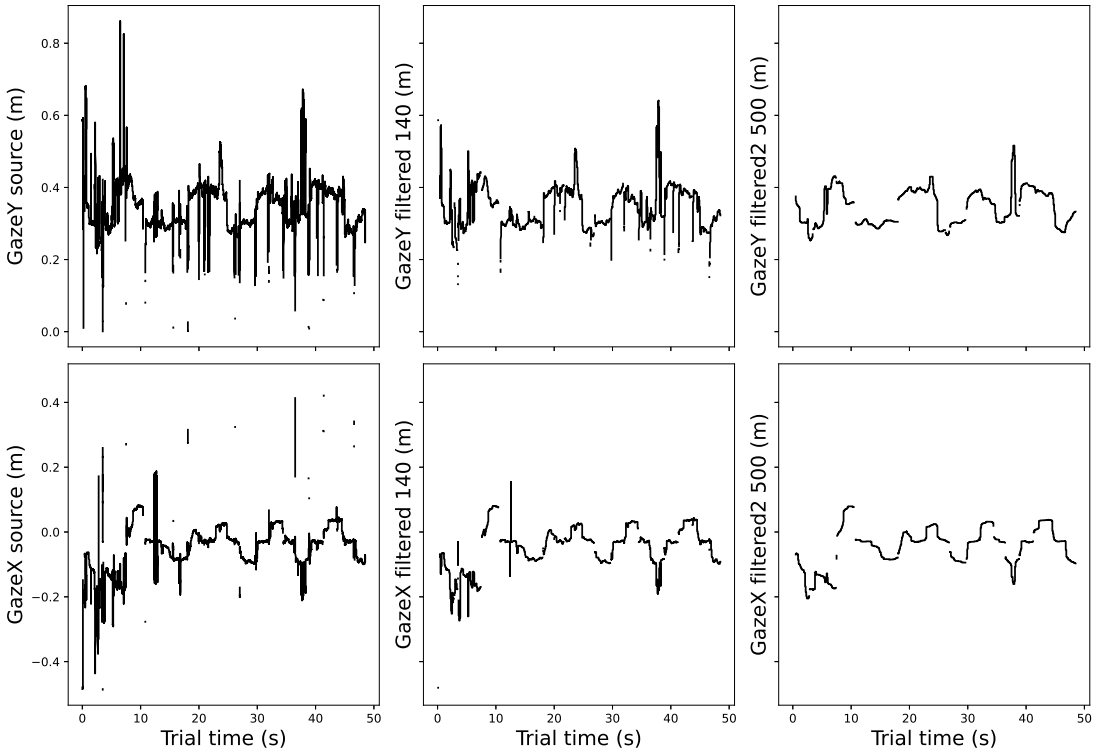

Figure 5: Median filter application: two different filter sizes applied to a *Ball On Bar* task result file. In this example application, extreme flickering values are effectively removed. On the left panel are the original Gaze X and Y over time. On the center panel a filter of size 140 is applied. On the right panel the filter is of size 500. The filter is centered on the current value if this value is not a NaN, as presented in Section (2.8).

Two different filter sizes are applied: 140 and 500, respectively, on the centre and right panels, with the filter centred on the replaced value. On the gaze Y, the range of values went from 0.0-0.83, to 0.17-0.61 in the 140-filtered time series, and to 0.22-0.46 in the 500-filtered time series. A similar result is obtained for the Gaze X values. Although some flickering outliers remain

in the 140-filtered time series, they are all smoothed in the 500-filtered time series. In this example, the smoothing appears to be effective. In practice, a 500-sized filter may be damaging for some tasks since it represents half a second of gaze movements; ruling out the gaze events with shorter durations. The filter of 500ms is used here as a display example of a high value.

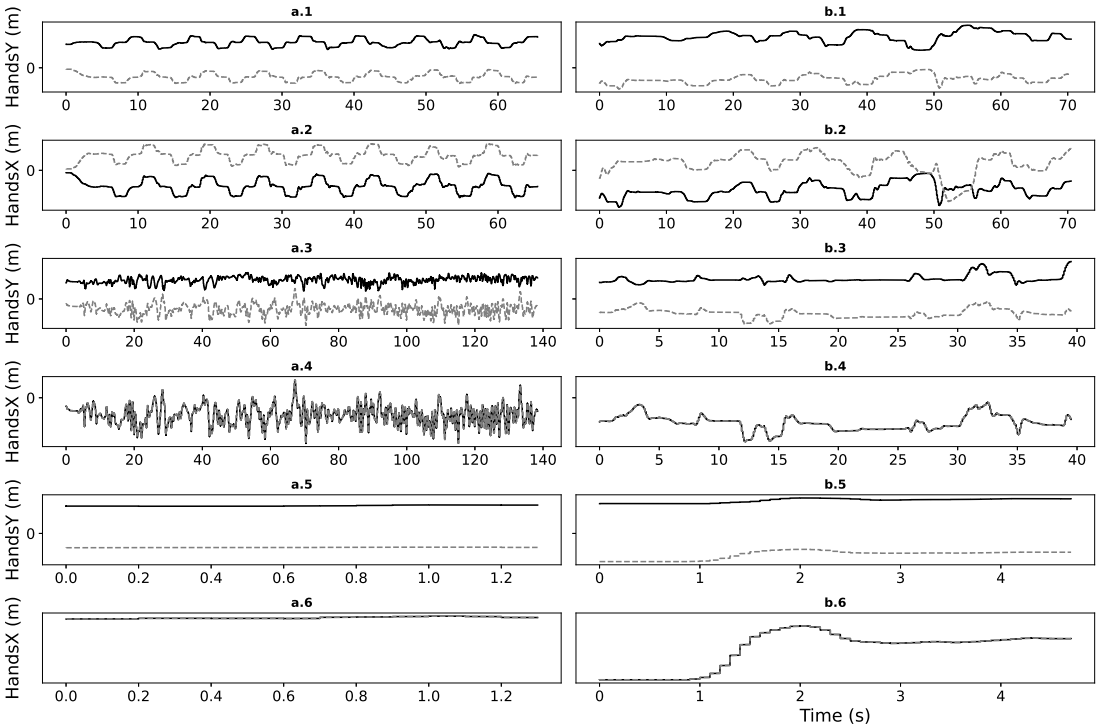

Figure 6: Hands movements comparison: group A and B. Group A and B tasks are represented on the left and right sides, respectively. Number 1 to 2 represent X and Y movements of the hands on the *Ball On Bar* tasks. The ball position is not plotted for visibility. Numbers 3 to 4 correspond to an *Object Hit* task, and numbers 5 to 6 correspond to the *Visually Guided Reaching* task. In black: left hand position, gray: right hand position.

5. Conclusions

Eye movement tracking combined with bimanual motor movement recording allows a complete experimental analysis during symmetrical and asymmetric tasks. From the combined measurements, precise parameters can be extracted and analysed. In this paper data extracted from measurements obtained with the experimental setup described in Section 2.1 and 2.2, is used to highlight the possible applications of the KiPy software analysis library. For each task, it is possible to extract the recorded parameters, including the gaze and hands positions with the timestamp, thanks to various automated functions. Additionally, statistics of ranges of movements and speeds can be individually calculated. If files with flickering and missing values

are present, the software can smooth the flickering signals, detect the size of missing value gaps, and effectively count the number of consecutive data sections. The visualisations and statistics on incomplete experimental data are therefore possible, allowing the analysis of all datasets, including those that present a high percentage of missing data. In the available data, half of the files displayed such problems.

The ability to obtain as much information as possible from the experiments is crucial. The variation of the median filter described in this paper can be applied to all kinds of datasets. To derive an optimal strategy for the choice of the parameter Q, more experimental and different data will be needed. This analysis is planned for a future publication.

To the best knowledge of the authors, no previous work has looked at the automatic detection and filtering of missing data in Kinarm report files. With access to more statistical samples, the KiPy software can be confidently used to extract the desired features and make the analysis much more robust. The authors plan to use and apply the KiPy software to the analysis of a larger dataset to study the eye-hand coordination in a group of children with unilateral cerebral palsy.

Acknowledgments

This work was supported by the project: "PARENT" funded by the European Union's Horizon 2020 Project MSCA-ITN-2020 – Innovative Training Networks Grant No. 956394.

References

[1] P. Rosenbaum, N. Paneth, A. Leviton, M. Goldstein, M. Bax, D. Damiano, B. Dan, B. Jacobsson, et al., A report: the definition and classification of cerebral palsy april 2006, Dev Med Child Neurol Suppl 109 (2007) 8–14.

[2] D. R. Patel, M. Neelakantan, K. Pandher, J. Merrick, Cerebral palsy in children: a clinical overview, Translational pediatrics 9 (2020) S125.

[3] M. Sadowska, B. Sarecka-Hujar, I. Kopyta, Cerebral palsy: Current opinions on definition, epidemiology, risk factors, classification and treatment options, Neuropsychiatric disease and treatment 16 (2020) 1505.

[4] Kinarm, National institute for health and care excellence (uk). cerebral palsy in under 25s: assessment and management, 2022. URL: https://www.ncbi.nlm.nih.gov/books/, available online.

[5] L. Mailleux, C. Simon-Martinez, K. Klingels, E. Ortibus, H. Feys, Brain lesion characteristics in relation to upper limb function in children with unilateral cerebral palsy, in: Factors Affecting Neurodevelopment, Elsevier, 2021, pp. 411–420.

[6] A. Guzzetta, B. Fazzi, E. Mercuri, B. Bertuccelli, R. Canapicchi, J. Van Hof-van Duin, G. Cioni, Visual function in children with hemiplegia in the first years of life, Developmental Medicine and Child Neurology 43 (2001) 321–329.

[7] E. Fazzi, S. G. Signorini, R. La Piana, C. Bertone, W. Misefari, J. Galli, U. Balottin, P. E. Bianchi, Neuro-ophthalmological disorders in cerebral palsy: ophthalmological, oculomotor, and visual aspects, Developmental Medicine & Child Neurology 54 (2012) 730–736.

[8] S. Chokron, G. N. Dutton, Impact of cerebral visual impairments on motor skills: implications for developmental coordination disorders, Frontiers in psychology 7 (2016) 1471.
[9] F. R. Sarlegna, R. L. Sainburg, The roles of vision and proprioception in the planning of reaching movements, Progress in motor control (2009) 317–335.
[10] S. A. Mutalib, M. Mace, H. T. Ong, E. Burdet, Influence of visual-coupling on bimanual coordination in unilateral spastic cerebral palsy, in: 2019 IEEE 16th International Conference on Rehabilitation Robotics (ICORR), IEEE, 2019, pp. 1013–1018.
[11] O. Martinie, C. Mercier, A. M. Gordon, M. T. Robert, Upper limb motor planning in individuals with cerebral palsy aged between 3 and 21 years old: A systematic review, Brain sciences 11 (2021) 920.
[12] C. von Hofsten, L. Rönnqvist, Preparation for grasping an object: a developmental study., Journal of experimental psychology: Human perception and performance 14 (1988) 610.
[13] M. Favilla, Reaching movements in children: accuracy and reaction time development, Experimental Brain Research 169 (2006) 122–125.
[14] A. Schenk-Rootlieb, O. Van Nieuwenhuizen, P. Van Waes, Y. Van der Graaf, Cerebral visual impairment in cerebral palsy: relation to structural abnormalities of the cerebrum, Neuropediatrics 25 (1994) 68–72.
[15] S. M. Surkar, R. M. Hoffman, B. Davies, R. Harbourne, M. J. Kurz, Impaired anticipatory vision and visuomotor coordination affects action planning and execution in children with hemiplegic cerebral palsy, Research in Developmental Disabilities 80 (2018) 64–73.
[16] S. Saavedra, A. Joshi, M. Woollacott, P. van Donkelaar, Eye hand coordination in children with cerebral palsy, Experimental brain research 192 (2009) 155–165.
[17] J. Verrel, H. Bekkering, B. Steenbergen, Eye–hand coordination during manual object transport with the affected and less affected hand in adolescents with hemiparetic cerebral palsy, Experimental brain research 187 (2008) 107–116.
[18] B. Steenbergen, W. Hulstijn, A. De Vries, M. Berger, Bimanual movement coordination in spastic hemiparesis, Experimental Brain Research 110 (1996) 91–98.
[19] S. James, J. Ziviani, R. S. Ware, R. N. Boyd, Relationships between activities of daily living, upper limb function, and visual perception in children and adolescents with unilateral cerebral palsy, Developmental Medicine & Child Neurology 57 (2015) 852–857.
[20] Kinarm, Kinarm exoskeleton product webpage, 2022. URL: https://kinarm.com/kinarm-products/kinarm-exoskeleton-lab/, last accessed on 2022-07-03.
[21] Kinarm, Kinarm exoskeleton integrated gaze-tracking datasheet, 2022. URL: https://kinarm.com/download/kinarm-gaze-tracker/, last accessed on 2022-07-03.
[22] F. R. Danion, J. R. Flanagan, Different gaze strategies during eye versus hand tracking of a moving target, Scientific reports 8 (2018) 1–9.
[23] M. Q. Khan, S. Lee, Gaze and eye tracking: Techniques and applications in adas, Sensors 19 (2019) 5540.
[24] R. A. Naqvi, M. Arsalan, G. Batchuluun, H. S. Yoon, K. R. Park, Deep learning-based gaze detection system for automobile drivers using a nir camera sensor, Sensors 18 (2018) 456.
[25] A. Kar, P. Corcoran, A review and analysis of eye-gaze estimation systems, algorithms and performance evaluation methods in consumer platforms, IEEE Access 5 (2017) 16495–16519.
[26] D. D. Salvucci, J. H. Goldberg, Identifying fixations and saccades in eye-tracking protocols,

in: Proceedings of the 2000 symposium on Eye tracking research & applications, 2000, pp. 71–78.

[27] B. Cassin, S. Solomon, M. L. Rubin, Dictionary of eye terminology, Triad Publishing Company Gainesville, 1990.

[28] S. Tangnimitchok, A. Barreto, F. R. Ortega, N. D. Rishe, et al., Finding an efficient threshold for fixation detection in eye gaze tracking, in: International Conference on Human-Computer Interaction, Springer, 2016, pp. 93–103.

[29] Kinarm, Kinarm standard tests summary, 2022. URL: https://kinarm.com/kinarm-products/kinarm-standard-tests/, last accessed on 2022-07-03.

[30] C. Lowrey, C. Jackson, S. Bagg, S. Dukelow, S. Scott, A novel robotic task for assessing impairments in bimanual coordination post-stroke, International Journal of Physical Medicine and Rehabilitation S3:002 (2014). doi:10.4172/2329-9096.S3-002.

[31] K. Tyryshkin, A. M. Coderre, J. I. Glasgow, T. M. Herter, S. D. Bagg, S. P. Dukelow, S. H. Scott, A robotic object hitting task to quantify sensorimotor impairments in participants with stroke, Journal of neuroengineering and rehabilitation 11 (2014) 1–12.

[32] A. M. Coderre, A. Abou Zeid, S. P. Dukelow, M. J. Demmer, K. D. Moore, M. J. Demers, H. Bretzke, T. M. Herter, J. I. Glasgow, K. E. Norman, et al., Assessment of upper-limb sensorimotor function of subacute stroke patients using visually guided reaching, Neurorehabilitation and neural repair 24 (2010) 528–541.

[33] Kinarm, Dexterit-e., 2022. URL: https://kinarm.com/kinarm-products/dexterit-e/, last accessed on 2022-07-13.

[34] G. Gupta, Algorithm for image processing using improved median filter and comparison of mean, median and improved median filter, International Journal of Soft Computing and Engineering (IJSCE) 1 (2011) 304–311.

[35] B. Justusson, Median filtering: Statistical properties, Two-Dimensional Digital Signal Prcessing II (1981) 161–196.

[36] TOELT, Github repository, 2022. URL: https://github.com/toelt-llc/KiPy, last accessed on 2022-08-20.

Automatic measurements of the corpus callosum in the follow-up of preterm children: Methodology and validation

Jaime Simarro[1,2,*], Manuel Lubián[4], Bahram Jafrasteh[3], Simón Lubián[3,4], Thibo Billiet[1], Els Ortibus[2,5,†] and Isabel Benavente-Fernández[3,4,6,†]

[1]*Research and Development, icometrix, Leuven, Belgium*

[2]*Department of Development and Regeneration, KU Leuven, Leuven, Belgium*

[3]*Biomedical Research and Innovation Institute of Cádiz (INiBICA) Research Unit, Puerta del Mar University Hospital, Cádiz, Spain*

[4]*Division of Neonatology, Department of Paediatrics, Puerta del Mar University Hospital, Cádiz, Spain*

[5]*Department of Pediatric Neurology, UZ Leuven, Belgium*

[6]*Area of Paediatrics, Department of Child and Mother Health and Radiology, Medical School, University of Cádiz, Cádiz, Spain*

Abstract

Brain injury in preterm infants is associated with a high risk of neurodevelopmental disability. One of the most frequent forms of brain injury is white matter injury. The largest white matter structure is the corpus callosum and measurements of this structure have been associated with white matter volume. Consequently, quantification of the corpus callosum could provide an insight into the white matter injury related to preterm birth. However, manual measurements require an experienced rater, are highly time-consuming and suffer from high inter- and intra-rater variability.

In this paper, we present an automated method for measuring the corpus callosum on T1-weighted images of children, and we evaluate the model in terms of accuracy performance. Automatic measurements of the anterior area, posterior area and length of the corpus callosum have a good intraclass correlation coefficient while relatively low absolute error compared to the same measurement performed manually by an expert child neurologist.

Keywords

MRI quantification, follow-up of preterm infant, corpus callosum, white matter injury

1. Introduction

Brain injury in preterm infants is associated with a high risk of neurodevelopmental disability [1]. White matter injury (WMI) is one of the most frequent forms of brain injury in this population [2]. It includes a spectrum of lesions from periventricular leukomalacia (PVL) to a diffuse pattern of WMI [2]. WMI is associated with adverse neurodevelopmental outcomes, for

DETERMINED 2022: Neurodevelopmental Impairments in Preterm Children — Computational Advancements, August 26, 2022, Ljubljana, Slovenia

*Corresponding author.

† EO and IBF are Joint Senior Authors.

jaime.simarro@icometrix.com (J. Simarro)

© 2022 Copyright for this paper by its authors. Use permitted under Creative Commons License Attribution 4.0 International (CC BY 4.0).

CEUR Workshop Proceedings (CEUR-WS.org)

CEUR-WS.org/Vol-3363/paper02.pdf

example, around 10 % of infants with very low birth weight (those born with 1500g or less) that develop PVL later exhibit cerebral palsy and 50% have cognitive and behavioral deficits [3].

The corpus callosum (CC) is the largest white matter (WM) structure and has a key role in interhemispheric functional connectivity [4]. As a result of the importance of this brain structure, the CC is defined as a region of interest in several assessment tools of brain abnormality in preterm infants[5] and children [6]. In addition, this WM structure is associated with WM volume in children with cerebral palsy [7].

Consequently, quantification of this structure could provide an insight into the WM injury related to preterm birth. In spite of the potential of manual quantification of CC [8, 9], these manual measurements require an experienced rater, are highly time-consuming and suffer from high inter- and intra-rater variability [10].

In contrast, artificial intelligence-based software for analysing magnetic resonance images (MRI) has proven to be highly successful in boosting accuracy and increasing time efficiency. In a systematic literature review, Cover et al. summarized the methods for segmentation and parcellation of CC divided in model-based, region-based, thresholding and machine learning [10].

A semi-automatic segmentation tool via constrained elastic deformation of flexible Fourier contour model was applied to a pediatric dataset [11]. Despite the high reliability of the method segmenting the CC (test-retest intra-class correlation coefficient of 0.99), user interaction is required to correct the automatic segmentation. The development of a fully automatic tool for quantification of CC in pediatrics is delayed significantly due to considerable challenges such as partial volume effect, intensity inhomogeneity, extremely variable anatomy, and image artifact (e.g. ghost artifact).

In this study, we aim to overcome these challenges and propose a novel methodology that automatically quantifies the CC and its subregions. Moreover, we will evaluate the performance of these measurements compared with those obtained by manual segmentation.

2. Dataset and methods

2.1. Dataset

The dataset is composed of 65 MRI scans from patients that had been admitted at the Neonatal Intensive Care Unit after being born preterm. These scans were performed during the follow-up of these children at 8 years of age.

Table 1: Demographics of the dataset

# Patients	65
Sex Female (%)	36 (55.3%)
Age (min-max)	8.48 (6.37-10.25) years
Gestational Age at birth (min-max)	29.6 (24.0-34.0) weeks
Birth Weight (min - max)	1325 (550 - 2345) g
Birth Weight<1500g (%)	48 (73.8%)

T1-weighted (T1w) images were acquired at the Hospital Puerta del Mar, Cadiz, using a Siemens Symphony 1.5T MRI system with two different scanning parameters (repetition time = 1910 ms, echo time = 3.5 ms, flip angle = 15 degrees, voxel, size = $1x1x1$ mm3) and (repetition time = 2200 ms, echo time = 3.25 ms, flip angle = 8 degrees, voxel, size = $0.5x0.5x1$ mm3). Two scans were

excluded due to low image quality. Table 1 summarizes the main demographic characteristics of this population.

2.2. MRI analysis

Automatic quantification of the CC from a T1w image was performed in several steps. Figure 1 illustrates the steps proposed in this algorithm. Below, we describe the different steps in detail.

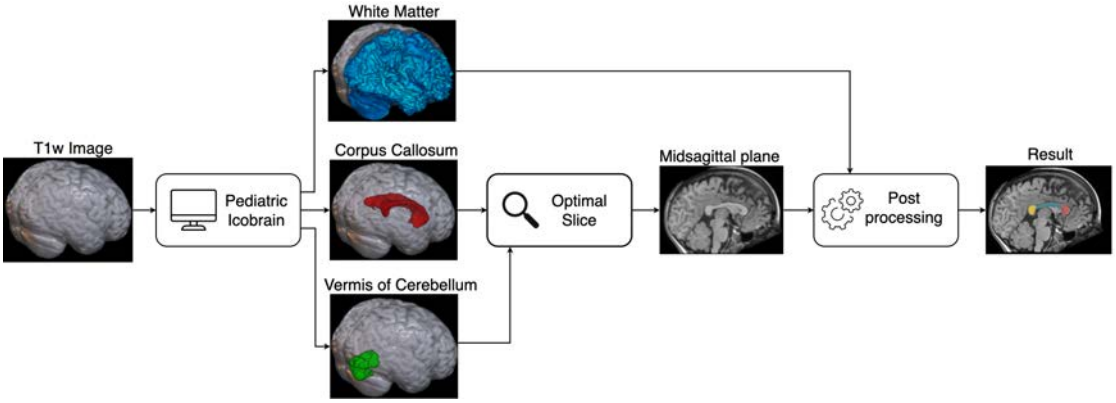

Figure 1: Main processing steps of the pipeline to obtain the automatic measurements of the corpus callosum

2.2.1. Pediatric icobrain

Pediatric icobrain is a model optimized for the pediatric population that is based on the medical device software of icobrain adult pipeline. In summary, the icobrain adult pipeline works as follows: After skull stripping, bias correction and atlas to image registration, the T1w image is segmented optimizing a Gaussian Mixture Model that considers the image intensity, the spatial prior knowledge, the intensity nonuniformities and the spatial consistency [12]. As icobrain is an adult-based pipeline, it was modified to be used for pediatric patients by including age-specific pediatric atlases [13, 14] . Automated segmentation of WM, CC and vermis of the cerebellum was performed on the T1w MR scans using the Pediatric Icobrain model.

2.2.2. Selection of the Optimal Slice

CC is well defined in the 2D midsagittal plane. However, this structure can not be defined in the axial plane and coronal plane since there is not a discontinuity in the WM tracks. Therefore, structural measurements of the CC are performed in the midsagittal plane.

Midsagittal plane is the sagittal slice in which the 4th ventricle and the vermis of the cerebellum are maximally visible. Taking into consideration these prior anatomical landmarks, we used the $argmax$ algorithm to select the midsagittal plane as the sagittal slice with maximum area of vermis.

$$\underset{x}{argmax}\, f(x) := \{x : f(s) \leq f(x) for\, all\, s\, \in X\} \tag{1}$$

where $f(x)$ denotes the amount of the vermis in an x sagittal slice and X the complete set of the sagittal slices.

Alignment with the horizontal axis. As there is considerable heterogeneity in the CC orientation within healthy brains, mainly following the orientation of the brainstem, expert readers typically align all the CC by manually defining the anterior and posterior points of the CC. The proposed algorithm takes advantage of the morphology of the CC to mimic this manual process. Firstly, the contour of the segmentation was fitted to an ellipse. The major axis of the ellipse represents the maximal anterior-posterior distance of the CC and therefore, it can be used to rotate and align all the images (see Figure 2). Alignment of all the images using the CC anterior-posterior axis facilitates the visual interpretation of the parcellation while enhancing the explainability of the algorithm.

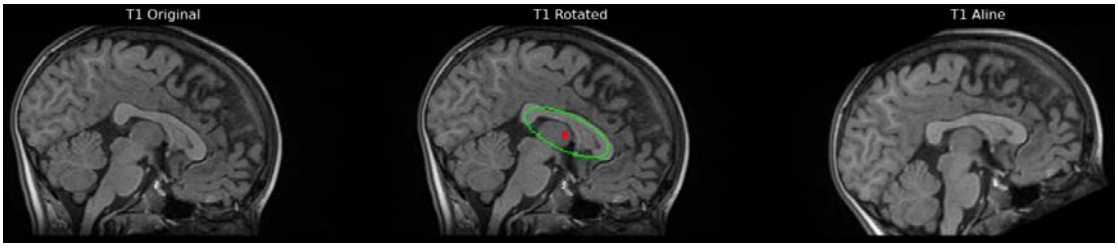

Figure 2: Midsagittal plane of T1-weighted image. Note how the corpus callosum is aligned with the horizontal axis by capturing the anterior-posterior axis of this structure with an ellipse fitting.

2.3. Post-processing

Several post-processing steps were conducted in order to fine-tune the segmentation of the CC.

Prior Anatomical Knowledge of the CC defines WM as the only tissue in this structure. Consequently, this anatomical knowledge was forced into the CC segmentation.

Smoothing of the contours. Alignment of the CC requires a rotation and therefore, an interpolation (bilinear), producing noisy sharp edges in the contour of the CC (which does not represent the anatomy of the structure). This noise was removed using a morphological operation of opening.

$$CC \circ K = (CC \ominus K) \oplus K \tag{2}$$

where $\circ$ denotes the morphological operation of opening, which is just an erosion [1] $\ominus$ followed by a dilation [2] $\oplus$, K denotes a $2x2$ kernel.

[1] Erosion. The value of the output pixel is the minimum value of all pixels in the neighborhood defined by the kernel.
[2] Dilation. The value of the output pixel is the maximum value of all pixels in the neighborhood defined by the kernel.

Largest connected component. CC appears in the midsagittal plane as a single component. However, in some patients the CC is over-segmented, capturing another WM structure, the fornix. The selection of the largest connected component (i.e. the CC) removed the unconnected segmentation of the fornix. This step has the potential limitation of removing an unconnected region of the CC mask, although, as consequence of the robust pediatric icobrain pipeline were atlas to image registration is used, there are no cases with an unconnected CC mask.

Equidistant parcellation and area computation The subdivision of the CC into smaller regions, such as rostrum, genu, body and splenium, is known as parcellation [10]. Our parcellation is based on the study by Park et al. [4], which was also used in prior manual segmentation. The subdivision in 3 sub-regions is proposed in this work in order to be easily reproducible in the clinical setting. In our model, a longitudinal division of 5 equidistant regions was computed. These regions were then clustered as follows: the anterior region, including the rostrum and genu; the central region, including the 2nd, 3er and 4th equidistant regions of the body of the CC; and the posterior region, including the splenium. The anterior-posterior length was also computed.

2.4. Statistical methodology

Accuracy can be defined as the degree of closeness of measurements of a quantity (e.g. area of the CC) to that quantity's actual value. In most cases, this actual value will not be known and, therefore, the accuracy is assessed by comparing the measurements produced by the algorithm, with reference values (ground truth), in this case, produced by an independent child neurologist.

Intraclass correlation coefficient (ICC) computes the reliability of measurements of two raters (i.e. manual and automatic). We selected the two-way random-effects model with absolute agreement. Interpretation of ICC follows the well-known guidelines presented in [15].

Mean absolute error (MAE) is a measure of errors between automatic and manual quantification of the regions.

$$MAE = \frac{\sum_{i=1}^{n} |y_i - \hat{y}_i|}{n} \tag{3}$$

where n denotes the number of patients, y_i the measurement of the manual expert and $\hat{y}_i$ the automatic measurement.

3. Results

3.1. Quantitative analysis

The ICC (CI 95%) performance of the algorithm is not uniform in all the measurements, ranging from 51.23 (2.03-74.06) for the central region to 94.77 (85.86 - 97.53) in the measurement of the length. Automatic measurements of the anterior area and length show a good ICC with the manual measurements with a relatively low percentage of mean absolute error (i.e. <10%). A

more detailed description of this inter-rater reliability experiment can be seen in Figure 3 and Table 2.

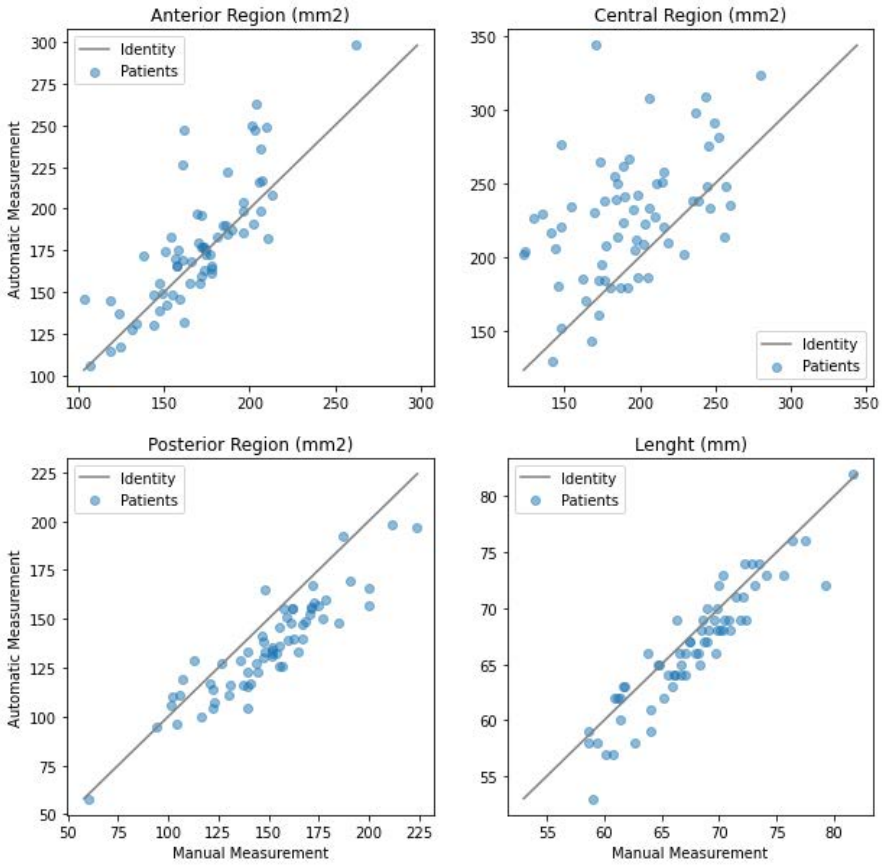

Figure 3: Scatter plots illustrating the corpus callosum quantification compared to the manual quantification of an expert child neurologist.

Table 2
Accuracy of the automatic measurements compared with expert manual quantification. The reference for the Mean Absolute Error is the manual measurement

Region	ICC (CI 95%)	Mean Absolute Error (%)
Anterior	86.48 (76.25 - 92.08)	16.33 mm2, (9,61%)
Central	51.23 (2.03 - 74.06)	40.83 mm2, (21,12%)
Posterior	88.12 (20.34 - 96.11)	16.40 mm2, (10,94%)
Length	94.77 (85.86 - 97.53)	1.89mm, (2,79%)

The central region has a mean absolute error higher than 20%. As illustrated in Figure 4, measurements in this region have a non-zero difference due to an overestimation of the automatic method.

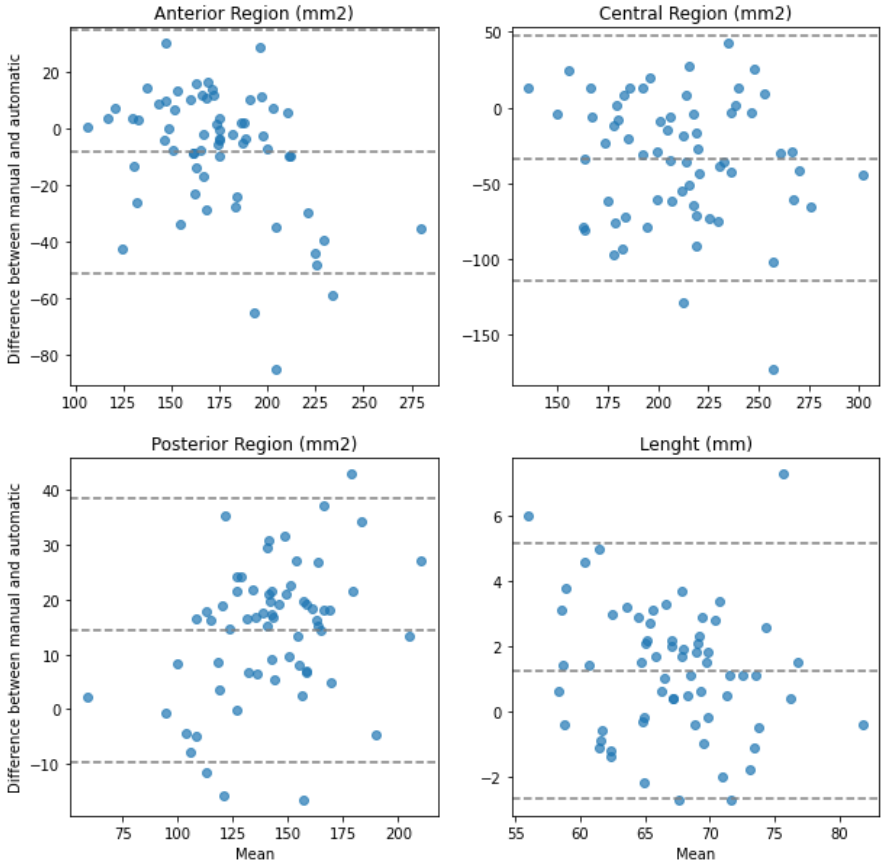

Figure 4: Bland–Altman plot of the corpus callosum measurements. Horizontal lines represent the average difference and the 95% limits of agreement (i.e. average difference ± 1.96 standard deviation of the difference).

3.2. Qualitative analysis

Figure 5 illustrates the automatic parcellation of the CC in three patients. We can observe an accurate segmentation in patients A and B. In contrast, in patient C, there is prominent thinning of the CC producing an extreme variability from the healthy anatomy and consequently, an inaccurate quantification (see red circle in Figure 5).

4. Discussion and conclusions

In this paper, we presented a preliminary evaluation of the proposed automatic method. Results seem to be in line compared with other proposed methods, although direct comparison is not possible as no other work computes the same region of interest.

Measurements of the anterior area and length of the CC have a good ICC while relatively low absolute error compared to manual measurement of an expert child neurologist. In the posterior region, the ICC is high although the poor level of reliability of 95% confident interval should be

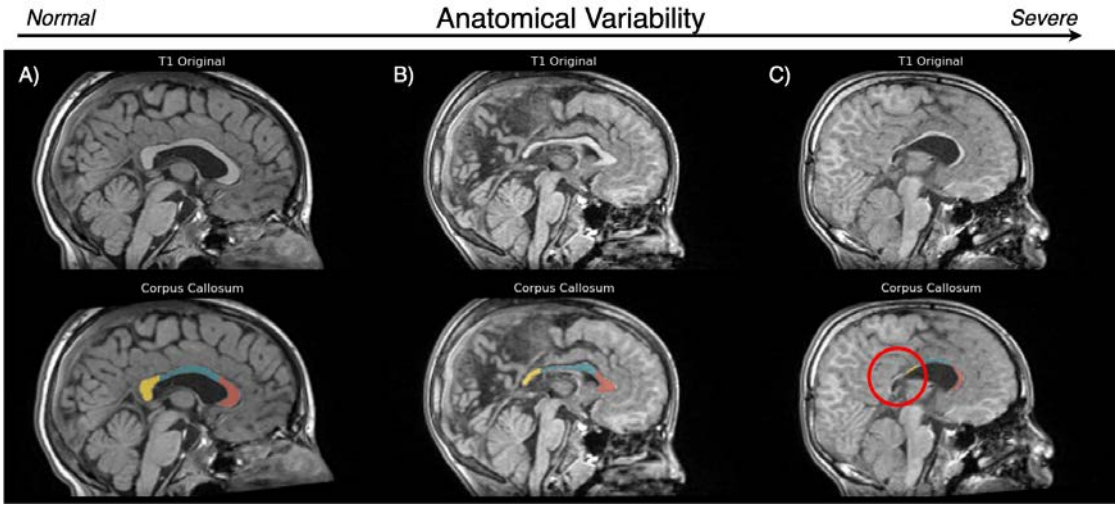

Figure 5: Illustration of the corpus callosum parcellation for several anatomical variabilities.

further studied. These promising results allow a quantitative and objective future investigation of the relationship between the anatomy of the CC and white matter injury related to preterm birth.

In contrast, the automatic measurement of the area of the central region of the CC shows a high error with respect to the manual measurement. This overestimation of the area is consequence of the over-segmentation of the CC including the fornix in this central region. Segmentation of CC without including the fornix is a complex task as both structures are similar and proximal [10].

We have been able to show that the methodology has the potential to properly handle the main challenges in pediatric quantification of the CC (e.g. intensity heterogeneity, minor image artifact). However, in some cases where there is extremely variable anatomy (i.e. prominent thinning of the CC) the algorithm under-segments this structure, proving an even lower volume quantification. Nevertheless, this low volume quantification also highlights the volume abnormality.

The methodology will be further improved in order to face the mentioned challenges. The pediatric icobrain block could be updated with a more advance supervised learning methodology (i.e. deep convolutional neural networks) which will allow to remove consistent errors, such as the over-segmentation of the fornix or under-segmentation in cases with extremely variable anatomy, by adding new training cases [16]. Moreover, the current turn-around-time of 30 minutes could be potentially improved by removing the computationally expensive registrations. In addition, the performance of the model could be further validated in a multi-center study and the reliability could be assessed in a test-retest study. After these improvements and additional validations, we will investigate the relationship of the CC measurement with the clinical outcome and WM volume.

Acknowledgments

The PARENT project has received funding from the European Union's Horizon 2020 research and innovation program under the Marie Sklodowska-Curie Innovative Training Network 2020. Grant Agreement N 956394.

References

[1] J. J. Volpe, H. C. Kinney, F. E. Jensen, P. A. Rosenberg, The developing oligodendrocyte: key cellular target in brain injury in the premature infant, International Journal of Developmental Neuroscience 29 (2011) 423–440.

[2] M. Guillot, S. P. Miller, The dimensions of white matter injury in preterm neonates, in: Seminars in Perinatology, volume 45, Elsevier, 2021, p. 151469.

[3] J. J. Volpe, Cerebral white matter injury of the premature infant-more common than you think, Pediatrics 112 (2003) 176–176.

[4] H.-J. Park, J. J. Kim, S.-K. Lee, J. H. Seok, J. Chun, D. I. Kim, J. D. Lee, Corpus callosal connection mapping using cortical gray matter parcellation and dt-mri, Human brain mapping 29 (2008) 503–516.

[5] H. Kidokoro, J. J. Neil, T. E. Inder, New mr imaging assessment tool to define brain abnormalities in very preterm infants at term, American Journal of Neuroradiology 34 (2013) 2208–2214.

[6] S. Fiori, A. Guzzetta, K. Pannek, R. S. Ware, G. Rossi, K. Klingels, H. Feys, A. Coulthard, G. Cioni, S. Rose, et al., Validity of semi-quantitative scale for brain mri in unilateral cerebral palsy due to periventricular white matter lesions: Relationship with hand sensorimotor function and structural connectivity, NeuroImage: Clinical 8 (2015) 104–109.

[7] A. Panigrahy, P. D. Barnes, R. L. Robertson, L. A. Sleeper, J. W. Sayre, Quantitative analysis of the corpus callosum in children with cerebral palsy and developmental delay: correlation with cerebral white matter volume, Pediatric radiology 35 (2005) 1199–1207.

[8] I. S. Gousias, A. D. Edwards, M. A. Rutherford, S. J. Counsell, J. V. Hajnal, D. Rueckert, A. Hammers, Magnetic resonance imaging of the newborn brain: manual segmentation of labelled atlases in term-born and preterm infants, Neuroimage 62 (2012) 1499–1509.

[9] J. Piven, J. Bailey, B. J. Ranson, S. Arndt, An mri study of the corpus callosum in autism, American Journal of Psychiatry 154 (1997) 1051–1056.

[10] G. Cover, W. G. Herrera, M. P. Bento, S. Appenzeller, L. Rittner, Computational methods for corpus callosum segmentation on mri: A systematic literature review, Computer methods and programs in biomedicine 154 (2018) 25–35.

[11] C. Vachet, B. Yvernault, K. Bhatt, R. G. Smith, G. Gerig, H. C. Hazlett, M. Styner, Automatic corpus callosum segmentation using a deformable active fourier contour model, in: Medical Imaging 2012: Biomedical Applications in Molecular, Structural, and Functional Imaging, volume 8317, SPIE, 2012, pp. 79–85.

[12] H. Struyfs, D. M. Sima, M. Wittens, A. Ribbens, N. P. de Barros, T. Vân Phan, M. I. F. Meyer, L. Claes, E. Niemantsverdriet, S. Engelborghs, et al., Automated mri volumetry as a

diagnostic tool for alzheimer's disease: Validation of icobrain dm, NeuroImage: Clinical 26 (2020) 102243.
[13] T. Vân Phan, D. M. Sima, C. Beelen, J. Vanderauwera, D. Smeets, M. Vandermosten, Evaluation of methods for volumetric analysis of pediatric brain data: the childmetrix pipeline versus adult-based approaches, NeuroImage: Clinical 19 (2018) 734–744.
[14] T. Vân Phan, D. Sima, D. Smeets, P. Ghesquière, J. Wouters, M. Vandermosten, Structural brain dynamics across reading development: A longitudinal mri study from kindergarten to grade 5, Human Brain Mapping 42 (2021) 4497–4509.
[15] T. K. Koo, M. Y. Li, A guideline of selecting and reporting intraclass correlation coefficients for reliability research, Journal of chiropractic medicine 15 (2016) 155–163.
[16] L. Henschel, S. Conjeti, S. Estrada, K. Diers, B. Fischl, M. Reuter, Fastsurfer-a fast and accurate deep learning based neuroimaging pipeline, NeuroImage 219 (2020) 117012.

Eye-tracking test battery for detecting cognitive impairments in premature children

Andrea De Gobbis[1,*], Marta Malavolta[2], Emiliano Trimarco[3], Isabel Benavente-Fernández[3,4,5], Simón Pedro Lubián-López[3,4], Aleksander Sadikov[1,2] and Vida Groznik[1,2,6]

[1]NEUS Diagnostics d.o.o., Ljubljana, Slovenia
[2]University of Ljubljana, Faculty of Computer and Information Science, Ljubljana, Slovenia
[3]Biomedical Research and Innovation Institute of Cádiz (INiBICA) Research Unit, Puerta del Mar University, Cádiz, Spain
[4]Division of Neonatology, Department of Paediatrics, Puerta del Mar University Hospital, Cádiz, Spain
[5]Area of Paediatrics, Department of Child and Mother Health and Radiology, Medical School, University of Cádiz, Cádiz, Spain
[6]University of Primorska, Faculty of Mathematics, Natural Sciences and Information Technologies, Koper, Slovenia

Abstract

Premature birth exponentially increases the risk for impaired neurological outcomes later in life, and early diagnosis is critical to optimise therapeutic options. There is evidence that oculomotor movements can be used as biomarkers for cognitive impairment (CI) in adults and young children. The aim of this study is to develop a prototype of a test battery using screen-based eye-tracking for detecting early signs of CI in preterm children and monitoring their neurological development. The study will also delve into identifying potential biomarkers of cognitive functions based on oculomotor movements found in medical literature, and provide methods to design explainable features and models. Finally, we summarise the most common experimental design practices, and propose an eye-tracking test battery that, by combining different stimuli, could be able to measure CI in different cognitive domains.

Keywords

Eye-tracking, premature children, neurodevelopment impairment

CEUR-WS.org/Vol-3363/paper03.pdf

1. Introduction

An estimated 15 million births in the world every year are preterm, amounting to 9.4% of all live births [1]. Prematurity leads to an increased risk of altered neurodevelopmental outcomes in childhood and adolescence (such as Autism Spectrum Disorder [2], altered brain development [3], or cognitive and motor delays [4]), with many survivor children facing a lifetime of disability [5]. Despite that advances in neonatal care have greatly improved survival of preterm born

DETERMINED 2022: Neurodevelopmental Impairments in Preterm Children — Computational Advancements, August 26, 2022, Ljubljana, Slovenia
*Corresponding author.
andrea.dg@neus-diagnostics.com (A. De Gobbis); marta.malavolta@fri.uni-lj.si (M. Malavolta); emiliano.trimarco@inibica.es (E. Trimarco); isabel.benavente@uca.es (I. Benavente-Fernández); simonp.lubian.sspa@juntadeandalucia.es (S. P. Lubián-López); aleksander.sadikov@fri.uni-lj.si (A. Sadikov); vida@neus-diagnostics.com (V. Groznik)
0000-0002-3993-5116 (A. De Gobbis); 0000-0002-7462-0822 (M. Malavolta)
© 2022 Copyright for this paper by its authors. Use permitted under Creative Commons License Attribution 4.0 International (CC BY 4.0).
CEUR Workshop Proceedings (CEUR-WS.org)

infants even at an extremely low gestational age, long-term neurodevelopmental outcomes have not improved significantly. For this reason, early diagnosis is an important strategy that could lead to a quick treatment and a wider array of therapeutic options.

There is evidence that oculomotor movements during specific tasks, such as smooth pursuit [6, 7], reading [8] and dot counting [9] are biomarkers for impaired cognitive processes in adults (e.g. linked to Alzheimer or Parkinson's disease). In the case of children, eye-tracking has been used to measure sensory [10], cognitive [11] and social [12] functions. Thus, a combined eye-tracking test battery able to summarise the state of the patient's cognitive development appears feasible; and it would help identifying early signs of altered brain maturation and detect a wider spectrum of symptoms.

The objective of this work is to summarise the current standard practices in test design and data analysis, and to provide the reader with a handbook of eye-tracking-based diagnostics. Moreover, we propose a novel testing paradigm that, by combining existing methodologies, allows to monitor the neurodevelopment of young children. In the Sections 2-3 we describe the state of the art in using a screen-based eye-tracking with children, highlighting the most common issues and challenges of creating a test battery for very young patients. We will also present existing eye-tracking test batteries based on machine learning [8, 13] used as part of a clinical decision support system. In Section 4 we present a prototype of our combined test battery for children (as young as 3 months corrected age) and briefly describe how data may be parsed.

2. Related Work

The non-invasiveness of eye-tracking methods has made them a particularly appealing approach with younger patients and has inspired a variety of works in the last two decades [14]. In Section 3, we build upon the previous work by Venker *et al.* [15], which presents an overview of using eye-tracking with children afflicted by Autism Spectrum Disorders, and Gredeback *et al.* [7] which summarises how eye-tracking can be used to monitor neurodevelopment in children. We review the state-of-the-art in diagnosing with oculomotor movements and highlight the challenges of testing younger patients with eye-tracking.

Different test procedures have been used with children to measure cognitive functions such as ability to smooth pursuit [10], attention [11], spatial inhibition [16], memory [17], and social orienting [12], these works offer adaptations of existing cognitive tests to the eye-tracking paradigm. An alternative approach is proposed by Oakes [18], who advises against using the device to adapt tests that could be conducted by medical professionals and instead suggests a more exploratory approach of gaze trajectories during everyday activities. Data disruption is investigated by Wass *et al.* [19], where they describe how age can impact the quality of eye-tracking data and design some strategies to preprocess raw data. Other factors that have been found to influence data quality are eye colour [20] and head positioning [21]. Moreover, as reported in previous studies [15, 10], standard calibration procedures can prove difficult with younger patients.

Test batteries using oculomotor movements as a biomarker to detect cognitive impairment have been employed with ageing patients for an early diagnosis of dementia [22, 13, 8]. With a

similar approach, Kaul *et al.* relate eye movements during smooth pursuit to neuropsychological tests taken at 6.5 years. These methodologies, once properly adapted by age group, provide a blueprint for our combined test battery.

3. Eye-tracking tests overview

From a physiological point of view, there are three main types of eye movements: *saccades* are very rapid movements that align a stimulus to the area of highest acuity (fovea), a *fixation* is defined as the moment where gaze position is fixed on the image, usually between two saccades. Finally, *smooth pursuit* is the type of movement where eyes remain fixed on a moving object without saccadic activity and thus the gaze position changes slowly. Smooth pursuit develops early in life [10] and it is a biomarker of cognitive functions [6, 23].

There are two main types of eye-tracking devices used in infancy research: head-mounted and screen-based [24]. In the former case, the device is fitted on a helmet and can be carried as the patient moves in an environment; in the latter case, the eye-tracker is fixed under a screen where the stimuli are presented. In both setups the gaze is recorded by capturing the cornea reflection of a small infrared light with a camera and reconstructing the person's point of view. Since we aim at creating a test battery that can be applied to patients as young as 3 months old and a head mounted tracker could prove uncomfortable for infants, in this work we focus our attention on the screen-based eye-tracker. This choice allows us to create different types of tests for the same instrument and monitor patients during early development. Nonetheless, both methods present advantages and disadvantages in a clinical setting and for an overview we refer to [24].

In the next section we compare the setup and of medical studies using eye-tracking in children, especially if preterm, describe tests batteries based on eye-tracking, and present how the data can be parsed and analysed.

3.1. Patient setup and calibration procedure

During testing, the patient is seated comfortably in front of the screen from a distance that varies from 60 cm [17, 25, 16] to around 120 cm [26, 10, 27, 11, 28], younger patients can be positioned in either a baby seat by themselves [26, 16] or in their caretaker's lap [10, 11]. Ben Itzhak *et al.* [29] compile a set of good practices to follow when setting up the environment (e.g. having natural light coming from the side). The authors warn about having the caretaker behind the patient, which is a very common practice, since the eye-tracking device could erroneously detect their gaze, and suggest to employ sunglasses to solve this problem. Another difference that can influence analysis [19] is the sampling rate of the eye-tracker, which can reach the 300 Hz [26, 17] in a hospital setting but for a widespread application the commercially available 60 Hz sampling device is more affordable due to cost.

Calibration is an essential first step when using an eye-tracker. The participant needs to look at different points spanning the entire screen, this allows the device to adapt to the patient and map camera signals to gaze positions. For adults and older children ($\geq$ 6 years) the procedure poses no issue, the patient can simply be instructed to look at the dots. Thus, a higher (5 to 8) number of dots is used to ensure high precision in the measurements during testing, the

sufficient number of dots is suggested by the device's manufacturer. In case of younger patients, calibration becomes challenging since the participant cannot be instructed and might not pay attention to the screen. The common solution employed [19, 10] is using a lower number of points (2 to 4), substituting dots with attractive stimuli such as smiling faces and coloured balls, and animating the stimuli and playing a rhythmic sound.

3.2. Type of stimuli and analysis

We divide the stimuli in three macro categories depending on the type of eye-movements the test should elicit:

1. *Smooth pursuit tasks* present an object (usually a dot but sometimes a smile for younger patients [10]) moving in a periodic pattern, usually a sinus wave [10, 22, 9] but some works use in addition triangular waves [26, 6, 23]. The stimulus can move either in one dimension along the horizontal or vertical direction [26, 6, 9, 22, 23] or in a circular pattern to test both directions simultaneously [10]. One approach is to study smooth pursuit from an input/output dynamical system prospective, with the moving stimulus as input term and the gaze position as output [23, 10]. Features encoded within this paradigm are inspired by dynamical systems and time series analysis (e.g. gain ratio, phase shift, cross-correlation, and mean squared error between input and output). It is detected that with high frequency stimuli often the patient starts compensating with anticipatory saccades [9, 10, 23], in this case it is possible to separate the saccadic and smooth pursuit contributions and analyse them separately.
2. *Fixation and saccade tasks* measure how quickly (time to first fixation) and how long (looking time) the patient fixates on a new stimulus. This paradigm covers a wide variety of approaches aimed at monitoring different cognitive functions, depending on the type and timing of the stimuli. Attention tests measure reaction time to a stimulus given different cues [11, 28, 25]. Memory capabilities are measured by presenting a pattern, letting the patient get acclimatised to it, displaying the same image with some differences and measuring the looking time to the novel stimuli [16, 17]. Social interaction is tested by presenting images containing or not human presence and measuring the difference in looking pattern [30, 12, 31]. The study by Oyama *et al.* [13] proposes an example of a test battery consisting exclusively of fixation tasks, displaying the versatility of this type of tasks.
3. *General tasks* that mimic everyday activities instead of adapting existing neuropsychological tests, and as such can elicit saccades, fixations and smooth pursuit. In contrast with the other categories, in this case the objective is data exploration and the challenge is feature design, since there is no well-defined cognitive ability under scrutiny. The approach then consists in finding differences in gaze behaviours during complex activities, and the challenge lies in designing suitable features and parsing methods without specific domain knowledge. An example is given by paper [8], where the authors show that there is a significant difference in reading behaviour between healthy and cognitively impaired individuals when measuring reading time and the distribution of forward (right) and backward (left) saccades.

4. Combined test battery

Combining the works presented in Section 3 and building up from existing test batteries to diagnose cognitive impairment in adults [8, 9], we present a first prototype of test battery designed to identify and monitor cognitive impairment due to premature birth. The test is appropriate for 4 months old participants and as such it contains no complex tasks and no instructions.

The present study was conducted on 23 babies (10 females and 13 males, 15 term babies ranging from 3 to 24 months of age, and 8 preterm babies ranging from 3 to 20 months of corrected age) at the Hospital Universitario Puerta del Mar, Cadiz (ethical committee code PIEBA 0672-N-22, register number 44.22). The babies' caretakers voluntarily accepted to participate in the pilot study after routine visits at the hospital. The aim of this pilot study is designing a first version of a test battery to study the feasibility of employing eye-tracking to find statistically significant differences in gaze behaviour of premature children. In particular, we investigate if the tasks can be presented in a single session and how long we could feasibly keep the participant's attention. The considerations in the current paper are mostly qualitative, and data analysis is left for future work. The setup is inspired by previous works in the field described in Section 3: the procedure is conducted in a small room lighted from the side, the patient is seated on their caretaker's lap at 60 cm from a 24 inches computer screen. A simple seven points calibration procedure using a sequence of white crosses as fixation stimuli proved to work correctly for the majority of the patients, as such we do not employ different stimuli for the calibration process in this test. All tests were conducted using a Tobii 4C Eye-Tracker working at 90 Hz.

The test battery is designed to measure responses across a wide variety of cognitive functions while at the same time being short enough that an average young child will not become fussy before the end. The test battery is comprised of the following tasks, which are presented on a black background to offer the maximal contrast with the stimuli, and are interspersed with a smile appearing at the centre of the screen to attract the patient's attention:

- *Sensation task*: a smooth pursuit task with a sinusoidal $\sim$0.4 Hz one dimensional wave and a smiling face as stimulus. The original study [10] reports that 5 months old children are able to follow a smiling face in a circular movement and the optimal frequency to minimise missing data is between 0.1 and 0.4 Hz. The movement is exclusively horizontal since it develops earlier than vertical smooth pursuit [6, 9]. The stimulus remains on the screen for a total of 8 s. Figure 1a shows an explicative diagram of the task.
- *Attention task*: this task takes inspiration from similar existing methodologies [11, 28] to measure the response of the patient given a cue. First a smile appears in the centre to induce a fixation, then an auditory aid accompanies a visual cue to one side of the screen along the horizontal axis followed by an attractive target (the colourful image of an animal). The cue can appear in the same position of the target (*valid anticipation*), in the opposite side (*invalid anticipation*), in both sides (*double*) or not appear at all (*baseline*). If the child inhibits correctly then we expect the *valid* modality to show faster reactions time compared to *baseline*, while the *invalid* modality should be slower than both. A summarising picture can be found in Figure 1b. The smile appears for 1.5 s followed by the cue that lasts 100 ms, then after a 100 ms delay the target appears and remains on the screen for 1 s.

- *Memory task*: a task inspired by [17] that checks the predisposition of children to fixate on novel stimuli. Two pictures are shown to the patient for 1 s, followed by a blank screen lasting 500 ms, then the pictures are presented again with one of them substituted with a new image and remain on the screen for 3 s. We use three types of differences to measure what the child is able to identify: colour, shape, and faces. The face pictures are taken from the London Set Dataset [32]. A summarising picture can be found in Figure 1c.
- *Social orienting task*: the aim of this task is measuring if the children displays social responses to human stimuli, and is inspired by the previous similar studies [12, 31]. The patient is presented with two pictures for 5 s, one containing a human face and the other containing the front of a house, and the looking time to the former is measured. The face pictures are taken from the London Set Dataset [32] and the house pictures are taken from the DalHouses Dataset [33]. An example of how the task appears to the participant can be found in Figure 1d.
- *Face exploration task*: in this task the patient is presented with the image of a human face with a neutral expression viewed from the front and taken from the London Set Dataset [32] (see Figure 1e for an example). Telford *et al.* [12] showed how the gaze trajectories while observing a human face, and in particular the difference of looking time with respect to the eyes and the mouth could be influenced by premature birth. In total the face remains on the screen for 10 s.

Table 1
Order and duration of each task composing the test battery. The block described in the table is repeated four times, for a total duration of 223.2 s.

Task	Task duration	Cumulative duration
Smile	1.5 s	1.5 s
Sensation	7.5 s	9 s
Attention	2.7 s	11.7 s
Attention	2.7 s	14.4 s
Attention	2.7 s	17.1 s
Attention	2.7 s	19.8 s
Smile	1.5 s	21.3 s s
Memory (colour)	4.5 s	25.8 s
Smile	1.5 s	27.3 s s
Memory (shape)	4.5 s	31.8 s
Smile	1.5 s	33.3 s s
Memory (face)	4.5 s	37.8 s
Smile	1.5 s	39.3 s
Social orienting	5.0 s	44.3 s
Smile	1.5 s	45.8 s
Social orienting	10.0 s	55.8 s

Each task is repeated four times and the test battery lasts approximately 223 s, which during the pilot study appeared to be a time frame where we can expect the the children to be able to maintain their attention. The timings of the singular tasks were kept as specified in the studies that inspired them. Gaze trajectories acquired during the test battery are parsed and a first set

of features can be computed following the original works that inspired the different tasks, as found in Section 3.

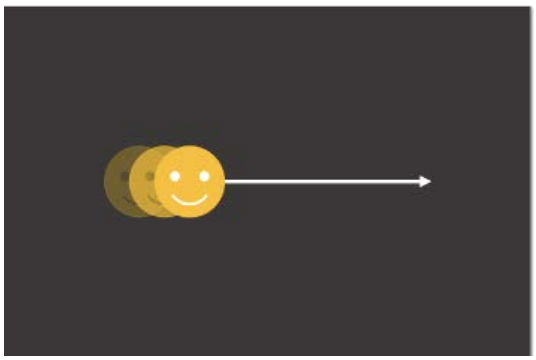

(a) The *sensation task* shows a smile moving horizontally in a sinusoidal pattern.

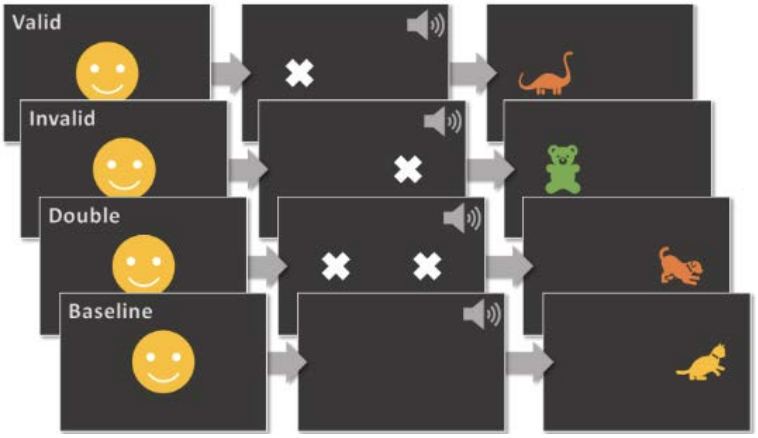

(b) The attention task. From top to bottom: *valid*, *invalid*, *double*, and *baseline*.

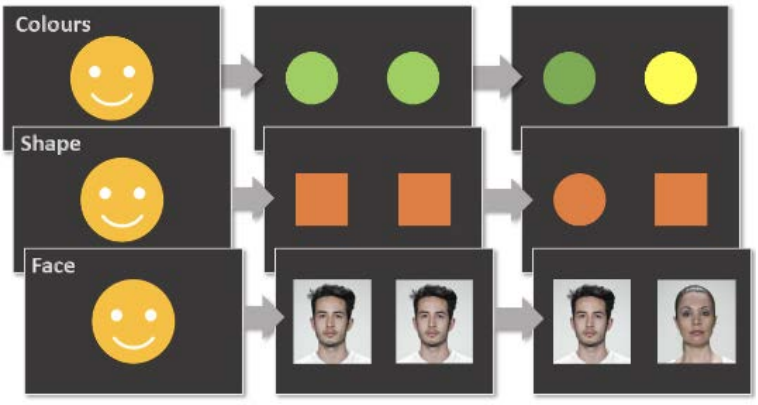

(c) The memory task. From top to bottom: *colour*, *shape*, and *face* differences.



(d) Pictures appearing on the screen during the *Social orienting task*.



(e) Picture appearing on the screen during the *Face exploration task*.

Figure 1: Example of how the tasks appear on the screen.

5. Conclusions

In this study, we have reviewed current medical literature on the topic of eye movements and in particular the recent advances in the application of eye-tracking to young children and infants. We supplied a general guideline on how similar tests have been conducted: how the calibration procedure should be modified to address the needs of younger patients, how to avoid fussiness in the participant through a correct experimental setup, and how to optimise the quality of acquired data. Then, we reported which stimuli can be employed to monitor neuropsychological development in children. Finally, we presented a prototype transversal test battery that, by combining and shortening existing experimental paradigms, might supply information on the state of different cognitive functions in developing children.

Future works will consist in analysing the eye-tracking data obtained with the test battery by defining features and comparing different classifiers. This analysis could lead to insights on how to design the tasks, and may result in an improved test battery. Evaluation will be conducted with different metrics (accuracy, Area under the Roc curve, explained variance etc.) and, by integrating modern machine learning methods, we aim at improving current state-of-the-art results. Moreover, we will judge our results by their clinical utility as per hospital requirements,

and compare evaluation metrics to similar studies on adults.

Acknowledgments

The authors would like to thank all the parents and the children for their participation in the pilot study. This research was partly founded by H20202 MSCA-ITN project PARENT, Grant Agreement N° 956394.

References

[1] World Health Organization, Born too soon: the global action report on preterm birth (2012).

[2] A. Leavey, L. Zwaigenbaum, K. Heavner, I. Burstyn, Gestational age at birth and risk of autism spectrum disorders in Alberta, Canada, J Pediatr 162 (2013) 361–368.

[3] G. Ball, J. P. Boardman, D. Rueckert, P. Aljabar, T. Arichi, N. Merchant, I. S. Gousias, A. D. Edwards, S. J. Counsell, The effect of preterm birth on thalamic and cortical development, Cereb Cortex 22 (2012) 1016–1024.

[4] A. Pascal, P. Govaert, A. Oostra, G. Naulaers, E. Ortibus, C. Van den Broeck, Neurodevelopmental outcome in very preterm and very-low-birthweight infants born over the past decade: a meta-analytic review, Dev Med Child Neurol 60 (2018) 342–355.

[5] M. Delobel-Ayoub, C. Arnaud, M. White-Koning, C. Casper, V. Pierrat, M. Garel, A. Burguet, J. C. Roze, J. Matis, J. C. Picaud, M. Kaminski, B. Larroque, B. Larroque, P. Y. Ancel, B. Blondel, G. Bréart, M. Dehan, M. Garel, M. Kaminski, F. Maillard, C. du Mazaubrun, P. Missy, F. Sehili, K. Supernant, L. Marchand, M. Durant, J. Matis, J. Messer, A. Treisser, A. Burguet, L. Abraham-Lerat, A. Menget, P. Roth, J. P. Schaal, G. Thiriez, C. Lévêque, S. Marret, L. Marpeau, P. Boulot, J. C. Picaud, A. M. Donadio, B. Ledésert, M. André, J. Fresson, J. M. Hascoët, C. Arnaud, S. Bourdet-Loubère, H. Grandjean, M. Rolland, C. Leignel, P. Lequien, V. Pierrat, F. Puech, D. Subtil, P. Truffert, G. Boog, V. Rouger-Bureau, J. C. Rozé, P. Y. Ancel, G. Bréart, M. Kaminski, C. du Mazaubrun, M. Dehan, V. Zupan-Simunek, M. Vodovar, M. Voyer, Behavioral problems and cognitive performance at 5 years of age after very preterm birth: the EPIPAGE Study, Pediatrics 123 (2009) 1485–1492.

[6] G. R. Barnes, Cognitive processes involved in smooth pursuit eye movements, Brain Cogn 68 (2008) 309–326.

[7] G. Gredeb ack, S. Johnson, C. von Hofsten, Eye tracking in infancy research, Dev Neuropsychol 35 (2010) 1–19.

[8] V. Groznik, M. Možina, T. Lazar, D. Georgiev, A. Sadikov, Gaze behaviour during reading as a predictor of mild cognitive impairment, in: 2021 IEEE EMBS International Conference on Biomedical and Health Informatics (BHI), 2021, pp. 1–4. doi:10.1109/BHI50953.2021.9508586.

[9] A. Gerbasi, V. Groznik, D. Georgiev, L. Sacchi, A. Sadikov, Detecting mild cognitive impairment using smooth pursuit and a modified Corsi task, in: A. Tucker, P. Henriques Abreu, J. Cardoso, P. Pereira Rodrigues, D. Riaño (Eds.), Artificial Intelligence in Medicine, Springer International Publishing, Cham, 2021, pp. 168–172.

[10] G. Gredebäck, C. von Hofsten, J. Karlsson, K. Aus, The development of two-dimensional tracking: a longitudinal study of circular pursuit, Exp Brain Res 163 (2005) 204–213.
[11] S. Ross-Sheehy, S. Schneegans, J. P. Spencer, The infant orienting with attention task: Assessing the neural basis of spatial attention in infancy, Infancy : the official journal of the International Society on Infant Studies 20 (2015) 467–506. doi:10.1111/infa.12087.
[12] E. J. Telford, S. Fletcher-Watson, K. Gillespie-Smith, R. Pataky, S. Sparrow, I. C. Murray, A. O'Hare, J. P. Boardman, Preterm birth is associated with atypical social orienting in infancy detected using eye tracking, J Child Psychol Psychiatry 57 (2016) 861–868.
[13] A. Oyama, S. Takeda, Y. Ito, T. Nakajima, Y. Takami, Y. Takeya, K. Yamamoto, K. Sugimoto, H. Shimizu, M. Shimamura, T. Katayama, H. Rakugi, R. Morishita, Novel method for rapid assessment of cognitive impairment using high-performance eye-tracking technology, Scientific Reports 9 (2019) 12932. doi:10.1038/s41598-019-49275-x.
[14] J. P. Boardman, S. Fletcher-Watson, What can eye-tracking tell us?, Archives of Disease in Childhood 102 (2017) 301–302. doi:10.1136/archdischild-2016-311693.
[15] C. E. Venker, S. T. Kover, An Open Conversation on Using Eye-Gaze Methods in Studies of Neurodevelopmental Disorders, J Speech Lang Hear Res 58 (2015) 1719–1732.
[16] M. Downes, D. Kelly, K. Day, N. Marlow, M. de Haan, Visual attention control differences in 12-month-old preterm infants, Infant Behav Dev 50 (2018) 180–188.
[17] S. Ross-Sheehy, B. Eschman, Assessing visual stm in infants and adults: eye movements and pupil dynamics reflect memory maintenance, Visual Cognition 27 (2019) 78–92. doi:10.1080/13506285.2019.1600089.
[18] L. Oakes, Advances in eye tracking in infancy research, Infancy 17 (2012). doi:10.1111/j.1532-7078.2011.00101.x.
[19] S. V. Wass, L. Forssman, J. Leppänen, Robustness and precision: How data quality may influence key dependent variables in infant eye-tracker analyses, Infancy 19 (2014) 427–460. doi:https://doi.org/10.1111/infa.12055.
[20] R. Hessels, R. Andersson, I. Hooge, M. Nyström, C. Kemner, Consequences of eye color, positioning, and head movement for eye-tracking data quality in infant research, Infancy 20 (2015). doi:10.1111/infa.12093.
[21] D. C. Niehorster, T. H. W. Cornelissen, K. Holmqvist, I. T. C. Hooge, R. S. Hessels, What to expect from your remote eye-tracker when participants are unrestrained, Behav Res Methods 50 (2018) 213–227.
[22] R. J. Molitor, P. C. Ko, B. A. Ally, Eye movements in Alzheimer's disease, Journal of Alzheimer's disease : JAD 44 (2015) 1–12. URL: https://pubmed.ncbi.nlm.nih.gov/25182738. doi:10.3233/JAD-141173.
[23] K. Fukushima, J. Fukushima, T. Warabi, G. R. Barnes, Cognitive processes involved in smooth pursuit eye movements: behavioral evidence, neural substrate and clinical correlation, Frontiers in systems neuroscience 7 (2013) 4–4. URL: https://pubmed.ncbi.nlm.nih.gov/23515488. doi:10.3389/fnsys.2013.00004.
[24] D. Corbetta, Y. Guan, J. L. Williams, Infant Eye-tracking in the Context of Goal-Directed Actions, Infancy 17 (2012) 102–125.
[25] S. Ross-Sheehy, E. Reynolds, B. Eschman, Evidence for attentional phenotypes in infancy and their role in visual cognitive performance, Brain Sciences 10 (2020). doi:10.3390/brainsci10090605.

[26] Y. F. Kaul, K. Rosander, C. von Hofsten, K. Strand Brodd, G. Holmström, L. Hellström-Westas, Visual tracking at 4 months in preterm infants predicts 6.5-year cognition and attention, Pediatric Research (2021). doi:10.1038/s41390-021-01895-8.

[27] D. Amso, S. P. Johnson, Learning by selection: visual search and object perception in young infants, Dev Psychol 42 (2006) 1236–1245.

[28] S. Ross-Sheehy, S. Perone, K. L. Macek, B. Eschman, Visual orienting and attention deficits in 5- and 10-month-old preterm infants, Infant Behavior and Development 46 (2017) 80–90. doi:10.1016/j.infbeh.2016.12.004.

[29] N. Ben Itzhak, M. Kooiker, J. van der Steen, J. Pel, J. Wagemans, E. Ortibus, The relation between visual orienting functions, daily visual behaviour and visuoperceptual performance in children with (suspected) cerebral visual impairment, Research in Developmental Disabilities 119 (2021) 104092. doi:https://doi.org/10.1016/j.ridd.2021.104092.

[30] T. Falck-Ytter, G. Gredebäck, C. von Hofsten, Infants predict other people's action goals, Nature Neuroscience 9 (2006) 878–879. URL: https://doi.org/10.1038/nn1729. doi:10.1038/nn1729.

[31] B. Dean, L. Ginnell, V. Ledsham, A. Tsanas, E. Telford, S. Sparrow, S. Fletcher-Watson, J. P. Boardman, Eye-tracking for longitudinal assessment of social cognition in children born preterm, J Child Psychol Psychiatry 62 (2021) 470–480.

[32] L. DeBruine, B. Jones, Face Research Lab London Set (2017). doi:10.6084/m9.figshare.5047666.v5.

[33] J. H. Filliter, J. M. Glover, P. A. McMullen, J. P. Salmon, S. A. Johnson, The DalHouses: 100 new photographs of houses with ratings of typicality, familiarity, and degree of similarity to faces, Behavior Research Methods 48 (2016) 178–183. doi:10.3758/s13428-015-0561-8.

Eye-tracking test battery for newborns: A pilot feasibility study

Marta Malavolta[1,*], Andrea De Gobbis[2], Emiliano Trimarco[3], Isabel Benavente-Fernández[3,4,5], Simón Pedro Lubián-López[3,4], Vida Groznik[1,2,6] and Aleksander Sadikov[1,2]

[1]University of Ljubljana, Faculty of Computer and Information Science, Ljubljana, Slovenia
[2]NEUS Diagnostics, d.o.o., Ljubljana, Slovenia
[3]Biomedical Research and Innovation Institute of Cádiz (INiBICA) Research Unit, Puerta del Mar University, Cádiz, Spain
[4]Division of Neonatology, Department of Paediatrics, Puerta del Mar University Hospital, Cádiz, Spain
[5]Area of Paediatrics, Department of Child and Mother Health and Radiology, Medical School, University of Cádiz, Cádiz, Spain
[6]Faculty of Mathematics, Natural Sciences and Information Technologies, University of Primorska, Koper, Slovenia

Abstract

Preterm birth is one of the leading causes of neurodevelopmental disabilities. Many efforts have been made to improve the well-being and quality of life of preterm infants and their families, especially during the first months of life. Several authors investigated cognitive impairments in children, such as social disorders or attention deficit, using various remote eye-tracking techniques. However, this tool remains poorly used in newborn infants, particularly in the first three months old children. Therefore, we aim to create a neuropsychological test battery using screen-based eye-tracking that can also be used on the above-mentioned population.

The aim of this study is to analyse the feasibility of the created pilot eye-tracking test battery and the suitability of the different stimuli used. We also investigate how the current paradigm evolved based on observations made during data acquisition, and how it was modified to achieve an appropriate test in terms of composition and length to keep children's attention.

Keywords

Eye-tracking test battery, Cognitive Impairments, Feasibility Study, Premature Children

1. Introduction

Every year 15 million babies worldwide are born preterm, 7.1% of them with some degree of impairment. The World Health Organization (WHO) considers an infant as preterm if

DETERMINED 2022: Neurodevelopmental Impairments in Preterm Children — Computational Advancements, August 26, 2022, Ljubljana, Slovenia

*Corresponding author.
marta.malavolta@fri.uni-lj.si (M. Malavolta); andrea.dg@neus-diagnostics.com (A. De Gobbis); emiliano.trimarco@inibica.es (E. Trimarco); isabel.benavente@uca.es (I. Benavente-Fernández); simonp.lubian.sspa@juntadeandalucia.es (S. P. Lubián-López); vida@neus-diagnostics.com (V. Groznik); aleksander.sadikov@fri.uni-lj.si (A. Sadikov)
0000-0002-7462-0822 (M. Malavolta); 0000-0002-3993-5116 (A. De Gobbis); 0000-0001-9276-1912 (I. Benavente-Fernández); 0000-0001-8925-926X (V. Groznik); 0000-0001-8697-3556 (A. Sadikov)

© 2022 Copyright for this paper by its authors. Use permitted under Creative Commons License Attribution 4.0 International (CC BY 4.0).
CEUR Workshop Proceedings (CEUR-WS.org)

CEUR-WS.org/Vol-3363/paper04.pdf

birth occurs before the 37th week of gestational age (GA). Furthermore, the WHO provided a classification of preterm infants according to the gestational time window, thereby further dividing children into late and moderate preterm, very preterm and extremely preterm [1, 2]. As the time span of gestation decreases (lower GA), the risk of complications caused by preterm birth significantly increases. The primary causes of long-term disabilities, such as behavioural alterations or neurological disorders (e.g. cerebral palsy), are related to brain injury occurring in the neonatal period in the case of premature births [3]. Furthermore, the burden of preterm birth extends beyond the well-being and overall health of the infants themselves as it also includes economic impact on the healthcare system, e.g. in the form of a longer stay in neonatal intensive care units (NICU) as well as an increased overall burden on the family [1, 2].

To date, a troubling dichotomy arises: despite the great improvement of the quality of prenatal care in recent years, which dramatically improved the survival of preterm babies, the diagnosis of motor and cognitive impairments has not progressed at the same pace, mostly relying on monitoring the clinical parameters. Indeed, clinicians need a more robust and timely set of biomarkers to assess the risk of disability of preterm infants to provide early intervention to reduce the developmental delays associated with this condition.

Many authors in the past decades relied on eye-tracking to investigate the possible connection between cognitive deficits and gaze behaviour in response to selected stimuli, both in adults and children. Indeed, eye-tracking has been employed in children to study social orientation [4], attention and memory [5, 6] or pursuit of moving objects [7]. In the specific context of the term- vs. preterm-born infants, Stand-Brodd et al. showed that premature children would appear to have delayed eye movements in following objects in comparison with term-born children of the same age [8]. Other works highlighted that the ability to visually follow a moving object at 4 months of age not only has a robust predictive power for neurodevelopment at 3 years in children born very preterm [9], but can also predict future memory and attention problems at 6 years of age [10]. Nevertheless, very few of these works are performed in the very first months after birth.

Whithin this framework of investigation, we created a neuropsychological test battery to study different types of cognitive processes in children born prematurely, using screen-based eye-tracking. The underlying goal is to give a quantitative and early prediction of possible future impairments. For the development of this prototype, we studied 23 children with an average age of 11 months (std 6 months), including eight babies born prematurely (8 months old, 6 months old CA). The purpose of this study is to analyse the evolution of the test battery and to pinpoint and implement any needed changes, to obtain a tool that can capture and hold the child's attention and at the same time ensure the correct gathering of sufficient data for analysis. Lastly, despite the young age of the studied population, we demonstrate the data acquisition feasibility of the proposed test battery by measuring missing values and attention for each child of the piloting cohort.

The article is organised as follows. First, we analyse the population studied during the implementation of the test battery. In the subsequent section, we introduce the neuropsychological test battery with a brief explanation and representation of the tasks. We explain in detail how we optimised the testing protocol, explaining the technical aspects in the fourth section. Finally, the last paragraph concludes the article.

2. Subjects

During the implementation of the neuropsychological test battery, we tested 23 subjects born at the Hospital Universitario Puerta del Mar, Cadiz (ethical committee code PIEBA 0672-N-22, register number 44.22), of whom 8 were premature. Table 1 summarises the subject data during the implementation of the neuropsychological test battery.

Table 1
Summary of the performed tests with the different setups, including information about the involved subjects. Total test times and inattention of the children during the test are also reported.

Prototype (test length)	*Setup*	*Sex*	*Preterm*	*Age [CA] (months)*	*Calibration*	*Test time (min)*	*Inattention time (min)*	*Missing values (%)*
#1 (10 min)	All-in-one room, 24-inch monitor	F	No	12	Completed	04:42	02:29	57%
	Partitioned room,	M	No	12	Completed	02:53	00:30	17%
	24-inch monitor,	F	No	6	Completed	02:32	00:29	20%
	Artificial light	M	Yes	5 [3]	Completed	03:10	00:57	27%
#2 (3 min)		M	No	9	Failed			
	Partitioned Room,	M	No	7	Completed	03:00	01:33	52%
	27-inch Monitor,	M	No	24	Completed	03:00	00:31	17%
	Artificial Light,	M	No	12	Completed	03:00	00:52	29%
	Covered Table	F	No	18	Failed			
		F	No	6	Completed	03:00	00:16	9%
	Partitioned Room,	M	No	9	Completed	03:00	01:21	45%
	24-inch Monitor,	F	No	18	Completed	03:00	00:23	13%
	Artificial Light,	M	Yes	15 [12]	Completed	02:17	00:45	35%
	Covered Lateral Table	F	Yes	8 [6]	Completed	03:00	00:16	9%
#3 (4 min)		M	Yes	23 [20]	Completed	04:00	00:48	20%
	Partitioned Room,	F	No	4	Completed	04:00	00:58	24%
	24-inch Monitor,	M	Yes	12 [10]	Completed	04:00	00:34	14%
	Artificial Light,	M	Yes	6 [5]	Completed	04:00	00:02	1%
	Covered Lateral Table	M	No	18	Completed	02:26	00:15	19%
		F	Yes	6 [3]	Completed	04:00	00:26	11%
	Partitioned Room,	M	No	15	Completed	04:00	01:00	25%
	18-inch Monitor,	F	Yes	6 [3]	Completed	*Test aborted due to child crying.*		
	Artificial Light,	F	No	3	Completed	04:00	02:02	51%
	Covered Lateral Table							

There were 10 females and 13 males, and their ages ranged from 3 to 24 months. The premature babies ranged from 3 months CA to 20 months CA. Only three of the children did not want to take the test (two of these completed the calibration). We also noticed that it is useful to help the children perform the instrument calibration. During the actual test, however, the children were mostly well-engaged. In fact, only in few cases the parents had to call the child's attention to the screen. The initial prototype was updated with minor changes as described later, mostly regarding test design and not task design. The first child differed the most from the other children in terms of the test setup. As a matter of fact, we noticed that there was a need for separation between the examination area, where the child was tested, and the examiners' space. In fact, the child was very distracted as witnessed by the percentage of missing values in Table 1. As can be seen from the table, some differences in the length of the test emerge between the prototypes. Specifically, with prototypes #1 and #2, where the tasks were consecutive, we could get a maximum of three minutes of testing. Instead, with the last prototype, where task repetitions were alternated, we were able to get up to four minutes of testing. The maximum

distraction was approximately 25 seconds which corresponds to the length of one task. In conclusion, we also noticed that although it is not evident from the data, from 15-18 months of age it was more challenging to keep the children's attention and therefore, there is likely a need to develop a different test for that age group (and older).

3. The neuropsychological test battery

The test is composed of four different types of tasks (smooth pursuit task, attention task, memory task and social orienting task), taken from the literature and adapted to test the children's cognitive development. Each task is consecutively repeated four times, obtaining the total test battery duration of four minutes. As described in the subsequent paragraph, the procedure proved able to engage the subjects for meaningful periods of time. The calibration process was also largely successful.

3.1. Smooth pursuit task

In the smooth pursuit task, the child has to follow with the gaze a smiling face moving horizontally with sinusoidal movements at a frequency of 0.4 Hz. This task is widely used for the detection of possible cognitive deficits in adults [11]. An illustration of the task is shown in Figure 1. The specific parameters which we plan to sample and analyse are related to how the child follows the moving smiling face: examples include e.g. the quantitative assessment of the anticipation of the movement of the dot, the delay in following the object and the latency in starting the smooth pursuit movement.

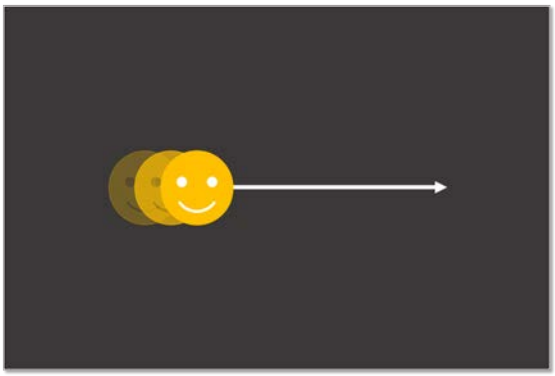

Figure 1: A graphical representation of the smooth pursuit task.

3.2. Attention task

The attention task was created to analyse the differences in the children's response to specific variations of the stimulus, inspired by the IOWA test [12, 13]. In detail, the test first presents a white cross for a fraction of a second (a visual cue) along with a warning sound to keep the child's attention. Subsequently, a black screen is shown briefly, followed by a target image

located either at the same location or at the opposite position of the initial white cross. In one version of the task, the white cross is shown on both sides of the screen. Furthermore, an additional baseline test instead consists of only the auditory stimulus prior to the appearance of the target, without the appearance of the cross. The task is visually summarised in Figure 2.

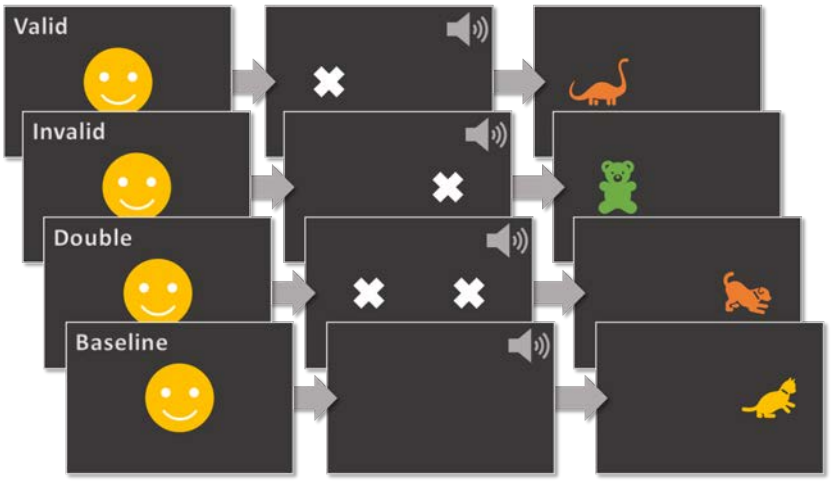

Figure 2: A schematic visualisation of the attention task.

3.3. Memory task

The memory task is inspired by [14] and it checks the predisposition of children to fixate on novel stimuli. Initially, two identical pictures are shown to the child. The screen is subsequently blanked, and then the pictures are presented again, with one of them substituted by a new, unseen image. This test is performed using three types of differences in image content to measure what the child is able to identify, namely differences in colour, shape, and faces. A summarising picture can be found in Figure 3.

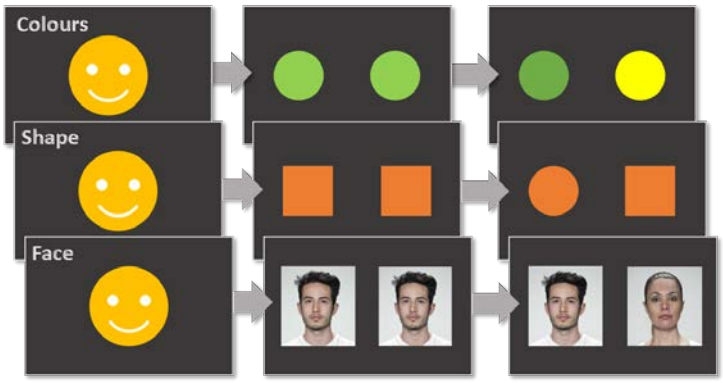

Figure 3: A schematic visualisation of the memory task. The face image dataset was taken from [15].

3.4. Social orienting task

The goal of the social orienting task is to measure if the children display responses to stimuli with social content, and it is inspired by the work of [4, 16]. The child is presented with two pictures, one depicting a person and the other depicting an inanimate object. The test measures the duration of the child's focus on the human picture. This task can be visualised in Figure 4.



Figure 4: An illustration of the social orienting task. The face image dataset was taken from [15] and the house image dataset was extracted from [17].

4. Optimisation of the testing protocol: operational and technical aspects

4.1. Duration of the testing procedure and repetitions

The first prototype we developed was composed of the four above-mentioned tasks with 10 repetitions per task, leading to a total test length of around 8 minutes. During the initial tests involving children under 12 months of age, we noticed how none of them successfully finished the test as they started to get fussy, or were otherwise easily distracted. This allowed us to estimate the maximum attention span of the tested children to at most 3 minutes. Hence, subsequent tests consisted of a reduced testing protocol with only three repetitions of each task. In most of the cases, the length of this updated test was adequate, but a few infants were still unable to finish the test as they were too active or too nervous. These aspects were hard to control in the experimental setting and, since the tasks were always administered in the same order, this lead to an imbalance in the collected data for different tasks. We thus decided to present the tasks in batches of one task of each type and we repeated the batches for three or four times depending on the prototype. This ensured the availability of experimental data for each individual task.

4.2. Child activity level and distracting elements

In the initial testing configuration, the child was seated on their parent's lap at a distance of 60 cm from the 24-inch computer screen. For collecting the data on the child's eye-movements, we

used a Tobii 4C eye-tracker (Tobii AB, Danderyd, Sweden) mounted to the computer screen. The test operators and the other parent were located behind the computer screen, inside the child's field of view. This condition led to the loss of concentration of the children as they were distracted by the people around the testing area. Thus, in the subsequent testing setup, we decided to use a white separator screen (a curtain as seen in Figure 5) to divide the testing area from the operator space. In this way, the children could not see the operators except for the parent who was holding them in their lap. We also decided to increase the room lighting after introducing the separator screen. Lastly, we covered the table in the testing area with a white blanket as the light in the room gave rise to the reflections on the table surface that distracted the child.

4.3. Technical aspects

We noticed that bigger screen sizes increased the occurrence of distractions in the children, especially in the case of the attention task. Therefore, we fixed the computer screen size to 18 inches. We also noticed that the calibration procedure initially did not catch the children's attention as the crosses on the screen were too small in size. Hence, we made the calibration more attractive in subsequent examinations by visualising larger crosses. Also, the presented stimuli during the tests were increased in size to better keep the attention of the children. Lastly, we noticed how the currently used testing protocol was only suitable for children of ages up to 15-18 months since older children are less compliant to the testing procedure and are more easily distracted (e.g. by wanting to touch the screen or wandering around the examination room). The operators repeatedly made this observation during the examinations.

4.4. Room setup

The room setup comprises two separate parts: an examination room and an operator space divided by a white separator screen. The child is inside the examination room and is seated at a distance of 60 cm from the computer screen on his parent's lap. All parents inside the examination room wear sunglasses so their gaze is not interfering with the test. The eye-tracker is held on a 24-inch monitor using magnets (not visible to the child). In this space, the child can only see the parent and not the operators, which stay behind the white separator screen. The lighting in the examination room is artificial and from the side, while there is no light in the operator space. There is a table inside the examination room to the left of the child reflecting the artificial light, and we covered it with a white blanket. The setup is shown in Figure 5.

5. Discussion and Conclusion

In this work, we briefly described our test battery exploiting screen-based eye-tracking for the early detection of neuropsychological impairments in preterm babies. We explained how the test battery evolved since the deployment of the first prototype giving the reasons behind the changes. During the development of the test battery, we managed to increase the attention span of the tested children to up to four minutes, with a progressive improvement in the amount of missing values. Also, based on our findings, the current version of the test battery allows for a



Figure 5: A representation of the final testing setup.

successful calibration of the test in more than 90% of the runs. Furthermore, we highlighted some of the shortcomings and crucial aspects which emerged during the study, such as the physical location of the examiners and operators in the room during the tests, or the need to switch between the different tasks to keep the children's concentration longer. We ultimately demonstrated the feasibility of the current test battery and how it can be successfully applied starting from the first three months of life up to a likely maximum of two years. Lastly, in contrast to our previous belief, we saw that with children older than two years, we necessarily need to change the design of the test to make it dynamic and interactive, using e.g. cartoons to spark and maintain the child's interest.

Our findings described herein pave the way for the refinement and deployment of an optimised test battery suitable for the collection of eye-tracking data in preterm children, with the ultimate goal of early detection of possible developmental impairments.

Acknowledgments

The PARENT project has received funding from the European Union's Horizon 2020 research and innovation programme under the Marie Sklodowska-Curie – Innovative Training Network 2020, Grant Agreement N° 956394.

References

[1] C. P. Howson, M. V. Kinney, J. E. Lawn, Born too soon: the global action report on preterm birth., volume 25, 2012 ed., March of Dimes, Partnership for Maternal, Newborn and Child Health (PMNCH), Save the Children, WHO. World Health Organization. Geneva, 2012., 2012.

[2] J. E. Lawn, R. Davidge, V. K. Paul, S. von Xylander, J. de Graft Johnson, A. Costello, M. V. Kinney, J. Segre, L. Molyneux, Born Too Soon: Care for the preterm baby, Reproductive Health 10 (2013) S5. doi:10.1186/1742-4755-10-S1-S5.

[3] R. S. Jois, Understanding long-term neurodevelopmental outcomes of very and extremely preterm infants: A clinical review, Aust. J. Gen. Pract. 48 (2019) 26–31. doi:10.31128/AJGP-04-18-4545.

[4] E. J. Telford, S. Fletcher-Watson, K. Gillespie-Smith, R. Pataky, S. Sparrow, I. C. Murray, A. O'Hare, J. P. Boardman, Preterm birth is associated with atypical social orienting in infancy detected using eye tracking, J. Child Psychol. Psychiatry 57 (2016) 861–868. doi:10.1111/jcpp.12546.

[5] S. Ross-Sheehy, S. Schneegans, J. P. Spencer, The infant orienting with attention task: Assessing the neural basis of spatial attention in infancy, Infancy : the official journal of the International Society on Infant Studies 20 (2015) 467–506. doi:10.1111/infa.12087.

[6] S. Ross-Sheehy, B. Eschman, Assessing visual stm in infants and adults: eye movements and pupil dynamics reflect memory maintenance, Visual Cognition 27 (2019) 78–92. doi:10.1080/13506285.2019.1600089.

[7] G. Gredebäck, C. von Hofsten, J. Karlsson, K. Aus, The development of two-dimensional tracking: a longitudinal study of circular pursuit, Exp Brain Res 163 (2005) 204–213.

[8] K. Strand-Brodd, U. Ewald, H. Grönqvist, G. Holmström, B. Strömberg, E. Grönqvist, C. von Hofsten, K. Rosander, Development of smooth pursuit eye movements in very preterm infants: 1. General aspects, Acta Paediatr. 100 (2011) 983–991. doi:10.1111/j.1651-2227.2011.02218.x.

[9] Y. F. Kaul, K. Rosander, C. Von Hofsten, K. S. Brodd, G. Holmström, A. Kaul, B. Böhm, L. Hellström-Westas, Visual tracking in very preterm infants at 4 mo predicts neurodevelopment at 3 y of age, Pediatr. Res. 80 (2016) 35–42. doi:10.1038/pr.2016.37.

[10] Y. F. Kaul, K. Rosander, C. von Hofsten, K. Strand Brodd, G. Holmström, L. Hellström-Westas, Visual tracking at 4 months in preterm infants predicts 6.5-year cognition and attention, Pediatr. Res. (2021) 1–8. doi:10.1038/s41390-021-01895-8.

[11] A. Gerbasi, V. Groznik, D. Georgiev, L. Sacchi, A. Sadikov, Detecting Mild Cognitive Impairment Using Smooth Pursuit and a Modified Corsi Task, in: Springer (Ed.), Int. Conf. Artif. Intell. Med., Springer International Publishing, 2021, pp. 168–172. doi:10.1007/978-3-030-77211-6_19.

[12] S. Ross-Sheehy, S. Schneegans, J. P. Spencer, The Infant Orienting With Attention Task: Assessing the Neural Basis of Spatial Attention in Infancy, Infancy 20 (2015) 467–506. doi:10.1111/infa.12087.

[13] S. Ross-Sheehy, S. Perone, K. L. Macek, B. Eschman, Visual orienting and attention deficits in 5- and 10-month-old preterm infants, Infant Behav. Dev. 46 (2017) 80–90. doi:10.1016/j.infbeh.2016.12.004.

[14] S. Ross-Sheehy, B. Eschman, Assessing visual STM in infants and adults: eye movements and pupil dynamics reflect memory maintenance, Vis. cogn. 27 (2019) 78–92. doi:10.1080/13506285.2019.1600089.

[15] J. H. Filliter, J. M. Glover, P. A. McMullen, J. P. Salmon, S. A. Johnson, The Dal-Houses: 100 new photographs of houses with ratings of typicality, familiarity, and degree of similarity to faces, Behavior Research Methods 48 (2016) 178–183. doi:10.3758/s13428-015-0561-8.

[16] B. Dean, L. Ginnell, V. Ledsham, A. Tsanas, E. Telford, S. Sparrow, S. Fletcher-Watson, J. P. Boardman, Eye-tracking for longitudinal assessment of social cognition in children born preterm, J. Child Psychol. Psychiatry 62 (2021) 470–480. doi:10.1111/jcpp.13304.

[17] L. DeBruine, B. Jones, Face Research Lab London Set (2017). doi:10.6084/m9.figshare.5047666.v5.

Automatic neonatal cranial ultrasound segmentation using deep learning: A review

Roa'a Khaled[1,2,*], Arantxa Ortega-Leon[3], Joaquín Pizarro[2], Isabel Benavente Fernández[4], Simón P. Lubián López[4] and Lionel C. Gontard[1,5]

[1]*Applied Optics and Magnetism Research Group, University of Cádiz, 11510 Puerto Real, Spain*
[2]*Department of Computer Engineering, University of Cádiz, 11519 Puerto Real, Spain*
[3]*Intelligent Modelling of Systems Research Group, University of Cádiz, 11202 Algeciras, Spain*
[4]*Biomedical Research and Innovation Institute of Cádiz (INiBICA) Research Unit, Puerta del Mar University Hospital, 11009 Cádiz, Spain*
[5]*IMEYMAT, University of Cádiz, 11510 Puerto Real, Spain*

Abstract

Ultrasound is widely used as a clinical routine tool for neonates' brain assessment, especially for preterm neonates. This population is at high risk of developing serious complications leading to neurocognitive and motor impairments. However, the analysis of Cranial Ultrasound requires experienced personnel to perform a time-consuming visual assessment, which is nontrivial due to the low quality and artifacts in the images. For this analysis to be more objective, fast, and accurate, many automatic methods have been proposed. Such methods usually rely on segmenting brain structures or regions of interest for the extraction of subsequent clinically useful measurements. Deep Learning methods are being more adopted recently as they proved to have a huge potential in many medical image analysis tasks.

In this review article, we present and discuss the Deep Learning-based methods developed for the automatic segmentation of preterm neonatal ultrasound images, more specifically the methods developed for segmenting the Cerebral Ventricle System. The performance and evaluation results of these methods are compared, and their major contributions are outlined. Furthermore, we discuss the main challenges of neonatal ultrasound automatic segmentation and possible ways to address these challenges. Finally, we discuss the future directions in this very specific context.

Keywords

Cranial Ultrasound analysis, Deep Learning, Medical image segmentation, Preterm neonates, Cerebral Ventricle System segmentation,

1. Introduction

Ultrasound (US) imaging has been widely used in clinical practice as the first screening and diagnostic tool in many medical domains, including fetal and neonatal care. In neonatal care,

DETERMINED 2022: Neurodevelopmental Impairments in Preterm Children — Computational Advancements, August 26, 2022, Ljubljana, Slovenia
*Corresponding author.
roaa.khaled@uca.es (R. Khaled); arantxa.ortega@uca.es (A. Ortega-Leon); joaquin.pizarro@uca.es (J. Pizarro); isabel.benavente@uca.es (I. B. Fernández); simonplubian@gmail.com (S. P. L. López); lionel.cervera@uca.es (L. C. Gontard)
0000-0002-5231-8462 (R. Khaled); 0000-0002-0793-3677 (A. Ortega-Leon); 0000-0002-4295-6743 (J. Pizarro); 0000-0001-9276-1912 (I. B. Fernández); 0000-0001-8603-7119 (L. C. Gontard)
© 2022 Copyright for this paper by its authors. Use permitted under Creative Commons License Attribution 4.0 International (CC BY 4.0).
CEUR Workshop Proceedings (CEUR-WS.org)

CEUR-WS.org/Vol-3363/paper05.pdf

Cranial US is extensively used for routine brain assessment of newborn infants and more specifically preterm infants. This widespread use of US is due to its several advantages over other imaging modalities, such as the low cost, non-invasive nature, non-ionizing radiation, real-time display, operator comfort, portability, and accessibility [1, 2, 3, 4].

Cranial US can only be used in the newborn period during which the anterior fontanelle is still open (usually until 18 months of age), but it is mostly used during the first 5-6 months of age when the best US images can be obtained. After that age brain structures will start to be less visible due to the processes of brain membranes thickening and fontanelle closure [5, 6].

Cranial US allows the detection of most neonatal hemorrhagic and ischemic lesions in addition to the main congenital and maturational anomalies [7]. However, the use of US entitles some challenges. For instance, US has low imaging quality and suffers from noise and artifacts. Moreover, it requires trained and experienced operators to acquire good images and perform a tedious visual assessment, which leads to high inter- and intra-observer variability across different institutes and US systems manufacturers [1, 7].

Since the standard clinical practice is based on visual assessment and some 2D linear measurements, much research has been conducted to propose the use of better quantitative analysis over the visual assessment and to prove the usefulness of other measurements than the 2D linear ones, such as volumetric measurements. This has the potential to improve the diagnosis and prognosis of neurodevelopmental disorders in preterm neonates. However, this could not be adopted in clinics yet because it requires manually segmenting anatomical structures of interest in the brain, which is time-consuming and prone to inter- and intra-observer variability [7].

Developing automatic methods for the analysis of Cranial US images can alleviate these challenges by making such analysis more objective, accurate, and fast. Automatic methods include segmentation as an important preliminary step for the extraction of clinical parameters that neonatologists need in order to perform an assessment and diagnosis based on quantitative measurements [8].

One of the important structures to be segmented in Cranial US images of preterm neonates is the Cerebral Ventricle System (CVS). CVS can be affected by some serious complications such as germinal matrix-intraventricular hemorrhage leading to posthemorrhagic ventricular dilatation (PHVD). This happens because of preterm birth and causes neurocognitive and motor impairments.

Currently, the clinical standard is to perform 2D measurements manually on 2D US images to estimate the CVS volume. This practice, apart from being time-consuming and subjective, is imprecise due to the unavailability of 3D information [2, 7]. Therefore, developing automatic segmentation methods and quantitative analysis methods based on 3D US can help clinicians to perform timely medical interventions and improve the outcome of those infants [9, 10]. However, the task of automatically segmenting anatomical structures from Cranial US is very challenging due to several reasons, such as the variable image quality, presence of noise and shading artifacts, unclear and incomplete boundaries, similar intensities among different structures, variable size and anatomical shape of the ventricles for neonates with abnormalities. Moreover, the differences in shape, size, and texture characteristics caused by the change in blood pressure [11].

Recently, there has been an increasing trend in the use of Deep Learning (DL) algorithms

to segment CVS from neonatal Cranial US images. This is due to the success that DL methods have been achieving in the field of medical image analysis in the last years.

There are several reviews focused on neonatal neuroimage segmentation, but most of them focused on MRI [12, 13]. Although few reviews have been conducted on US segmentation methods based on DL [1, 14], they were generic and included studies on different medical domains (i.e. not focused on neonatal US segmentation). To this date, and to the best of our knowledge, no reviews have been written on segmentation methods of neonatal US images specifically.

Therefore, we conducted a literature search for all studies published in this field from 2018 until 2022 July 1st, by specifying keywords such as (preterm neonatal AND cerebral ventricles AND ultrasound AND segmentation AND deep learning) in Google Scholar database. Abstracts of papers resulting from this search were screened and only (8) relevant papers were chosen.

In this review we present a systematic overview of DL methods in segmenting Cranial US images of preterm neonates, more specifically, segmenting the CVS. In Section 2 we briefly mention the evolution of segmentation methods in this specific context and review several DL methods developed for preterm neonatal ventricles segmentation from US images. In Section 3 we discuss the challenges of US image segmentation and the possible ways to address these challenges in the future. Finally, in Section 4 we present our conclusions.

2. Cranial Ultrasound Image Segmentation

2.1. Non-DL Based Image Segmentation

Many studies have been conducted for automating US image analysis of different organs but very few studies have focused on US neuroimaging [15, 16]. Most segmentation methods were initially based on well-established image processing techniques. In those methods, images are first pre-processed for denoising using image filtering. Then segmentation is carried out using intensity thresholding or edge detection filters. Finally, image analysis of binary images is carried out using morphological operations. For instance, Gontard et al. [17] used median filtering followed by a global intensity threshold calculated automatically from the 3D volume for segmenting cerebrospinal fluid (CSF).

Nevertheless, boundary incompleteness in US images raises great challenges to automatic segmentation. Therefore, most methods were semi-automatic where some input from the user is required. Additionally, shape prior can provide strong guidance in estimating the missing boundary. Qiu et al. [18] proposed a semi-automatic convex segmentation algorithm for ventricle segmentation in 3D US images. In [19] a geometric-based method using a 3D ellipsoid estimation technique was proposed for ventricle segmentation. However, traditional shape models often suffer from being reliable on hand-crafted descriptors and losing local information in the fitting procedure, hence, such methods had poor generalization.

A semi-automatic approach was proposed in [20] for ventricle segmentation. In this study, the image is denoised using complex wavelets and then 3 seed points are required to be manually selected in order to perform an active contour segmentation where the contour is parametrized implicitly using a level-set function. The most advanced non-DL-based segmentation method for segmenting ventricles was developed by Qiu et al [21]. This method made use of a phase

congruency map, multi- atlas initialization technique, atlas selection strategy, and a multiphase geodesic level-sets evolution combined with a spatial shape prior derived from multiple pre-segmented atlases. Nevertheless, the method proposed required 54 min to segment one volume, which is too long to be used in clinical routine.

In addition to the previously mentioned methods, Machine Learning based methods have also been proposed for US image segmentation. Tabrizi et al. [22] proposed an automatic method for ventricle segmentation in 2D US images based on a hybrid approach consisting of fuzzy c-means, adaptive thresholding, template matching, phase congruency, and active contour algorithms.

2.2. Deep Learning for Image Segmentation

Nowadays, DL methods represent the state-of-the-art methods for image analysis and have outperformed any other conventional methods in both performance and speed in terms of the specific task.

Two main methodologies are currently used to address boundary detection-segmentation in US:
1) A top-down manner that takes advantage of prior shape information to guide segmentation. For example, Yang et al. [23] formulated boundary completeness as a sequential problem and a model of the shape in a dynamic manner using Recurrent Neural Networks. Authors in [24] modified Convolutional Neural Network (CNN) architectures like the Hough-CNN which include explicitly transforms for edge detection.
2) A bottom-up manner that classifies each pixel into foreground (object) or background in a supervised manner. Most studies apply this approach by classifying each pixel in an image in an end-to-end and fully supervised learning manner employing CNNs with encoder-decoder architectures.

The first widely recognized encoder-decoder network was Seg-Net [25]. Later, UNet [26] brought a major breakthrough in medical image segmentation, and became the backbone of almost all the leading methods recently, such as UNet++, UNet3+, 3D UNet, V-Net, Res-UNet, and Dense-UNet. In these extensions of UNet, the contribution was either in skip connections, using better convolutional layer connections, or in applications. For instance, UNet++ [27], [28] utilizes nested and dense skip connections for further reduction of the semantic gap between the encoder and decoder feature maps. In UNet3+ [29], skip connections between different scales are used. 3D UNet [30] and V-Net [31] are extensions of UNet for volumetric segmentation of 3D medical images. In Res-UNet [32] the encoder and decoder convolutional blocks consist of residual connections [33], while in Dense-UNet [34], they consisted of dense blocks [35].

Due to the difficulty of 3D DL, the DL methods that are currently applied in medical US analysis mostly use 2D images as inputs, although these 2D images might be taken from available 3D volumes. In fact, 3D DL is still a challenging task, due to the following limitations:
1) Training a deep network on a large volume might be too computationally expensive for real clinical application (i.e. with a significantly increased memory and computational requirement).
2) A deep network with a 3D volume as input requires more training samples since a 3D network contains parameters that are orders of magnitude higher than a 2D network. This may dramatically increase the risk of overfitting, given the limited training samples. Alternatively, there are authors that formulate the problem of optimizing 3D image segmentation as a patch-

level classification task, as was proposed in [36].

In fact, there are not so many DL methods proposed for neonatal US segmentation, and in this review (Section 2.3) we are reviewing the DL methods for CVS segmentation specifically.

2.3. Deep Learning for CVS segmentation from Cranial US images

In this subsection, we review 8 papers that were selected after a literature search for studies published on the use of DL for segmenting lateral ventricles or the whole CVS from Cranial US. The search included papers that were published from 2018 until 2022 July 1st. Those 8 papers were the only studies found that utilize DL for this task and they are summarized in Table 1.

	Architecture (2D/3D)	Dataset	2D/3D segmentation	Augmentation	Loss function	Evaluation	Inference time (s)
Martin et al. (2018) [10]	UNet (2D)	15 volumes (private)	3D	-	Soft Dice	DSC = 0.816 HD = 13.6 MAD = 0.62	5 s
Wang et al. (2018) [37]	UNet and SegNet combination (2D)	687 slices (private)	2D	horizontal flip, random crop	MAE	DSC = 0.908 IoU = 84.84% Pix. Acc. = 92.14%	0.022 s
Valanarasu et al. (2020) [38]	CBAS (2D)	1629 (private)	2D	horizontal and vertical flips, random crop	confidence guided	DSC = 0.8901 IoU = 81.03%	0.01 s
Tabrizi et al. (2020) [39]	UNet like (2D)	1253 slices (private)	2D	vertical flip, affine transformation	probabilistic atlas-based	DSC = 0.86 HD = 0.3 mm	17.4 s
Gontard et al. (2021) [40]	pretrained SegNet (2D)	152 volumes (private)	3D	translation, rotation, scale, shear	weighted BCE	DSC = 0.8	< 60 s
Martin et al. (2021) [41]	V-Net/ UNet with CPPN (2D and 3D)	25 volumes (private)	2D and 3D	-	BCE then soft Dice	(for V-Net) DSC = 0.822 MAD = 0.5 mm δ Va = 0.35 cm^3 δ Vr = 11.1%	3.5 s (for 2D)
Valanarasu et al. (2022) [42]	KiUNet (2D)	1629 slices (private)	2D	-	BCE	DSC = 0.8943	-
Szentimrey et al. 2022 [43]	UNet ensemble (3D)	190 volumes (private)	3D	translation	combined BCE and Dice loss (with MSE for the 3rd model)	DSC = 0.72 VD = 3.7 cm^3 MAD = 1.14 mm	5 s

Table 1: Comparison of DL based methods for automatic CVS segmentation from Cranial US images. Loss Functions: **MAE** is Mean Absolute Error loss, **BCE** is Binary Cross Entropy loss, and **MSE** is Mean Squared Error loss. Evaluation Metrics: **DSC** is Dice Similarity Coefficient, **HD** is Hausdorff Distance, **MAD** is Mean Absolute Distance, **IoU** is Intersection over Union, **Pix. Acc.** is Pixel Accuracy, δ **Va** is Absolute volume difference, δ **Vr** is Relative volume difference, and **VD** is Absolute Volumetric Difference

It is worth mentioning that to get an estimation of the CVS volume, clinicians usually obtain various linear measurements manually from 2D images. However, this practice is imprecise (since 3D information is missing), time-consuming, and operator dependent. Therefore, the studies reviewed here mainly aimined to improve the accuracy and reduce the time required to perform manual segmentation by automating this task and therefore paving the way for

obtaining clinical measurements automatically. Some of the reviewed studies were also aiming to improve the performance of automatic segmentation by utilizing 3D information, which may result in more accurate and representative volumetric clinical measurements.

In 2018 Martin et al. [10] extended CVS volume estimation to 3D. They used a 2D UNet to first segment 2D angular image sequence. Then they propose an algorithm for 3D reconstruction to reconstruct 3D segmentation. This method can significantly reduce the extensive computation cost and memory requirement of 3D processing. A limitation of this study is the small dataset, which affects the ability of the model to generalize.

Wang et al. [37] proposed a CNN that combines the advantages of both UNet and SegNet architectures to segment lateral ventricles from 2D US. The proposed network consists of two components: a pre-trained DenseNet as the encoder to extract deep features, and a multi-scale decoder that first applys pooling of the feature maps (resulted from the encoder) into four different sizes and then applies a series of transposed convolutions to transform lower dimensional feature maps into higher ones in steps. Moreover, the output of each transposed convolution is concatenated with existing feature maps of the same size and then fed into the next transposed convolution.

Since the resolution of small features is gradually lost along the deeper layers of a CNN, the resulting coarse features can miss the details of small structures. This leads to poor performance of traditional CNN architectures in segmenting small anatomical structures (as in the case of normal ventricles for example). To address that, Valanarasu et al. [38] propose a network (Confidence-guided Brain Anatomy Segmentation-CBAS), where segmentation and corresponding confidence maps are estimated at different scales. Aleatoric uncertainty is computed as the confidence scores to indicate how confident the CBAS network is about the segmentation output. This allows CBAS to learn how to differentiate regions with higher error (low confidence score) and therefore focus more on those regions in subsequent layers and block the propagation of error while computing the segmentation output.

Tabrizi et al. [39] proposed a method to segment lateral ventricles from 2D US images. The proposed method integrates anatomical information into a CNN by defining a new weighted loss function and an image-specific adaption. First, a deep CNN was used to detect the cranium and brain interhemispheric fissure to estimate the anatomical position of ventricles and correct the cranium rotation. Then, lateral ventricles were segmented using a CNN with a similar structure to that of a 2D UNet. The CNN learning was integrated with a prior model of the lateral ventricles through a probabilistic atlas-based weighted loss function and an image-specific adaption. Moreover, the authors performed posthemorrhagic hydrocephalus (PHH) outcome prediction (necessity of intervention) using a support vector machine classifier that was trained on ventricular morphology and clinical parameters. The segmentation performance was affected by the unclear boundaries caused by the build-up of hemorrhage pressure, but this is a challenge that experts also experience when doing manual segmentation. Regarding PHH output prediction, although the prediction performance was good, the features used were hand-crafted and based on 2D measurements. We believe that 3D features learned by the DL model may improve the PHH output prediction accuracy.

Gontard et al. [40] utilized a pre-trained SegNet model based on VGG16 to obtain 3D ventricular segmentation from 2D thickened sagittal slices (i.e. 3 consecutive slices). After that 3D ventricular volumes were estimated using the segmented 2D slices.

Martin et al. [41] utilized both V-Net and UNet (for both 2D and 3D images) to estimate CVS volume in a dataset including both normal and dilated ventricles. Moreover, the use of a Compositional Pattern Producing Network (CPPN) was proposed to enable the CNNs to learn spatial information about the CVS location. Their results showed a comparative performance for both V-Net and UNet, with V-Net being slightly better (especially in segmenting normal ventricles). They also reported that CPPN increased the accuracy of the CNNs when having fewer layers. It would be interesting to investigate the benefits of the CPPN for multi-structural brain segmentation. Results reported in this study show that a 3D architecture is overall more accurate for this task. Nevertheless, a 2D architecture was as accurate as a 3D architecture for segmenting dilated ventricles. Moreover, it was shown that a 2D architecture enables to perform the segmentations in clinical time with hardware that requires fewer memory resources and therefore may be preferable to a 3D architecture in a clinical context.

To address the issue of poor segmentation of smaller structures and boundary regions in medical image segmentation in general, Valanarasu et al. [42] proposed an architecture (KiUNet) that consists of two branches. The first branch is an overcomplete convolutional network (Kite-Net) which learns to capture fine details and accurate edges of the input by projecting the input image into a higher dimension such that the receptive field is being constrained from increasing in the deep layers of the network. The second part is a UNet which learns high-level features. A cross-residual fusion strategy was proposed to combine the features across the two branches. Moreover, the architecture was proposed in both 2D and 3D settings, and a Res-KiUNet and a Dense-KiUNet architectures where also proposed for improving the learning of the network, where residual connections and dense blocks are utilized. Finally, the proposed method was tested on 5 different datasets of different medical image applications and modalities, including lateral ventricles from US, and was proved to generalize well to different modalities.

Nevertheless, only one metric was used for evaluation in [42], that is the Dice Similarity Coefficient (DSC), which might not be very indicative of the improvement in segmentation unless the segmented structure is small. For instance, dice values for US ventricular segmentation dataset were not significantly improved compared to other methods reported in this study, which is expected since dilated ventricles are not very small structures (compared to tumors datasets for example where improvement was reported to be clearer). Therefore, other metrics might also be more useful for showing the improvement in segmenting ventricle boundaries. Also, it would be interesting to test this method on 3D ventricles segmentation and use volumetric metrics to evaluate the performance, since volumetric measurements might be more susceptible to slight improvements in segmenting the surface or boundaries. Another contribution of this work is that the network's memory requirements are less while maintaining decent performance. However, it would be interesting to compare with a deeper KiUNet that is as deep as the UNet they compared with.

To address the limitations of 2D US, Szentimrey et al. [43] developed a method to segment lateral ventricles from 3D US images using a 3D UNet ensemble model composed of three UNet variants. Each variant highlights various aspects of the segmentation task such as the shape and boundary of the ventricles. The ensemble is made of a UNet++, attention UNet, and UNet with a DL-based shape prior combined using a mean voting strategy. The UNet++ has more skip connections compared to the basic UNet, to allow for a more flexible fusion of feature maps at the decoder pathway and make the semantic maps between the encoder and decoder

more similar which is believed to make the learning task easier for the optimizer and either improve the speed and/or performance of the model. The attention UNet incorporates attention gates to improve the ventricle surface segmentation boundary (which is challenging in US images) by improving the sensitivity to foreground voxels while adding minimal complexity to the model. The UNet with a DL-based shape prior utilizes a shape prior loss function to add surface regularization by conforming the predicted ventricle shape to that of the ground truth segmentation.

Even though incorporating shape prior resulted in improving the segmentation of ventricles according to [43], it might not be the case if an unseen test image has a unique ventricle shape not captured in the training data, which is likely to happen because ventricles might have several deformations. Another limitation is that the ensemble model is computationally heavy, especially due to the UNet++ model. Therefore, GPU resources are required even during test time, which might not always be available at healthcare points. Moreover, the ventricles were manually annotated on the sagittal plane every 1mm such that slices between each manual contour required interpolation, leading to possible inaccuracies of the ground truth volume. On the other hand, they utilized bigger data compared to previous studies, and they included scans with varying degrees of intraventricular hemorrhage and scans with only one ventricle being visible due to the limited field of view. Several metrics were used for evaluating the proposed method's performance, including metrics that are clinically useful, especially absolute volumetric difference (VD), which has been used for patients with PHVD to determine those who need intervention [44].

All methods reviewed in this section seem to have good performance according to the reported results (both in terms of accuracy and speed). Each method had its contributions and limitations. However, it is worth mentioning that the comparability of methods, in this case, is not straightforward since each method was developed using a different private dataset that varies in the number of cases, image quality...etc. Moreover, in most cases, small datasets were used, and it was not mentioned about the number of data resulting from Augmentation. This becomes more of a problem in the case of training on 3D volumes. Therefore, we believe that efforts are still needed to form large open datasets that will allow researchers to develop new methods and compare them with others.

Another area that we believe needs to be further investigated is whether segmenting 3D data would improve the performance. One would expect that incorporating 3D information using 3D architectures would increase the accuracy of segmentation. Authors in [41] reported comparative performance of both 2D and 3D architectures for segmenting dilated ventricles, however, they used a small dataset.

Regarding the applicability of the proposed methods in clinical settings, memory, and computational requirements are also important (besides the accuracy and speed). Even though inference time was reported in most of these studies, it was not always mentioned whether the developed methods can be used in machines with lower memory and computational resources, or if they need special requirements. We believe that most of the proposed methods were computationally heavy and therefore novel methods are still needed to tackle this issue.

3. Challenges in US segmentation and Possible solutions

3.1. Limited availability of annotated data and Image Synthesis

One of the major problems in medical image analysis is the limited number of annotated data. This is due to the difficulty of sharing patient data publicly and the difficulty of obtaining clinical annotations since it is expensive and time-consuming.

However, most advanced research on automation of US analysis is based on supervised learning which is strongly dependent on the access to open and considerable amounts of data, acquired on different populations and with different operating conditions (and with different US scanners). This leads to a lack of generalization and validation of the AI models. Moreover, not having access to open large data makes it difficult to reproduce and compare the proposed methods.

In this context, federated learning or data augmentation strategies are important for developing better algorithms. Moreover, novel image synthesis methods are proposed in the literature to synthesize high-quality data that could be added to the training dataset. Generative Adversarial Networks (GANs) [45] and their variants are powerful architectures capable of generating synthetic images to be used for training other networks, for example, UNet-based networks. In addition, GANs are favored over traditional methods for handling data imbalance [46] by synthesizing realistic-looking minority class samples, thereby balancing the class distribution, and avoiding overfitting. GANs are being applied for generating 3D medical imaging data [47], however, generating realistic-looking data samples in US neuroimaging is an open research problem [48] and further research is required to improve and validate the quality of the synthesized samples. Another challenge is that while using GANs in medical imaging to synthesize new images solves the issue of limited available data, the problem of annotations still exists in this setup. Therefore, novel methods are needed to synthesize annotations as well. To tackle this issue, Valanarasu et al. [38] proposed a method for image synthesis using multi-scale self-attention generator where 2D Cranial US images are synthesized directly from manipulated segmentation masks (ventricle and septum pellucidi masks). Thus, there is no need for annotation of the synthesized data.

Alternatively, data can be generated through the simulation of US images [49]. This is a field largely unexplored in the context of neuroimaging. For example, we suggest that 3D models of neonatal brain gyrification might be generated as in [50] and then used for simulating US images using computing simulation toolboxes like MUST [51] or FIELD II [52].

3.2. Segmentation of other brain structures

MRI is used in neonatology to segment not only the lateral ventricles and external CSF but also white matter, cortical gray matter, cerebellum, or brain stem [53]. US neuroimaging might complement better MRI neuroimages if US data could provide information on other brain structures. For example, most studies with US report measurements related only to ventricular dilation but it would be more interesting to assess those measurements relative to the total brain volume [19]. With appropriate data labeling US might also be used for the detection and quantification of white matter injuries. Finally, the folding dynamics of the brain, occurring mostly before normal-term birth, are vastly unknown. US might help to better understand this

process by looking into the development of cortical sulci in infants. For instance, longitudinal studies of the central brain sulcus could in principle be carried out with 3D US like it is done with MRI [54].

3.3. Inherent US image limitations and Image preprocessing

US acquisition introduces noise in the signal, which corrupts the resulting image and affects further processing steps, e.g., segmentation and quantitative analysis. US segmentation can clearly benefit from the application of preprocessing methods for improving image quality (denoising, deblurring, increasing resolution). DL is being applied to improve the resolution and contrast-to-noise ratio of the reconstruction algorithms of the signal acquired with the US sensors [55, 56]. And DL will certainly be very promising for US image enhancement and denoising using super-resolution methods [57, 58].

3.4. Novel AI architectures

The aforementioned encoder-decoder CNN architectures achieved state-of-the-art performance in medical imaging segmentation. UNet, has become the de-facto standard and achieved tremendous success. However, due to the intrinsic locality of convolution operations, UNet generally demonstrates limitations in explicitly modeling long-range dependency (i.e., they lack focus in extracting low-level features) since the networks are built to be deeper and hence more high-level features get extracted. As a result, they fail in providing a good segmentation of small structures with blurred boundaries, which is the case with US image segmentation. This implies the need for novel architectures or variants.

GANs for example are explored for image segmentation using image transfer methods [45]. And Transformers, designed for sequence-to-sequence prediction, with innate global self-attention mechanisms, have emerged strongly as alternative architectures [59] to Encoder-Decoder architectures for medical image segmentation. To name some recent examples, TransUNet [60] merits both Transformers and UNet CNNs, UNetFormer [61] increases the efficiency of conventional UNet architectures, and MedFormer can generalize to different medical domains[62].

4. Conclusions

DL has meant a change of paradigm in medical imaging analysis, and new techniques and architectures are in continuous development which will certainly impact US imaging and analysis. Synthetic data generation, transformers, and super-resolution methods can help to overcome some limitations of US image analysis with respect to MRI.

Automatic methods that yield reliable 3D measurements of the ventricles are expected to provide a more accurate assessment of preterm neonates' ventricles and other cerebral structures, which can improve the monitoring and treatment decisions of preterm born infants. Overall, the studies reviewed in this review demonstrate the possibility of achieving an accurate segmentation of preterm neonates' CVS in a clinical time in 3D US images and therefore pave the way to prove the clinical benefits of 3D US in monitoring cerebral structures of preterm

neonates, not only for CVS dilation but also for brain growth, sulci formation or detection of white matter injuries.

In the future, studies that compare volumetric measurements obtained from both US and MRI are needed, to show whether the measurements obtained from 3D US can be competitive with those obtained from MRI. Moreover, models utilizing both US and MRI can be developed to study whether both modalities contain complementary information that could help improve the accuracy.

Another important future direction is automatic outcome prediction based on automatic ventricular segmentation and measurements, this can include predicting the progression of PHH which offers an opportunity for early interventions to improve outcome [39]. Developing AI tools that combine measurements of other cerebral structures, like those related to White Matter damage or Sulci malformation, can also be used to predict the long-term outcome of preterm infants and the probability of them developing neurodevelopmental impairments. To the best of our knowledge, this has not been achieved yet, but with the continuous developments of methods in this field, this can be achieved in the following few years.

References

[1] S. Liu, Y. Wang, X. Yang, B. Lei, L. Liu, S. X. Li, D. Ni, T. Wang, Deep Learning in Medical Ultrasound Analysis: A Review, Engineering 5 (2019) 261–275. URL: https://www.sciencedirect.com/science/article/pii/S2095809918301887. doi:https://doi.org/10.1016/j.eng.2018.11.020.

[2] M. J. Brouwer, L. S. De Vries, L. Pistorius, K. J. Rademaker, F. Groenendaal, M. J. Benders, Ultrasound Measurements of the Lateral Ventricles in Neonates: Why, How and When? A Systematic Review, Acta paediatrica 99 (2010) 1298–1306.

[3] M. Riccabona, Potential Role of 3D US in Infants and Children, Pediatric radiology 41 Suppl 1 (2011) S228–37. doi:10.1007/s00247-011-2051-1.

[4] I. Timor-Tritsch, A. Monteagudo, P. Mayberry, Three-dimensional Ultrasound Evaluation of the Fetal Brain: the Three Horn View, Ultrasound in Obstetrics and Gynecology: The Official Journal of the International Society of Ultrasound in Obstetrics and Gynecology 16 (2000) 302–306.

[5] L. Pogliani, G. Zuccotti, M. Furlanetto, V. Giudici, A. Erbetta, L. Chiapparini, L. Valentini, Cranial ultrasound is a reliable first step imaging in children with suspected craniosynostosis, Child's nervous system : ChNS : official journal of the International Society for Pediatric Neurosurgery 33 (2017). doi:10.1007/s00381-017-3449-3.

[6] P. Gupta, K. Sodhi, A. Saxena, N. Khandelwal, P. Singhi, Neonatal cranial sonography: A concise review for clinicians, Journal of Pediatric Neurosciences 11 (2016) 7. doi:10.4103/1817-1745.181261.

[7] I. Benavente-Fernández, E. Ruiz-González, M. Lubian-Gutiérrez, et al., Ultrasonographic Estimation of Total Brain Volume: 3D Reliability and 2D Estimation. Enabling Routine Estimation During NICU Admission in the Preterm Infant, Frontiers in Pediatrics 9 (2021). doi:10.3389/fped.2021.708396.

[8] J. P. Kusanovic, J. K. Nien, L. F. Gonçalves, J. Espinoza, W. Lee, M. Balasubramaniam,

E. Soto, O. Erez, R. Romero, The Use of Inversion Mode and 3D Manual Segmentation in Volume Measurement of Fetal Fluid-filled Structures: Comparison with Virtual Organ Computer-aided AnaLysis (VOCAL™), Ultrasound in obstetrics & gynecology 31 (2008) 177–186.

[9] M. N. Cizmeci, N. Khalili, N. H. P. Claessens, et al., Assessment of Brain Injury and Brain Volumes after Posthemorrhagic Ventricular Dilatation: A Nested Substudy of the Randomized Controlled ELVIS Trial, The Journal of Pediatrics 208 (2019) 191–197.e2. doi:10.1016/j.jpeds.2018.12.062.

[10] M. Martin, B. Sciolla, M. Sdika, et al., Automatic Segmentation of the Cerebral Ventricle in Neonates Using Deep Learning with 3D Reconstructed Freehand Ultrasound Imaging, in: 2018 IEEE International Ultrasonics Symposium (IUS), 2018, pp. 1–4. doi:10.1109/ULTSYM.2018.8580214.

[11] K. M. Meiburger, U. R. Acharya, F. Molinari, Automated Localization and Segmentation Techniques for B-mode Ultrasound Images: A review, Computers in Biology and Medicine 92 (2018) 210–235. URL: https://www.sciencedirect.com/science/article/pii/S0010482517303888. doi:https://doi.org/10.1016/j.compbiomed.2017.11.018.

[12] C. N. Devi, A. Chandrasekharan, V. Sundararaman, Z. C. Alex, Neonatal brain MRI segmentation: A review, Computers in Biology and Medicine 64 (2015) 163–178. URL: https://www.sciencedirect.com/science/article/pii/S0010482515002346. doi:https://doi.org/10.1016/j.compbiomed.2015.06.016.

[13] A. Makropoulos, S. J. Counsell, D. Rueckert, A Review on Automatic Fetal and Neonatal Brain MRI Segmentation, NeuroImage 170 (2018) 231–248. URL: https://www.sciencedirect.com/science/article/pii/S1053811917305451. doi:https://doi.org/10.1016/j.neuroimage.2017.06.074, segmenting the Brain.

[14] Z. Wang, Deep Learning in Medical Ultrasound Image Segmentation: a Review, 2021. arXiv:2002.07703.

[15] J. A. Noble, D. Boukerroui, Ultrasound Image Segmentation: a Survey, IEEE Transactions on medical imaging 25 (2006) 987–1010.

[16] M. H. Mozaffari, W. Lee, 3D Ultrasound Image Segmentation: A Survey, arXiv preprint arXiv:1611.09811 (2016).

[17] L. C. Gontard, J. Pizarro, I. Benavente-Fernández, S. P. Lubián-López, Automatic Measurement of the Volume of Brain Ventricles in Preterm Infants from 3D Ultrasound Datasets, in: ECCOMAS Thematic Conference on Computational Vision and Medical Image Processing, Springer, 2019, pp. 323–329.

[18] W. Qiu, J. Yuan, J. Kishimoto, J. McLeod, Y. Chen, S. de Ribaupierre, A. Fenster, User-Guided Segmentation of Preterm Neonate Ventricular System from 3-D Ultrasound Images Using Convex Optimization, Ultrasound in Medicine Biology 41 (2015) 542–556. URL: https://www.sciencedirect.com/science/article/pii/S0301562914006371. doi:https://doi.org/10.1016/j.ultrasmedbio.2014.09.019.

[19] M.-A. Boucher, S. Lippé, A. Damphousse, R. El-Jalbout, S. Kadoury, Dilatation of Lateral Ventricles with Brain Volumes in Infants with 3D Transfontanelle US, in: MICCAI, 2018.

[20] B. Sciolla, M. Martin, P. Delachartre, P. Quetin, Segmentation of the Lateral Ventricles in 3D Ultrasound Images of the Brain in Neonates, in: 2016 IEEE International Ultrasonics Symposium (IUS), IEEE, 2016, pp. 1–4.

[21] W. Qiu, Y. Chen, J. Kishimoto, S. de Ribaupierre, B. Chiu, A. Fenster, J. Yuan, Automatic Segmentation Approach to Extracting Neonatal Cerebral Ventricles from 3D Ultrasound Images, Medical image analysis 35 (2017) 181–191.

[22] P. Roshani Tabrizi, R. Obeid, J. Cerrolaza, A. Penn, A. Mansoor, M. G. Linguraru, Automatic Segmentation of Neonatal Ventricles from Cranial Ultrasound for Prediction of Intraventricular Hemorrhage Outcome, volume 2018, 2018, pp. 3136–3139. doi:10.1109/EMBC.2018.8513097.

[23] X. Yang, L. Yu, L. Wu, Y. Wang, D. Ni, J. Qin, P.-A. Heng, Fine-grained Recurrent Neural Networks for Automatic Prostate Segmentation in Ultrasound Images, 2016. URL: https://arxiv.org/abs/1612.01655. doi:10.48550/ARXIV.1612.01655.

[24] F. Milletari, S.-A. Ahmadi, C. Kroll, A. Plate, V. Rozanski, J. Maiostre, J. Levin, O. Dietrich, B. Ertl-Wagner, K. Bötzel, N. Navab, Hough-CNN: Deep Learning for Segmentation of Deep Brain Regions in MRI and Ultrasound, Computer Vision and Image Understanding 164 (2017) 92–102. URL: https://www.sciencedirect.com/science/article/pii/S1077314217300620. doi:https://doi.org/10.1016/j.cviu.2017.04.002, deep Learning for Computer Vision.

[25] V. Badrinarayanan, A. Kendall, R. Cipolla, SegNet: A Deep Convolutional Encoder-Decoder Architecture for Image Segmentation, IEEE Transactions on Pattern Analysis and Machine Intelligence 39 (2017) 2481–2495. doi:10.1109/TPAMI.2016.2644615.

[26] O. Ronneberger, P. Fischer, T. Brox, U-Net: Convolutional Networks for Biomedical Image Segmentation, in: N. Navab, J. Hornegger, W. M. Wells, A. F. Frangi (Eds.), Medical Image Computing and Computer-Assisted Intervention – MICCAI 2015, Springer International Publishing, Cham, 2015, pp. 234–241.

[27] Z. Zhou, M. M. Rahman Siddiquee, N. Tajbakhsh, J. Liang, UNet++: A Nested U-Net Architecture for Medical Image Segmentation: 4th International Workshop, DLMIA 2018, and 8th International Workshop, ML-CDS 2018, Held in Conjunction with MICCAI 2018, Granada, Spain, September 20, 2018, Proceedings, volume 11045, 2018, pp. 3–11. doi:10.1007/978-3-030-00889-5_1.

[28] Z. Zhou, M. M. Rahman Siddiquee, N. Tajbakhsh, J. Liang, UNet++: Redesigning Skip Connections to Exploit Multiscale Features in Image Segmentation, IEEE transactions on medical imaging (2019). doi:10.1109/TMI.2019.2959609.

[29] H. Huang, L. Lin, R. Tong, H. Hu, Q. Zhang, Y. Iwamoto, X. Han, Y.-W. Chen, J. Wu, UNet 3+: A Full-Scale Connected UNet for Medical Image Segmentation, ICASSP 2020 - 2020 IEEE International Conference on Acoustics, Speech and Signal Processing (ICASSP) (2020) 1055–1059.

[30] Çiçek, S. Lienkamp, T. Brox, O. Ronneberger, 3D U-Net: Learning Dense Volumetric Segmentation from Sparse Annotation, 2016, pp. 424–432. doi:10.1007/978-3-319-46723-8_49.

[31] F. Milletari, N. Navab, S.-A. Ahmadi, V-Net: Fully Convolutional Neural Networks for Volumetric Medical Image Segmentation, 2016, pp. 565–571. doi:10.1109/3DV.2016.79.

[32] X. Xiao, S. Lian, Z. Luo, S. Li, Weighted Res-UNet for High-Quality Retina Vessel Segmentation, in: 2018 9th International Conference on Information Technology in Medicine and Education (ITME), 2018, pp. 327–331. doi:10.1109/ITME.2018.00080.

[33] K. He, X. Zhang, S. Ren, J. Sun, Deep Residual Learning for Image Recognition, in: 2016

IEEE Conference on Computer Vision and Pattern Recognition (CVPR), 2016, pp. 770–778. doi:10.1109/CVPR.2016.90.

[34] X. Li, H. Chen, X. Qi, Q. Dou, C.-W. Fu, P.-A. Heng, H-DenseUNet: Hybrid Densely Connected UNet for Liver and Tumor Segmentation From CT Volumes, IEEE Transactions on Medical Imaging 37 (2018) 2663–2674. doi:10.1109/TMI.2018.2845918.

[35] G. Huang, Z. Liu, L. Van Der Maaten, K. Q. Weinberger, Densely Connected Convolutional Networks, in: 2017 IEEE Conference on Computer Vision and Pattern Recognition (CVPR), 2017, pp. 2261–2269. doi:10.1109/CVPR.2017.243.

[36] R. Khaled, J. Vidal, J. C. Vilanova, R. Martí, A U-Net Ensemble for Breast Lesion Segmentation in DCE MRI, Computers in Biology and Medicine (2022) 105093.

[37] P. Wang, N. G. Cuccolo, R. Tyagi, et al., Automatic Real-Time CNN-based Neonatal Brain Ventricles Segmentation, in: 2018 IEEE 15th International Symposium on Biomedical Imaging (ISBI 2018), 2018, pp. 716–719. doi:10.1109/ISBI.2018.8363674.

[38] J. M. Jose Valanarasu, R. Yasarla, P. Wang, I. Hacihaliloglu, V. M. Patel, Learning to Segment Brain Anatomy From 2D Ultrasound With Less Data, IEEE Journal of Selected Topics in Signal Processing 14 (2020) 1221–1234. doi:10.1109/JSTSP.2020.3001513.

[39] P. R. Tabrizi, A. Mansoor, R. Obeid, J. J. Cerrolaza, D. A. Perez, J. Zember, A. Penn, M. G. Linguraru, Ultrasound-Based Phenotyping of Lateral Ventricles to Predict Hydrocephalus Outcome in Premature Neonates, IEEE Transactions on Biomedical Engineering 67 (2020) 3026–3034. doi:10.1109/TBME.2020.2974650.

[40] L. C. Gontard, J. Pizarro, B. Sanz-Peña, et al., Automatic Segmentation of Ventricular Volume by 3D Ultrasonography in Post Haemorrhagic Ventricular Dilatation Among Preterm Infants, Scientific Reports 11 (2021). doi:10.1038/s41598-020-80783-3.

[41] M. Martin, B. Sciolla, M. Sdika, et al., Automatic Segmentation and Location Learning of Neonatal Cerebral Ventricles in 3D Ultrasound Data Combining CNN and CPPN, Computers in Biology and Medicine 131 (2021) 104268. doi:10.1016/j.compbiomed.2021.104268.

[42] J. M. J. Valanarasu, V. A. Sindagi, I. Hacihaliloglu, V. M. Patel, KiU-Net: Overcomplete Convolutional Architectures for Biomedical Image and Volumetric Segmentation, IEEE Transactions on Medical Imaging 41 (2022) 965–976. doi:10.1109/TMI.2021.3130469.

[43] Z. Szentimrey, S. de Ribaupierre, A. Fenster, et al., Automated 3D U-Net based Segmentation of Neonatal Cerebral Ventricles from 3D Ultrasound Images, Medical Physics 49 (2022) 1034–1046. doi:10.1002/mp.15432.

[44] J. Kishimoto, A. Fenster, D. S. C. Lee, S. de Ribaupierre, Quantitative 3-D Head Ultrasound Measurements of Ventricle Volume to Determine Thresholds for Preterm Neonates Requiring Interventional Therapies Following Posthemorrhagic Ventricle Dilatation, Journal of Medical Imaging 5 (2018) 1 – 9. URL: https://doi.org/10.1117/1.JMI.5.2.026001. doi:10.1117/1.JMI.5.2.026001.

[45] S. Kazeminia, C. Baur, A. Kuijper, B. van Ginneken, N. Navab, S. Albarqouni, A. Mukhopadhyay, GANs for Medical Image Analysis, Artificial Intelligence in Medicine 109 (2020) 101938.

[46] R. J. Chen, M. Y. Lu, T. Y. Chen, D. F. Williamson, F. Mahmood, Synthetic Data in Machine Learning for Medicine and Healthcare, Nature Biomedical Engineering 5 (2021) 493–497.

[47] S. Hong, R. Marinescu, A. V. Dalca, A. K. Bonkhoff, M. Bretzner, N. S. Rost, P. Golland,

3D-stylegan: A Style-based Generative Adversarial Network for Generative Modeling of Three-dimensional Medical Images, in: Deep Generative Models, and Data Augmentation, Labelling, and Imperfections, Springer, 2021, pp. 24–34.

[48] A. Montero, E. Bonet-Carne, X. P. Burgos-Artizzu, Generative Adversarial Networks to Improve Fetal Brain Fine-grained Plane Classification, Sensors 21 (2021) 7975.

[49] H. Rivaz, D. L. Collins, Simulation of Ultrasound Images for Validation of MR to Ultrasound Registration in Neurosurgery, in: Workshop on Augmented Environments for Computer-Assisted Interventions, Springer, 2014, pp. 23–32.

[50] X. Wang, A. Bohi, M. A. Harrach, M. Dinomais, J. Lefèvre, F. Rousseau, On Early Brain Folding Patterns using Biomechanical Growth Modeling, in: 2019 41st Annual International Conference of the IEEE Engineering in Medicine and Biology Society (EMBC), 2019, pp. 146–149. doi:10.1109/EMBC.2019.8856670.

[51] D. Garcia, SIMUS: An Open-source Simulator for Medical Ultrasound Imaging. Part I: Theory & Examples, Computer Methods and Programs in Biomedicine 218 (2022) 106726.

[52] J. A. Jensen, Field: A Program for Simulating Ultrasound Systems, Medical & Biological Engineering & Computing 34 (1997) 351–353.

[53] A. Largent, J. De Asis-Cruz, K. Kapse, S. D. Barnett, J. Murnick, S. Basu, N. Andersen, S. Norman, N. Andescavage, C. Limperopoulos, Automatic Brain Segmentation in Preterm Infants with Post-hemorrhagic Hydrocephalus using 3D Bayesian U-Net, Human brain mapping 43 (2022) 1895–1916.

[54] H. de Vareilles, D. Rivière, Z.-Y. Sun, C. Fischer, F. Leroy, S. Neumane, N. Stopar, R. Eijsermans, M. Ballu, M.-L. Tataranno, et al., Shape Variability of the Central Sulcus in the Developing Brain: a Longitudinal Descriptive and Predictive Study in Preterm Infants, NeuroImage 251 (2022) 118837.

[55] A. A. Nair, T. D. Tran, A. Reiter, M. A. L. Bell, A Deep Learning based Alternative to Beamforming Ultrasound Images, in: 2018 IEEE International conference on acoustics, speech and signal processing (ICASSP), IEEE, 2018, pp. 3359–3363.

[56] S. Khan, J. Huh, J. C. Ye, Adaptive and Compressive Beamforming using Deep Learning for Medical Ultrasound, IEEE transactions on ultrasonics, ferroelectrics, and frequency control 67 (2020) 1558–1572.

[57] S. Cammarasana, P. Nicolardi, G. Patanè, Real-time Denoising of Ultrasound Images based on Deep Learning, Medical & Biological Engineering & Computing (2022) 1–16.

[58] A. Sawant, S. Kulkarni, Ultrasound Image Enhancement using Super Resolution, Biomedical Engineering Advances (2022) 100039.

[59] S. Zheng, J. Lu, H. Zhao, X. Zhu, Z. Luo, Y. Wang, Y. Fu, J. Feng, T. Xiang, P. H. Torr, et al., Rethinking Semantic Segmentation from a Sequence-to-sequence Perspective with Transformers, in: Proceedings of the IEEE/CVF conference on computer vision and pattern recognition, 2021, pp. 6881–6890.

[60] J. Chen, Y. Lu, Q. Yu, X. Luo, E. Adeli, Y. Wang, L. Lu, A. L. Yuille, Y. Zhou, Transunet: Transformers Make Strong Encoders for Medical Image Segmentation, arXiv preprint arXiv:2102.04306 (2021).

[61] A. Hatamizadeh, Z. Xu, D. Yang, W. Li, H. Roth, D. Xu, UNetFormer: A Unified Vision Transformer Model and Pre-Training Framework for 3D Medical Image Segmentation, 2022. URL: https://arxiv.org/abs/2204.00631. doi:10.48550/ARXIV.2204.00631.

[62] Y. Gao, M. Zhou, D. Liu, Z. Yan, S. Zhang, D. N. Metaxas, A Data-scalable Transformer for Medical Image Segmentation: Architecture, Model Efficiency, and Benchmark, 2022. URL: https://arxiv.org/abs/2203.00131. doi:10.48550/ARXIV.2203.00131.

Neural correlates of visuomotor functions in preterm children: a literature review focused on unilateral Cerebral Palsy

Monica Crotti[1,*], Nofar Ben Itzhak[1], Lisa Mailleux[2], Umberto Michelucci[3,4] and Els Ortibus[1,*]

[1]University of Leuven, Department of Development and Regeneration, Leuven, Belgium
[2]University of Leuven, Department of Rehabilitation Sciences, Leuven, Belgium
[3]TOELT LLC, Research and Development, Dübendorf, Switzerland
[4]Lucerne University of Applied Sciences and Arts, Computer Science Department, Lucerne, Switzerland

Abstract

Cerebral Palsy (CP) is the most common developmental disorder in preterm infants with spastic CP as the most prevalent motor type. Several aspects of visual perception and visuomotor control remain unsolved in children with spastic unilateral Cerebral Palsy (uCP). This is remarkable since CP is recognized as the leading cause of childhood motor disability, and comorbidities, such as visual problems, are well recognized in this condition. The co-occurrence of visual and motor impairments is related to the fact that the lesions to motor pathways are anatomically close to visual pathways in children with uCP. Previous studies attempted to define the relationship between visual disorders and brain damage in uCP, finding no specific correlation between the type and timing of the lesions and visual functions. Furthermore, research investigating which brain regions and tracts are responsible for specific visual functions and deficits is limited. The present review, therefore, aims to describe neurological correlates (i.e., structural MRI and diffusion MRI) of visuomotor deficits in children with uCP to identify the gaps in the current literature which could be addressed in future studies.

Keywords

Cerebral Palsy, Visual perception, Visuomotor control, Neuroimaging, Diffusion MRI

1. Introduction

Preterm birth, defined as birth before 37 completed weeks of gestation [1], can result in long term developmental impairments due to brain immaturity or damage occurring during the prenatal or perinatal period. The main disorders associated with prematurity are intellectual disability, hearing loss, visual impairment, and cerebral palsy [2].

DETERMINED 2022: Neurodevelopmental Impairments in Preterm Children — Computational Advancements, August 26, 2022, Ljubljana, Slovenia

*Corresponding author.
monica.crotti@kuleuven.be (M. Crotti); nofar.benitzhak@kuleuven.be (N. Ben Itzhak); lisa.mailleux@kuleuven.be (L. Mailleux); umberto.michelucci@toelt.ai (U. Michelucci); els.ortibus@uzleuven.be (E. Ortibus)
0000-0003-3206-2006 (M. Crotti)

© 2022 Copyright for this paper by its authors. Use permitted under Creative Commons License Attribution 4.0 International (CC BY 4.0).
CEUR Workshop Proceedings (CEUR-WS.org)

CEUR-WS.org/Vol-3363/paper06.pdf

Visual impairments refer to any degree of impairment to a person's ability to see, that affects his or her daily life [3]. For years, retinopathy of prematurity (ROP) was considered the most common cause of visual loss in infants with low birth weight [4]. ROP is an eye disorder caused by abnormal blood vessel growth in the light-sensitive part of the retina. However, recent studies [5] have shown that cerebral visual impairment (CVI) has replaced ROP as the main cause of visual disability in ex-preterm children [6]. CVI refers to a heterogeneous group of visual dysfunctions which *"cannot be attributed to disorders of the anterior visual pathways or any potentially co-occurring ocular impairment"* [7]. It includes disorders of basic visual functions such as acuity and stereopsis, but also higher visual dysfunctions of visual attention, depth and motion perception, object recognition and spatial cognition [8, 9]. A gestational age of less than 26 weeks is the most important factor associated with CVI (5.21%) [10, 2].

Cerebral Palsy (CP) is the most common developmental disorder in preterm infants. According to the literature, over 50% of children with CP are born preterm [11]. The prevalence of CP increases with decreasing gestational age at delivery [12]. In a meta-analysis, the pooled prevalence of CP in preterm infants is estimated to be 6.8% [13]. However, in extremely preterm born children (i.e. born before 28 weeks of gestation), the prevalence of CP increases up to 10%. CP is defined as a non-progressive permanent disorder of movement and posture due to disturbances in the developing fetal and infant brain [14]. In addition to impairments of gross and fine motor function (i.e., muscle tone, posture, and movement), CP manifests with deficits in sensory modalities such as visual function [14]. CVI in particular is reported in over half of children with CP [15, 16]. The presence of such impairments can have an important impact on planning and performing movements, due to a lack of information about the position of the hands as well as the target [17, 18]. As a consequence, visuo-motor integration and motor coordination skills might be hampered in children with CP not only due to their motor impairment.

CP also is a heterogeneous disorder and can be classified by its motor type and distribution. According to the Surveillance of Cerebral Palsy in Europe (SCPE) the motor type can be described as spastic, dyskinetic, ataxic, or mixed pattern [19], and the distribution of limb involvement as unilateral or bilateral. Spastic CP, characterized by pyramidal signs (i.e., spasticity, weakness), increased muscle tone, and joint stiffness, is the prevailing type [20], and the most common one in preterm infants or those with low birth weight [2]. Spastic CP can be further classified into unilateral CP (uCP), if only one side of the body is affected, and bilateral CP, if both sides are involved [21]. Children with uCP, who make up 30% of the total cases of CP [22], are often physically less impaired than those with bilateral CP, showing a higher degree of impairment in the upper limb in comparison to the lower limbs. Such impairments result from an injury predominantly lateralized to one brain hemisphere [23] which leads to a lower degree of deficits when compared to bilateral CP. Up to now, the majority of studies on children with uCP have been focusing on motor control [24] describing an irregular movement pattern of the impaired arm and difficulties with performing bimanual tasks [25]. On the contrary, visual impairments, also common in uCP [26, 15], have been less well investigated despite their impact on guiding and planning motor actions. As a result, several aspects of

visual perception and visuomotor control remain unsolved in children with uCP.

The present review, therefore, aims to summarize the current knowledge about visuomotor deficits in children with uCP and identify the gaps in the current literature to be addressed in future studies. In Section 2, we describe the anatomy and functions of the visuomotor system and the related impairments in children with uCP. Section 3 highlights the findings on structural and diffusion neuroimaging in children with CP, focusing first on those related to motor function and secondly on those related to visual and visuomotor function. Lastly, Section 4 provides a summary of the findings described in previous sections, highlighting the need of future research to address the link between neuroimaging and visual and visuomotor function in children with uCP.

2. Visuomotor network in children with uCP

2.1. Anatomy and functions

The visual network is highly complex with 40% of the brain serving visual functions [27]. Visual information from the retina reaches the posterior visual pathways through the optic nerves and the optic chiasm (i.e., optic tracts). The optic tracts are the first structures of the posterior visual pathways which transfer information together with the lateral geniculate nucleus (LGN), the pulvinar, the superior colliculus and the optic radiations to the primary visual cortex (V1) located in the occipital lobe [28]. Damage to the optic tract, LGN, or optic radiations leads to visual field defects, which can vary depending on the site of the lesion [28]. Extension of the damage to V1 results in acuity loss [28]. From V1, visual information is sent to the higher visual areas located in the parietal and temporal lobes, where higher order visual processing takes place [28].

Historically, CVI has been explained within the framework of two distinct and interacting systems, the dorsal and the ventral stream [29]. The former is responsible for motion and object's spatial location and damage to the dorsal stream results in impairments in visual guidance of movement and simultaneous perception [27]. The latter is involved in object identification and damage to the ventral stream results in difficulties with object and face recognition and orientation in the environment [30]. In the last decades, a growing body of evidence [31, 32] has proposed more refined functional and anatomical circuits for visuo-motor processing. According to Pisella et al. [32], in the visuomotor system we can identify three different streams:
(1) a dorso-dorsal pathway, including the dorsal part of the parietal and pre-motor cortices, for immediate visuo-motor control [33, 34]. Damage to the dorso-dorsal pathway can result in optic ataxia, a deficit of visuo-manual guidance.
(2) a ventral prefrontal pathway with connections from the ventral visual stream to pre-frontal areas for spatial or temporal control of action. Damage to the ventral prefrontal pathway results in visual agnosia, a deficit of visual recognition.
(3) a ventro-dorsal pathway, including the ventral part of the parietal lobe and the pre-motor and pre-frontal areas, for complex planning and programming with a more bilateral organisation

and a hemispheric lateralization. Damage to the ventro-dorsal pathway results in mirror apraxia, characterized by misreaching errors when the controlesional hand is guided to a visual goal through a mirror. Another common deficit is limb apraxia, a brain disease affecting the performance of skilled and learned object-related movements [35]. Moreover, spatial neglect, a syndrome affecting the left space in the domains of perception, representation and action can also occur when this pathway is damaged.
An illustration of the visual network is provided in Figure 1.

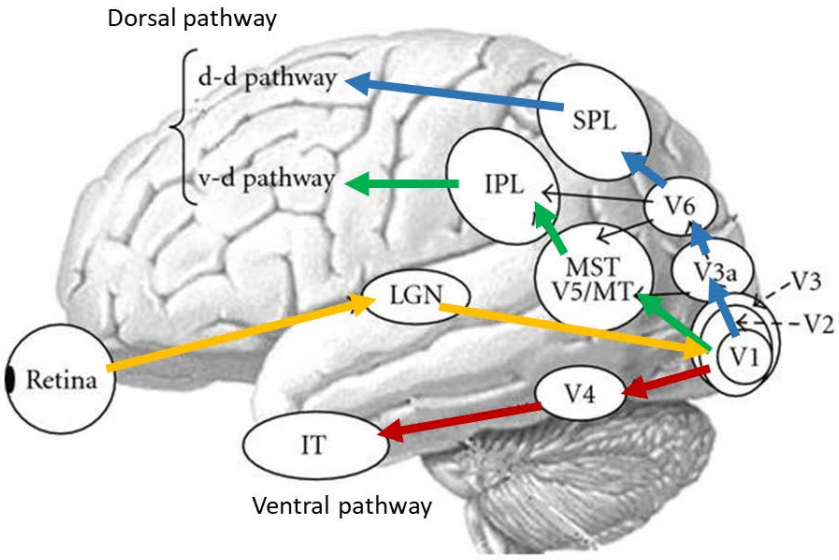

Figure 1: The visual network in humans. Dorso-dorsal pathway (d-d pathway) is shown in blue, ventrodorsal pathway (v-d pathway) in green, and the ventral pathway in red. In addition, the visual pathway from the retina to the primary visual cortex (V1) is highlighted in yellow. Lateral geniculate nucleus (LGN); secondary, tertiary, quaternary, and senary visual cortices (V2, 3, 4, and 6); accessory visual cortex (V3a, V3); quinary visual cortex/middle temporal area (V5/MT); medial superior temporal area (MST); inferior parietal lobule (IPL,); superior parietal lobule (SPL); inferior temporal cortex (IT). Figure adapted and modified from [36] with Open Access distributed under the Creative Commons Attribution License.

Overall, visual problems can be classified as peripheral or ocular (e.g., strabismus, refractive error, decreased acuity) if the damage occurs anterior to the optic chiasm and retrochiasmatic or cerebral when the damage occurs after the level of the optic chiasm [15]. Cerebral visual problems include visual perception (VP) and visuomotor integration impairments [30]. A full overview of visual functions is provided in Table 1 [37, 38, 15, 39].

Table 1
Overview of visual functions with the division in oculomotor [38], geniculostriate functions [37, 28], visual perceptual functions and visuomotor integration [15, 39].

Category	Name of function	Definition
Oculomotor functions	*Fixations*	Maintenance of the gaze on a single location or area
	Smooth Pursuit	Slower tracking movements of the eyes designed to keep a moving stimulus on the fovea
	Saccades	Rapid, ballistic movements of the eyes that abruptly change the point of fixation
Geniculostriate functions	*Visual acuity*	Ability of the eye to distinguish shapes and the details of objects at a given distance
	Visual field	Total area in which objects can be seen in the side (peripheral) vision as eyes are focused on a central point
	Contrast sensitivity	Ability to distinguish an object against its background
	Stereopsis	Perception of depth and three-dimensional structure through binocular vision
Visual perceptual (VP) functions	*Visual discrimination and matching*	Ability to detect features for processing the differences and similarities among visual stimuli
	Object recognition or visual closure	Ability to recognize an object when shown under an incomplete representation (i.e., noise on top of an image or missing parts)
	Visual spatial perception	Ability to determine spatial relations within and between objects, perceive depth, topographic orientation, and wayfinding
	Figure-ground perception	Ability to differentiate relevant object information from distracting background information
	Motion perception	Ability to understand a constantly changing visual environment
	Visual memory	Ability to integrate visual information with previous experience
Visuomotor integration	*Visually guided motor activity*	Reaching, locomotion
	Eye-hand coordination	Ability to coordinate the information received through the eyes to control the hands in the accomplishment of a given task

2.2. Visual and visuomotor impairments in children with unilateral cerebral palsy (uCP)

In children with CP, the prevalence of visual problems, including both ocular and cerebral impairments, varies between 40% and 50% while the prevalence of only CVI increases up to 70% [15, 16]. Several studies have attempted to describe high-level visual dysfunctions, however, these studies showed mixed results. Kozeis et al. [40] investigated visual perception in 105

children with spastic CP (aged 6–15 years), finding a reduced near visual acuity and abnormal or absent stereopsis. In addition, the scores on the Motor Free Visual Perception Test [41] used to assess visual discrimination, figure-ground perception, visual memory, visual closure, and visual spatial perception, were less than or equal to that of 6-year-old typically developing children. In a study of Fazzi et al. [15], different types of CP were found to be associated with different patterns of visual impairments. Furthermore, VP impairments seem to occur more frequently in children with spastic CP compared to other types of CP, in whom visuo-motor integration is more impaired than non-motor visual–perceptual skills [26, 42].

In the present paragraph, we specifically focus on results in children with uCP, starting with findings on oculomotor and geniculostriate functions, followed by higher-order visual deficits. A summary of the main studies on visual and visuomotor impairments in children with CP is reported in Table 2. According to the study of Fazzi et al. [42], children with uCP showed oculomotor impairment (e.g., altered smooth pursuit and saccades), a slight reduction in visual acuity and visual field, and altered stereopsis. With regard to higher-order visual functions, the systematic review of Auld [43] identified three assessments (i.e., Motor-Free Visual Perception Test [41]; Test of Visual Perceptual Skills [44, 45]; Developmental Test of Visual Perception [46]) for measuring high-level visual perception in children with uCP which showed good psychometric properties. Results from Burtner et al. [47] showed that children with uCP have significantly lower scores on the Motor-Free Visual Perceptual Test-Revised and on the Developmental Test of Visual Perception when compared to typically developing children. Specifically, only children with left hemiplegia scored significantly lower than typically developing children on the Motor-Free Visual Perceptual Test-Revised. These findings are in line with the recent study of Berelowitz and Franzsen [48], which investigated specific VP impairments in children aged 4-18 in South Africa, finding that left spastic uCP demonstrated consistently lower scores on all of the subtests of the Test of Visual Perceptual Skills and composite scores than those with right spastic uCP.

Additional studies [49, 50] report that children with uCP have deficits in sensorimotor integration and visuo-perceptual modalities, leading to difficulties in the execution of motor actions. Also, visual perceptual ability assessed by the Test of Visual Perceptual Skills, and unimanual capacity of the dominant upper limb evaluated by the Jebsen–Taylor Test of Hand Function, were found to be associated with activities of daily living process skills which were measured by Assessment of Motor and Process Skills) in children with uCP [51]. In addition, during object manipulation and reaching, children with uCP closely monitor the actions of the affected hand [52] by increasing the visual attention towards the impaired limb [53]. The increased attention could be explained as a compensation strategy for underlying visuomotor deficits [54] such as visual exploration and eye-hand coordination. Lastly, in the study of Surkar et al. [54], children with uCP showed impaired anticipatory visual control and eye-hand coordination which affects the planning of goal-directed actions. Hence, impairments in action execution are closely related to the ones in visuomotor coordination, suggesting important implications to take into account for diagnosis and rehabilitation of children with uCP.

Table 2
Studies on visual and visuomotor impairments in children with cerebral palsy.

Authors	N CP and age	CP	Main findings in visual and visuomotor functions
Kozeis et al., 2007 [40]	105 (range 6–15 yrs)	Spastic CP	Impairment in: · Visual acuity · Stereopsis · Visual discrimination · Figure-ground perception · Visual memory · Visual closure · Visual spatial perception
Fazzi et al., 2004 [42]	20 (range 5 – 8 yrs)	Spastic CP	Impairment in: · Visual acuity · Visual field · Stereopsis · Smooth pursuit · Saccades
Fazzi et al., 2012 [15]	17 (age not reported)	uCP	· Refractive errors · Strabismus Impairment in: · Visual field · Oculomotor behaviour
Burtner et al., 2006 [47]	20 (range 4-10 yrs)	uCP	· Impaired visual perception (i.e., Developmental Test of Visual Perception, Motor-Free Visual Perceptual, Test-Revised and School Function Assessment) · Left uCP lower scores on motor-free visual tests
Berelowitz and Franzsen., 2021 [48]	20 (range 5-18 yrs)	uCP	· Left uCP low scores on the test of Visual Perceptual Skills
Verrel et al., 2008 [52]	6 (range 14–19 yrs)	uCP	· Increased visual monitoring of impaired limb
Steenbergen et al.,1996 [53]	14 (range 15-20 yrs)	uCP	· Increased attention to impaired limb
Surkar et al., 2018 [54]	13 (mean age 6.8 + 2.9 yrs)	uCP	Impairment in: · Anticipatory visual control · Eye-hand coordination

CP, cerebral palsy; uCP, unilateral CP

3. Brain lesion in children with uCP

Visuomotor impairments result from brain damage that is highly heterogeneous in children with uCP.
Neuroimaging techniques allow the study of lesion extension and location which is needed to better understand and inform about the integrity of the different pathways responsible for visuomotor function. Among neuroimaging techniques, brain structural MRI (sMRI) and diffusion-weighted MRI (DWI) can provide high-resolution images of anatomy and white matter architecture of the cerebral structures of children with uCP [55].

3.1. Neuroimaging techniques

3.1.1. Structural MRI (sMRI)

Conventional MRI is used in hospital environments for the diagnosis and characterization of perinatal brain injury in pathologies such as CP and CVI [56, 57, 58]. With respect to CP, MRI sheds light on the location (e.g., lobe, hemisphere, structures), timing and extent of brain damage (i.e., cerebral hemispheres uni- or bilaterally). In the last decades, several classifications of MRI findings in CP have been proposed [31, 59, 60]. Below, we describe examples of qualitative and semi-quantitative interpretation of MRI data in children with CP.

Qualitative methods The MRI classification system (MRICS), developed by the Surveillance of Cerebral Palsy in Europe, SCPE [19, 59], defines the predominant neuroimaging pattern which most likely is the cause of the CP. MRICS is primarily a qualitative system including some simple quantitative aspects (e.g. uni- vs bilaterality, severity of a pattern such as basal ganglia/thalamus lesions). This classification has been found to be reliable based on the Reference and Training Manual and annual exchange and discussions among SCPE registered partners (i.e., clinicians dealing with CP, epidemiologists, and experts who work with CP registers from 18 countries). In the manual, which is available online with open access (https://eu-rd-platform.jrc.ec.europa.eu/scpe/reference-and-training-manual_en), brain abnormalities are classified into three major groups and subgroups. For a complete overview of the classification, see Table 3.

In a recent systematic review, Franki et al. [61] described the type of the underlying brain lesions in children with uCP. Taken together, approximately 5% of children with uCP had brain malformations. White matter lesions were the most common lesion type (57.8%) finding periventricular leukomalacia (PVL) in the majority of cases, followed by intraventricular haemorrhage (IVH) and the combination of PVL and IVH. Grey matter lesions were found in 14.8% of children with uCP while in 5% of these children, no visible lesions were found on sMRI.

Table 3
The harmonized classification of MRI, based on pathogenic patterns (MRI classification system) proposed by the SCPE network. Table adapted from [59].

Classification		Subclassification		Subtypes and/or examples
A	Maldevelopments	A1	Disorders of cortical formation	Disorders of proliferation
				Disorders of migration
				Disorders of organization
		A2	Other maldevelopments	Holoprosencephaly, Dandy Walker malformation, Corpus callosus agenesis, Cerebellar hypoplasia, etc.
B	White matter lesions	B1	Periventricular leukomalacia (PVL)	
		B2	Sequelae of intra-ventricular hemorrhage (IVH) or periventricular hemorrhagic infarction	
		B3	Combination of PVL and IVH sequelae	
C	Gray matter lesions	C1	Basal ganglia / thalamus lesions	Mild Moderate Severe
		C2	Cortico-subcortical lesions	
		C3	Arterial infarctions (middle cerebral artery or others)	
D	Miscellaneous			Cerebellar atrophy, cerebral atrophy, delayed myelination, ventriculomegaly not covered under B, hemorrhage not covered under B, brainstem lesions, calcifications, etc.
E	Normal			

Semi-Quantitative scale In the last years, a semi-quantitative scale (SQS) has been developed to describe the extent and location of lesions in MRI data of children with CP aged above 3 years old [62]. The SQS is structured in three main sections: (1) information on the technical characteristics of the scan and the type of lesion based on previous classification; (2) the graphical template for the brain hemispheres; (3) the scoring system for the hemispheres, subcortical structures (basal ganglia, thalamus, and brainstem), corpus callosum, and cerebellum. In section (2) of the SQS, lesions are traced onto a graphical black and white reproduction of six axial slices selected from the Montreal Neurological Institute (MNI) template. The scale makes a distinction between the cortical outline, the subcortical line separating the grey from the white matter, and a periventricular line bordering the periventricular white matter. Based on this subdivision, the brain template is made of three layers, namely a periventricular layer, a

middle white matter layer, and a cortico/subcortical layer. In section (3), hemispheric subscores include the number of affected slices; the number of affected lobes, the sum of the lobar scores for periventricular layer, the middle layer, and the cortico/subcortical layer. Right, left, and total scores are marked separately. Summary scores are calculated for the hemispheres, the basal ganglia and brainstem as total, right, and left scores, while for the corpus callosum and the cerebellum, scores are calculated as total scores only. The summary scores give a global score on the extent of a lesion, ranging from 0 to 40, with higher scores indicating more extensive lesions while information on topography is provided when subscores are considered. A detailed description of the methodology can be found in the study of Fiori et al. [62].

The reliability of the semi-quantitative scale was investigated in a study with 34 children with CP, among which 17 had uCP [62]. High interrater and intra-rater reliability of the total score was found with indices above 0.87 (kappa (k); intraclass correlation coefficients (ICC)). Nevertheless, a possible limitation of the semi-quantitative scale is that it uses the Montreal Neurological Institute template which is the international standard template for adults [63]. Indeed, to objectively analyse an MRI scan, it is necessary to compare the patient's MRI with an atlas built from the mean anatomical and physiological metrics as a function of disease and age [63]. Consequently, the use of age-specific brain atlases, built from averaging brain images of children in a specific age-range, is recommended [64]. Furthermore, the SQS scale [62] requires time investment in manual segmentation and anatomical knowledge of the examiner, which leads to its suboptimal application in population-based studies and in clinical practice. In the last decades, novel tools such as the use of automated volumetric segmentation, where the boundaries of a specific brain segment are measured automatically by a software program, have been developed. Pagnozzi et al. [65] developed an automated lesion segmentation pipeline for both white matter (WM) and grey matter (GM) lesions validated in 107 children with uCP. This tool showed positive correlations between lesions and clinical performance such as the Assisting Hand Assessment (AHA) which assesses the contribution of the impaired hand to bimanual activities [66] and the Test of Visual Perception Skills. Although the use of automated volumetric segmentation is not fully established in routine practice, such results highlight the important application of artificial intelligence techniques to optimize clinical research.

3.1.2. Diffusion MRI (dMRI)

Diffusion MRI (dMRI) provides insight into the microstructural development of the brain by measuring the random motion of water molecules [67]. In fibrous tissue, such as in the brain white matter (WM), water molecules tend to diffuse along the fibers, enabling the study of the orientation of the underlying structures. Different methods are used for measuring WM orientation, among which the most common are diffusion tensor imaging (DTI) and constrained spherical deconvolution (CSD) [68, 69].
DTI measures the three-dimensional diffusion of water as a function of spatial location [67]. In white matter, the presence of axons and bundles running in parallel constrains the free motion of water molecules, a condition known as diffusion anisotropy. This feature can be exploited to calculate different scalar measures namely fractional anisotropy (FA), mean diffusivity (MD),

radial diffusivity (RD), and axial diffusivity (AD) [67]. FA measures the degree of uniformity of water diffusion for a specific orientation [70]. Higher values are found in tissues with oriented structures organized in a common direction, such as white-matter tracts while lower values are found in damaged tissues due to the loss of coherence in the main diffusion direction. AD describes the diffusivity of water molecules parallel to fibers bundles while RD refers to the diffusivity of water molecules which is perpendicular to fibers bundles. Decreased AD but unchanged RD is typically assumed to indicate white matter damage. MD is a measure of the average diffusion in a certain time [71] and it is higher in damaged tissues as a result of increased free diffusion. The accuracy of the DTI model is limited in brain regions with crossing fibers where many voxels contain contributions from different oriented fiber populations and make it challenging to interpret metrics such as FA [72, 73]. To overcome this problem, one alternative method is constrained spherical deconvolution [68] which models the diffusion signal in each voxel as a function of all fiber orientations within the voxel (i.e., fiber orientation distribution - fOD). FOD can be used to calculate quantitative measures of microscopic and macroscopic white matter morphology (i.e., fiber density, fiber-bundle cross-section, fiber density and cross-section) and also to perform tractography [74, 68, 75, 76]. From both DTI and CSD metrics, it is possible to infer long-range connectivity patterns between distant brain regions namely Fibre Tractography (FT) [77, 78]. Fiber tractography is computed through algorithms that can be classified into deterministic [79] and probabilistic [80]. The former reconstructs the most likely trajectory from a given point (i.e., region of interest; ROI), the latter produces a distribution of trajectories, reflecting the degree of uncertainty of the trajectories.
As described above, dMRI has the potential application to describe the anatomic connections between different parts of the brain on an individual basis. This allows the possibility to investigate white matter tracts in a non-invasive way in clinical populations such as uCP.

3.2. Findings related to motor function

Diffusion MRI (dMRI) can provide a precise measures of structural connections of the brain. Over the past years, several studies applied dMRI to investigate structure-function relationships in children with uCP. The systematic review of Mailleux et al. [81] showed that in uCP, consistent relationships were found between white matter integrity of the corticospinal tract and somatosensory pathways (e.g., thalamocortical projections, medial lemniscus) with upper limb sensorimotor function. In addition, in uCP white matter abnormalities were widespread across the brain including non-motor areas. In additional studies, lower FA (i.e., loss of coherence in the main diffusion direction due to tissue damage) and higher MD (i.e., increased free diffusion due to tissue damage) were found in the posterior limb of internal capsule (PLIC) and along the affected corticospinal tract (CST) [82, 83, 84], in thalamocortical projections, and fronto-parietal association pathways [84] of children with uCP when compared to the less affected hemisphere or the brain of typically developing children. Furthermore, tractography studies showed decreased white matter integrity in the CST, projections traversing the PLIC, thalamocortical projections, the medial lemniscus, the corpus callosum, and the corticopontocerebellar tracts of the lesioned hemisphere in children with uCP compared to the dominant hemisphere of typically developing children [85, 86, 87, 88, 83]. A summary of the main neuroimaging studies in children with uCP is provided in Table 4.

Table 4
Studies on neuroimaging in children with unilateral cerebral palsy (uCP).

Authors	N CP	MRI	Main findings
Pagnozzi et al., 2016 [65]	107 (mean age 10.9 yrs)	sMRI	· Lesion segmentation correlation to clinical outcomes
Mackey et al., 2014 [82]	20 (mean age 15 ± 3 yrs)	dMRI	· Lower FA, higher MD in the PLIC and in the affected CST
Weinstein et al., 2014 [83]	14 (mean age 10.6 ± 2.7 yrs)	dMRI	· Lower FA, higher MD in the PLIC and in the affected CST
Pannek et al., 2014 [84]	50 (range 5-17 yrs)	dMRI	· Low FA in CST, thalamocortical projections, and fronto-parietal association pathways
Fiori et al., 2015 [85]	36 (mean age 12.61 ± 3.2)	dMRI	· Disruption of structural cerebrocerebellar connectivitylinked to impaired hand function in bimanual skills
Hodge et al., 2017 [86]	28 (range 6-18 yrs)	dMRI	· Lower FA and RD associated with decreased size of CST and AHA and MA assessments
Kim et al., 2015 [87]	36 (mean age 5.6 ± 3.2 months)	dMRI	· Lower FA in CST associated with Functional Level of Hemiplegia scale
Kuczynski et al., 2017 [88]	29 (range 6-19 yrs)	dMRI	· Lower FA and higher MD, RD, and AD compared with the non-dominant hemisphere of controls · Impairments in proprioception correlated with lesioned hemisphere DCML tract
Kuczynski et al., 2018 [89]	33 (range 6-19 yrs)	dMRI	· FA, MD, RD, AD of lesioned CST correlated with visually guided reaching task performance
Weinstein et al., 2014 [83]	14 (mean age 10.6 ± 2.7 yrs)	dMRI	· Reduced WM integrity in CC, affected CST and affected PLIC related to hand function

CP, cerebral palsy; sMRI, structural MRI, dMRI, diffusion MRI; FA, fractional anisotropy; MD, mean diffusivity; RD, radial diffusivity; AD, axial diffusivity; PLIC, posterior limb of the internal capsule; CST, corticospinal tract; CC, corpus callosum; DCML, dorsal column-medial lemniscus; WM, white matter; AHA, assisting hand assessment; MA, Melbourne assessment

As highlighted in previous findings [81], most of the studies investigated the relationship between white matter integrity and motor function in children with uCP. Nevertheless, in children born very preterms dMRI findings (i.e., thalamic radiations, inferior longitudinal fasciculus, superior longitudinal fasciculus, inferior fronto-occipital fasciculus) also suggest the presence of white matter damage in brain regions not only involved in motor but also visual functions [90].

3.3. Findings related to visual and visuomotor function

Previous studies [91, 92, 93] have attempted to define a relationship between visual disorders and brain damage in children with CP. Results showed that PVL is the most common causative lesion in children with spastic CP and also frequently affects the visual pathways [94, 95, 96]. With regard to grey matter structures, damage to the thalamus has been associated with severe visual impairment [97, 98, 99, 100]; lesions to occipital-parietal areas with impairments in visual

crowding [101, 102], and reduction of the thickness of the primary visual cortex with motion perception in children with PVL [103]. The study of Tinelli et al. [96] explored the relationship between type and severity of brain lesion on sMRI and visual function in children with bilateral CP and PVL. Brain damage scores (i.e., global structural, hemispheric, and subcortical) were calculated with the semi-quantitative template of Fiori et al [62]. Visual functions were assessed with age-specific tests for fixation, smooth pursuit, saccades, nystagmus, visual acuity, visual field, stereopsis, and colour perception. For each test they provided a score of 0 if it was not compromised or 1 when there was an impairment. A visual total score was obtained from the sum of all of the items, ranging from 0 to 8. Results showed that brain lesion severity strongly correlated with visual function total score. Specifically, visual acuity, visual field, stereopsis, and colour were compromised when cortical damage was present, while fixation and saccades were affected in the presence of subcortical brain damage. Similarly, a study of Sakki et al. [9] investigated the association of brain lesions with visual function (i.e., visual acuity, visual fields, contrast sensitivity, stereopsis, visual perception, visuomotor integration) in children with VP impairments with and without CP. Results showed that approximately half of the participants had abnormalities in the frontal, temporal, or striatum areas, and approximately three quarters in the occipital or parietal areas. Cerebellar or brainstem abnormalities were present in less than a fifth of the participants. Nevertheless, no clear associations were found between regions or number of brain lesions and degree of visual acuity and contrast sensitivity. As reported by the authors, this result differs from the findings of Tinelli et al. [96] who showed that cortical and subcortical lesions strongly correlated with visual function total score. One possible explanation is that Tinelli et al. [96] used a single category of "visual dysfunction" including fixation, saccades, nystagmus, acuity, visual field, stereopsis, colour perception, whereas Sakki et al. [9] investigated acuity and contrast sensitivity separately from visuoperceptual functions. Furthermore, a previous study [92] showed that visual field defects were not always related to damage in the optic radiations or the visual cortex and the review of Philip et al. [30] reported a low correlation between MRI and different patterns of visuoperceptual deficits. Indeed, it is important to mention, that not all damage of the brain leading to visual deficits is visible on sMRI. For example, Guzzetta et al. [104] studied 26 school-aged preterm born children, among which only 13 had PVL with significant visible brain damage on structural MRI. However, all 26 children showed significantly lower perception of pure global motion relative to full-term controls, irrespective of the presence of brain damage visible on MRI [104]. The lack of association between visual skills and observed anatomical brain anomalies can be explained by the fact that conventional MRI techniques do not reveal all structural injuries within the visual pathways [99, 8]. For example, premature infants frequently suffer from diffuse white matter injury not easily detectable on anatomical images [105]. Therefore, the application of more advanced neuroimaging techniques such as dMRI can further enhance the understanding of the visuomotor system in children with uCP .

Changes in the structural and functional integrity of white matter pathways such as the optic radiations, detected by dMRI, were found to be associated with reduced visual acuity and visual perceptual dysfunctions [106, 107, 102, 108]. More specifically, abnormalities in the inferior longitudinal fasciculus have been implicated in object recognition difficulties in children with CVI [102], while abnormal white matter connections of the visual cortex to the

temporal lobe was found in individuals previously diagnosed with CVI (mean age = 17.36 years ± 3.03 SD) [108]. Furthermore, recent findings from Chandwani et al. [90] showed that CSD metrics in several white matter tracts of the visual pathways (i.e., the splenium of the corpus callosum, bilateral representations of the inferior longitudinal fasciculus, inferior fronto-occipital fasciculus, superior longitudinal fasciculus, and posterior thalamic radiations) were significantly associated with abnormal visual attention scores in very preterm infants at 3–4 months corrected age. Such results start to clarify that already at a young age the link between visual-behavioral scores and brain structures can be demonstrated. Hence, follow up of visual-behavioural outcome is crucial for determining possible biomarkers. A summary of the main studies linking neuroimaging to visual and visuomotor outcomes is provided in Table 5. Although these studies bring important insights in the relation between brain damage and visual function, this has not been specifically investigated in children with uCP.

Table 5
Studies linking neuroimaging to visual and visuomotor outcomes.

Authors	N CP	Diagnosis	MRI	Main findings
Fazzi et al., 2009 [91]	22 (range 6–15 yrs)	Preterm, PVL, spastic diplegia	sMRI	· Deficit in visual functions not related to parietal and temporal WM, or GM of area of visual associative functions
Van den Hout et al., 2004 [93]	7 (mean age 5 yrs)	Preterm, PVL	sMRI	· Lower peritrigonal WM volume · Gliosis and cortical damage associated with poorer visuo-perceptual skill
Lanzi et al., 1998 [95]	38 (range 20 m to 5 yrs)	Preterm, PVL	sMRI	· Lesions in optic radiations and calcarinecortex related to lower visual acuity
Tinelli et al., 2020 [96]	72 (mean age 3.2–14.4 yrs)	Bilateral CP and PVL	sMRI	· Impaired visual acuity, visual field, stereopsis and colour associated with cortical damage · Impaired fixation and saccades associated with subcortical brain damage
Cioni et al., 1996 [97]	80 (age not reported)	Neonatal encepha-lopathy	sMRI	· Visual acuity related to damage to visual cortex and optic radiations
Ortibus et al., 2009 [99]	70 (range 4 –20 yrs)	Preterm, CP	sMRI	· Perceptual visual impairment related to dorsal stream impairments
Ricci et al., 2006 [100]	12 (mean age 1 yr)	PVL	sMRI	· Thalami atrophy and abnormal optic radiations related to visual functions
Bhat et al., 2021 [103]	13 (mean age 11.2 ± 4.5 yrs)	Preterm, PVL spastic diplegia	sMRI	· V1 cortical thickness negatively correlated with motion coherence sensitivity
Sakki et al., 2022 [9]	28 (range 5 –15 yrs)	CVI	sMRI	· Main damage in the postgeniculate visual pathways and visual cortex · No relation between brain scores (i.e., Fiori scale) and acuity and contrast sensitivity
Guzzetta et al.,2009 [104]	26 (range 8.2–12.9 yrs)	Preterm, PVL	sMRI	· Low score on motion perception compared to controls · Ventral stream-related functions related to the presence of PVL
Bauer et al., 2014 [106]	2 (range 16 – 22 yrs)	CVI	dMRI	· Lower density of WM in inferior frontal-occipital fasciculus and superior and inferior longitudinal fasciculi
Ortibus et al., 2012 [102]	11 (range 3y5mo–13 yrs)	CVI	dMRI	· Lower FA in the inferior longitudinal fasciculus related to impaired object recognition
Pamir et al., 2021 [108]	12 (range 14 –24 yrs)	CVI	dMRI	· Higher RD within cortico-cortical but not thalamo-hMT+ connections
Chandwani et al., 2022 [90]	191 (3–4 m corrected age)	Very preterm	sMRI dMRI	· FDC of the left posterior thalamic radiations, left inferior longitudinal fasciculus, right superior longitudinal fasciculus, and left inferior fronto occipital fasciculus associated with visual attention scores

CP, cerebral palsy; PVL, periventricular leukomalacia; CVI, cerebral visual impairment; sMRI, structural MRI, dMRI, diffusion MRI; FA, fractional anisotropy; RD, radial diffusivity; FDC, fibre density and bundle cross-section; hMT+, human middle temporal complex; WM, white matter; GW, grey matter

4. Conclusion and gaps

In sum, children with uCP are not only affected by their motor impairment, but they also present with heterogeneous visual dysfunctions, that potentially further impact their already compromised manual function.
Whereas the motor part of the clinical picture of children with uCP has been extensively studied, the visual deficits have not been systematically mapped and certainly, the relation between brain damage and visual dysfunction and the interplay with visuomotor function remains to be elucidated.
Previous findings showed that children with uCP have impairments in oculomotor, geniculostriate functions, visual perceptual, and visuomotor functions. Neuroimaging findings revealed that PVL is the most common structural brain lesion in children with uCP. With regard to dMRI, findings are mainly focused on children with CVI, showing lesions in the optic radiations and inferior longitudinal fasciculus and on very preterm infants conditions. Hence, research investigating which brain regions and tracts are implicated in specific visual functions and deficits in children with uCP is limited.
To our knowledge, no previous work has systematically and comprehensively mapped the neurological correlates (i.e., sMRI and dMRI) of the visual and visuomotor dysfunction in children with CP. Since little is known about the relevance of non-motor pathways, further studies are needed to investigate the contribution of visual pathway to visuomotor function in children with uCP.

Acknowledgments

This work was supported by the project: "PARENT" funded by the European Union's Horizon 2020 Project MSCA-ITN-2020 – Innovative Training Networks Grant No. 956394.

References

[1] J.-A. Quinn, F. M. Munoz, B. Gonik, L. Frau, C. Cutland, T. Mallett-Moore, A. Kissou, F. Wittke, M. Das, T. Nunes, et al., Preterm birth: Case definition & guidelines for data collection, analysis, and presentation of immunisation safety data, Vaccine 34 (2016) 6047–6056.
[2] F. Soleimani, F. Zaheri, F. Abdi, Long-term neurodevelopmental outcomes after preterm birth, Iran. Red Crescent Med. J. 16 (2014) e17965.
[3] W. Sapp, Visual impairment, in: International Encyclopedia of Education, Elsevier, 2010, pp. 880–885.
[4] A. Zamani, A. Karimi, M. Naseri, E. Amini, M. Milani, A. A. Sazgar, S. M. S. Hosseini, M. S. H. Abadi, F. Nayeri, F. Nili, et al., Prevalence of hearing loss among high risk newborns hospitalized in hospitals affiliated to tehran university of medical sciences., Tehran University Medical Journal 68 (2010).
[5] S. H. Ingvaldsen, T. S. Morken, D. Austeng, O. Dammann, Visuopathy of prematurity: is retinopathy just the tip of the iceberg?, Pediatr. Res. 91 (2022) 1043–1048.

[6] J. S. Rahi, N. Cable, British Childhood Visual Impairment Study Group, Severe visual impairment and blindness in children in the UK, Lancet 362 (2003) 1359–1365.
[7] H. E. A. Sakki, N. J. Dale, J. Sargent, T. Perez-Roche, R. Bowman, Is there consensus in defining childhood cerebral visual impairment? a systematic review of terminology and definitions, Br. J. Ophthalmol. 102 (2018) 424–432.
[8] E. Ortibus, E. Fazzi, N. Dale, Cerebral visual impairment and clinical assessment: The european perspective, Semin. Pediatr. Neurol. 31 (2019) 15–24.
[9] H. Sakki, N. J. Dale, K. Mankad, J. Sargent, G. Talenti, R. Bowman, Exploratory investigation of brain mri lesions according to whole sample and visual function subtyping in children with cerebral visual impairment, Frontiers in human neuroscience 15 (2021).
[10] P. García, L. San Feliciano, F. Benito, R. García, J. Guzmán, S. Salas, C. Fernández, N. Del Prado, D. Ciprián, J. Figueras, hospitales pertenecientes a SEN1500, Evolución a los 2 años de edad corregida de una cohorte de recién nacidos con peso inferior o igual a 1.500 g de los hospitales pertenecientes a la red neonatal SEN1500, An. Pediatr. (Barc.) 79 (2013) 279–287.
[11] M. Oskoui, F. Coutinho, J. Dykeman, N. Jetté, T. Pringsheim, An update on the prevalence of cerebral palsy: a systematic review and meta-analysis, Dev. Med. Child Neurol. 55 (2013) 509–519.
[12] M. Stavsky, O. Mor, S. A. Mastrolia, S. Greenbaum, N. G. Than, O. Erez, Cerebral palsy-trends in epidemiology and recent development in prenatal mechanisms of disease, treatment, and prevention, Front. Pediatr. 5 (2017) 21.
[13] A. Pascal, P. Govaert, A. Oostra, G. Naulaers, E. Ortibus, C. Van den Broeck, Neurodevelopmental outcome in very preterm and very-low-birthweight infants born over the past decade: a meta-analytic review, Dev. Med. Child Neurol. 60 (2018) 342–355.
[14] P. Rosenbaum, N. Paneth, A. Leviton, M. Goldstein, M. Bax, D. Damiano, B. Dan, B. Jacobsson, et al., A report: the definition and classification of cerebral palsy april 2006, Dev Med Child Neurol Suppl 109 (2007) 8–14.
[15] E. Fazzi, S. G. Signorini, R. LA Piana, C. Bertone, W. Misefari, J. Galli, U. Balottin, P. E. Bianchi, Neuro-ophthalmological disorders in cerebral palsy: ophthalmological, oculomotor, and visual aspects, Dev. Med. Child Neurol. 54 (2012) 730–736.
[16] A. J. Schenk-Rootlieb, O. van Nieuwenhuizen, P. F. van Waes, Y. van der Graaf, Cerebral visual impairment in cerebral palsy: relation to structural abnormalities of the cerebrum, Neuropediatrics 25 (1994) 68–72.
[17] S. A. Mutalib, M. Mace, H. T. Ong, E. Burdet, Influence of visual-coupling on bimanual coordination in unilateral spastic cerebral palsy, in: 2019 IEEE 16th International Conference on Rehabilitation Robotics (ICORR), IEEE, 2019.
[18] F. R. Sarlegna, R. L. Sainburg, The roles of vision and proprioception in the planning of reaching movements, in: Advances in Experimental Medicine and Biology, Advances in experimental medicine and biology, Springer US, Boston, MA, 2009, pp. 317–335.
[19] C. Cans, Surveillance of cerebral palsy in europe: a collaboration of cerebral palsy surveys and registers, Dev. Med. Child Neurol. 42 (2007) 816–824.
[20] A. Papavasiliou, H. Ben-Pazi, S. Mastroyianni, E. Ortibus, Cerebral palsy: New developments, Frontiers in Neurology 12 (2021).
[21] K. Klingels, I. Demeyere, E. Jaspers, P. De Cock, G. Molenaers, R. Boyd, H. Feys, Upper

limb impairments and their impact on activity measures in children with unilateral cerebral palsy, Eur. J. Paediatr. Neurol. 16 (2012) 475–484.
[22] K. Himmelmann, P. Uvebrant, The panorama of cerebral palsy in sweden. XI. changing patterns in the birth-year period 2003-2006, Acta Paediatr. 103 (2014) 618–624.
[23] F. Hadzagic-Catibusic, E. Avdagic, S. Zubcevic, S. Uzicanin, Brain lesions in children with unilateral spastic cerebral palsy, Med. Arch. 71 (2017) 7–11.
[24] C. Simon-Martinez, E. Jaspers, L. Mailleux, E. Ortibus, K. Klingels, N. Wenderoth, H. Feys, Corticospinal tract wiring and brain lesion characteristics in unilateral cerebral palsy: Determinants of upper limb motor and sensory function, Neural Plast. 2018 (2018) 2671613.
[25] Y.-C. Hung, J. Charles, A. M. Gordon, Bimanual coordination during a goal-directed task in children with hemiplegic cerebral palsy, Dev. Med. Child Neurol. 46 (2007) 746–753.
[26] A. Ego, K. Lidzba, P. Brovedani, V. Belmonti, S. Gonzalez-Monge, B. Boudia, A. Ritz, C. Cans, Visual-perceptual impairment in children with cerebral palsy: a systematic review, Dev. Med. Child Neurol. 57 Suppl 2 (2015) 46–51.
[27] G. N. Dutton, 'dorsal stream dysfunction' and 'dorsal stream dysfunction plus': a potential classification for perceptual visual impairment in the context of cerebral visual impairment?, Dev. Med. Child Neurol. 51 (2009) 170–172.
[28] D. J. Swienton, A. G. Thomas, The visual pathway–functional anatomy and pathology, Semin. Ultrasound CT MR 35 (2014) 487–503.
[29] L. L. Cloutman, Interaction between dorsal and ventral processing streams: where, when and how?, Brain Lang. 127 (2013) 251–263.
[30] S. S. Philip, G. N. Dutton, Identifying and characterising cerebral visual impairment in children: a review, Clin. Exp. Optom. 97 (2014) 196–208.
[31] R. Benini, L. Dagenais, M. I. Shevell, Registre de la Paralysie Cérébrale au Québec (Quebec Cerebral Palsy Registry) Consortium, Normal imaging in patients with cerebral palsy: what does it tell us?, J. Pediatr. 162 (2013) 369–74.e1.
[32] L. Pisella, F. Binkofski, K. Lasek, I. Toni, Y. Rossetti, No double-dissociation between optic ataxia and visual agnosia: multiple sub-streams for multiple visuo-manual integrations, Neuropsychologia 44 (2006) 2734–2748.
[33] F. Binkofski, L. J. Buxbaum, Two action systems in the human brain, Brain and language 127 (2013) 222–229.
[34] G. Rizzolatti, M. Matelli, Two different streams form the dorsal visual system: anatomy and functions, Experimental brain research 153 (2003) 146–157.
[35] R. C. Leiguarda, C. D. Marsden, Limb apraxias: higher-order disorders of sensorimotor integration, Brain 123 (2000) 860–879.
[36] T. Yamasaki, H. Muranaka, Y. Kaseda, Y. Mimori, S. Tobimatsu, Understanding the pathophysiology of alzheimer's disease and mild cognitive impairment: A mini review on fmri and erp studies, Neurology research international 2012 (2012).
[37] I. P. Howard, B. J. Rogers, et al., Binocular vision and stereopsis, Oxford University Press, USA, 1995.
[38] D. Purves, G. J. Augustine, D. Fitzpatrick, L. C. Katz, A.-S. LaMantia, J. O. McNamara, S. M. Williams, et al., Types of eye movements and their functions, Neuroscience 20 (2001) 361–390.

[39] N. Ben Itzhak, K. Vancleef, I. Franki, A. Laenen, J. Wagemans, E. Ortibus, Quantifying visuoperceptual profiles of children with cerebral visual impairment, Child Neuropsychology 27 (2021) 995–1023.
[40] N. Kozeis, A. Anogeianaki, D. T. Mitova, G. Anogianakis, T. Mitov, A. Klisarova, Visual function and visual perception in cerebral palsied children, Ophthalmic Physiol. Opt. 27 (2007) 44–53.
[41] R. P. Colarusso, D. D. Hammill, Motor-free visual perception test, Academic Therapy Pub., 1972.
[42] E. Fazzi, S. M. Bova, C. Uggetti, S. G. Signorini, P. E. Bianchi, I. Maraucci, M. Zoppello, G. Lanzi, Visual-perceptual impairment in children with periventricular leukomalacia, Brain Dev. 26 (2004) 506–512.
[43] M. Auld, R. Boyd, G. L. Moseley, L. Johnston, Seeing the gaps: a systematic review of visual perception tools for children with hemiplegia, Disabil. Rehabil. 33 (2011) 1854–1865.
[44] C. Menken, S. A. Cermak, A. Fisher, Evaluating the visual-perceptual skills of children with cerebral palsy, Am. J. Occup. Ther. 41 (1987) 646–651.
[45] L.-T. Tsai, K.-C. Lin, H.-F. Liao, C.-L. Hsieh, Reliability of two visual-perceptual tests for children with cerebral palsy, Am. J. Occup. Ther. 63 (2009) 473–480.
[46] D. D. Hammill, N. A. Pearson, J. K. Voress, DTVP-3: Developmental test of visual perception, Pro-ed, 2014.
[47] P. A. Burtner, A. Dukeminier, B. Lynette, C. Qualls, K. Scott, Visual perceptual skills and related school functions in children with hemiplegic cerebal palsy, New Zealand Journal of Occupational Therapy 53 (2006) 24–29.
[48] S. Berelowitz, D. Franzsen, Visual perceptual deficits in different types of cerebral palsy, S. Afr. J. Occup. Ther. 51 (2021).
[49] J. P. Wann, The integrity of visual-proprioceptive mapping in cerebral palsy, Neuropsychologia 29 (1991) 1095–1106.
[50] A. M. Gordon, J. Charles, B. Steenbergen, Fingertip force planning during grasp is disrupted by impaired sensorimotor integration in children with hemiplegic cerebral palsy, Pediatr. Res. 60 (2006) 587–591.
[51] S. James, J. Ziviani, R. S. Ware, R. N. Boyd, Relationships between activities of daily living, upper limb function, and visual perception in children and adolescents with unilateral cerebral palsy, Dev. Med. Child Neurol. 57 (2015) 852–857.
[52] J. Verrel, H. Bekkering, B. Steenbergen, Eye-hand coordination during manual object transport with the affected and less affected hand in adolescents with hemiparetic cerebral palsy, Exp. Brain Res. 187 (2008) 107–116.
[53] B. Steenbergen, W. Hulstijn, A. de Vries, M. Berger, Bimanual movement coordination in spastic hemiparesis, Exp. Brain Res. 110 (1996) 91–98.
[54] S. M. Surkar, R. M. Hoffman, B. Davies, R. Harbourne, M. J. Kurz, Impaired anticipatory vision and visuomotor coordination affects action planning and execution in children with hemiplegic cerebral palsy, Res. Dev. Disabil. 80 (2018) 64–73.
[55] I. Krägeloh-Mann, V. Horber, The role of magnetic resonance imaging in elucidating the pathogenesis of cerebral palsy: a systematic review, Dev. Med. Child Neurol. 49 (2007) 144–151.
[56] J. B. De Vis, J. Hendrikse, E. T. Petersen, L. S. de Vries, F. van Bel, T. Alderliesten, S. Negro,

F. Groenendaal, M. J. Benders, Arterial spin-labelling perfusion mri and outcome in neonates with hypoxic-ischemic encephalopathy, European radiology 25 (2015) 113–121.
[57] M. Rutherford, C. Malamateniou, A. McGuinness, J. Allsop, M. M. Biarge, S. Counsell, Magnetic resonance imaging in hypoxic-ischaemic encephalopathy, Early Hum. Dev. 86 (2010) 351–360.
[58] N. Tusor, T. Arichi, S. J. Counsell, A. D. Edwards, Brain development in preterm infants assessed using advanced MRI techniques, Clin. Perinatol. 41 (2014) 25–45.
[59] K. Himmelmann, V. Horber, J. De La Cruz, K. Horridge, V. Mejaski-Bosnjak, K. Hollody, I. Krägeloh-Mann, SCPE Working Group, MRI classification system (MRICS) for children with cerebral palsy: development, reliability, and recommendations, Dev. Med. Child Neurol. 59 (2017) 57–64.
[60] S. J. Korzeniewski, G. Birbeck, M. C. DeLano, M. J. Potchen, N. Paneth, A systematic review of neuroimaging for cerebral palsy, J. Child Neurol. 23 (2008) 216–227.
[61] I. Franki, L. Mailleux, L. Emsell, M.-L. Peedima, A. Fehrenbach, H. Feys, E. Ortibus, The relationship between neuroimaging and motor outcome in children with cerebral palsy: A systematic review - part a. structural imaging, Res. Dev. Disabil. 100 (2020) 103606.
[62] S. Fiori, G. Cioni, K. Klingels, E. Ortibus, L. Van Gestel, S. Rose, R. N. Boyd, H. Feys, A. Guzzetta, Reliability of a novel, semi-quantitative scale for classification of structural brain magnetic resonance imaging in children with cerebral palsy, Dev. Med. Child Neurol. 56 (2014) 839–845.
[63] A. C. Evans, A. L. Janke, D. L. Collins, S. Baillet, Brain templates and atlases, Neuroimage 62 (2012) 911–922.
[64] T. V. Phan, D. Smeets, J. B. Talcott, M. Vandermosten, Processing of structural neuroimaging data in young children: Bridging the gap between current practice and state-of-the-art methods, Dev. Cogn. Neurosci. 33 (2018) 206–223.
[65] A. M. Pagnozzi, N. Dowson, J. Doecke, S. Fiori, A. P. Bradley, R. N. Boyd, S. Rose, Automated, quantitative measures of grey and white matter lesion burden correlates with motor and cognitive function in children with unilateral cerebral palsy, NeuroImage Clin. 11 (2016) 751–759.
[66] L. Krumlinde-Sundholm, M. Holmefur, A. Kottorp, A.-C. Eliasson, The assisting hand assessment: current evidence of validity, reliability, and responsiveness to change, Dev. Med. Child Neurol. 49 (2007) 259–264.
[67] D. Le Bihan, Looking into the functional architecture of the brain with diffusion MRI, Nat. Rev. Neurosci. 4 (2003) 469–480.
[68] B. Jeurissen, J.-D. Tournier, T. Dhollander, A. Connelly, J. Sijbers, Multi-tissue constrained spherical deconvolution for improved analysis of multi-shell diffusion MRI data, Neuroimage 103 (2014) 411–426.
[69] D. Le Bihan, J. F. Mangin, C. Poupon, C. A. Clark, S. Pappata, N. Molko, H. Chabriat, Diffusion tensor imaging: concepts and applications, J. Magn. Reson. Imaging 13 (2001) 534–546.
[70] C. Pierpaoli, S. Marenco, G. Rohde, D. Jones, A. Barnett, Analyzing the contribution of cardiac pulsation to the variability of quantities derived from the diffusion tensor, in: Proceedings of the 11th Annual Meeting of ISMRM, Toronto, Canada, Citeseer, 2003, p. 70.

[71] M. M. Bahn, Comparison of scalar measures used in magnetic resonance diffusion tensor imaging, J. Magn. Reson. 139 (1999) 1–7.
[72] A. L. Alexander, K. M. Hasan, M. Lazar, J. S. Tsuruda, D. L. Parker, Analysis of partial volume effects in diffusion-tensor MRI, Magn. Reson. Med. 45 (2001) 770–780.
[73] J.-D. Tournier, F. Calamante, D. G. Gadian, A. Connelly, Direct estimation of the fiber orientation density function from diffusion-weighted MRI data using spherical deconvolution, Neuroimage 23 (2004) 1176–1185.
[74] A. M. Auriat, M. R. Borich, N. J. Snow, K. P. Wadden, L. A. Boyd, Comparing a diffusion tensor and non-tensor approach to white matter fiber tractography in chronic stroke, NeuroImage Clin. 7 (2015) 771–781.
[75] Y. D. Reijmer, A. Leemans, S. M. Heringa, I. Wielaard, B. Jeurissen, H. L. Koek, G. J. Biessels, Vascular Cognitive Impairment Study group, Improved sensitivity to cerebral white matter abnormalities in alzheimer's disease with spherical deconvolution based tractography, PLoS One 7 (2012) e44074.
[76] J.-D. Tournier, F. Calamante, A. Connelly, Robust determination of the fibre orientation distribution in diffusion MRI: non-negativity constrained super-resolved spherical deconvolution, Neuroimage 35 (2007) 1459–1472.
[77] M. Lazar, Mapping brain anatomical connectivity using white matter tractography, NMR Biomed. 23 (2010) 821–835.
[78] J.-D. Tournier, S. Mori, A. Leemans, Diffusion tensor imaging and beyond, Magn. Reson. Med. 65 (2011) 1532–1556.
[79] S. Mori, W. E. Kaufmann, C. Davatzikos, B. Stieltjes, L. Amodei, K. Fredericksen, G. D. Pearlson, E. R. Melhem, M. Solaiyappan, G. V. Raymond, H. W. Moser, P. C. M. van Zijl, Imaging cortical association tracts in the human brain using diffusion-tensor-based axonal tracking, Magn. Reson. Med. 47 (2002) 215–223.
[80] T. E. J. Behrens, H. J. Berg, S. Jbabdi, M. F. S. Rushworth, M. W. Woolrich, Probabilistic diffusion tractography with multiple fibre orientations: What can we gain?, Neuroimage 34 (2007) 144–155.
[81] L. Mailleux, I. Franki, L. Emsell, M.-L. Peedima, A. Fehrenbach, H. Feys, E. Ortibus, The relationship between neuroimaging and motor outcome in children with cerebral palsy: A systematic review-part B diffusion imaging and tractography, Res. Dev. Disabil. 97 (2020) 103569.
[82] A. Mackey, C. Stinear, S. Stott, W. D. Byblow, Upper limb function and cortical organization in youth with unilateral cerebral palsy, Frontiers in neurology 5 (2014) 117.
[83] M. Weinstein, D. Green, R. Geva, M. Schertz, A. Fattal-Valevski, M. Artzi, V. Myers, S. Shiran, A. M. Gordon, V. Gross-Tsur, D. B. Bashat, Interhemispheric and intrahemispheric connectivity and manual skills in children with unilateral cerebral palsy, Brain Struct. Funct. 219 (2014) 1025–1040.
[84] K. Pannek, R. N. Boyd, S. Fiori, A. Guzzetta, S. E. Rose, Assessment of the structural brain network reveals altered connectivity in children with unilateral cerebral palsy due to periventricular white matter lesions, NeuroImage Clin. 5 (2014) 84–92.
[85] S. Fiori, K. Pannek, R. Pasquariello, R. S. Ware, G. Cioni, S. E. Rose, R. N. Boyd, A. Guzzetta, Corticopontocerebellar connectivity disruption in congenital hemiplegia, Neurorehabil. Neural Repair 29 (2015) 858–866.

[86] J. Hodge, B. Goodyear, H. Carlson, X.-C. Wei, A. Kirton, Segmental diffusion properties of the corticospinal tract and motor outcome in hemiparetic children with perinatal stroke, J. Child Neurol. 32 (2017) 550–559.
[87] J. H. Kim, Y. M. Kwon, S. M. Son, Motor function outcomes of pediatric patients with hemiplegic cerebral palsy after rehabilitation treatment: a diffusion tensor imaging study, Neural Regen. Res. 10 (2015) 624–630.
[88] A. M. Kuczynski, H. L. Carlson, C. Lebel, J. A. Hodge, S. P. Dukelow, J. A. Semrau, A. Kirton, Sensory tractography and robot-quantified proprioception in hemiparetic children with perinatal stroke, Hum. Brain Mapp. 38 (2017) 2424–2440.
[89] A. M. Kuczynski, S. P. Dukelow, J. A. Hodge, H. L. Carlson, C. Lebel, J. A. Semrau, A. Kirton, Corticospinal tract diffusion properties and robotic visually guided reaching in children with hemiparetic cerebral palsy, Hum. Brain Mapp. 39 (2018) 1130–1144.
[90] R. Chandwani, K. Harpster, J. E. Kline, V. Mehta, H. Wang, S. L. Merhar, T. L. Schwartz, N. A. Parikh, Brain microstructural antecedents of visual difficulties in infants born very preterm, NeuroImage Clin. 34 (2022) 102987.
[91] E. Fazzi, S. Bova, A. Giovenzana, S. Signorini, C. Uggetti, P. Bianchi, Cognitive visual dysfunctions in preterm children with periventricular leukomalacia, Dev. Med. Child Neurol. 51 (2009) 974–981.
[92] A. Guzzetta, E. Mercuri, G. Cioni, Visual disorders in children with brain lesions: 2. visual impairment associated with cerebral palsy, Eur. J. Paediatr. Neurol. 5 (2001) 115–119.
[93] B. M. van den Hout, L. S. de Vries, L. C. Meiners, P. Stiers, Y. T. van der Schouw, A. Jennekens-Schinkel, D. Wittebol-Post, D. van der Linde, E. Vandenbussche, O. van Nieuwenhuizen, Visual perceptual impairment in children at 5 years of age with perinatal haemorrhagic or ischaemic brain damage in relation to cerebral magnetic resonance imaging, Brain Dev. 26 (2004) 251–261.
[94] L. K. Jacobson, G. N. Dutton, Periventricular leukomalacia, Surv. Ophthalmol. 45 (2000) 1–13.
[95] G. Lanzi, E. Fazzi, C. Uggetti, A. Cavallini, S. Danova, M. G. Egitto, O. F. Ginevra, R. Salati, P. E. Bianchi, Cerebral visual impairment in periventricular leukomalacia, Neuropediatrics 29 (1998) 145–150.
[96] F. Tinelli, A. Guzzetta, G. Purpura, R. Pasquariello, G. Cioni, S. Fiori, Structural brain damage and visual disorders in children with cerebral palsy due to periventricular leukomalacia, NeuroImage Clin. 28 (2020) 102430.
[97] G. Cioni, B. Fazzi, A. E. Ipata, R. Canapicchi, J. v. H.-v. Duin, Correction between cerebral visual impairment and magnetic resonance imaging in children with neonatal encephalopathy, Dev. Med. Child Neurol. 38 (2008) 120–132.
[98] L. B. Merabet, D. L. Mayer, C. M. Bauer, D. Wright, B. S. Kran, Disentangling how the brain is "wired" in cortical (cerebral) visual impairment, Semin. Pediatr. Neurol. 24 (2017) 83–91.
[99] E. Ortibus, L. Lagae, I. Casteels, P. Demaerel, P. Stiers, Assessment of cerebral visual impairment with the L94 visual perceptual battery: clinical value and correlation with MRI findings, Dev. Med. Child Neurol. 51 (2009) 209–217.
[100] D. Ricci, S. Anker, F. Cowan, M. Pane, F. Gallini, R. Luciano, V. Donvito, G. Baranello, L. Cesarini, F. Bianco, M. Rutherford, C. Romagnoli, J. Atkinson, O. Braddick, F. Guzzetta,

E. Mercuri, Thalamic atrophy in infants with PVL and cerebral visual impairment, Early Hum. Dev. 82 (2006) 591–595.
[101] S. R. Drummond, G. N. Dutton, Simultanagnosia following perinatal hypoxia: a possible pediatric variant of balint syndrome, J. AAPOS 11 (2007) 497–498.
[102] E. Ortibus, J. Verhoeven, S. Sunaert, I. Casteels, P. de Cock, L. Lagae, Integrity of the inferior longitudinal fasciculus and impaired object recognition in children: a diffusion tensor imaging study, Dev. Med. Child Neurol. 54 (2012) 38–43.
[103] A. Bhat, L. Biagi, G. Cioni, F. Tinelli, M. C. Morrone, Cortical thickness of primary visual cortex correlates with motion deficits in periventricular leukomalacia, Neuropsychologia 151 (2021) 107717.
[104] A. Guzzetta, F. Tinelli, M. M. Del Viva, A. Bancale, R. Arrighi, R. R. Pascale, G. Cioni, Motion perception in preterm children: role of prematurity and brain damage, Neuroreport 20 (2009) 1339–1343.
[105] J. J. Volpe, Cerebral white matter injury of the premature infant-more common than you think, Pediatrics 112 (2003) 176–176.
[106] C. M. Bauer, G. Heidary, B.-B. Koo, R. J. Killiany, P. Bex, L. B. Merabet, Abnormal white matter tractography of visual pathways detected by high-angular-resolution diffusion imaging (HARDI) corresponds to visual dysfunction in cortical/cerebral visual impairment, J. AAPOS 18 (2014) 398–401.
[107] F. H. Boot, J. J. M. Pel, J. van der Steen, H. M. Evenhuis, Cerebral visual impairment: which perceptive visual dysfunctions can be expected in children with brain damage? a systematic review, Res. Dev. Disabil. 31 (2010) 1149–1159.
[108] Z. Pamir, C. M. Bauer, E. S. Bailin, P. J. Bex, D. C. Somers, L. B. Merabet, Neural correlates associated with impaired global motion perception in cerebral visual impairment (CVI), NeuroImage Clin. 32 (2021) 102821.

A. Online Resources

- SCPE Reference and Training manual
- Creative Commons Attribution License

Particle image velocimetry image processing to assess cell distribution within bioreactors

Michele Pistillo[1,*,†], Margherita Scamarcio[1,†], Federica Liguori[1,†], Maurizio Mastantuono[1,†], Simona Gramazio[2,†], Alfredo Ambrico[3,†], Rosaria Alessandra Magarelli[3,†], Maria Martino[3,†], Mario Trupo[3,†], Miriam Merco[4,†], Mario Ledda[4,†] and Giuseppe Falvo D'urso Labate[1,†]

[1]*Cellex Srl, Piazzale delle Belle Arti, 2 00196 Rome, Italy*

[2]*AKKA Technologies Italy, Life Sciences division, via Enrico Tazzoli 215/12b 10137 Torino*

[3]*Italian National Agency for New Technologies, Energy and Sustainable Economic Development (ENEA), Trisaia Research Centre SS 106 Jonica, Km 419+500, 75026 Rotondella (Matera), Italy*

[4] *Institute of Translational Pharmacology, National Research Council (CNR), Via Fosso del Cavaliere 100, 00133 Rome, Italy*

Abstract

Cell cultures suspended in bioreactors in a fluid environment are the basis for cell expansion and important medical products manufacturing. Assessing local cell distribution within bioreactors may provide information to increase cell production efficiency. Hydrodynamics characterizations of bioreactors are typically performed via Particle Image Velocimetry (PIV) with fluorescent polystyrene microspheres or Computational Fluid Dynamics (CFD), while local cell distribution is monitored through expensive sensors or direct sampling. However, PIV and CFD analysis lack of cell behaviour representativity, while direct sampling give average and local information and may impact cell culture conditions. In this study a novel non-invasive method, focusing on the optical investigation of suspended fluorescent nanoparticles (NPs) -labelled Chinese hamster ovary (CHO) cells distribution within SUSPENCE® bioreactor through PIV image processing, is presented. Our investigation showcases the favourable effect of an innovative NPs internalisation approach in terms of cellular uptake efficiency and fluorescence brightness. Moreover, NPs-labelled CHO cells (NP-CHO) PIV image processing and analysis robustness is validated by cell sampling and sample processing. Furthermore, the turbulent kinetic energy distribution to gain insight of the impact of hydrodynamic conditions on cell culture is evaluated.

Keywords

Biomedical image processing, Particle Image Velocimetry, Bioreactors, Nanoparticles

DETERMINED 2022: Neurodevelopmental Impairments in Preterm Children — Computational Advancements, August 26, 2022, Ljubljana, Slovenia

*Corresponding author.

† These authors contributed equally.

michelepistillo94@gmail.com (M. Pistillo); margherita.scamarcio@cellex.it (M. Scamarcio); federica.liguori@cellex.it (F. Liguori); maurizio.mastantuono85@gmail.com (M. Mastantuono); Simona.GRAMAZIO@akka.eu (S. Gramazio); alfredo.ambrico@enea.it (A. Ambrico); rosaria.magarelli@enea.it (R. A. Magarelli); maria.martino@enea.it (M. Martino); mario.trupo@enea.it (M. Trupo); Miriam.merco.15@gmail.com (M. Merco); mario.ledda@ift.cnr.it (M. Ledda); management@cellex.it (G. Falvo D'urso Labate)

0000-0002-8487-9723 (A. Ambrico); 0000-0001-5419-62543 (R. A. Magarelli); 0000-0002-2640-050X (M. Trupo)

© 2022 Copyright for this paper by its authors. Use permitted under Creative Commons License Attribution 4.0 International (CC BY 4.0).

CEUR Workshop Proceedings (CEUR-WS.org)

CEUR-WS.org/Vol-3363/paper07.pdf

1. Introduction

Bioreactors have become fundamental devices in the biomedical industry since they are employed in different fields such as tissue engineering and cell-based therapies [1]. The use of bioreactor for suspension cells culture gives many potential advantages over the static cell culture, including homogeneity of cell conditions, possibility of sampling, automated systems for controlling parameters such as pH, temperature and dissolved oxygen concentration, thus allowing to obtain very high cell densities [2].
Assessing cell and nutrients distribution and fluid flow field is important to evaluate bioreactors performances. In this regard, in the current study turbulent kinetic energy (TKE), a fluid dynamic parameter, and cell concentration distribution have been determined. A homogeneous distribution of all components inside bioreactors, including cells, is a key property to promote nutrients exchange and to avoid cell deposition and local cell accumulation, thus increasing cell growth [3]. On the other hand, TKE is a fluid parameter often employed to evaluate bioreactors mixing mechanisms [4]. As regards to evaluate fluid flow field inside bioreactors, Particle Image Velocimetry (PIV) is a technique used to investigate fluid parameter such as flow pattern information, velocity field and local energy dissipation rates. PIV experimentations are usually conducted using a fluid model composed by water and specific fluorescent tracking particles. Also, through PIV it is possible to study the fluid dynamic characteristics inside bioreactors for cell culture [4]. However, even though tracking particles may possess the same size and density of living cells they not have the same biological properties, so they are unable to mimic the cell behaviour inside cell culture chambers.
Premature new-born children strongly risk to develop health problems in childhood and adolescence, early diagnostics are fundamental to prevent and ensure the welfare of the child [5]. Different cell types can be analysed in newborns, for instance studies have shown the role of nasal epithelial cells in neonates with asthma and allergic rhinitis and so their impact on respiratory disease in adulthood [6]. Another example is represented by peripheral blood mononuclear cells from umbilical cord blood of premature born babies, that can be cultured in bioreactors for suspended cell culture and that can be employed to investigate inflammatory processes that are a cornerstone of pathophysiology in the developing organs of preterm born children [7][8]. As it is reported in the mentioned studies, the improvement in cell culture through the employment of bioreactors will lead to obtain a higher number of cells and a higher amount of biomolecules production compared to static cell culture, thus facilitating the downstream early diagnosis processes for preterm new-borns. In the current study, CHO cells were tested with the possibility of extending the same analysis to other cell types.
In this study a novel non-invasive method has been developed, focusing on the optical investigation of suspended fluorescent nanoparticles (NPs) -labelled Chinese hamster ovary (CHO) cells distribution within SUSPENCE® bioreactor, through PIV image processing. PMMA-FluoRed-COOH NPs were internalized by CHO cells and the experiments were conducted using cell culture medium as the liquid phase. Moreover, NPs-labelled CHO cells (NP-CHO) distribution analysis robustness was confirmed by comparing it to direct cell sampling measurements.
The current work is structured as follows. Section 2.1 describes how cell culture was performed, both in static and in dynamic conditions. In section 2.2 cell label techniques and NPs internalisation inside cells methods are presented (results reported in Section 3.1). In section 2.3

the experimental setup used for PIV images acquisition of NP-CHO, including bioreactor set up and PIV system description, are reported. Section 2.4 describes the techniques used for PIV-images post processing: firstly the algorithm used for background noise reduction and then the methods employed for cell and TKE distribution estimation (results reported in Section 3.2).

2. Materials and Methods

2.1. Cell culture

In recent years, NPs have gained increasing interest in various research fields, especially in the biotechnological and biomedical fields [9]. Moreover, fluorescent NPs can be internalised by living cells, and their uptake can be assessed via fluorescence microscopy, at the same light wavelength emitted by tracer particles used for PIV analysis [10] [9]. Methods to obtain NPs internalisation within CHO cells growth in adherence can be easily found in literature [11]. For these reasons, and since the aim of this work was to study cell distribution within a bioreactor for cell growth in suspension via PIV, we choose to use NPs to label CHO cells, firstly starting from CHOs growth in adherence and subsequently with CHOs growth in suspension.

2.1.1. Adherence cell culture

CHO cells (American Type Culture Collection) were grown in Corning® TC-Treated Multiple Well Plates using Ham's F-12K (Kaighn's) medium supplemented with 10 % heat-inactivated fetal bovine serum (FBS, Euroclone), 2 mM L-glutamine (Sigma), 1.0 unit ml1 penicillin (Sigma), and 1.0 mg-1 streptomycin (Sigma). The cell line was cultured on a plastic Petri dish at 37°C in a humidified incubator containing 5% CO2.

2.1.2. Suspension cell culture

The content of one vial from the cryopreserved CHO cell bank was thawed and suspended in 80 mL pre-warmed CD FORTI CHO medium (Thermo Fisher) supplemented with 4 mM L-glutamine (Biowest, France) and 1% Penicillin/Streptomycin (GE Healthcare Bio-Sciences, Sweden). The CHO suspension was grown in ventilate Erlenmeyer flask and kept in a shaker incubator (80-85 RPM) at 37°C and with 5-7% CO2 for 96 hours.

2.2. Cell labelling and nanoparticles internalisation inside cells

2.2.1. Fluorescent nanoparticles cell internalisation

Red-fluorescent monodisperse polymethylmethacrylate carboxylated particles (microParticles Gmbh, Germany) with a mean diameter of 286 nm (PMMA-FluoRed-COOH, SD = 7nm, abs/em = 530/607 nm, COOH >30 μmol/g) were used to stain cells. The internalisation of NPs in CHO cells grown in adherence was performed as follow: firstly, cells were seeded in a Corning® TC-Treated Multiple Well Plates, where each well contained 3mL of suspended cells at a cell concentration of $8{,}33 \cdot 10^5$ cells/mL. A 0,0025 g/mL NPs starting solution was obtained by diluting PMMA-FluoRed-COOH stock solution at room temperature with cell culture medium.

0,1 mL of starting solution were added to each well to obtain a NPs concentration of 68000 NPs/cell, expressed also as $1{,}7 \cdot 10^{12}$ NPs/mL and 83,3 µg/mL, the latter comparable to NPs concentration values for cell internalisation found in literature [12]. Cells were incubated for different time periods (1 hour, 3 hour and overnight) under growth conditions in order to identify proper incubation periods to maximize the number of internalised NPs. Then, cell medium containing residual NPs was discarded and cells were washed thrice with Dulbecco's phosphate buffered saline (DPBS). DNA staining was performed by using Hoechst dye (Thermo Scientific™ Solution Hoechst 33342) 20 nM. Cells were harvested with 0.05% trypsin/EDTA 1 × and via centrifugation (980 RPM, 5 minutes) and suspended in fresh cell culture medium. Finally, NPs-labelled cells (NPs-CHO) were examined using a fluorescence microscope (Olympus IX51, RT Slider SPOT—Diagnostic Instruments, Sterling Heights, MI, USA), equipped with a 20 × objective and with a cooled CCD camera (Spot RT Slider, full frame; Diagnostic Instruments). Moreover, the effect of fluorescence microscope exposition time (10, 100 and 1000 ms) on images quality, intended as the easiness for the user to recognise NPs inside cells, was qualitatively evaluated.
Regarding suspended CHO cells, a different method was developed and used to ensure NPs internalisation. Firstly, PMMA-FluoRed-COOH NPs working solution at the same concentration used for adherent cells internalisation (as mentioned above: 68000 NPs/cell; $1{,}7 \cdot 10^{12}$ NPs/mL NPs/mL; 83,3 µg/mL) was obtained by diluting PMMA-FluoRed-COOH NPs stock solution in fresh cell culture medium. CHO cells were seeded and expanded in suspension cell growth conditions, and when the required cell number was reached, they were harvested via centrifugation (700 RPM - 6 minutes) and re-suspended in PMMA-FluoRed-COOH NPs working solution, transferred into a T175 Corning® cell culture flasks (Falcon) and incubated at different time periods in static condition. Then, cells were washed thrice via centrifugation (700 RPM - 6 minutes) and re-suspended in fresh cell culture medium. Images of fluorescent nanoparticles labelled – suspended CHO cells (NPs-SCHO) were collected using a fluorescence microscope (Nikon Eclipse E400) with B-2A filter (Ex=450-490, DM=500, BA=515).
In order to compare the effect of NPs encapsulation in terms of fluorescence intensity to different cell staining procedures, NPs-SCHO fluorescence intensity was compared to the one of CHO cells stained with CellTracker®Orange probe (Invitrogen, UK), a largely used cell dye [13] [14].

2.2.2. CellTracker® staining

Cell staining was performed, according to manufacturer's protocols, by using CellTracker® Orange probe (Invitrogen, UK). 10 mM CellTracker® Orange (Invitrogen, UK) stock solution was prepared by dissolving CellTracker® in high-quality, anhydrous dimethylsulfoxide (DMSO). 25µM staining solution was obtained diluting stock solution to CD FORTI CHO medium. The working solution was added to suspended cells after harvesting them via centrifugation (700 RPM, 6 minutes), and cells were incubated for 45 minutes under growth conditions. Then, the working solution was replaced with fresh media and the cells were examined using two fluorescence microscope, depending on the laboratory availability: (i) Nikon Eclipse E400 with B-2A filter (Ex=450-490, DM=500, BA=515) and (ii) Olympus IX51, RT Slider SPOT equipped with a 20 × objective and with a cooled CCD camera Spot RT Slider, full frame, Diagnostic Instruments USA).

2.3. Experimental set up for PIV images acquisition

2.3.1. Bioreactor set up

Suspence® (Cellex, Italy) was the bioreactor used in this work: it consists of a device in which cell culture fluids are continuously pumped in its semi-transparent vessel from the bottom and exit from an outlet in the upper part. Cell suspension in CD FORTI CHO medium (Thermo Fisher) supplemented with 4 mM L-glutamine (Biowest, France) and 1% Penicillin/Streptomycin (GE Healthcare Bio-Sciences, Sweden) was inoculated in the bioreactor with a starting volume of 1500 mL, at a starting density of $5{\cdot}10^5$ cells/mL, where the 5% of the total were NPs-SCHO cells. Medium perfusion was guaranteed by using a peristaltic pump (MASTERFLEX® L/S® 07522-20) setting a flow of 80 mL/min. Figure 1 illustrates the inner geometry of Suspence® vessel. Cell samples were withdrawn at different time points after the cell seeding (30, 180 and 300 minutes) in three different areas inside the bioreactor: the "Bottom" area, located approximately near the bottom inner surface of the vessel, the "Centre" area, at approximately 70 mm from the bottom, and the "Top", located near the liquid free surface.



Figure 1: 3D rendering of the inner geometry of the vessel of Suspence® bioreactor. Cells are seeded inside the vessel and they move from the bottom part to the top.

2.3.2. PIV acquisition system

Suspence® bioreactor was positioned inside a parallelepipedal glass tank filled with distilled water, to reduce errors caused by refractive and diffractive light phenomena on the cylindrical surface of the bioreactor. PIV analysis were carried out by employing planar PIV system (Dantec Dynamics, Denmark) with a green laser (Dantec Dynamics, Denmark) providing a light beam of 532 nm and a Flow Sense USB camera (Dantec Dynamics, Denmark). The camera was

positioned perpendicularly to the laser beam. Figure 2 illustrates the PIV acquisition system and the bioreactor configuration for PIV images acquisition employed during this work.



Figure 2: PIV system and the bioreactor configuration for images acquisition employed during this work. The Suspence® bioreactor was positioned inside a glass tank filled with distilled water to reduce refractive and diffractive light phenomena. A green laser and a camera (Dantec Dynamics, Denmark), positioned perpendicularly to the laser beam, were also used.

Planar images for cell distribution were acquired at nine different levels of frontal plane of the bioreactor, with the first level located at the zone in direct contact with the bottom surface of the bioreactor and the last level covering the sections next to the free surface of the cell suspension and the bioreactor outlet. A Cartesian coordinate system was used, with the vertical and horizontal coordinates indicated respectively by y and x. The system origin was located at the left end of the bioreactor bottom inner surface. The laser was oriented to acquire the horizontal and vertical direction of cells' speed. Figure 3 illustrates the spatial distribution of the nine investigated sections. Images length along the y-axis was approximately 6 mm, while images width along the x-axis ranged from 45,7 to 49,1 mm, corresponding to the laser-illuminated area dimensions. Laser beam thickness was approximately 1 mm.

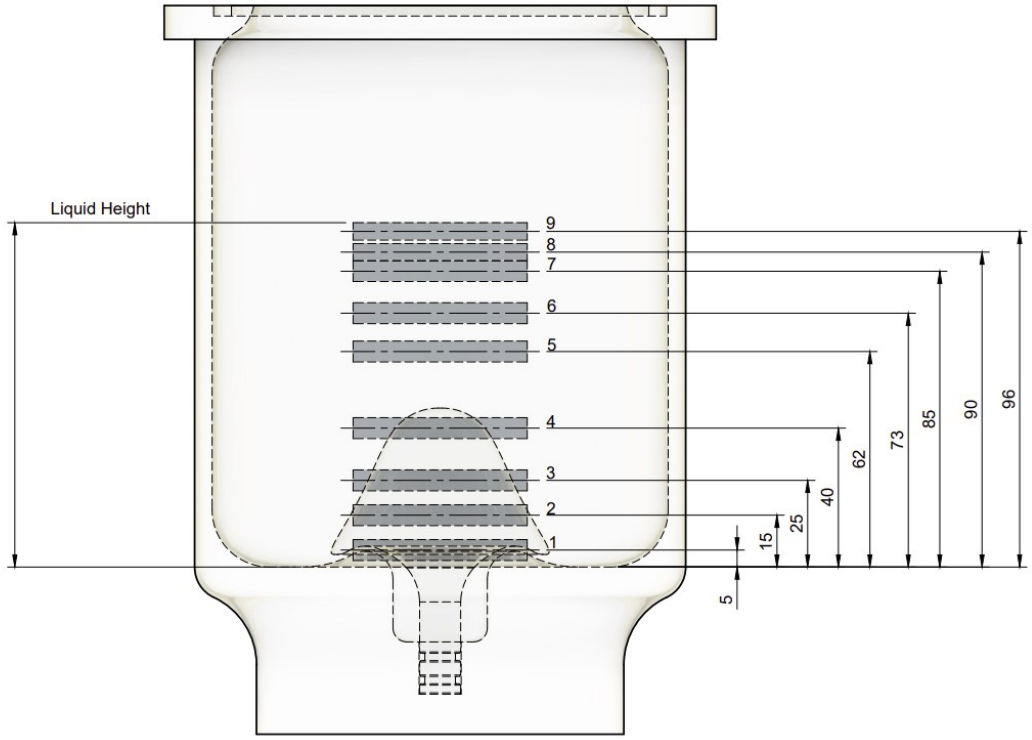

Figure 3: Spatial distribution of the nine planar sections investigated via PIV. These sections were analysed in order to evaluate cell distribution and flow speed along all the vessel height. Section vertical length is approximately 6 mm, while horizontal width ranges from 45,7 to 49,1 mm. Dimension on the right are expressed in millimeters.

2.4. PIV images post processing

2.4.1. PIV images background noise removal

A Dantec Dynamic PIV system was used to acquire the images in the vertical plane; nine sections, as shown in Figure 3, were recorded and at different time points. For each condition 100 images, subsequentially used for TKE distribution estimation, were taken and imported into Python to estimate the percentage of cells in suspension. Two images for each section were analysed at a time. Background noise removal is fundamental for biomedical image processing [15]. During the PIV images post processing the background noise, caused by the presence of refractive and diffractive light phenomena, was reduced by using a Python script. In our application the MedianBlur value, obtained computing the median of all pixels under the kernel window and the central pixel, represented the background noise, since noise corresponded with a diffuse background halo. Different kernel size, consisting in the product between the filter mask width and height in pixels, were used (7x7, 11x11, 15x15, 21x21) [16]. Thus, the background value was subtracted from the starting images. The subtraction was performed because the significant content of PIV images was assumed to be the single pixel value, that represented the absence

or the presence of single or aggregate cells. The threshold binary function was also used to separate even more the objects (NPs-SCHO) considered as a foreground from its background. In brief, the images were modified by this function so that all pixel intensity values higher than the threshold were assigned the maximum value (white), or the minimum value (black). More specifically, when pixel values were greater or equal than the set threshold value (50 or 100), they were set to 255, in the other case they were set to 0 (black) [17]. Basic Python libraries have been used, such as "cv2" to read images, "numpy" for scientific computing and "matplotlib" to plot images.

2.4.2. Cell distribution estimation

For each of the nine sections, the number of nonzero pixels of the two images was determined, and the result of the mean between these numbers gave an estimation of the amount of cells in suspension. PIV image processing and analysis robustness was assessed by comparing it to cell distribution analysis carried out via cell sampling and sample processing. Since three cell sampling points were used, three mean areas close to the point where cells were withdrawn were investigated. These three areas, which account for cell distribution in the bottom, centre and upper part of the bioreactor, were named "Bottom", "Centre" and "Top" and represented respectively the mean between values measured in section (1, 2, 3), (4, 5) and (6, 7, 8, 9). For each area, values were normalised to the total value, equal to the sum of the total values of the tree areas, calculated at time 0 (cell seeding into the bioreactor). The results were shown as bar graphs and compared with values obtained from the 3 cell samples. Total cell counts were determined by hemocytometer, as Bürker chamber, using a fluorescence microscope. The cell samples and the images acquired by the PIV system and post-processed with the above-mentioned Python Script were taken at different time points after bioreactor seeding (30, 180 and 300 minutes).

2.4.3. Ensemble-averaged turbulent kinetic energy distribution analysis

TKE is an index that can be employed to understand mass transfer and cell viability within bioreactors [18] [19] [20]. TKE distribution was obtained by re-adapting a previous PIV data processing method developed by Odeleye et. al. [10]. Measurements were carried out with a bioreactor fill volume of 1500 mL and at a flow rate of 80 mL/min. For each frontal plane section of the bioreactor, 100 image pairs were collected to obtain 100 instantaneous NPs-SCHOs velocity components (along the x and y axis) vector maps. The two components along the x and y axis of NPs-SCHOs velocity from the PIV measurements were calculated employing the adaptive PIV processing algorithm provided within Dynamic Studio software (Dantec Dynamics, Denmark). Interrogation areas were set from 16x16 to 32x32 pixels, while a universal outlier detection in neighbourhoods of 5x5 pixels was used for validating vectors. For velocity gradient adaptivity, the absolute value of each component of the velocity gradient was limited to 0.1 while the total magnitude of the gradients (square root of the sum of the squares) was limited to 0.2. Spatial resolution obtained within vector maps ranged between 0.4 x 0.4 and 0.48 x 0.48 mm. The mean value between vector maps was calculated in order to obtain vector maps representing the "Bottom", "Centre" and "Top" areas respectively between velocity values calculated in section (1,

2 ,3), (4, 5) and (6, 7 ,8, 9). These were post-processed by using a second Python script to obtain the ensemble-averaged turbulent kinetic energy through equations presented by Odeleye et. al. [10]. Since in the latter work kinetic energy was divided to the square of spinner tip speed and Suspence® bioreactor does not have an impeller, in this work turbulent kinetic energy has been divided to the square of the input fluid speed. For simplicity, turbulent kinetic energy distribution was normalised to the maximum value found in all the investigated frontal plane levels.
Figure 4 illustrates the steps, from the acquisition one to those executed in the post processing phase, performed in this work.

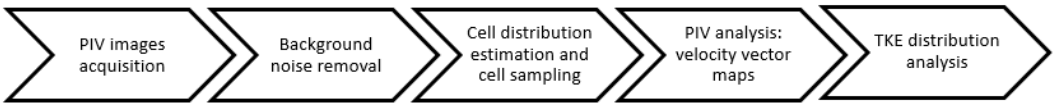

Figure 4: Schematics of PIV images acquisition and post processing steps performed in this work.

3. Results and discussion

3.1. Fluorescent cell labelling

PMMA-FluoRed-COOH NPs uptake in CHO was monitored via fluorescence microscope (Figure 5). Images show that, at each investigated incubation time, NPs appear to be localised around cell nuclei, and this may reveal that NPs were able to accumulate within cells. Also, Figure 5 shows that the number of red spots around cell nuclei tend to increase over incubation time, to such an extent that after incubating cells overnight, red fluorescence light appears to be predominant (Figure 5c). In this case, NPs can be considered internalised since some nuclei appear to be purple due to light overlap. For these reasons, NPs incubation time was subsequently set at 10 hours. These findings may suggest that the internalised NPs number increase over incubation time. This result is in line with findings shown by dos Santos et. al. [12]. Further studies are needed to fully understand the internalisation mechanisms.

Figure 6 shows PMMA-FluoRed-COOH NPs uptake in CHO cells at three different exposure times. As can be recognised from these images, an exposure time of about 100 ms was considered suitable to assess NPs internalisation.

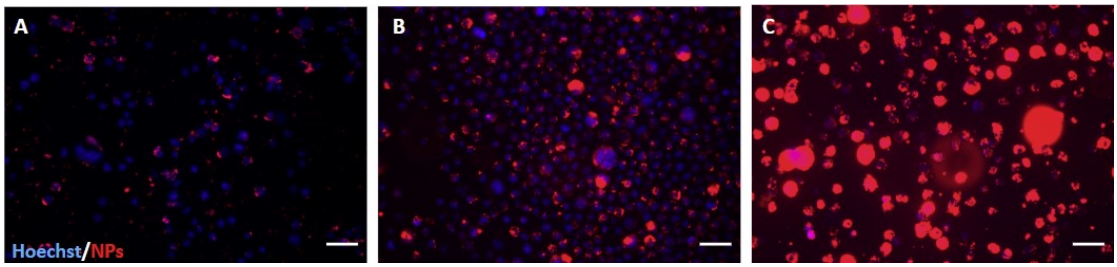

Figure 5: Internalisation evaluation of PMMA-FluoRed-COOH NPs inside CHO cells (NPs-CHO) via fluorescence microscope at different incubation times under cell culture conditions: (A) 1 hour, (B) 3 hours and (C) overnight. Cells nuclei were stained in blue while NPs are visualised in red. Exposition time: 1000ms. Scale bar = 100 μm.

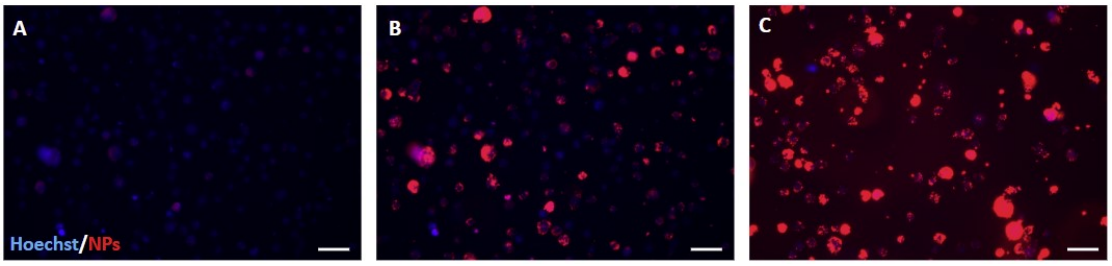

Figure 6: Internalisation of PMMA-FluoRed-COOH NPs inside CHO cells (NPs-CHO) evaluation performed via fluorescence microscope at different exposition times: (A) 10 ms, (B) 100 ms and (C) 1s. Cell nuclei were stained in blue while NPs are visualized in red. Scale bar = 100 µm.

Figure 7A illustrates CHO cells stained with cell tracker CellTracker®. In this case, few cells, shown as red spots, can be distinguished (e.g in the upper-right corner of the image). Figure 7B shows PMMA-FluoRed-COOH NPs uptake in CHO cells. In order to compare the results, the incubation time for NPs encapsulation was set to 1 hour (similar to the incubation time set for CellTraker dye, 45 min). From these images the difference in the obtained fluorescence intensity between the two used methods is appreciable, with the NPs-CHO cells fluorescence being more intense than CellTracker® one. Further quantitative fluorescence intensity analysis are needed to confirm this result.

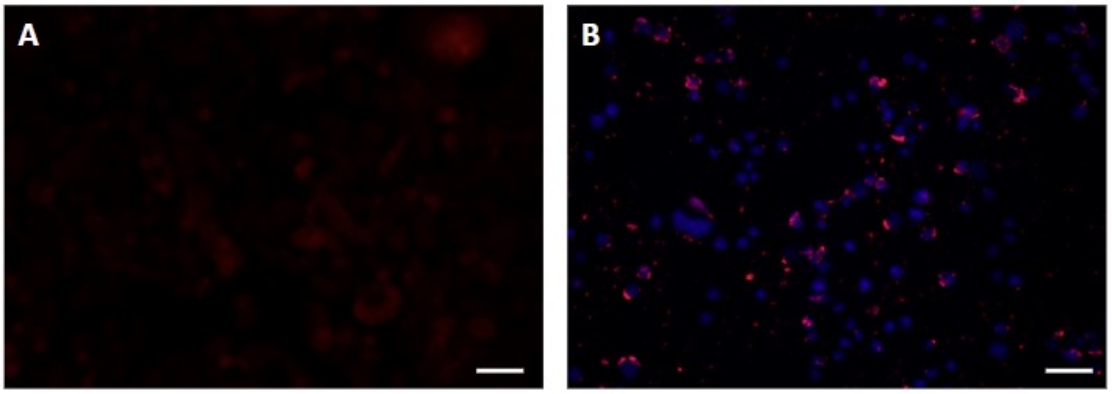

Figure 7: Comparison of the fluorescence intensity obtained via CellTracker® cell dye staining and via NPs internalisation. (A) CHO cells stained with CellTracker® (Incubation Time: 45 minutes), cells are visualized as red spots and (B) PMMA-FluoRed-COOH NPs inside CHO cells (NPs-CHO), cells nuclei were stained in blue while NPs are visualized in red (Incubation time: 1 hour). Images were acquired via fluorescence microscope. Exposition time: 100 ms. Scale bar = 100 µm.

3.1.1. Fluorescent nanoparticles internalisation in cells growth in suspension

The effectiveness of the new method developed to ensure NPs internalisation within CHO cells growth in suspension was demonstrated by comparing fluorescence intensity of CHO cells growth in adhesion stained with CellTracker® (Figure 8A) to the one emitted by NPs-SCHO (Figure 8B). These images provide evidence that cells can be clearly distinguished with both methods. Also, fluorescence intensity of NPs-SCHO appears to be comparable to CellTracker® one. Further quantitative fluorescence intensity analysis is needed to confirm this result.

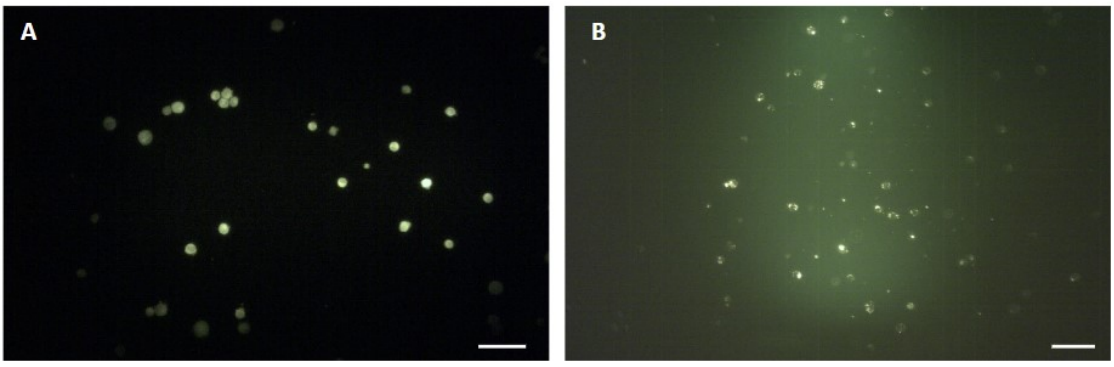

Figure 8: Evaluation of the NPs internalisation within CHO cells growth in suspension in terms of fluorescence intensity. Fluorescence microscope images: (A) CHO cells growth in adhesion stained with CellTracker®: cells are visualized in green and (B) PMMA-FluoRed-COOH NPs inside CHO cells growth in suspension (NPs-SCHO), NPs are visualized in green too. Incubation time: overnight. Exposition time: 69 ms. Scale bar = 50 µm.

3.2. PIV images post processing

3.2.1. PIV images background noise removal

Section three of one of the nine sections acquired using the PIV system was used to evaluate the performance of the developed Python filter and is shown in Figure 9. In this case, the kernel size was set to 21, while the value of the Threshold Binary function was set to 50. Figure 9A, 9B and 9C represent respectively the non-filtered image, the image containing only the background noise, and the filtered image obtained via the employed Python script processing. As can be seen from these figures, the reduction of noise is clearly distinguished on the filtered image (Figure 9C) single fluorescent dot, that can be associated with single cells or cell aggregates, can be distinguished.

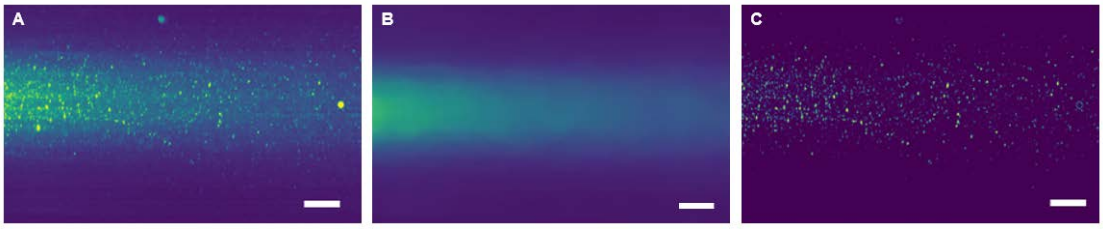

Figure 9: Effect of the background noise removal filter on PIV images of NPs-SCHO within SUSPENCE®. (A) Non filtered PIV image (B) PIV image containing only the background noise and (C) Filtered PIV image using Python script. Analysed section number: 3. Scale bar = 5mm.

3.2.2. Cell distribution estimation

Figure 10 shows cell distribution results obtained via PIV images post processing and via cell sampling. The results of the two different used methods may be considered comparable, especially in the first two time points considered. In addition, a homogeneous distribution of the cell distribution inside the vessel is highlighted, indeed values found in different areas (Bottom, Centre and Top) appear to be similar. After 30 minutes from seeding the percentage of the cell concentration is about 33%, instead after 180 minutes about 34%, in both systems described. This highlights how cell suspension is maintained over time. Anyway, a difference between the two methods can be seen in the last time point considered (300 minutes). In both systems the percentage of cell concentration in the Top area is about 40%. While the Bottom area is about 28% and 32% and the Centre area is about 33% and 27%, in the PIV system and cell samples respectively. This difference may be due to human errors occurring during PIV image acquisition procedures. In the latter case, the measurements obtained from the cell samples are considered more truthful, showing a non homogeneity of the cell concentration inside the vessel.

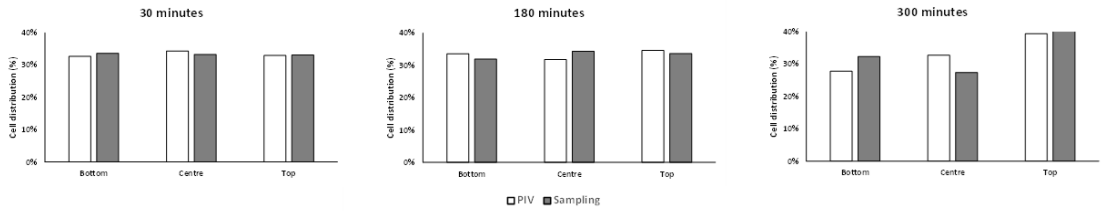

Figure 10: Bar graphs showing cell distribution results obtained via PIV images acquisition and Python script postprocessing (PIV) compared to the one obtained via cell sampling and cell counting (Sampling), at different time points.

3.2.3. Ensemble-averaged turbulent kinetic energy distribution analysis

Figure 11 shows the ensemble averaged turbulent kinetic energy (TKE) distribution of NPs-SCHO in the tree investigated bioreactors areas. A high normalized TKE area can be found in the central region of the Bottom area, corresponding to the region close to the bioreactor inlet. In this area the value of TKE appears to gradually decrease when moving away from the central zone, and this may suggest that the considered area is well mixed, since TKE is considered the portion of kinetic energy that provides a mixing mechanism due to turbulent dispersion [4]. Mixing is fundamental to obtain homogeneity of nutrients and oxygen and to reduce gradients induced by addition of cell culture media and acid/base tirants and to increase mass transfer. However, an increase in turbulent energy may be related to an increase in hydrodynamic stresses that can hinder cell viability [18][19][20]. Another high normalized TKE area is found along the length of the top area, corresponding to the region close to the bioreactor outlet. Differently from the TKE distribution of the bottom area, TKE appears to be high also in the peripheral zones. Moreover, TKE distribution in the Centre zone appears to be similar to the one observed in the bottom zone but with a lower intensity. TKE intensity in this area appears to be higher than the one observed by Odeleye et. al.[10], and this can be associated to a higher mixing mechanism in the central area of the bioreactor and also to the presence of an inlet and an outlet in the Suspence® bioreactor, which are absent in the bioreactor tested in the above-mentioned study.

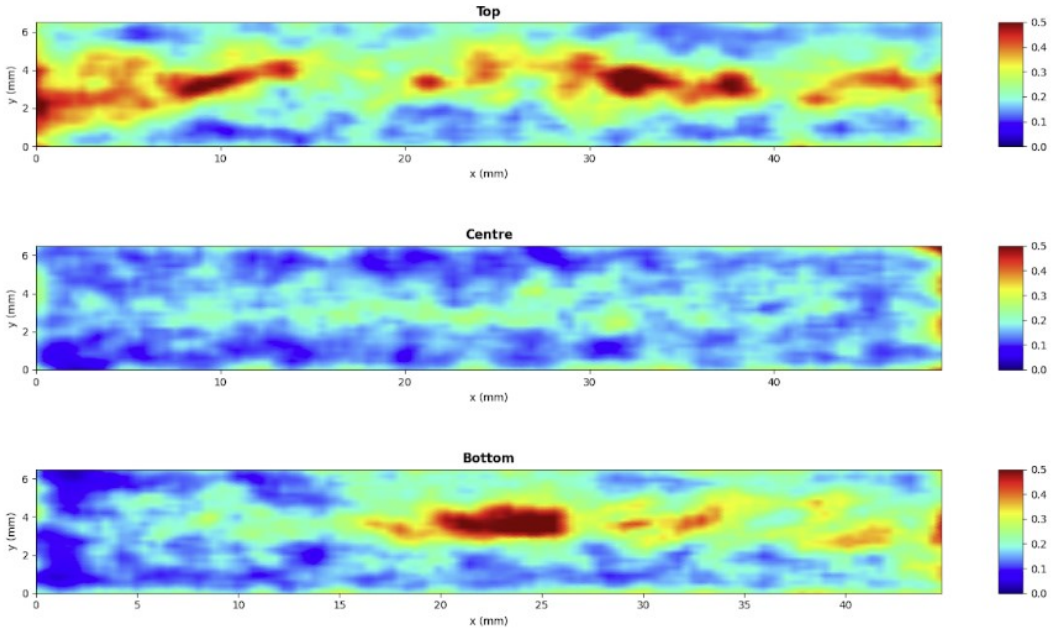

Figure 11: Ensemble-averaged turbulent kinetic energy (TKE) distribution of NPs-SCHO normalized to the maximum TKE value found the investigated bioreactors areas (Top, Centre, Bottom). TKE is considered the portion of kinetic energy that provides a mixing mechanism, fundamental to obtain homogeneity of nutrients and oxygen. High normalised TKE regions can be seen near the inlet and the outlet of the bioreactor, where flow speed is higher than the rest of the considered volume.

4. Conclusions

In this work we have demonstrated the effectiveness of the new method developed to ensure NPs internalisation within CHO cells growth in suspension and we have exploited NPs-SCHO to study cell and kinetic energy distribution within SUSPENCE® bioreactor via PIV analysis and data processing. Fluorescent particles are typically employed for fluid dynamic characterization of bioreactors and are monitored in different conditions and under various stimuli (e.g. chemico-physical). The ability to internalise fluorescent nanoparticles inside CHO cells allowed the use of the PIV system as a non-invasive image acquisition tool for bioreactors for cell culture in suspension. To the extent of our knowledge, in this work for the first time living cells with encapsuled fluorescent NPs have been employed, instead of tracer particles alone, for PIV analysis. The quantification of cell distribution and hydrodynamic parameters, in the same condition in which the cells are used to grow, within a bioreactor using PIV may allow a complete and strict study upon local cell culture conditions. Regarding PIV images post processing, firstly images background noise was successfully filtered by using our Python Script. Then, a second script was used to calculate cell distribution within the bioreactors. Cell distribution values appeared to be comparable, especially in the first two time points investigated, to the one obtained via cell sampling. The ensemble averaged turbulent kinetic energy (TKE) distribution

of NPs-SCHO was obtained in the three investigated bioreactors areas. High normalised TKE regions were found near the inlet and the outlet of the bioreactor, where flow speed is higher than the rest of the considered volume. Also, in the central area of Suspence® TKE intensity appeared to be higher than the one observed in the same area of other bioreactors. In these regions, mixing of nutrients and oxygen is promoted, but also high levels of TKE may hinder cell viability. Future development would be employing PIV cell distribution and TKE distribution analysis on different types of cells to predict cell distribution and behaviour within bioreactors during longer-lasting cell culture. In conclusion, PIV cell distribution and TKE distribution analysis inside bioreactors may represent two new methods to optimize culture conditions for cells (e.g. Peripheral Blood Mononuclear Cells) used for preterm new-borns diagnosis and therapy.

References

[1] M. Stephenson, W. Grayson, Recent advances in bioreactors for cell-based therapies, F1000Research 7 (2018).

[2] K. S. Carswell, E. T. Papoutsakis, Culture of human t cells in stirred bioreactors for cellular immunotherapy applications: Shear, proliferation, and the il-2 receptor, Biotechnology and bioengineering 68 (2000) 328–338.

[3] R. Olmer, A. Lange, S. Selzer, C. Kasper, A. Haverich, U. Martin, R. Zweigerdt, Suspension culture of human pluripotent stem cells in controlled, stirred bioreactors, Tissue Engineering Part C: Methods 18 (2012) 772–784.

[4] A. Håkansson, D. Arlov, F. Carlsson, F. Innings, Hydrodynamic difference between inline and batch operation of a rotor-stator mixer head-a cfd approach, The Canadian Journal of Chemical Engineering 95 (2017) 806–816.

[5] A. R. Hayward, Development of lymphocyte responses and interactions in the human fetus and newborn, Immunological reviews 57 (1981) 39–60.

[6] D. Miller, S. W. Turner, D. Spiteri-Cornish, N. McInnes, A. Scaife, P. J. Danielian, G. Devereux, G. M. Walsh, Culture of airway epithelial cells from neonates sampled within 48-hours of birth, PLoS One 8 (2013) e78321.

[7] J. Baier, A. C. Gwellem, R. Haase, I. Volkmer, B. Bartling, M. S. Staege, Co-culture of peripheral blood mononuclear cells and endothelial colony forming cells from cord blood of preterm born babies, in: In Vitro Models for Stem Cell Therapy, Springer, 2021, pp. 107–124.

[8] P. C. Collins, L. K. Nielsen, S. D. Patel, E. T. Papoutsakis, W. M. Miller, Characterization of hematopoietic cell expansion, oxygen uptake, and glycolysis in a controlled, stirred-tank bioreactor system, Biotechnology progress 14 (1998) 466–472.

[9] A. Bhattacharyya, P. Datta, P. Chaudhuri, B. Barik, Nanotechnology-a new frontier for food security in socio economic development, in: Disaster risk vulnerablity conference, 2011, pp. 116–120.

[10] A. Odeleye, D. Marsh, M. Osborne, G. Lye, M. Micheletti, On the fluid dynamics of a laboratory scale single-use stirred bioreactor, Chemical Engineering Science 111 (2014) 299–312.

[11] V. B. Bregar, J. Lojk, V. Šuštar, P. Veranič, M. Pavlin, Visualization of internalization of functionalized cobalt ferrite nanoparticles and their intracellular fate, International journal of nanomedicine 8 (2013) 919.
[12] T. Dos Santos, J. Varela, I. Lynch, A. Salvati, K. A. Dawson, Quantitative assessment of the comparative nanoparticle-uptake efficiency of a range of cell lines, Small 7 (2011) 3341–3349.
[13] O. Uckermann, I. Iandiev, M. Francke, K. Franze, J. Grosche, S. Wolf, L. Kohen, P. Wiedemann, A. Reichenbach, A. Bringmann, Selective staining by vital dyes of müller glial cells in retinal wholemounts, Glia 45 (2004) 59–66.
[14] M. Hsu, T. Andl, G. Li, J. L. Meinkoth, M. Herlyn, Cadherin repertoire determines partner-specific gap junctional communication during melanoma progression, Journal of cell science 113 (2000) 1535–1542.
[15] S. R. Sternberg, Biomedical image processing, Computer 16 (1983) 22–34.
[16] B. Chen, J. Liang, N. Zheng, J. C. Príncipe, Kernel least mean square with adaptive kernel size, Neurocomputing 191 (2016) 95–106.
[17] S. Parveen, J. Shah, A motion detection system in python and opencv, in: 2021 third international conference on intelligent communication technologies and virtual mobile networks (ICICV), IEEE, 2021, pp. 1378–1382.
[18] S. Mishra, V. Kumar, J. Sarkar, A. S. Rathore, Cfd based mass transfer modeling of a single use bioreactor for production of monoclonal antibody biotherapeutics, Chemical Engineering Journal 412 (2021) 128592.
[19] A. Nienow, Hydrodynamics of stirred bioreactors (1998).
[20] A. R. Lara, E. Galindo, O. T. Ramírez, L. A. Palomares, Living with heterogeneities in bioreactors, Molecular biotechnology 34 (2006) 355–381.

A review on computational tools for analytical visualisation and molecular interactions of sncRNAs: prospects in NDDs

Konstantinos Panagiotopoulos[1,*], Lolia Ibanibo[2,*], Benedetta Perrone[1], Caterina Marchetti[1], Martina Tumsich[1], Giovanni Traetta[1], Konstantinos Theofilatos[3,4] and Marco A. Deriu[1,*]

[1]*PolitoBIOMed Lab, Department of Mechanical and Aerospace Engineering, Politecnico di Torino, Turin, Italy*
[2]*Instituto de investigación e innovación biomédica de Cádiz, Cadiz, Spain*
[3]*School of Cardiovascular and Metabolic Medicine & Sciences, King's College, London, United Kingdom*
[4]*Intelligent Systems Biology (InSyBio) PC, Patras Science Park building Platani, Patras, Greece*

Abstract

Neurodevelopmental disorders (NDD) including cognitive impairments, motor disabilities, and psychosocial disorders are common among infants that are born prematurely, but the molecular mechanisms behind them are still not clear. Nevertheless, recent studies have shown that there are some shared molecular pathways driving NDDs and neurodegenerative diseases with sncRNAs having a significant role in their manifestation. It is important to study and reveal the mechanism behind the development of these disorders to predict them as soon as possible, using biomarkers and allowing medical doctors to intervene early on, while neuroplasticity in newborns still allows for recovery to some extent. In this work, we examine the role of sncRNAs and some of the shared pathways in NDDs, but most importantly, we present some of the existing computational tools and databases for predicting target interactions, and tools to perform network analysis and visualization.

Keywords

Bioinformatics, Computational tools, Biological Databases, sncRNA, molecular pathways

CEUR-WS.org/Vol-3363/paper08.pdf

1. Introduction

Preterm babies are considered those who have been born before the 37th week of gestation, while births given before the 32nd week, are considered very preterm [1, 2]. Premature deliveries have an average rate of more than 10% of total labors with an upward tendency

DETERMINED 2022: Neurodevelopmental Impairments in Preterm Children — Computational Advancements, August 26, 2022, Ljubljana, Slovenia
*Corresponding author.
konstantinos.panagiotopoulos@polito.it (K. Panagiotopoulos); loliaibanibo@gmail.com (L. Ibanibo); konstantinos.theofilatos@kcl.ac.uk (K. Theofilatos); marco.deriu@polito.it (M. A. Deriu)
https://www.dimeas.polito.it/it/personale/scheda/(nominativo)/konstantinos.panagiotopoulos (K. Panagiotopoulos); https://kclpure.kcl.ac.uk/portal/en/persons/konstantinos-theofilatos(cc24751e-4e2b-4471-aa12-380645c8e9b2).html (K. Theofilatos); https://www.dimeas.polito.it/en/personale/scheda/(nominativo)/marco.deriu (M. A. Deriu)
0000-0001-5034-378X (K. Panagiotopoulos); 0000-0001-6799-0553 (K. Theofilatos); 0000-0003-1918-1772 (M. A. Deriu)
© 2022 Copyright for this paper by its authors. Use permitted under Creative Commons License Attribution 4.0 International (CC BY 4.0).
CEUR Workshop Proceedings (CEUR-WS.org)

worldwide [3]. From the clinical point of view, preterm infants with low birth weight have higher chances of experiencing short- or long-term neurodevelopmental disorders (NDDs) and related comorbidities [4]. Common NDDs are related to motor deficits such as cerebral palsy (CP), cognitive and speech delays, visual and hearing impairments, and some psychosocial and behavioral disorders such as Autism Spectrum Disorder (ASD) and Schizophrenia. The most common methods of assessment of the developing brains in infants are using magnetic resonance imaging (MRI), ultra-sound wave imaging, and Neuropsychological battery tests [5]. But this is a way of seeing the phenotype itself or predicting the outcome rather than finding the source of the problem. Previous works have shown that genetic factors such as copy number variations (CNVs) - which are repeated segments of DNA with higher (duplications) or lower (deletions) abundance than the reference genome - are linked to both intellectual disabilities [6] and motor impairments [7], and have a statistically significant relationship with NDDs and psychiatric comorbidities [4, 8, 9].

It is well known that even though most of the human genome (>76%) can be transcribed into RNA products, only a small fraction (∼3%) of it encodes for proteins [10]. These RNA molecules that do not follow the central dogma of molecular biology [11], are called non-coding RNAs (ncRNAs) and for many years were considered byproducts with low biological meaning. This perspective started to change, and scientists began to unravel the ncRNA mystery over the last decades with the help of advancements in sequencing methods and computational tools. Projects such as The Human Genome Project and The Encyclopedia of DNA Elements (ENCODE) [12], promoted the discovery of novel genes and shed light on functional elements encoded in the human genome, especially in non-coding areas, expanding our knowledge of their importance and their regulatory mechanisms. Studies and computational predictions suggest that even though NDDs and neuropsychiatric diseases are highly heterogenous, there are common enriched pathways and genetic factors between some of them [13, 14, 15]. As an example, ASD, Tourette syndrome (TS), and Schizophrenia share some genetic modifications that may lead to dysregulation of gene expression related to micro RNAs (miRNAs); a specific regulatory group of short non-coding RNA molecules [10].

According to their average size, ncRNAs can be categorized into two general groups: long non-coding (lncRNA) and small or short non-coding (sncRNA). LncRNAs extend to over 200 nucleotides (nt) and usually have a similar size to messenger RNAs which is more than 1000nt [16], while sncRNAs typically have a length below 200nt and they are separated into two groups based on their role in the cell; Housekeeping and Regulatory [10]. Except for other important functional roles in the cell, lncRNAs such as pseudogenes and circular RNAs can interact with some classes of sncRNAs, lowering their abundance in the free form through complementarity sequences. Housekeeping sncRNAs were discovered relatively early and are well studied, due to their abundance and their fundamental roles in the function of the cell. For example, their roles can be the amino acid transfer (tRNAs) at protein synthesis or being involved in RNA processing and splicing in the nucleus (snRNAs). Regulatory sncRNAs have drawn the attention of scientists only in the last decades when technological advancements allowed for it. Since then, their important role started to unravel and it was found that they actively interact and interfere with other molecules, regulate gene expression, and involve in important molecular pathways [17, 18, 19, 20, 21]. This control over the gene expression of the regulatory sncRNAs is important because, in many diseases dysregulation of sncRNAs sequentially causes

dysregulation of functional elements that then lead to pathological phenotypes [22, 23]. Because of the great importance of these molecules, bioinformatics tools and dedicated databases have been developed in the last decades to explore their role as biomarkers and their potential in medicine. A visual taxonomy of the classification of RNA molecules can be seen in figure 1.

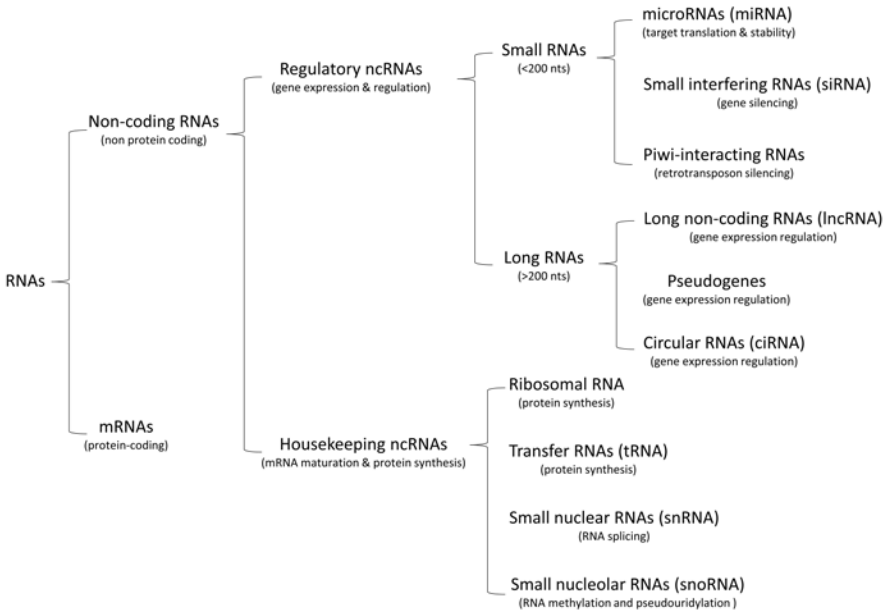

Figure 1: Classification of RNAs. The first split is based on the transcript product (coding/non-coding), followed by a discrimination on the general role of the non-coding RNAs and further on the size of these molecules. This is a modified version of the Figure 1 in the work of Gomes et al. (2020) [24].

After the systematic studies of sncRNAs, biologists clustered them by similarity and function with the most common ones being: microRNAs (miRNA) and small interfering RNA (siRNA) which regulate gene expression, small nuclear (snRNAs) that involve in RNA splicing, and piwi-interacting RNA (piRNA) that mainly interfere with transposable elements (or transposons) [10]. It is well established that sncRNAs hold a significant role also in many diseases in humans, and they can be used as biomarkers for diagnosis or prognosis, as drug targets, and as potential therapeutic methods [25]. Special attention has been given to miRNAs due to their high theoretical and experimental total number, the number of their interactions, and the role they have in both defending the homeostasis in the cell, but also related to diseases like cancer if they are dysregulated [26].

Because of the numerous interactions of sncRNAs and other molecules in the manifestation of diseases, a common approach is to handle this complexity with the use of interaction networks. Since our understanding of the underlying mechanisms is still unclear for the majority of these diseases, studying individual relationships is not enough to unravel and understand the dynamic of these pathologies. Rather than this, a more holistic view is needed with the help of multi-layer networks integrating instances belonging to different levels of complexity and domains (RNAs, proteins, diseases, functions, etc.) [27]. In this context, computational modeling can help in

reconciling the advancements in high throughput technologies with studies under the scope of systems and also explore the pathogenesis of diseases by understanding the molecular relations driving them, promoting treatments, drug discoveries, and precision medicine [28].

There are multiple tools nowadays that have been developed to predict the interactions of sncRNAs and especially miRNAs. Computational methods try to predict targets of these molecules [29, 30], pathways, and mechanisms involved in multiple diseases and disorders. Due to their interesting nature, ncRNAs have been systematically studied and there are multiple databases available where one can find experimental and computational information about them, based on their categorization. Most of these databases are open-access and publicly available. This makes the contained information accessible to everyone, helping scientists to build predictive models for diseases, discover potential biomarkers, and even design potential therapeutic targets.

Relevant studies were identified in PubMed, Scopus, ScienceDirect, and IEEE Xplore with no language restrictions. The first search from these databases was performed by the first author of this review and double-checked by the other corresponding authors. The following keywords were used: (sncRNAs OR miRNA OR siRNA OR piRNA OR RNAi), (neurodevelopmental co-morbidities OR co-occurrence of neurodevelopmental disorders), non-coding RNA Databases, (bioinformatics tools AND target prediction of sncRNA). We included only papers from January 2000 up to August 2022. Older papers were excluded, with the exception of papers explaining concepts or statistical and mathematical techniques

In this article, we review some of the most widely used molecular biology-related databases for the characterization and functionality of sncRNAs, and the state-of-the-art of computational tools for the analysis of these RNA molecules in various comorbidities, such as NDDs observed in some preterm infants [31, 32]. The main objective is to comprehensively collect in one article information on the effectiveness and usability of biological databases and databanks, as well as some computational tools for different types of bioinformatics analysis that are considered or could be considered in the future for research in the field of neurodevelopmental disorders, also considering preterm infants.

2. Features of sncRNAs

Regulatory sncRNAs can derive usually from individual genes or introns of other genes, but it is known that by the procedure of alternative splicing they may also contain some exon sequences. The most studied categories are miRNAs and siRNAs which have been found to involve in many pathologies [33] and the developmental processes [34]. The biogenesis of miRNAs has five main steps: transcription into a primary (pri-miRNA) form of a stem-loop, cleavage into a shorter stem-loop precursor (pre-miRNA) known as hairpin, transportation of the hairpin out of the nucleus, and a second cleavage followed by the unstranding of the two counterparts to produce the mature miRNA. These molecules are typically 20-24nt long [20, 35] and bind to their targets through partial complementarity -not necessarily perfect- of their seed (nucleotides 2-8), and their mRNA target sequences in the 3' untranslated region (3'UTR) which are called miRNA response elements (MREs). This leads to degradation of the mRNA molecule, or the disruption of translation by preventing the binding of ribosomes on

the mRNA. In both cases, translational inhibition results in the silencing of the target gene, a process also called RNA interference (RNAi). MREs can be found also in other types of RNAs like in lncRNAs and pseudogenes, which increases the number of targets for miRNAs since they are not strictly target-specific. This lower specificity gave rise to the idea of competitive endogenous RNAs (ceRNA). In the ceRNA field, miRNAs become the target of other competing molecules which based on their concentration, affinity, and the number of MREs regulate the abundance of available miRNAs resulting in an indirect regulation of their own expression.

Similarly, siRNAs regulate the gene expression of their target. These molecules by structure, are almost identical to miRNAs, but with the difference of having very high specificity to their target since they usually have perfect complementarity of base pairing with them [36]. The function of siRNAs lies in the interference with gene expression by degrading their transcript-targets which are far fewer targets than those of miRNAs. piRNAs on the other hand, follow a different biogenesis process which remains unclear to some extent, and also have different mechanisms of action. They are produced by a process related to the P-element induced wimpy testis or PIWI subfamily members, and recently they have been associated with cancer biology. The structure of piRNAs is single-stranded molecules of length range 26-31nt and they are known for epigenetic regulation through histone modification, but mostly for interfering with transposable elements or "genomic parasites", protecting the genome of the host [37].

The biogenesis and the mechanism of interaction of regulatory sncRNAs are important since this knowledge is also implemented in the computational tools that predict their targets. Common features on which the majority of target prediction tools are based are: the seed match, conservation sequences, free energy, and site accessibility [38].

2.1. sncRNAs in neurological disorders

sncRNAs are crucial in the maintenance of homeostasis since they coordinate the expression of genes through the RNAi process. It has been reported by many studies that sncRNAs have a linked role in neurodegenerative diseases, various types of cancers [26, 37] where the expression of sncRNAs is heavily dysregulated due to mutations, and neurodevelopmental disorders [20, 39, 40]. Specifically, sncRNAs have been found to be part of enriched molecular pathways in numerous neurodevelopmental disorders and comorbidities like Rett syndrome, ASD, Down syndrome, and others [7, 10, 39, 40]. In fact, a known commonly altered pathway in neurodevelopmental and psychiatric disorders is the mTOR pathway [41, 42]. This may indicate that there are similar mechanisms between these disorders that lead to higher probabilities of comorbidity. The role of sncRNAs in pathologies makes these molecules perfect candidates for biomarkers for early detection of diseases and mechanisms of diagnosis [43], as they are also highly ranked as therapeutic targets and in drug discovery research [44, 45]. From what is known, although there are some sncRNAs that have been identified to have different expression levels and to involve in the manifestation of NDDs, they do not show specific characteristics or significant features compared to other sncRNAs. However, mutations in the genes of the regulatory ncRNAs may be responsible for the occurrence of specific NDDs [46].

3. Computational tools to investigate molecular mechanisms and characteristics of sncRNAs

With the emergence of clinical and biological databases, as well as with the new technologies in sequencing (micro-arrays, next generation sequencing (NGS), tiling arrays, etc.), new opportunities arose for computational biology and the exploration of microscopic and macroscopic processes. Methods and tools started developing to tackle the challenges of massive amounts of data and the complication of biological systems. Results of multiple focused experiments started gathering and the findings were made easily accessible for further analysis. Additionally, databases started implementing online tools for processing information, predicting, and storing multiple-level entities because of the interoperability between different databases [47]. The ever-increasing number of databases along with the availability of data due to the new technologies of high throughput techniques led to the development of new tools, methods, and pipelines for handling the amount of available data and the extraction of new knowledge.

3.1. Biological Databases

The need for databases comes from the scattered information in literature. Having a comprehensive dataset helps researchers -especially in the clinical industry- to use the obtained knowledge from multiple and different experiments easily and find associations between instances leading to a better understanding of some conditions and processes. Biological databases can be manually or automatically curated, which means that they are constantly updated with new knowledge coming either from experiments or computational predictions. Additional to databases of linked information, there are databanks where raw data from experiments are stored. This, except for being a source of information for the databases, allows for meta-analysis of the data and merging of experiments to increase the amount of data in individual studies.

In the last decades, many efforts have been done to summarize the information about ncRNAs, as it is a game-changer in the study of cellular processes and gene regulation. Two commonly used sources of raw data are the Gene Expression Omnibus (GEO) [48] and the Sequence Read Archive (SRA) [49]. Both are from the National Institutes of Health (NIH), a part of the United States Department of Health and Human Services. In GEO, one can find collections of genomic data grouped by studies for multiple instances, and information about the protocols followed in the conducted studies. Genome browsers such as Ensembl, UCSC, and NCBI, provide interactive and comprehensive annotations of the genes on the human genome, as well as multiple tools for further bioinformatics analysis such as variant predictors and sequence comparison tools. The sequences they contain for ncRNAs are usually imported from other sources that have been created for storing information. GeneCards and HUGO Gene Nomenclature Committee (HGNC) are examples of generic databases containing information about both coding and non-coding genes. Location, aliases, description, and links to other databases can be found here, but still they only host the information contained in the sncRNA-specific databases. There are also multiple browser-based available tools for the analysis of the datasets such as gene identification tools for differential expression analysis on two or more groups. SRA is a repository of high throughput sequencing data, containing the raw sequences and alignment information, promoting reproducibility and new discoveries

through data analysis. Similar to GEO and still from the NIH is the database of Genotypes and Phenotypes (dbGaP), which provides also a controlled access space, meaning that some of the datasets stored needs authorization to get access. Finally, ArrayExpress [50] supported by the European Bioinformatics Institute (EMBL-EBI), stores high-throughput data from functional genomics experiments. The difference with the previous databanks is that ArrayExpress contains both the processed data and the raw sequences as well as links to the European Nucleotide Archive (ENA). All of these repositories contain both coding and non-coding sequences which are the building blocks for the biological databases holding information about the structure, attributes, and interactions of molecules.

General Biological Databases

A large number of biological databases for sncRNAs have been created through the years with diverse purposes such as annotation, structural information, function, interactions, location, sequence, and others. There is a large part of overlapping and redundant results contained in the databases, because of the interoperability and the information exchange between different providers. For many years now, there have been efforts to map and annotate all genes and transcripts, especially in the ever-increasing field of non-coding RNAs. The reason for non-coding-specific databases is that knowing the sequence of these molecules is the most crucial information for finding their interactions and developing computational tools for their analysis.

sncRNA sources

miRBase. The miRBase founded in 2003 [51] is among the most significant databases for miRNA sequences storage and annotation, with the latest version v22.1 (2019) containing 1917 hairpin instances and 2500 mature miRNAs for the human species alone. miRbase integrated multiple tools for sequence annotation, target prediction, and new sequence registration [52]. Additionally, it includes both experimentally verified and computationally predicted active sites and targets, and it is one of the main sources of miRNA information for other databases. Currently, there is an effort to synchronize the miRbase with Rfam; a collection of RNA families including sncRNAs with additional information about secondary structures. Both of these databases contain classifications for microRNA families but so far obtained with different methods and have a consensus of only 28% between them.

miRTarBase is a biological database that mainly provides generally validated experimentally miRNA-Target Interactions (MTI) collected in a manual way [53]. miRTarBase contains more than 4.4M interactions of about 3000 miRNAs for humans and has search filters based on specific miRNA names, their targets, and diseases.

miRCarta [54] implements the information of precursor and mature miRNAs coming from miRBase as well as predicted ones resulted from the online pipeline **miRMaster** [55]. The import of these predicted miRNAs which are based on the sequence of the sample data, results in a huge number of miRNAs in the database which is around 25k mature miRNAs and 15k precursors for the human species alone.

An interesting and recently published comprehensive database for circulating sncRNAs is **EVAtlas** [56]. It contains information for multiple families of non-coding RNAs from disease and control datasets originated from different tissues and sources. Data collection for EVAtlas is

made from 57 GEO and SRA manually reviewed registries, making it a great tool for circulating biomarker studies.

Interactions and Targets databases

miRNet [57] visualization of miRNA and other molecule interactions, can be used for multilayer network construction and ceRNA networks. It links miRNAs to coding and non-coding molecules, transcription factors, and diseases. These features make miRNet a great tool for multi-layer network reconstruction.

Pathways and enrichment analysis databases

Other than databases with structural details and interactions for ncRNAs, there are databases containing information on the involvement of ncRNAs in molecular pathways and processes, linking them in a functional role beyond their immediate first-degree interactions. The Kyoto Encyclopedia of Genes and Genome (**KEGG**) is among the most used databases for pathways, storing genomic and pathway information, and providing manually drawn maps of interactions, regulations, and signal cascading. Despite the fact that it is so well organized, KEGG has a limited amount of information about sncRNAs, and most of them are related to cancers. **Reactome**, is another generic human curated biological pathway database, that cross-references its information with NCBI, Ensebml, KEGG and others [58]. It implements online tools for analyzing and interpreting interactions and visualization of networks, but it also has relatively limited information about ncRNAs. For this reason, miRPathDB [59] has been created to indirectly link the regulatory information of miRNAs to the molecular pathways. Although **miRPathDB** [59] does not calculate the interactions, it uses context mining techniques to gather information from different enrichment analysis and pathway generic sources (KEGG, GO), linking them to information of ncRNA databases as miRBase or miRCarta.

RISE is a repository for RNA-RNA interactions coming mainly from transcriptome-wide studies [60]. Although RISE contains information about interactions between sncRNAs and other RNA molecules, it mostly focuses on lncRNA interactions. Thus, the use in sncRNA studies can be used in a validation step of a ceRNA network. **NPinter** [61] contains interactions between ncRNAs (except tRNAs and rRNAs) and biomolecules (proteins, RNAs, and DNAs) with the additional feature of visualizing the network of first-degree interactions between the query and the target. The drawback of this database is the limitation to interactions.

Lastly, a broader open-source RNA interaction database is starBase or **ENCORI** [62] which integrates information for 23 species from which it has more than 4.1 million miRNA-ncRNA interactions and 2.9 million miRNA-mRNA interactions. The data for ENCORI comes from the analysis of high throughput datasets, gene co-expression analysis, and signaling pathways sources [62]. ENCORI offers the option of searching for interactions based on the type of interaction (miRNA-Target, RNA-RNA) as well as ceRNA-Network and pathways based on KEGG terms.

3.2. Bioinformatics Tools

Bioinformatics tools are used to make the analysis of complex biological systems possible, fast and reliable. Once the sequence of sncRNAs is known through experiments and/or

prediction techniques (e.g. miRMaster), and the information of interactions is available in databases, the analysis usually proceeds with the creation of networks. Networks of single or multiple-level instances such as molecules, diseases, and pathways coexist and interact in one graph. In the case of novel transcripts, where there is no experimental evidence or previous knowledge of the targets of ncRNAs, computational tools try to predict the most probable interactions of these molecules in various ways. A list of the databases and tools discussed in this work can be found in Table 1

Target prediction tools

Binding site prediction for sncRNAs is usually referred to miRNAs and siRNA targets which are calculated based on thermodynamic criteria, anti-correlation of target genes, and miRNA/siRNA expression, but most significantly by nucleotide sequences in the target's 3'UTR MREs. Many tools developed in the last decades for this difficult task, with the most popular one being the **TargetScan**. An online computational tool for target prediction of miRNAs, based on the complementarity between the query gene transcript and the seed of the miRNA along with other multiple features related to the nucleotide sequence of the targets [63]. **DIANA** is a set of tools with the microT algorithm predicting miRNA targets in canonical (3'UTR) regions and the microT-CDS [64] algorithm for the non-canonical (coding) regions. DIANA implements also the LncBase and TarBase [65] databases for experimentally verified miRNA-target interactions with non-coding and coding transcripts respectively, and mirPath tool for identifying potential altered pathways based on miRNA expression profiles. There is a plethora of other tools and databases related to target prediction such as **miRecords** [66] or **miR2Disease** [67] which contains information about miRNAs related to specific diseases, but they are not as comprehensive or updated as the previously mentioned ones even though they are holding valuable information and are sources for databases.

Network reconstruction and visualization

The use of networks in molecular interactions is crucial to depict and tackle the complexity of biological systems. One of the uses of biological networks is the visualization of interactions, which in small networks is easy to interpret but when there are hundreds or thousands of nodes and edges it gets overwhelming for a human to handle. So, a more useful application for these systems is the analysis based on the graph theory. Metrics of centrality and affinity can be used to evaluate significant nodes and pathways, leading to important conclusions such as potential therapeutic targets [68]. Moreover, instances belonging to different categories (e.g. genes, variations, and phenotypes) can be integrated into an interactive network and help to draw conclusions about difficult problems. Tools that are used in bioinformatics for visualization of networks and analysis derive from generic network-reconstruction tools that are based on maths and the graph-theory. Functionality related to the field of biology was added through the years, mostly in the form of add-on modules that extend the basic metrics and enrich them with biological information through the available databases.

Pajek [69] is a generic, more than 20 years old, Microsoft Windows-based network visualization tool, initially implemented for social network analysis. It is also considered an immensely powerful application for analysis and visualization of massive networks because it can easily visualize a million nodes with billion connections in an average computer. For Pajek there

are available implementations that are optimized to handle faster and with a lower need for memory larger structures (Pajek-XXL or Pajek-3XL). It also implements numerous features such as Graph layout, node merging, neighborhood detection, identification of strongly connected components, clustering, and many other network analysis metrics and tools. This feature makes it a great tool for massive networks but with lower quality visualization potential.

Gephi [70] is a free offline open-source, leading visualization and exploration software and runs on all main operating systems. It is not designed specifically for biological networks, rather it is a general-purpose tool for exploratory data analysis, social networks, and biological network analysis. In Gephi there are multiple plugin modules designed for clustering of nodes and statistical analysis. It is user-friendly, allowing for customization in the visualization and due to its flexible multi-task architecture is very fast even for large datasets.

Cytoscape [71] is probably the most popular open-source desktop application for 2D network visualization in biology and health sciences. It supports all kinds of networks (e.g. weighted, unweighted, bipartite, directed, undirected, and multi-edged) and comes with an enormous library of plugins with more than 250 modules. It was initially designed for research related to biology, as its first aim was to analyze molecular interaction networks and biological pathways, integrating them with other state data such as gene expression profiles. It can handle big networks, but it requires more memory and time for clustering and layout routines than other tools which makes it less scalable, and it is recommended to run such processes in the command line and then load the results as node/edge attributes. It is a good compromise between analysis and visualization, and it comes with a great plethora of layout, clustering, and topological network analysis algorithms, such as AutoSOME, Eisen's hierarchical and k-Means clustering (in the ClusterMaker plugin), and the basic network metrics of average connectivity betweenness centrality and others. Finally, plugins for the connection of biological databases of functional enrichment, GO annotations, data retrieval, and others have been developed making it very convenient to work with.

Other solutions for network analysis may include market products or whole pipelines of processing. These solutions are usually less customizable but require less knowledge of the underlying methods and fewer resources of computational power from the user. One such example is InSyBio's suite, which implements multiple tools from the level of RNA-sequence analysis up to the network analysis by InSyBio BioNets [72] for identifying important nodes and potential biomarkers using machine learning approaches.

4. Conclusion

Since their discovery, the importance of non-coding transcripts has become clear, and they stop being considered as "Junk" DNA regions. With the advancements in technology allowing for the detection of these molecules and especially sncRNAs, a huge number of ncRNAs were discovered and got annotated. Even though some of their mechanisms of action have been decoded, their full functionality still remains to be discovered. Despite what is unknown, the focus on regulatory sncRNAs, led to significant improvements in our understanding of the molecular mechanisms driving certain diseases, and the prognosis of pathologies. It is not known if there are specific characteristics and features of the sncRNAs that are involved in

	Name	URL
Bio Databases	**Genome Browsers**	
	Ensembl	http://www.ensembl.org/index.html
	NCBI	https://www.ncbi.nlm.nih.gov/genome/51
	UCSC	https://genome.ucsc.edu/
	Non-codingRNA related	
	miRBase	https://www.mirbase.org
	miRTarBase	https://mirtarbase.cuhk.edu.cn
	miRCarta	https://mircarta.cs.uni-saarland.de
	EVAtlas	http://bioinfo.life.hust.edu.cn/EVAtlas
	miRNet	https://www.mirnet.ca
	Molecular Pathways	
	KEGG	https://www.genome.jp/kegg
	REACTOM	https://reactome.org
	miRPathDB	https://mpd.bioinf.uni-sb.de
	RISE	http://rise.life.tsinghua.edu.cn
	NPinter	http://bigdata.ibp.ac.cn/npinter4
	ENCORI	https://starbase.sysu.edu.cn
Bioinformatics Tools	**Target prediction**	
	miRMaster	https://ccb-compute.cs.uni-saarland.de/mirmaster2
	TargetScan	https://www.targetscan.org/vert_80
	DIANA	https://diana.e-ce.uth.gr/home
	miRecords	http://c1.accurascience.com/miRecords
	miR2Disease	http://www.mir2disease.org
	Network Visualization	
	Pejek	http://mrvar.fdv.uni-lj.si/pajek
	Gephi	https://gephi.org
	Cytoscape	https://cytoscape.org

Table 1
List of databases and tools discussed in the present work and the uniform resource locator (URL) for each of these sources

NDDs, so further studies are needed to understand and unravel the sources of these disorders. Computer science and Bioinformatics have a tremendous impact on systems biology, with the ever-improving development of tools helping scientists draw important conclusions from the massive amounts of available data. And this is why it is so important to have comprehensive, curated, open-source, and well-organized databases as the ones presented in this work.

The availability of datasets stored in databanks along with the interoperability and the organization of information in databases has dramatically shifted the nature of biological studies from small- to large-scale and gave rise to data-driven methods. This alternation of viewing multiple interactions and functions brought the use of multi-layer networks into the foreground as an important tool. This allowed for broader and more holistic computational approaches, which model much better the real biological systems.

To date, none of the presented tools is specific to neurodevelopmental disorders. In fact, these tools are of general use, but there is an interesting potential for application in various fields, including neurological and neurodevelopmental disorders. This derives from the fact that RNA

molecules and specifically sncRNAs have simple structures, with no particular biochemical features. Thus, the individual tools that analyse these molecules are general. Despite that, their combination -depending on the question every time- can lead to pathology-specific methods which are related to the emerged properties of more complex structures such as tissues, organs, diseases etc. The purpose of this paper is to collect the most well-known and important tools and to give an insight into their functionality and effectiveness. This is an important step towards understanding their potential in specific fields such as neurodevelopmental disorders.

Of course, except for the presented tools and databases in the current work, there are numerous others online and offline tools that could not be included because of their high number and redundancy of information. In bioinformatics, there is a continuous need for new tools and additional functionality which makes the review of new tools a hard task. As one can see, information is shared between platforms, databases, and databanks in the spirit of scientific collaboration and the pursuit of new knowledge.

In this review, we introduced tools that are needed for starting an analysis of genomic data from a high level (disease or phenotype), ending with the reconstruction of networks of interactions for ncRNAs and specifically short non-coding molecules. We did not get into methodologies of analysis of the data which is a whole field of study alone and needs special focus. The presented tools, even though not oriented only in NDDs, can be used to identify the common molecular pathways in these disorders and the comorbidity that is often present in preterm babies with NDDs.

A. Abbreviations

- NDD : neurodevelopmental disorder
- CP : ceribral palsy
- MRI : magnetic resonance imaging
- 3'UTR : 3' (prime) untranslated region
- ADS : autism disorder spectrum
- NGS : next generation sequencing
- PIWI : P-element induced wimpy testis
- mRNA : messenger RNA
- ncRNA : non-coding RNA
- sncRNA : short/small non-coding RNA
- miRNA : micro RNA
- siRNA : small interference RNA
- piRNA : P-element-induced wimpy testis-interacting RNA (piwi RNA)
- RNAi : RNA interference
- ceRNA : competitive endogenous RNA
- MRE : miRNA response element

References

[1] R. L. Goldenberg, J. F. Culhane, J. D. Iams, R. Romero, Epidemiology and causes of preterm birth, The Lancet 371 (2008) 75–84. URL: https://doi.org/10.1016/S0140-6736(08)60074-4. doi:10.1016/S0140-6736(08)60074-4, doi: 10.1016/S0140-6736(08)60074-4.

[2] H. Blencowe, S. Cousens, M. Z. Oestergaard, D. Chou, A.-B. Moller, R. Narwal, A. Adler, C. V. Garcia, S. Rohde, L. Say, J. E. Lawn, National, regional, and worldwide estimates of preterm birth rates in the year 2010 with time trends since 1990 for selected countries: a systematic analysis and implications, The Lancet 379 (2012) 2162–2172. URL: https://www.sciencedirect.com/science/article/pii/S0140673612608204. doi:https://doi.org/10.1016/S0140-6736(12)60820-4.

[3] H.-L. Li, L.-L. Chen, G. Qian, W.-S. Wang, X.-N. Feng, M.-Q. Yu, L.-Z. Ren, A birth cohort study of neurodevelopmental outcomes from birth to 2 years of age in preterm infants under 34 weeks of gestation, Journal of Healthcare Engineering 2022 (2022) 7496785. URL: https://doi.org/10.1155/2022/7496785. doi:10.1155/2022/7496785.

[4] D. Dewey, What is comorbidity and why does it matter in neurodevelopmental disorders?, Current Developmental Disorders Reports 5 (2018) 235–242. URL: https://doi.org/10.1007/s40474-018-0152-3. doi:10.1007/s40474-018-0152-3.

[5] D. J. Zgaljardic, R. O. Temple, Neuropsychological assessment battery (nab): Performance in a sample of patients with moderate-to-severe traumatic brain injury, Applied Neuropsychology 17 (2010) 283–288. URL: https://doi.org/10.1080/09084282.2010.525118. doi:10.1080/09084282.2010.525118, doi: 10.1080/09084282.2010.525118.

[6] L. E. L. M. Vissers, C. Gilissen, J. A. Veltman, Genetic studies in intellectual disability and related disorders, Nature Reviews Genetics 17 (2016) 9–18. URL: https://doi.org/10.1038/nrg3999. doi:10.1038/nrg3999.

[7] A. H. MacLennan, S. C. Thompson, J. Gecz, Cerebral palsy: causes, pathways, and the role of genetic variants, American Journal of Obstetrics & Gynecology 213 (2015) 779–788. URL: https://doi.org/10.1016/j.ajog.2015.05.034. doi:10.1016/j.ajog.2015.05.034, doi: 10.1016/j.ajog.2015.05.034.

[8] J. H. Thygesen, K. Wolfe, A. McQuillin, M. Viñas-Jornet, N. Baena, N. Brison, G. D'Haenens, S. Esteba-Castillo, E. Gabau, N. Ribas-Vidal, A. Ruiz, J. Vermeesch, E. Weyts, R. Novell, G. V. Buggenhout, A. Strydom, N. Bass, M. Guitart, A. Vogels, Neurodevelopmental risk copy number variants in adults with intellectual disabilities and comorbid psychiatric disorders, British Journal of Psychiatry 212 (2018) 287–294. doi:DOI:10.1192/bjp.2017.65.

[9] M. K. Licari, A. Finlay-Jones, J. E. Reynolds, G. A. Alvares, A. J. Spittle, J. Downs, A. J. O. Whitehouse, H. Leonard, K. L. Evans, K. Varcin, The brain basis of comorbidity in neurodevelopmental disorders, Current Developmental Disorders Reports 6 (2019) 9–18. URL: https://doi.org/10.1007/s40474-019-0156-7. doi:10.1007/s40474-019-0156-7.

[10] P. Zhang, W. Wu, Q. Chen, M. Chen, Non-coding RNAs and their integrated networks, Journal of Integrative Bioinformatics 16 (2019) 20190027. URL: https://doi.org/10.1515/jib-2019-0027. doi:doi:10.1515/jib-2019-0027.

[11] F. CRICK, Central dogma of molecular biology, Nature 227 (1970) 561–563. URL: https://doi.org/10.1038/227561a0. doi:10.1038/227561a0.

[12] I. D. et al., An integrated encyclopedia of DNA elements in the human genome, Nature

489 (2012) 57–74. URL: https://doi.org/10.1038/nature11247. doi:10.1038/nature11247.

[13] A. S. Cristino, S. M. Williams, Z. Hawi, J.-Y. An, M. A. Bellgrove, C. E. Schwartz, L. da F Costa, C. Claudianos, Neurodevelopmental and neuropsychiatric disorders represent an interconnected molecular system, Molecular Psychiatry 19 (2014) 294–301. URL: https://doi.org/10.1038/mp.2013.16. doi:10.1038/mp.2013.16.

[14] R. A. Clarke, S. Lee, V. Eapen, Pathogenetic model for tourette syndrome delineates overlap with related neurodevelopmental disorders including autism, Translational Psychiatry 2 (2012) e158–e158. URL: https://doi.org/10.1038/tp.2012.75. doi:10.1038/tp.2012.75.

[15] M. Sahin, M. Sur, Genes, circuits, and precision therapies for autism and related neurodevelopmental disorders, Science 350 (2015) aab3897. URL: https://www.science.org/doi/abs/10.1126/science.aab3897. doi:10.1126/science.aab3897. arXiv:https://www.science.org/doi/pdf/10.1126/science.aab3897.

[16] I. V. Novikova, S. P. Hennelly, K. Y. Sanbonmatsu, Sizing up long non-coding RNAs: do lncRNAs have secondary and tertiary structure?, Bioarchitecture 2 (2012) 189–199. URL: https://pubmed.ncbi.nlm.nih.gov/23267412https://www.ncbi.nlm.nih.gov/pmc/articles/PMC3527312/. doi:10.4161/bioa.22592.

[17] A. Mahfouz, M. N. Ziats, O. M. Rennert, B. P. F. Lelieveldt, M. J. T. Reinders, Shared pathways among autism candidate genes determined by co-expression network analysis of the developing human brain transcriptome, Journal of molecular neuroscience : MN 57 (2015) 580–594. URL: https://pubmed.ncbi.nlm.nih.gov/26399424https://www.ncbi.nlm.nih.gov/pmc/articles/PMC4644211/. doi:10.1007/s12031-015-0641-3.

[18] S. F. Zhang, J. Gao, C. M. Liu, The role of non-coding RNAs in neurodevelopmental disorders, 2019. doi:10.3389/fgene.2019.01033.

[19] S. K. Fineberg, K. S. Kosik, B. L. Davidson, MicroRNAs potentiate neural development, Neuron 64 (2009) 303–309. URL: https://www.sciencedirect.com/science/article/pii/S0896627309008502. doi:https://doi.org/10.1016/j.neuron.2009.10.020.

[20] C. N. Watson, A. Belli, V. D. Pietro, Small non-coding RNAs: New class of biomarkers and potential therapeutic targets in neurodegenerative disease, Frontiers in Genetics 10 (2019). URL: https://www.frontiersin.org/articles/10.3389/fgene.2019.00364. doi:10.3389/fgene.2019.00364.

[21] J. O'Brien, H. Hayder, Y. Zayed, C. Peng, Overview of microRNA biogenesis, mechanisms of actions, and circulation, Frontiers in Endocrinology 9 (2018). URL: https://www.frontiersin.org/article/10.3389/fendo.2018.00402. doi:10.3389/fendo.2018.00402.

[22] M. Muñoz-Culla, H. Irizar, M. Sáenz-Cuesta, T. Castillo-Triviño, I. Osorio-Querejeta, L. Sepúlveda, A. L. de Munain, J. Olascoaga, D. Otaegui, SncRNA (microRNA & snoRNA) opposite expression pattern found in multiple sclerosis relapse and remission is sex dependent, Scientific Reports 6 (2016) 20126. URL: https://doi.org/10.1038/srep20126. doi:10.1038/srep20126.

[23] O. Noronha, L. Mesarosovo, J. J. Anink, A. Iyer, E. Aronica, J. D. Mills, Differentially expressed miRNAs in age-related neurodegenerative diseases: A meta-analysis, Genes 13 (2022). URL: https://www.mdpi.com/2073-4425/13/6/1034. doi:10.3390/genes13061034.

[24] C. P. da Costa Gomes, B. Schroen, G. M. Kuster, E. L. Robinson, K. Ford, I. B. Squire, S. Heymans, F. Martelli, C. Emanueli, Y. Devaux, null null, Regulatory rnas in heart

failure, Circulation 141 (2020) 313–328. URL: https://doi.org/10.1161/CIRCULATIONAHA.119.042474. doi:10.1161/CIRCULATIONAHA.119.042474, doi: 10.1161/CIRCULATIONAHA.119.042474.

[25] E. S. Smith, E. Whitty, B. Yoo, A. Moore, L. F. Sempere, Z. Medarova, Clinical applications of short non-coding RNA-based therapies in the era of precision medicine, Cancers 14 (2022). URL: https://www.mdpi.com/2072-6694/14/6/1588. doi:10.3390/cancers14061588.

[26] Y. Peng, C. M. Croce, The role of microRNAs in human cancer, Signal Transduction and Targeted Therapy 1 (2016) 15004. URL: https://doi.org/10.1038/sigtrans.2015.4. doi:10.1038/sigtrans.2015.4.

[27] R. Bardini, G. Politano, A. Benso, S. D. Carlo, Multi-level and hybrid modelling approaches for systems biology, Computational and Structural Biotechnology Journal 15 (2017) 396–402. URL: https://www.sciencedirect.com/science/article/pii/S2001037017300314. doi:https://doi.org/10.1016/j.csbj.2017.07.005.

[28] Z. Ji, K. Yan, W. Li, H. Hu, X. Zhu, Mathematical and computational modeling in complex biological systems, BioMed Research International 2017 (2017) 5958321. URL: https://doi.org/10.1155/2017/5958321. doi:10.1155/2017/5958321.

[29] A. Oulas, N. Karathanasis, A. Louloupi, G. Pavlopoulos, P. Poirazi, K. Kalantidis, I. Iliopoulos, Prediction of miRNA targets, 2015. doi:10.1007/978-1-4939-2291-8_13.

[30] A. Korfiati, K. A. Theofilatos, D. Kleftogiannis, C. E. Alexakos, S. D. Likothanassis, S. Mavroudi, Predicting human miRNA target genes using a novel computational intelligent framework, Inf. Sci. 294 (2015) 576–585.

[31] M. N. Ziats, O. M. Rennert, Identification of differentially expressed microrna across the developing human brain, Molecular Psychiatry 19 (2014) 848–852. URL: https://doi.org/10.1038/mp.2013.93. doi:10.1038/mp.2013.93.

[32] H. J. Kang, Y. I. Kawasawa, F. Cheng, Y. Zhu, X. Xu, M. Li, A. M. M. Sousa, M. Pletikos, K. A. Meyer, G. Sedmak, T. Guennel, Y. Shin, M. B. Johnson, Željka Krsnik, S. Mayer, S. Fertuzinhos, S. Umlauf, S. N. Lisgo, A. Vortmeyer, D. R. Weinberger, S. Mane, T. M. Hyde, A. Huttner, M. Reimers, J. E. Kleinman, N. Šestan, Spatio-temporal transcriptome of the human brain, Nature 478 (2011) 483–489. URL: https://doi.org/10.1038/nature10523. doi:10.1038/nature10523.

[33] P. Paul, A. Chakraborty, D. Sarkar, M. Langthasa, M. Rahman, M. Bari, R. K. S. Singha, A. K. Malakar, S. Chakraborty, Interplay between miRNAs and human diseases, Journal of Cellular Physiology 233 (2018) 2007–2018. URL: https://doi.org/10.1002/jcp.25854. doi:https://doi.org/10.1002/jcp.25854, https://doi.org/10.1002/jcp.25854.

[34] H. Lv, Q. Wang, S. Wu, L. Yang, P. Ren, Y. Yang, J. Gao, L. Li, Neonatal hypoxic ischemic encephalopathy-related biomarkers in serum and cerebrospinal fluid, Clinica Chimica Acta 450 (2015) 282–297. doi:10.1016/j.cca.2015.08.021.

[35] M. Ha, V. N. Kim, Regulation of microRNA biogenesis, Nature Reviews Molecular Cell Biology 15 (2014) 509–524. URL: https://doi.org/10.1038/nrm3838. doi:10.1038/nrm3838.

[36] J. K. W. Lam, M. Y. T. Chow, Y. Zhang, S. W. S. Leung, siRNA versus miRNA as therapeutics for gene silencing, Molecular Therapy - Nucleic Acids 4 (2015). URL: https://doi.org/10.1038/mtna.2015.23. doi:10.1038/mtna.2015.23, doi: 10.1038/mtna.2015.23.

[37] C. B. Assumpção, D. Q. Calcagno, T. M. T. Araújo, S. E. B. dos Santos, Ândrea Kely Campos Ribeiro dos Santos, G. J. Riggins, R. R. Burbano, P. P. Assumpção, The role of piRNA

and its potential clinical implications in cancer, Epigenomics 7 (2015) 975–984. URL: https://doi.org/10.2217/epi.15.37. doi:10.2217/epi.15.37, doi: 10.2217/epi.15.37.

[38] S. Peterson, J. Thompson, M. Ufkin, P. Sathyanarayana, L. Liaw, C. B. Congdon, Common features of microRNA target prediction tools, Frontiers in Genetics 5 (2014). URL: https://www.frontiersin.org/articles/10.3389/fgene.2014.00023. doi:10.3389/fgene.2014.00023.

[39] K. T. Thomas, S. S. Zakharenko, MicroRNAs in the onset of schizophrenia, Cells 10 (2021). URL: https://www.mdpi.com/2073-4409/10/10/2679. doi:10.3390/cells10102679.

[40] S. Chang, S. Wen, D. Chen, P. Jin, Small regulatory RNAs in neurodevelopmental disorders, Human Molecular Genetics 18 (2009) R18–R26. URL: https://doi.org/10.1093/hmg/ddp072. doi:10.1093/hmg/ddp072.

[41] M. Costa-Mattioli, L. M. Monteggia, mTOR complexes in neurodevelopmental and neuropsychiatric disorders, Nature Neuroscience 16 (2013) 1537–1543. URL: https://doi.org/10.1038/nn.3546. doi:10.1038/nn.3546.

[42] I. Parenti, L. G. Rabaneda, H. Schoen, G. Novarino, Neurodevelopmental disorders: From genetics to functional pathways, Trends in Neurosciences 43 (2020) 608–621. URL: https://doi.org/10.1016/j.tins.2020.05.004. doi:10.1016/j.tins.2020.05.004, doi: 10.1016/j.tins.2020.05.004.

[43] G. Jain, A. Stuendl, P. Rao, T. Berulava, T. P. Centeno, L. Kaurani, S. Burkhardt, I. Delalle, J. Kornhuber, M. Hüll, W. Maier, O. Peters, H. Esselmann, C. Schulte, C. Deuschle, M. Synofzik, J. Wiltfang, B. Mollenhauer, W. Maetzler, A. Schneider, A. Fischer, A combined miRNA–piRNA signature to detect alzheimer's disease, Translational Psychiatry 9 (2019) 250. URL: https://doi.org/10.1038/s41398-019-0579-2. doi:10.1038/s41398-019-0579-2.

[44] M. A. Obeid, A. A. A. Aljabali, W. Alshaer, N. B. Charbe, D. K. Chellappan, K. Dua, S. Satija, M. M. Tambuwala, Chapter 35 - targeting siRNAs in cancer drug delivery, 2021. URL: https://www.sciencedirect.com/science/article/pii/B9780323855037000274. doi:https://doi.org/10.1016/B978-0-323-85503-7.00027-4.

[45] L. H. Madkour, Chapter 5 - therapeutic applications of siRNA gene delivery systems, 2019. URL: https://www.sciencedirect.com/science/article/pii/B9780128197776000056. doi:https://doi.org/10.1016/B978-0-12-819777-6.00005-6.

[46] T. N. Turner, E. E. Eichler, The role of de novo noncoding regulatory mutations in neurodevelopmental disorders, Trends in Neurosciences 42 (2019) 115–127. URL: https://www.sciencedirect.com/science/article/pii/S0166223618302960. doi:https://doi.org/10.1016/j.tins.2018.11.002.

[47] A. D. Baxevanis, The importance of biological databases in biological discovery, Current Protocols in Bioinformatics 34 (2011) 1.1.1–1.1.6. URL: https://doi.org/10.1002/0471250953.bi0101s34. doi:https://doi.org/10.1002/0471250953.bi0101s34, https://doi.org/10.1002/0471250953.bi0101s34.

[48] T. Barrett, S. E. Wilhite, P. Ledoux, C. Evangelista, I. F. Kim, M. Tomashevsky, K. A. Marshall, K. H. Phillippy, P. M. Sherman, M. Holko, A. Yefanov, H. Lee, N. Zhang, C. L. Robertson, N. Serova, S. Davis, A. Soboleva, NCBI GEO: archive for functional genomics data sets—update, Nucleic Acids Research 41 (2013) D991–D995. URL: https://doi.org/10.1093/nar/gks1193. doi:10.1093/nar/gks1193.

[49] N. R. Coordinators, Database resources of the national center for biotechnology information, Nucleic Acids Research 44 (2016) D7–D19. URL: https://doi.org/10.1093/nar/gkv1290. doi:10.1093/nar/gkv1290.

[50] A. Athar, A. Füllgrabe, N. George, H. Iqbal, L. Huerta, A. Ali, C. Snow, N. A. Fonseca, R. Petryszak, I. Papatheodorou, U. Sarkans, A. Brazma, ArrayExpress update – from bulk to single-cell expression data, Nucleic Acids Research 47 (2018) D711–D715. URL: https://doi.org/10.1093/nar/gky964. doi:10.1093/nar/gky964.

[51] S. Griffiths-Jones, The microRNA registry, Nucleic Acids Research 32 (2004) D109–D111. URL: https://doi.org/10.1093/nar/gkh023. doi:10.1093/nar/gkh023.

[52] S. Griffiths-Jones, H. K. Saini, S. van Dongen, A. J. Enright, miRBase: tools for microRNA genomics, Nucleic Acids Research 36 (2008) D154–D158. URL: https://doi.org/10.1093/nar/gkm952. doi:10.1093/nar/gkm952.

[53] H.-Y. Huang, Y.-C.-D. Lin, J. Li, K.-Y. Huang, S. Shrestha, H.-C. Hong, Y. Tang, Y.-G. Chen, C.-N. Jin, Y. Yu, J.-T. Xu, Y.-M. Li, X.-X. Cai, Z.-Y. Zhou, X.-H. Chen, Y.-Y. Pei, L. Hu, J.-J. Su, S.-D. Cui, F. Wang, Y.-Y. Xie, S.-Y. Ding, M.-F. Luo, C.-H. Chou, N.-W. Chang, K.-W. Chen, Y.-H. Cheng, X.-H. Wan, W.-L. Hsu, T.-Y. Lee, F.-X. Wei, H.-D. Huang, miRTarBase 2020: updates to the experimentally validated microRNA–target interaction database, Nucleic Acids Research 48 (2020) D148–D154. URL: https://doi.org/10.1093/nar/gkz896. doi:10.1093/nar/gkz896.

[54] C. Backes, T. Fehlmann, F. Kern, T. Kehl, H.-P. Lenhof, E. Meese, A. Keller, miRCarta: a central repository for collecting miRNA candidates, Nucleic Acids Research 46 (2018) D160–D167. URL: https://doi.org/10.1093/nar/gkx851. doi:10.1093/nar/gkx851.

[55] T. Fehlmann, F. Kern, O. Laham, C. Backes, J. Solomon, P. Hirsch, C. Volz, R. Müller, A. Keller, mirmaster 2.0: multi-species non-coding rna sequencing analyses at scale, Nucleic Acids Research 49 (2021) W397–W408. URL: https://doi.org/10.1093/nar/gkab268. doi:10.1093/nar/gkab268.

[56] C.-J. Liu, G.-Y. Xie, Y.-R. Miao, M. Xia, Y. Wang, Q. Lei, Q. Zhang, A.-Y. Guo, EVAtlas: a comprehensive database for ncRNA expression in human extracellular vesicles, Nucleic Acids Research 50 (2022) D111–D117. URL: https://doi.org/10.1093/nar/gkab668. doi:10.1093/nar/gkab668.

[57] L. Chang, G. Zhou, O. Soufan, J. Xia, miRNet 2.0: network-based visual analytics for miRNA functional analysis and systems biology, Nucleic Acids Research 48 (2020) W244–W251. URL: https://doi.org/10.1093/nar/gkaa467. doi:10.1093/nar/gkaa467.

[58] A. Fabregat, K. Sidiropoulos, P. Garapati, M. Gillespie, K. Hausmann, R. Haw, B. Jassal, S. Jupe, F. Korninger, S. McKay, L. Matthews, B. May, M. Milacic, K. Rothfels, V. Shamovsky, M. Webber, J. Weiser, M. Williams, G. Wu, L. Stein, H. Hermjakob, P. D'Eustachio, The reactome pathway knowledgebase, Nucleic Acids Research 44 (2016) D481–D487. URL: https://doi.org/10.1093/nar/gkv1351. doi:10.1093/nar/gkv1351.

[59] T. Kehl, F. Kern, C. Backes, T. Fehlmann, D. Stöckel, E. Meese, H.-P. Lenhof, A. Keller, miRPathDB 2.0: a novel release of the miRNA pathway dictionary database, Nucleic Acids Research 48 (2020) D142–D147. URL: https://doi.org/10.1093/nar/gkz1022. doi:10.1093/nar/gkz1022.

[60] J. Gong, D. Shao, K. Xu, Z. Lu, Z. J. Lu, Y. T. Yang, Q. C. Zhang, Rise: a database of rna interactome from sequencing experiments, Nucleic Acids Research 46 (2018) D194–D201.

URL: https://doi.org/10.1093/nar/gkx864. doi:10.1093/nar/gkx864.

[61] X. Teng, X. Chen, H. Xue, Y. Tang, P. Zhang, Q. Kang, Y. Hao, R. Chen, Y. Zhao, S. He, NPInter v4.0: an integrated database of ncRNA interactions, Nucleic Acids Research 48 (2020) D160–D165. URL: https://doi.org/10.1093/nar/gkz969. doi:10.1093/nar/gkz969.

[62] J.-H. Li, S. Liu, H. Zhou, L.-H. Qu, J.-H. Yang, starBase v2.0: decoding miRNA-ceRNA, miRNA-ncRNA and protein–RNA interaction networks from large-scale CLIP-Seq data, Nucleic Acids Research 42 (2014) D92–D97. URL: https://doi.org/10.1093/nar/gkt1248. doi:10.1093/nar/gkt1248.

[63] V. Agarwal, G. W. Bell, J.-W. Nam, D. P. Bartel, Predicting effective microRNA target sites in mammalian mRNAs, eLife 4 (2015) e05005. URL: https://doi.org/10.7554/eLife.05005. doi:10.7554/eLife.05005.

[64] M. D. Paraskevopoulou, G. Georgakilas, N. Kostoulas, I. S. Vlachos, T. Vergoulis, M. Reczko, C. Filippidis, T. Dalamagas, A. G. Hatzigeorgiou, DIANA-microT web server v5.0: service integration into miRNA functional analysis workflows, Nucleic Acids Research 41 (2013) W169–W173. URL: https://doi.org/10.1093/nar/gkt393. doi:10.1093/nar/gkt393.

[65] D. Karagkouni, M. D. Paraskevopoulou, S. Chatzopoulos, I. S. Vlachos, S. Tastsoglou, I. Kanellos, D. Papadimitriou, I. Kavakiotis, S. Maniou, G. Skoufos, T. Vergoulis, T. Dalamagas, A. G. Hatzigeorgiou, DIANA-TarBase v8: a decade-long collection of experimentally supported miRNA–gene interactions, Nucleic Acids Research 46 (2018) D239–D245. URL: https://doi.org/10.1093/nar/gkx1141. doi:10.1093/nar/gkx1141.

[66] F. Xiao, Z. Zuo, G. Cai, S. Kang, X. Gao, T. Li, miRecords: an integrated resource for microRNA–target interactions, Nucleic Acids Research 37 (2009) D105–D110. URL: https://doi.org/10.1093/nar/gkn851. doi:10.1093/nar/gkn851.

[67] Q. Jiang, Y. Wang, Y. Hao, L. Juan, M. Teng, X. Zhang, M. Li, G. Wang, Y. Liu, miR2Disease: a manually curated database for microRNA deregulation in human disease, Nucleic Acids Research 37 (2009) D98–D104. URL: https://doi.org/10.1093/nar/gkn714. doi:10.1093/nar/gkn714.

[68] P. N. Deepthi, R. Anitha, Applications of network analysis in bioinformatics, Springer International Publishing, 2020, pp. 79–84.

[69] A. Mrvar, V. Batagelj, Analysis and visualization of large networks with program package pajek, Complex Adaptive Systems Modeling 4 (2016) 6. URL: https://doi.org/10.1186/s40294-016-0017-8. doi:10.1186/s40294-016-0017-8.

[70] M. Bastian, S. Heymann, M. Jacomy, Gephi: An open source software for exploring and manipulating networks, Proceedings of the International AAAI Conference on Web and Social Media 3 (2009) 361–362. URL: https://ojs.aaai.org/index.php/ICWSM/article/view/13937.

[71] P. Shannon, A. Markiel, O. Ozier, N. S. Baliga, J. T. Wang, D. Ramage, N. Amin, B. Schwikowski, T. Ideker, Cytoscape: A software environment for integrated models of biomolecular interaction networks, Genome Research 13 (2003) 2498–2504. doi:10.1101/gr.1239303.

[72] K. Theofilatos, C. Dimitrakopoulos, C. Alexakos, A. Korfiati, S. Likothanassis, S. Mavroudi, InSyBio BioNets: an efficient tool for network-based biomarker discovery, EMBnet.journal 22 (2016) 871. doi:10.14806/ej.22.0.871.

Towards an AI driven early detection of brain injuries in neonates through non-contact audio and video recording

Janet Pigueiras-del-Real[1], Lionel C. Gontard[1,4], Simón P. Lubián-López[2], Isabel Benavente-Fernández[2] and Angel Ruiz-Zafra[3]

[1]*Applied Optics and Magnetism Research Group, University of Cádiz, 11510 Puerto Real, Spain*
[2]*Department of Paediatrics and with Biomedical Research and Innovation Institute of Cadiz (INiBICA) Research Unit, Puerta del Mar University, Cadiz, Spain*
[3]*Department of Software Engineering, University of Granada, Periodista Daniel Saucedo Aranda s/n, 18071, Granada*
[4]*IMEYMAT, University of Cádiz, 11510 Puerto Real, Spain*

Abstract

An early detection of brain injuries in preterm infants' development fosters early therapies and treatments that could significantly improve the health of babies. Recent research confirm that the use of audio and video as non-contact data sources could enable the diagnosis of a possible brain damage of a neonate through the use of AI, but advances in this area are still very much in its infancy. This paper introduces an approach for the design and validation of a non-contact monitoring system to be used in a Neonatal Intensive Care Unit (NICU) that would help to the early detection of neonates affected by brain injury. The research focuses on the identification of neurological injury markers through the development of AI-based techniques based on video and audio data, exploiting the different features related to the movements, crying and sounds, and vital signs data of healthy neonates and of those affected by a brain injury. The paper presents the methodology and focuses on the first stage (System deployment) where it is described a software platform designed to collect, record and label data from different video and audio sources in a NICU, including the physiological parameters of the neonates.

Keywords

methodology, monitoring device, preterm infants, audio and video technologies, artificial intelligence, video and data gathering

1. Introduction

Early diagnosis of problems that can lead to neurodevelopmental disorders in preterm neonates are considered one of the main concerns of the medical community [1]. These patients have some vital functions immature and they need special care in Neonatal Intensive Care Units (NICUs) where their physiological parameters (heart rate, respiration rate and oxygen saturation) are constantly monitored with wired sensors attached to the skin of the baby. These sensors are connected to a monitor screen, which is reviewed by medical staff. Although this technique

DETERMINED 2022: Neurodevelopmental Impairments in Preterm Children — Computational Advancements, August 26, 2022, Ljubljana, Slovenia
janet.pigueiras@uca.es (J. Pigueiras-del-Real); lionel.cervera@uca.es (L. C. Gontard); isabel.benavente@uca.es (I. Benavente-Fernández); angelr@ugr.es (A. Ruiz-Zafra)
© 2021 Copyright for this paper by its authors. Use permitted under Creative Commons License Attribution 4.0 International (CC BY 4.0).
CEUR Workshop Proceedings (CEUR-WS.org)

CEUR-WS.org/Vol-3363/paper09.pdf

is appropriate, use of non-invasive techniques are emerging in recent years as a solid and viable alternative [2, 3].

Clinical monitoring of preterm infants including by direct observation of motor activity, facial expression, skin color, or cry can also be used to detect potential problems in the neurodevelopment of the baby. However, not all newborns can get benefit from this clinical follow-up as it requires medical staff with especial training that it is not always available and if present they have to share their time among many babies in a NICU [4].

The collection and analysis of audio and video of the neonates has proven to be a feasible solution with advantages for their monitoring, since it offers the gathering of clinical data without the need to use invasive methods (sensors glued to the skin) that may lead to discomfort and stress periods for the preterm. These techniques are currently being widely used in other biomedical applications [4].

In this paper we present a draft of an approach for the early detection of brain injuries in neonates using audio and video and supported by different computing technologies and paradigms: artificial intelligence (AI), internet of things (IoT), edge computing and computer vision (CV). The goal of the proposal is the use of non-invasive technologies to gather information related to the neonate through audio and video recordings, and process this data sources along with physiological information through the implementation of novel AI and CV-based algorithms/models to detect related symptoms of brain injuries in early stages of the baby's development.

The paper introduces the approach showing the different 5 stages that compose it, and focuses in the first two, which described *1)* an edge computing-based device developed and deployed to gather audio/video information in NICUs and *2)* the description of the *Neonate Recording Platform*, or NRP, A recording software platform used to collect data from different sources: video cameras, microphones and also from the monitors that are used in NICU for visualizing the physiological parameters of the babies.

The paper has 4 sections and it is organized as follows. In section 2 we present a detailed literature review. Section 3 illustrates the proposed methodology, with the different stages of this approach and the Section 4 provides conclusion of the study.

2. Related work

The recording of video and audio enables a non-invasive way to collect relevant medical information of the patients and it is being applied in many biomedical domains [4]. Next, we review recent developments for the non-contact monitorization of preterm neonates.

Video

In the case of NICUs, the research presented in [5] measures with video physiological variables and automatically detect bradycardia in infants. Other authors [6, 7] have developed and improved algorithms to control oxygen saturation, showing that it is safe and effective for carrying out measurements of vital parameters in preterm infants with assisted mechanical ventilation. Other studies have proposed the use of computer vision for the identification of

sleep stages, combining information from eye movements, body movements, facial expressions, sound made by babies and breathing patterns [8, 9].

A trendy line of research in this area is the automatic analysis of video using artificial intelligence techniques with the aim to provide an early diagnosis of neurological disorders [10, 11, 12]. *AI-based* models are used to detect the baby's pose and group them (set of sequences) to check if it is a normal behavior or abnormal. For instance, it has been applied to detect signs of cerebral palsy in babies [13, 14]. Much research focuses on the investigation in babies with a gestational age of 36 weeks, in order to correlate the amount of movement of the body with pain [12]. In the same category, in the project presented in [15] the authors propose to analyse spontaneous movements in order to diagnose neurodevelopmental disorders. Although this area is of great interest also for neonates, most of the research related to study the sequences of movements of the baby is carried out with a population of children who already walk.

Audio

Regarding to the use of audio as data source, the investigations in paediatrics mostly relied on cry analysis. In the 2000s, the analysis of signals began to be automated thanks to the *AI* techniques [4]. There are research that addressed the classification of cry signal through the use of *AI* algorithms in order to determine when babies are hungry, sleepy, need attention, are uncomfortable or need a diaper change [16, 17]. Analysis of cries was also developed in other contexts, for instead, [18] shows that deep learning systems are a powerful machines that can be used for distinguishing between healthy and pathological infant cry records. The authors of these works state that the crying of the baby is a field that has not yet been widely explored since it is not a language that can be easily understood, despite the fact that it is the main means of communication for this population.

In [16, 18] the authors made used of the short-time Fourier transform (STFT) to analyze audio signals. They also apply techniques originally designed and used in automatic speech recognition to detect and recognize the features of the baby's cry, and compression sampling to analyze and classify these signals. In addition, other research apply tools that were developed for analysing the crying signal. We can mentioned the study of [17, 19]. The authors apply the BioVoice software tool, developed specifically for the acoustic analysis of a newborn audio signal, in order to address their work in the crying field.

Furthermore, another topic in the use of audio for neonates is the measurement and analysis of environmental noise in the NICU. Probably [20] is the current state of art in this topic, where the authors develop the automatic detection of acoustic alarms in a noisy environment by applying filtering in the frequency space.

It is important to notice that joint audio and video processing has not been widely addressed so far. Concerning to our knowledge, only one study that integrates audio and video processing was published in [21] with Digi-New B project, where non-invasive strategies are proposed for the early diagnosis of neonatal sepsis.

In this paper we present an approach that joints the use of audio and video for a non-invansive detection of brain injury in neonates in early stages. The rest of the paper presents the different stages of the approach and focus in the technology and main contributions developed to collect audio and video data.

3. The proposed approach

This section introduces the draft of the proposed approach, which consist in a methodology composed by five stages and different AI-based techniques, developed computer vision algorithms, etc. The five stages of the methodology are depicted in Figure 1 and each stage is described shortly thereafter.

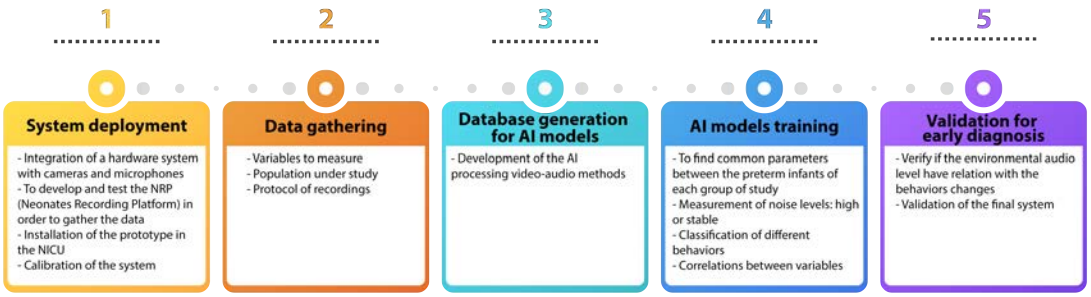

Figure 1: Proposed approach

Stage 1: *System deployment*

As first stage of the methodology, we need to set up the hardware-software system that must be used to record video as well as audio. Several commercials recording devices are available, however, we define a set of requirements that must accomplished by the devices, according to our expected outcomes once the approach completely implemented. The device required in our approach should meet, at least, the following features:

- *High quality recording video device.* In order to process in the best possible way the different frames captured of the neonate, we envise the use of a high quality recording camera.
- *Depth sensor supports in video recording.* The video captured will be used by AI-based techniques, so it is also desired to have a camera that also records or calculate depth in the recording raw video.
- *Physiological parameters collection.* So far, this approach does not address the automatic detection of some physiological parameters of the neonate such as heart rate, respiration rate, oxygen saturation, etc. In this way, our recording device will also have an additional camera to record the device where these neonate's parameters are shown, that is, the medical device located near to the neonate where are the wired sensors are connected. The software of these medical devices is not open source and the medical staff do not have the possibility of exporting the physiological parameters values.
- *Multiple audio recording.* At least, our approach must cover the recording audio about the sounds of the neonate but also the environment. However, could be interesting support an unknown number of recording audio devices in order to add as many data sources of audio as needed.

- *Data connectivity.* Although the recording of audio and video can be stored anywhere locally, could be interested have a device that can store the recordings but also send all the data (or part of it) to an external data warehouse.
- *Additional external storage.* Most of devices currently has an embedded internal storage or a free slot to insert a microSD card. Sometimes, especially if we record many hours, this storage capacity is not enough, so it is desired also that the devices has an extension to add additional storage devices like hard drives disks.
- *Comfortably and handy devices.* This recording device will be used probably by a medical staff or a research, that is, by a single user. So, the device must be easy to set up and easy to use.

With this restrictions about our needs in our approach, and after a concise search, we have not found an available commercial device that meets these requirements.

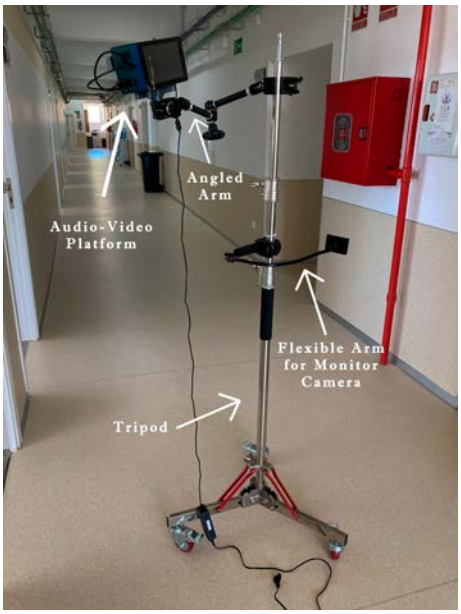

Figure 2: Prototype Support Equipment

In this first stage we have design, assembled and set up a hardware system with commercial components for the gathering of audio and video data from neonates, through the use of cameras and microphones. The system will record color videos with a camera focused on the baby, for gathering the body movements and facial expressions [22]. There will be a second camera that will be focused on recording the screen of the monitors that show the physiological parameters (heart rate, breathing, oxygen saturation) of the baby and that are placed next to the incubators. In addition the system will have 3 microphones, one omnidirectional to record environmental noise, and one directional to gather sounds made by the baby, and one additional from the physiological camera.

We have developed the system prototype (see Figure 2), that is composed of an OAK-D-CM4 (color camera), a Raspberry Pi where the operating system runs, an external hard drive,

the camera to register physiological parameters (web camera) and, in the first term, three microphones (aforementioned). One of the main features of the OAK is that it runs any AI model, even custom architecture/built ones. We are going to need this characteristic for future development of the recording platform, to offer a diagnosis on the possible presence of neurological problems signs in a preterm infants (Stage 4 of this approach).

In addition, for the right placement of the recording prototype, we have to place it where does not disturb the work of the clinicians, and easy-to-handle for them. The 3D housing is held near the incubator with a tripod and an angled arm. The second camera is also attached to the tripod with a second flexible arm. The housing includes a touch screen for the execution of the NRP.

This prototype is fully hardware, so the software is still required. Although the prototype could be used in many different areas, this first version has been developed aligned to the goals of this approach. In this way, a customized software to use the prototype as well as satisfy the requirements is required.

We have developed a customized software called *Neonates Recording Platform (NRP)*. The main view of NRP is illustrated in Figure 3.

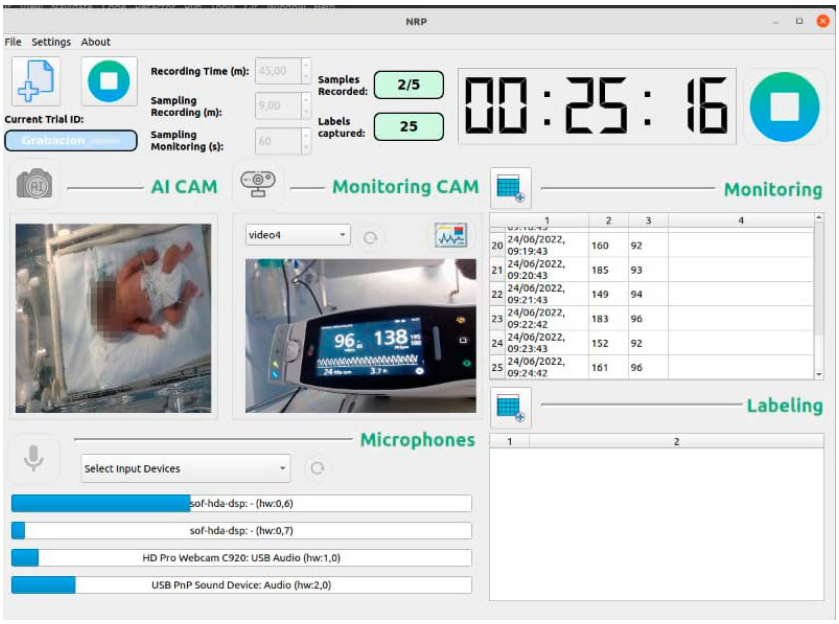

Figure 3: Neonate Recording Platform

The NRP (see Figure 3) supports the following different functionalities:

1. the recording of audio signals of different inputs/microphones. As many microphones as required can be added.
2. permanent recording of the neonate inside the incubator and the NICU (video).
3. video recording of the monitor that displays the neonate's physiological parameter.
4. automatic extraction and parsing of physiological parameters besides the entire video of the physiological parameters, a labeling system that automatically detects (using OCR

+ Machine learning neural network) from the video source *3)* and parse the neonate's parameters.
5. The software will enable healthcare professionals enabling to the addition of adding timestamps and comments
6. a trial-oriented structure to enable the exportation of the data in interoperable formats (XML, CSV, JSON) and enabling the exchange of trials between healthcare professionals
7. in order to ensure reliability, the recording interface supports the sampling of video and audio, recording content according to slots defined by end-user.

Stage 2: *Data gathering*

First of all, we need to calibrate the previous developed system in a real environment. For this purpose we are going to install the prototype in the NICU of the Puerta del Mar University Hospital located in Cadiz. The clinicians are going to choose one preterm infant and place him in an incubator with the same environmental conditions of the rest of the future recordings.

Secondly, we aim to be able to distinguish a healthy baby and a baby with brain injury. In order to achieve this goal, we need to analyse the different features of the behaviors of this 2 groups (crying, body movement and facial expressions), as well as the possible external triggers of the state changes. For this purpose, we propose to measure the following variables showed in the Table 1, that we have classified as external or internal variables depending on whether or not they are the baby's own.:

Table 1. Variables

Variable/Source	**Audio**	**Video**	**Other**
Internal	Crying	Movements	Heart frequency, Oxygen saturation, breathing frequency, clinical data
External	Environmental Audio	Presence/Absence of the baby	Comments and Labeling

The videos and audios will be recorded with the platform developed in the aforementioned Stage 1. At 36 weeks of post-menstrual age, the baby will be video-recorded for a period of 6 hours, 4hours before, and 2hours after the baby feeding. Around feeding time the baby is usually awake and we can gather his/her movements and crying. In addition, during this time controls are not usually carried out and the baby is not usually moved, so we can gather their movements and spontaneous crying without an external agent stimulating them.

The population under study will be made up of 2 groups of preterm infants, one of healthy babies and the other of babies with some neurological injury, who are admitted to the NICU of the University Hospital Puerta del Mar (Cadiz, Spain).

In order not to affect the possible movements of the baby, we propose to follow the protocol used for the authors [23, 24, 25] based on the Prechtl method [26] where it is proposed to carry out the recordings following the aspects:

- The child must remain in a supine position in the incubator
- Cosy incubator at a neutral temperature
- Free to move their body and all limbs, including fingers and toes
- Only wearing a diaper, no blankets or clothes
- Free disturbing environment

Stage 3: *Database generation for AI models*

Once all the data has been gathered, the pre-processing methods will be applied to provide the database for the training and later validation stage of the *AI* models.

The databases will save the different features that allow us to find the final correlation between variables in order to identify when a preterm present behaviors/state related to a possible brain injury. We could mention the following features:

- *Audio*: cry length, values of fundamental frequency (F0) and the first three resonant frequencies of the vocal tract (F1, F2 and F3), the decibels of environmental noise.
- *Movements/Motor activity*: value (angle and speed between adjacent joints) of the coordinates of 12 joints (left and right) shoulders, elbows, wrists, hips, knees and ankles.
- *Vital signs*: oxygen saturation value, breathing rate and heart rate.

Stage 4: *AI models training*

Through *AI* models, we aim to detect common data for each study groups that allow us to find behavioral features to differentiate a healthy baby from a baby with a possible neurological injury. In addition, classification methods will be applied in order to identify noise levels, high or stable.

On the other hand, through the application of the suitable *AI* model and using the data gathered previously, the different behaviors of the preterm infant will be classified, and finally identifying a neonate with brain damage from a healthy one.

At the end, we would like to develop a second platform (based on NRP platform) that will integrate IoT connectivity technologies, the visualization functionalities of the NRP platform, and a software system to support functionalities based on the use of artificial intelligence techniques, real-time notifications, etc. with the aim to support healthcare professionals in the behavioral understanding of preterm infants and diagnosis of possible signs of neurological injuries at real time.

Stage 5: *Validation for early diagnosis*

The goal is to get a software-hardware platform with TRL5 (Level 5 of Technology Readiness Level) [27], tested in a real environment by healthcare professionals. We will integrate a system with basic functionality that can record and process the audio-video stream, and offer a possible diagnosis of neurological injury sings.

Then we are planning to use the monitoring system in the NICU of the Puerta del Mar University Hospital located in Cadiz, and later to apply a survey (based on TAM-Technology Acceptance Model) [28] to the clinicians and nurses that allows us to know their opinions about

this contacless and non-invasive monitoring system, and if it has helped them when diagnosing the medical condition of a preterm infant.

4. Conclusions and Further Work

Brain injury is a frequent complication in preterms that need to be diagnosed as early as possible by medical staff in NICUs. At present, monitoring of the baby at NICUs is carried out 24/7 through empirical observation of nurses or medical staff along with the use of physiological parameters, gathered through wired-connected devices to the skin of the baby. As preterms cannot talk, clinical care include also intensive visual observation of the motor activity and aspect of the neonate with the aim to assess their health status.

There is much research through the use of audio and video data and AI-based techniques to support a non-contact monitoring of neonates with the goal of helping doctors in the early detection of brain damage, and improving the comfort of the babies in the incubators.

This paper presents an approach based on the use of cutting-edge technologies (AI, IoT, CV), the use of audio/video data sources and novel AI-based techniques to provides a support solution for medical staff to detect brain injuries in neonates at early stages of health development. The approach contains a methodology composed by five stages.

The paper describes the five stages but focus on the first stage (System deployment), presenting the first recording system prototype and NRP, a recording platform to gather information from different video and audio sources, providing also a labeling system and automatic recognition of physiological parameters.

As application example of this first, we described shortly the second stage, that is, the installation of the system in the NICU of University Hospital Puerta del Mar located in Cadiz, in order to gather the audio and video data. Likewise, we are going to keep progress on the research development in order to achieve the final goal.

Acknowledgments

Results incorporated in this publication received funding from the *EU Horizon 2020 MSCA-ITN-ETN "PremAtuRe nEwborn motor and cogNitive impairment: Early diagnosis - PARENT", GrantAgreement N° 956394.*. We would like to thank the clinicians, Isabel and Simon, of the hospitals hosting this work for their motivation, professionalism, and support to this research.

References

[1] Cabon, S., Porée, F., Simon, A., Met-Montot, B., Pladys, P., Rosec, O.,and Carrault, G. (2019). Audio-and video-based estimation of the sleep stages of newborns in Neonatal Intensive Care Unit. Biomedical Signal Processing and Control, 52, 362-370.

[2] Khanam, F. T. Z., Perera, A. G., Al-Naji, A., Gibson, K., and Chahl, J. (2021). Non-contact automatic vital signs monitoring of infants in a neonatal intensive care unit based on neural networks. Journal of Imaging, 7(8), 122.

[3] Khanam, F. T. Z., Al-Naji, A., Perera, A. G., Gibson, K., and Chahl, J. (2022). Non-contact automatic vital signs monitoring of neonates in NICU using video camera imaging. Computer Methods in Biomechanics and Biomedical Engineering: Imaging & Visualization, 1-8.
[4] Cabon, S., Porée, F., Simon, A., Rosec, O., Pladys, P., and Carrault, G. (2019). Video and audio processing in paediatrics: a review. Physiological measurement, 40(2), 02TR02.
[5] Villarroel, M., Guazzi, A., Jorge, J., Davis, S., Watkinson, P., Green, G. and Tarassenko, L. (2014). Continuous non-contact vital sign monitoring in neonatal intensive care unit. Healthcare technology letters, 1(3), 87-91
[6] Dargaville, P. A., Marshall, A. P., Ladlow, O. J., Bannink, C., Jayakar, R., Eastwood-Sutherland, C. and Gale, T. J. (2022). Automated control of oxygen titration in preterm infants on non-invasive respiratory support. Archives of Disease in Childhood-Fetal and Neonatal Edition, 107(1), 39-44.
[7] Nagy, Ádám, et al. "Continuous camera-based premature-infant monitoring algorithms for NICU." Applied Sciences 11.16 (2021): 7215.
[8] Bik, A., Sam, C., de Groot, E. R., Visser, S. S., Wang, X., Tataranno, M. L. and Dudink, J. (2022). A scoping review of behavioral sleep stage classification methods for preterm infants. Sleep Medicine.
[9] Sentner, T., Wang, X., de Groot, E. R., van Schaijk, L., Tataranno, M. L., Vijlbrief, D. C., and Dudink, J. (2022). The Sleep Well Baby project: an automated real-time sleep-wake state prediction algorithm in preterm infants. Sleep.
[10] Ihlen, E. A., Støen, R., Boswell, L., de Regnier, R. A., Fjørtoft, T., Gaebler-Spira, D., and Adde, L. (2019). Machine learning of infant spontaneous movements for the early prediction of cerebral palsy: A multi-site cohort study. Journal of clinical medicine, 9(1), 5.
[11] Sakkos, D., Mccay, K. D., Marcroft, C., Embleton, N. D., Chattopadhyay, S., and Ho, E. S. (2021). Identification of abnormal movements in infants: A deep neural network for body part-based prediction of cerebral palsy. IEEE Access, 9, 94281-94292.
[12] Leo, M., Bernava, G. M., Carcagnì, P., and Distante, C. (2022). Video-Based Automatic Baby Motion Analysis for Early Neurological Disorder Diagnosis: State of the Art and Future Directions. Sensors, 22(3), 866.
[13] Adde, L., Helbostad, J. L., Jensenius, A. R., Taraldsen, G., Grunewaldt, K. H., and StØen, R. (2010). Early prediction of cerebral palsy by computer-based video analysis of general movements: a feasibility study. Developmental Medicine and Child Neurology, 52(8), 773-778.
[14] Adde, L., Helbostad, J. L., Jensenius, A. R., Taraldsen, G., and Støen, R. (2009). Using computer-based video analysis in the study of fidgety movements. Early human development, 85(9), 541-547.
[15] Shin, H. I., Shin, H. I., Bang, M. S., Kim, D. K., Shin, S. H., Kim, E. K., and Lee, W. H. (2022). Deep learning-based quantitative analyses of spontaneous movements and their association with early neurological development in preterm infants. Scientific Reports, 12(1), 1-9.
[16] Liu, L., Li, Y., and Kuo, K. (2018, March). Infant cry signal detection, pattern extraction and recognition. In 2018 International Conference on Information and Computer Technologies (ICICT) (pp. 159-163). IEEE.
[17] Orlandi, S., Garcia, C. A. R., Bandini, A., Donzelli, G., and Manfredi, C. (2016). Application of pattern recognition techniques to the classification of full-term and preterm infant cry.

Journal of Voice, 30(6), 656-663.
[18] Liu, L., Li, W., Wu, X., and Zhou, B. X. (2019). Infant cry language analysis and recognition: an experimental approach. IEEE/CAA Journal of Automatica Sinica, 6(3), 778-788.
[19] Manfredi, C., Bandini, A., Melino, D., Viellevoye, R., Kalenga, M., and Orlandi, S. (2018). Automated detection and classification of basic shapes of newborn cry melody. Biomedical Signal Processing and Control, 45, 174-181
[20] Raboshchuk, G., Jančovič, P., Nadeu, C., Lilja, A. P., Köküer, M., Mahamud, B. M., and Veciana, A. R. D. (2015). Automatic detection of equipment alarms in a neonatal intensive care unit environment: A knowledge-based approach. In the Sixteenth Annual Conference of the International Speech Communication Association.
[21] Digi-NewB - GCS HUGO - CHU - monitoring system, http://www.digi-newb.eu, accessed 14 July 2022
[22] Cabon, S., Porée, F., Cuffel, G., Rosec, O., Geslin, F., Pladys, P. and Carrault, G. (2021). Voxyvi: A system for long-term audio and video acquisitions in neonatal intensive care units. Early Human Development, 153, 105303.
[23] Einspieler, C., Prechtl, H. F., Ferrari, F., Cioni, G., and Bos, A. F. (1997). The qualitative assessment of general movements in preterm, term and young infants—review of the methodology. Early human development, 50(1), 47-60.
[24] Porro, M., Fontana, C., Giannì, M. L., Pesenti, N., Boggini, T., De Carli, A.and Picciolini, O. (2020). Early detection of general movements trajectories in very low birth weight infants. Scientific Reports, 10(1), 1-7.
[25] Einspieler, C., and Prechtl, H. F. (2005). Prechtl's assessment of general movements: a diagnostic tool for the functional assessment of the young nervous system. Mental retardation and developmental disabilities research reviews, 11(1), 61-67
[26] Einspieler, C., Prechtl, H. F. R., Bos, A. F., Ferrari, F. and Cioni, G. Prechtl 's Method on the Qualitative Assessment of General Movements in Preterm, Term and Young Infants (Mac Keith Press, 2004).
[27] Martínez-Plumed, F., Gómez, E., and Hernández-Orallo, J. (2021). Futures of artificial intelligence through technology readiness levels. Telematics and Informatics, 58, 101525.
[28] Na, S., Heo, S., Han, S., Shin, Y., and Roh, Y. (2022). Acceptance Model of Artificial Intelligence (AI)-Based Technologies in Construction Firms: Applying the Technology Acceptance Model (TAM) in Combination with the Technology–Organisation–Environment (TOE) Framework. Buildings, 12(2), 90.

Intelligent system development to monitor the neonatal behaviour: A review

Syed Adil Hussain Shah[1,*,†], Angelo di Terlizzi[1,†] and Marco Agostino Deriu[2,†]

[1]Department of Research and Development (R&D), GPI SpA, Trento, Italy
[2]PolitoBIOMed Lab, Department of Mechanical and Aerospace Engineering, Politecnico di Torino, Turin, Italy

Abstract

The early birth of children can be associated with neurodevelopmental disease onset. In such cases, the lack of early diagnosis and early medical treatment negatively affects the rest of the child's life. In this context, recent developments in artificial intelligence (AI) in the medical field suggest a possible key role also in the cases of preterm birth through the integration of various sources of neurodiagnostic data in order to extract clinical information. In this manuscript, we have addressed the importance of the development of intelligent systems merging with the Internet of Medical Things (IoMT) for the analysis of the baby's movement. More in detail, we here consider a general prototype of an incubator for neonatal intensive care unit (NICU) and related tools capable of detecting/measuring vital signs and patient characteristics for newborns with particular attention to preterm infants. In this context, we will also provide a brief explanation of available datasets, such as BabyPose Dataset, MINI-RGBD, and MIA dataset. Furthermore, we will explore data mining techniques and the role of IoMT in the context of preterm infants and children. Finally, emphasis will be placed on technology communication, combination, and multidisciplinary research pursuing more accurate and improved self-guided techniques and systems.

Keywords

Preterm birth, Incubator system, Intensive care unit, Data mining, Baby motion analysis, Internet of medical things

1. Introduction

According to World Health Organization (WHO) observations, the first month of life is a very dangerous period for child survival, with 2.4 million newborns dying in 2020 [1, 2]. The highest neonatal mortality rate was recorded in sub-Saharan Africa and Central and South Asia, with about 25 deaths per 1000 births [3, 4].

The main causes of death from preterm birth are lack of breathing at birth, low birth weight, illness, and other infection factors. In general, preterm birth is divided into three categories according to the gestational age of delivery: moderate preterm (MP: 32-37 weeks), very preterm

DETERMINED 2022: Neurodevelopmental Impairments in Preterm Children — Computational Advancements, August 26, 2022, Ljubljana, Slovenia

*Corresponding author.
†These authors contributed equally.
syedadilhussain.shah@gpi.it (S. A. H. Shah); angelo.diterlizzi@gpi.it (A. d. Terlizzi); marco.deriu@polito.it (M. A. Deriu)
https://www.dimeas.polito.it/en/personale/scheda/(nominativo)/marco.deriu (M. A. Deriu)
0000-0003-1918-1772 (M. A. Deriu)

© 2022 Copyright for this paper by its authors. Use permitted under Creative Commons License Attribution 4.0 International (CC BY 4.0).
CEUR Workshop Proceedings (CEUR-WS.org)

CEUR-WS.org/Vol-3363/paper10.pdf

(VP - 28-32 weeks), and extremely preterm (EP - less than 28 weeks) [5].

The normal and stable duration of delivery is considered completed when the pregnancy cycle exceeds 37 weeks of gestation. The earlier the birth, the higher the risk of death, and the need to monitor the preterm infant in the neonatal intensive care unit (NICU) for a long-time increase. Because of this critical condition, artificial intelligence systems for example coupled with incubator sensor systems can play an important role in overcoming the preterm mortality rate and improving the quality of care.

In recent years, many researchers have been working on the development of intelligence systems to improve the performance of neonatal behavior monitoring and analysis. In this area, contact and noncontact clinical data sources are being used to design automated intelligent systems. In addition, computer systems that were previously inadequate at the home of traditional and handcrafted features are now performing very well mainly due to the integration of machine learning and deep learning algorithms. In this regard, a general software architecture for neonatal sensing and monitoring is shown in Figure 1, which includes various IoMT-related concepts and technologies such as artificial intelligence, devices, sensors, big data, mobile devices, and what is considered for the design of state-of-the-art NICU incubators.

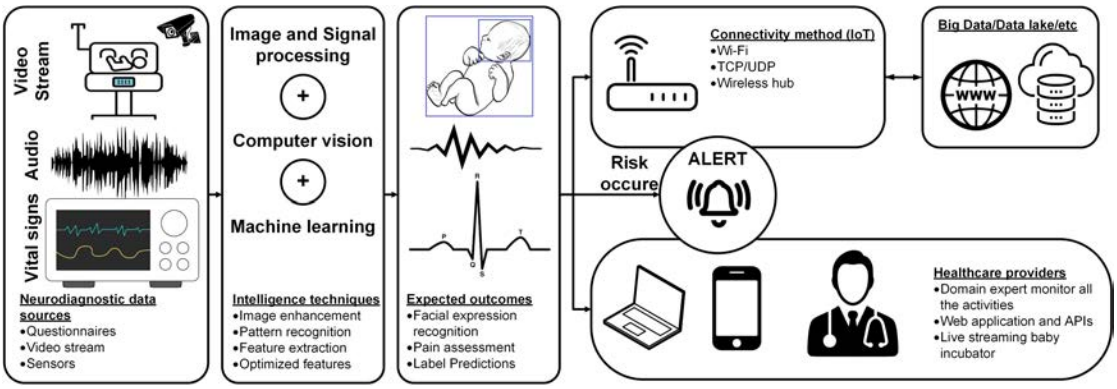

Figure 1: The general flow of an automated system to monitor neonatal behaviour.

As said, monitoring neonatal behaviors is a key clinical activity for early diagnosis of possible abnormalities or diseases. In this context, the AI and computer vision fields have given a lot of attention to the automated identification and classification of newborn behaviors [6, 7, 8]. The manual process to monitor the behaviour of newborn babies was complex and too much costly. Moreover, it is dangerous for neonatals to survive in low-resource environments. Therefore, an automated AI system with the implementation of hardware can be useful for neurologists and domain experts to monitor the baby's condition in a single incubator in a NICU. For the development of AI systems, the researchers believe that such applications will be helpful for doctors to analyze the behaviour of preterm birth.

Based on the above-mentioned premises in the present review work we will discuss issues related to the role of AI systems and IoT that may help in designing automated systems to obtain accurate results and reduce the complexity rate in the field of NICU incubator implementation. More specifically, the article focuses on issues concerning: i) the knowledge base on the

Neonatal Intensive Care Unit and related conditions; ii) data collection issues and publicly available reference datasets; iii) the role of data mining techniques for monitoring neurological disorders; iv) the role of IoT in the medical environment and the potential of the mentioned technologies in the field of incubator design and development.

2. General features of NICU Incubators

An incubator is a device used to monitor clinical parameters and maintain environmental conditions suitable for the life of a newborn baby. It is generally used in preterm birth or in cases of specific pathologies at birth. The device is equipped with sensors that are capable of monitoring/supporting the patient's condition through the detection of behavioural and physiological parameters (e.g. blood pressure, oxygenation, temperature, cardiac function, etc.) of newborns that help doctors to prevent any morbidity leading to the critical phase [9, 10]. The real-time analysis gives the advantage of early detection of any type of complication, which can help protect the infant and increase its survival rate [11, 12]. The single incubator in the NICU is a separate, self-contained area for each individual infant under the supervision of an expert. A NICU incubator usually requires multidisciplinary skills and highly qualified specialists, being built for those environments that manage the critical phase of preterm infants [13].

2.1. Main pathological conditions requiring the use of NICU incubators

In the following list, the main conditions requiring the use of incubators are detailed:
• Intraventricular hemorrhage (IVH)
Intraventricular hemorrhage (IVHs) causes the illness or disease and death of newborn infants. Infants whose birth weight is about 1500g usually develop an IVH. Mostly it occurs during the third day of birth and in some cases, it occurred before delivery. Important risk factors for IVHs are: increase atrial blood pressure, pneumothorax, and birth asphyxia [14, 15]. The potential of ML techniques to improve early detection of IVH has been highlighted in recent literature.
• Periventricular leukomalacia (PVL)
In this disease, the white matter near the cerebral ventricles dies. PVL is usually developed by premature infants, whose birthweight 1500g or 3lb 5oz. PVL affects infants (birth week < 25) when they are suffering from the deprivation of oxygen during delivery and at the time of birth [16]. The variation of oxygen and CO2 in the blood cause PVL while the surgeons predict this disease by applying standard psychological parameters to infants [17]. In the aspect of intelligent system development, many researchers have proposed several techniques to predict the PVL disease in neonates [18, 19].
• Nosocomial Infection
Infections are the most common cause of mortality and illness for infants [20]. Around 45% of infants born before 25-28 weeks of gestation and kept alive in NICU incubators face critical infections. This infection, mainly caused by pathogens present in the hospital, is difficult to be identified at an early stage given that symptoms appear at the advanced pathological stage. Clinical checkups are mainly responsible for the infection spread [21]. Few examples of intelligent system for recognition of the above-mentioned neonatal infection are reported in literature [22, 23].

• Pneumothorax
Pneumothorax occurs when air or gas accumulated in the process of inhaling and exhaling. In the body, the pleural cavity is a fluid-filled space that surrounds the lungs. Usually, 1-2% of infants face gas and air in their pleural cavities. There are two layers that surround the lungs. One is attached to the chest wall and the other is attached to the lungs. These layers move when we inhale or exhale, and in this process, fluid is emitted from the membrane for the lubrication of the lung's smooth movement [14]. In pneumothorax, researchers have also used machine learning techniques to improve the detection as details are presented in [24, 25].

2.2. Principles for design and implementation of NICU incubators

The implementation of a single intensive care unit is divided into two main types: real and simulated prototypes, where real prototype means the testing phase in a real environment while simulated prototypes are just computer-implemented and analyzed systems. In this regard, Figure 2 has shown the general prototype of the neonatal incubator.

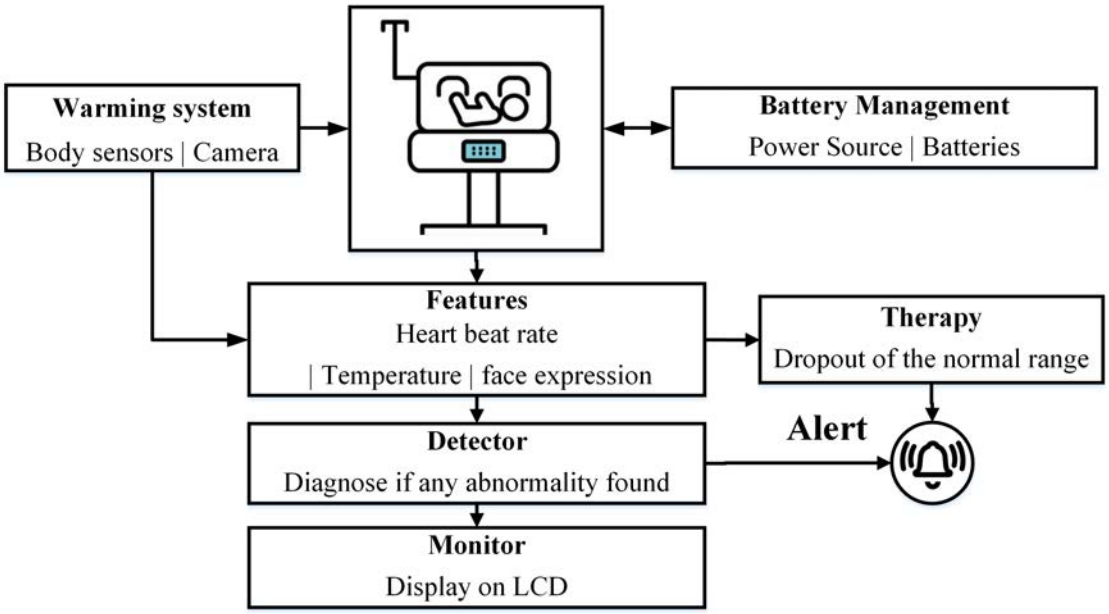

Figure 2: General prototype of neonatal Single intensive care unit [11].

There are several tools and systems which are usually connected with an incubator to monitor the condition of the baby at every moment. Due to these components, surgeons can easily analyze a number of vital signs and features like the warming system (body temperature, heart beat rate (HBR), and SpO2) and body behaviour systems (cameras). All these features of the neonatal are basically displayed on the incubator's LCD. Moreover, the power supply systems are also connected to the incubator to manage the battery system. In any condition, the behaviour, oxygen level, or temperature is sensed as a bad outcome by the machine, it generates an alert

buzzer which means the patient is in a critical stage. There are several parameters related to incubators that interact with IoT and further explanations are shown in table 1.

A. F. Symon et. al. [26] developed a system that detects the movement and crying sound of a newborn baby. The objective of this study was to analyze the contactless data modality to find the state of babies and also monitor their physical behaviour. It was suggested that previous systems were just controlling the temperature and humidity of the incubator without controlling the sound pollution which they found that it is a very mandatory parameter that can provide a comfortable environment to the baby. In another research [27], they designed a hardware system in combination with IoT's based model to monitor the preterm incubator environment. The hardware components used microcontroller along with the other body temperature sensors. The performance of the proposed system was better as compared to the other related measuring systems. In this way, N. A. Zakaria et. al. [28] addressed another device to detect the infant body temperature in an incubator system. The device was a wearable sensor that measures the vital signs of baby and also sends the information to their parents through a wireless network. Furthermore, the portable device is utilized to visualize the information and any alert related to the baby health.

All the above-mentioned studies have shown contactless systems in detail but are not physically installed in any hospital. In recent research implemented at the John Radcliffe Hospital in Oxford [22]. This work has been designed similarly to previously discussed methods. They have adapted the video-based technique to monitor neonatals' respiratory rate, heart rate, and oxygen saturation. By using these features, they have developed an algorithm that efficiently detects bradycardia events in the early stages.

Table 1
Incubator parameters interacting with IoT

References	*PARAMETERS*	*SYSTEM MONITORING WITH THE PARAMETERS*
[11]	Neonatal body temperature	This is a monitoring and risk management system, through cloud services, for neonates and it manages the critical stage alarm to domain experts for personal assistance.
[29]	Incubator heat	This parameter maintains the incubator heat which is sufficient for the development of the preterm baby.
[30]	Incubator Humidity	This parameter controls the humidity level in the incubator and it helps in maintaining the temperature of the incubator.
[29, 31]	Neonatal body weight	By the help of this measure, surgeons came to know about the weight of neonate. In this way, they can analyze the growth of neonate based on his/her weight.

3. Information Technology in biomedicine and potential for data collection and treatment at NICU

IT has cardinal importance in every aspect of our lives [32, 33, 34]. It has also proved itself as an important part of the medical field as well. Health IT is processing the information of different kinds of diseases using computer knowledge and its advancements. The capability of decision-making in health IT is a lot more than that of an individual human. As we know, computers can work more efficiently than humans. Health IT can assist all over the world's medical community in diagnosing different diseases. Due to advancements in IT, the medical field is also considering IT as an important part of it. The most tremendous thing in this IT domain is the amount of required data, that is available on the internet and anyone can access that information at any time [35].

However, this is not always the case with clinical data. Although there is a huge amount of clinical data that is collected by each hospital, this collection is usually very irregular and rough, both from one field to another but also in the same field in different countries and even in the same country from hospital to hospital. In fact, even today in many hospitals, data collection is done by hand by doctors or with the help of computer tools but often in a disorganized manner. This creates a huge problem in the pre- and post-processing of clinical data whose sets are often unusable. Added to this are the various problems of ethics and data privacy, which often require lengthy approval processes for their use. The case of the study of neurodevelopmental disorders presents a further degree of difficulty, given a large number of patients, which is certainly much smaller than in studies of cardiac diseases.

In this context, it is therefore crucial to develop systems that are able to automatically collect data in a standardized manner, but also to pre- and post-process collected data in order to boost the ability to extract useful clinical information from them. This is the context for all the IT technologies, IoMT that have been introduced above and that have the potential to drastically increase the quantity and quality of clinical data that could be available to data mining and ML-driven knowledge extraction algorithms. In this vision, a single NICU incubator becomes also a data collector for infant disease investigation based on real-world data. Nevertheless, some data for the analysis of the preterm‘s behaviour have already been collected and made available to the community. Those datasets are listed in Table 2.

3.1. Internet of medical things (IoMT) and potential for neonatal data sharing

Internet of Things (IoT) is an emerging technology that is increasing the data in various sectors daily. Big data analysis is a technique used to handle and evaluate enormous amounts of data using various methods. The IoT is a general paradigm. It changes its shape according to the environment, when we deal with the medical environment it is known as the IoMT. The objective of IoTs is to provide remote access to different physical devices and machines on service providers that cover location-based services, smart cities, smart streets, and homes. The IoT applications use invariably cloud storage combined with fog computing. Ubiquitous systems are increasing day by day and it reaches 50 billion in 2020 [31]. Nowadays, researchers have included many components in IoMT which have started to make the medical staff's life very easy like web portals, WSN (Wireless Sensor Nodes), RFID (Radio Frequency Identification),

Table 2
The publicly available dataset of infants, newborns, and toddlers

Dataset	*Modalities*	*Short Description*
Baby-Pose[36]	videos	The dataset contains 16 videos of 640 x 480 per frame size with 8–16-bit depth including 12 newborn cases with landmarks
MINI-RGBD[37]	videos	The dataset contains 12 videos having 640 x 480 per frame size with RGB Channels. This dataset is labeled on 25 infant babies
3D-AD[38]	videos	The dataset contains 100 videos with 512 x 424 frame size. In this dataset, the behaviour of toddlers is labeled
InfantsData[39]	videos	The dataset contains 85 videos with variant frame size and RGB channels. The dataset is labeled on 18 infant cases' landmarks
SyRIP[40]	images	The dataset contains the RGB channel images of 17 infant patients
SSBD[41]	videos	75 Youtube video, (m x n) frame size of RGB channels with benchmark dataset of behaviours of the preterm babies.

LCDs, detection sensors, etc [21, 42, 43]. In this scenario, L. Nachabe et. al. [44] designed a Distributed Neonatal Incubator Monitoring System (DNIMS) for neonates in which distributed software agents were used to connect different end-users like medical staff, parents, etc. This kind of system is the need of the current time because it is not just generating and storing the data in the servers but also in parallel, reformatting the data for the medical staff and caretakers [45].

3.2. Big Data Management tools and their potential application for future big data collection by novel generation of incubators

In the near future, we hope to have a massive amount of data coming from the next generation of incubators in NICUs. Several technologies for managing big data have already been developed and successfully employed in other medical fields. In this context, it is worth mentioning that five main strategies are recognized as successful in big data management: (1) create structured big data, (2) data sharing culture to develop information, (3) training to use big data analytics, (4) big data analytics with the combination of cloud computing, and (5) using big data analytics techniques to generate new business ideas. The need of analytics is linked with improvement in patient-centric services, detection of disease before it spreads, and -monitoring of the quality of services and methods of treatment. Some tools like Apache Hadoop is highly scalable storage platform. It provides cost-effective storage for large data. Apache Spark [46] is an open-source, in-memory processing machine. Its performance is much faster than Hadoop [47]. Another renowned platform namely MapReduce is used for interactive data mining. There are other large numbers of big data analytics tools/platforms which are publicly available and can be found at [48].

3.3. Data Mining techniques for extracting knowledge from collected data

Modern IT has radically amplified the capacity and power of data mining and information extraction from data. Classical or ML/DL driven data mining concern the analysis of observational datasets to extract knowledge from them unraveled unknown relationships and rationalize data in useful ways for the end-user. In the context of data coming from NICU incubators, Figure 3 can be helpful in the development of an efficient automated health care system.

Following the flow described in Figure 3, we may identify the main techniques/steps characterizing data mining technology. Those are general steps that can be specified depending on the chosen application. For example, preprocessing applied to data concerning studies in Table 3 will be principally used to upgrade the nature of an image with diminishing varieties. This is done to eradicate any infringements that cause entanglements in the preparing stage which cause broad utilization of reality assets [49]. Several key destinations can be accomplished with preprocessing which incorporates commotion evacuation, differentiate improvement, brightening, and recoloring revision. For evacuation, channels are broadly utilized, for example, mean and middle channels, Gaussian low-pass sifting, etc. Morphological strategies are additionally utilized for image sharpness upgrade purposes [50]. For differentiating improvement, differentiate extending strategies and histogram adjustment procedures have been generally used to enhance the contrast in the images. For brightening adjustment and recoloring varieties, shading standardization procedures have been mostly utilized [51].

Classification, data rationalization, knowledge extraction, and statistical formulation usually follow the preprocessing and can be combined or not. There are a high number of application examples of data mining techniques applied to the medical field. In Table 3 we report the most important application related to neonatal behavioral investigation. Again, all these approaches can be considered for further application in concert with the novel generation of NICU incubators for data analysis and knowledge extraction to support clinical decisions and precision medicine.

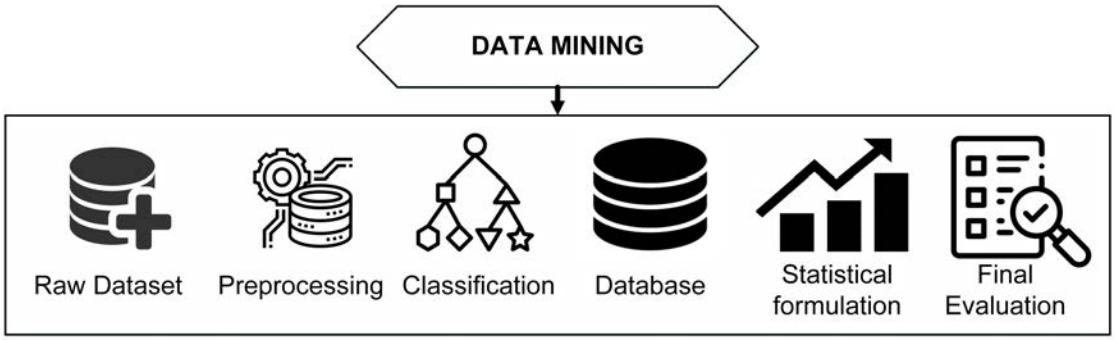

Figure 3: The block diagram of the data mining techniques for intelligent system development.

Table 3
Preprocessing and data mining research work

Study	*Environment*	*Data detail*	*Technique*	*Objectives*
[52]	Hospital	3D images	Key points recognition	Overall behaviour analysis
[53]	NICU	3D images	Convolutional neural networks (CNN's)	Overall behaviour analysis
[54]	Hospital	Multidimensional	Logistic regression algorithm	Classify normal/abnormal
[55]	Hospital	RGB images	supervised machine learning and handcrafting algorithm	Detect the Writhing movement
[56]	N/A	Synthetic	Convolutional neural network (CNN)	Classify abnormal Infant Movements
[57]	Hospital	RGB Images	Gaussian mixture model	Classify 4 type of movements
[58]	Hospital	RGB Images	Motion features, Decision Tree algorithm	Analysis CP risk
[59]	Hospital	RGB Images	Neural network	Detect the nervous condition of baby
[60]	Home/Hospital	RGB Images	Pre-trained CNN + LSTN	Detect Fidgety Movement

4. Conclusion

In the context of neonatal care, software architectures for storing data, to be then analyzed by data mining techniques, should consider innovative tools for heterogeneous (structured and unstructured) data collection as data that may be collected through hardware diagnostic devices, custom sensors, and software solutions installed in a NICU incubator (or a set of NICU incubators). Those data either the raw data or the processed data – should thus be handled as sensitive data, considering the appropriate ethical and privacy procedures, amongst which compliance to the General Data Protection Regulation (GDPR). Examples of data sources are (a) clinical data and Electronic health records (EHRs); (b) imaging data; (c) IoT device data streams. It is worth noticing that developing data collectors and management systems for neonatal care may take advantage of existent tools already applied to manage data in other fields of medicine and explicitly developed to manage patient health data with all the protection systems that need to be used for this type of sensitive data.

Acknowledgment

The present research work has been developed as part of the PARENT project, funded by the European Union's Horizon 2020 research and innovation program under the Marie Sklodowska-Curie-Innovative Training Network 2020, Grant Agreement N° 956394 (https://parenth2020.com/).

Conflicts of Interest

The authors declare no conflict of interest.

References

[1] Newborn mortality, 2021. URL: https://www.who.int/news-room/fact-sheets/detail/levels-and-trends-in-child-mortality-report-2021, accessed Mar. 15, 2022).

[2] Newborn mortality, 2020. URL: https://www.who.int/news-room/fact-sheets/detail/newborns-reducing-mortality, accessed Mar. 15, 2022).

[3] T. Tekelab, C. Chojenta, R. Smith, D. Loxton, The impact of antenatal care on neonatal mortality in sub-saharan africa: A systematic review and meta-analysis, PLOS ONE 14 (2019) 0222566,. doi:10.1371/JOURNAL.PONE.0222566.

[4] Towards maternal and newborn survival in the WHO South-East Asia Region i Implementation experience of the WHO SEARO model of point-of-care quality improvement (POCQI) Towards maternal and newborn survival in the WHO South-East Asia Region Implementation experience of the WHO SEARO model of point-of-care quality improvement, POCQI), 2020.

[5] B. Koullali, The association between parity and spontaneous preterm birth: A population based study, BMC Pregnancy and Childbirth 20 (2020) 1–8,. doi:10.1186/S12884-020-02940-W/TABLES/3.

[6] S. M. Mathews, Explainable artificial intelligence applications in nlp, biomedical, and malware classification: a literature review, in: Intelligent computing-proceedings of the computing conference, Springer, 2019, pp. 1269–1292.

[7] M. S. Salekin, P. R. Mouton, G. Zamzmi, R. Patel, D. Goldgof, M. Kneusel, S. L. Elkins, E. Murray, M. E. Coughlin, D. Maguire, et al., Future roles of artificial intelligence in early pain management of newborns, Paediatric and Neonatal Pain 3 (2021) 134–145.

[8] P. K. D. Pramanik, S. Pal, P. Choudhury, Beyond automation: the cognitive iot. artificial intelligence brings sense to the internet of things, in: Cognitive computing for big data systems over IoT, Springer, 2018, pp. 1–37.

[9] J. Nates, Icu admission, discharge, and triage guidelines: A framework to enhance clinical operations, development of institutional policies, and further research, Critical Care Medicine 44 (2016) 1553–1602,. doi:10.1097/CCM.0000000000001856.

[10] A. Ehteshami, F. Sadoughi, M. Ahmadi, P. Kashefi, Intensive care information system impacts, Acta Informatica Medica 21 (2013) 185,. doi:10.5455/AIM.2013.21.185-191.

[11] A. Zaylaa, M. Rashid, M. Shaib, I. Majzoub, A handy preterm infant incubator for providing

intensive care: Simulation, 3d printed prototype, and evaluation, Journal of Healthcare Engineering 2018 (2018). doi:10.1155/2018/8937985.

[12] E. Küng, L. Aichhorn, A. Berger, T. Werther, Mirrored ribs: A sign for pneumothorax in neonates, Pediatric Critical Care Medicine (2020) 944– 947,. doi:10.1097/PCC.0000000000002381.

[13] C. Bassford, Decisions regarding admission to the icu and international initiatives to improve the decision-making process, Critical Care 21 (2017) 1–3,. doi:10.1186/S13054-017-1749-3/METRICS.

[14] D. Szpecht, M. Szymankiewicz, I. Nowak, J. Gadzinowski, Intraventricular hemorrhage in neonates born before 32 weeks of gestation—retrospective analysis of risk factors, Child's Nervous System 32 (2016) 1399–1404,. doi:10.1007/S00381-016-3127-X/TABLES/1.

[15] N. Shah, C. Wusthoff, Intracranial hemorrhage in the neonate, Neonatal Network 35 (2016) 67–72,. doi:10.1891/0730-0832.35.2.67.

[16] M. Deshmukh, S. Patole, Antenatal corticosteroids in impending preterm deliveries before 25 weeks' gestation, Archives of Disease in Childhood - Fetal and Neonatal Edition 103 (2018) 173– 176,. doi:10.1136/ARCHDISCHILD-2017-313840.

[17] N. Zaghloul, H. Patel, M. Ahmed, A model of periventricular leukomalacia (pvl) in neonate mice with histopathological and neurodevelopmental outcomes mimicking human pvl in neonates, PLOS ONE 12 (2017) 0175438,. doi:10.1371/JOURNAL.PONE.0175438.

[18] A. Jalali, A. F. Simpao, J. A. Gálvez, D. J. Licht, C. Nataraj, Prediction of periventricular leukomalacia in neonates after cardiac surgery using machine learning algorithms, Journal of medical systems 42 (2018) 1–11.

[19] D. Bender, D. J. Licht, C. Nataraj, A novel embedded feature selection and dimensionality reduction method for an svm type classifier to predict periventricular leukomalacia (pvl) in neonates, Applied Sciences 11 (2021) 11156.

[20] S. Edwardson, C. Cairns, Nosocomial infections in the icu, Anaesthesia Intensive Care Medicine 20 (2019) 14–18,. doi:10.1016/J.MPAIC.2018.11.004.

[21] H. Khan, F. Baig, R. Mehboob, Nosocomial infections: Epidemiology, prevention, control and surveillance, Asian Pacific Journal of Tropical Biomedicine 7 (2017) 478–482,. doi:10.1016/J.APJTB.2017.01.019.

[22] J.-F. Hsu, Y.-F. Chang, H.-J. Cheng, C. Yang, C.-Y. Lin, S.-M. Chu, H.-R. Huang, M.-C. Chiang, H.-C. Wang, M.-H. Tsai, Machine learning approaches to predict in-hospital mortality among neonates with clinically suspected sepsis in the neonatal intensive care unit, Journal of Personalized Medicine 11 (2021) 695.

[23] M. Beltempo, G. Bresson, G. Lacroix, Using machine learning to predict nosocomial infections and medical accidents in a nicu (2020).

[24] C. Mehanian, S. Kulhare, R. Millin, X. Zheng, C. Gregory, M. Zhu, H. Xie, J. Jones, J. Lazar, A. Halse, et al., Deep learning-based pneumothorax detection in ultrasound videos, in: Smart Ultrasound Imaging and Perinatal, Preterm and Paediatric Image Analysis, Springer, 2019, pp. 74–82.

[25] S. Röhrich, T. Schlegl, C. Bardach, H. Prosch, G. Langs, Deep learning detection and quantification of pneumothorax in heterogeneous routine chest computed tomography, European radiology experimental 4 (2020) 1–11.

[26] A. Symon, N. Hassan, H. Rashid, I. Ahmed, S. Reza, Design and development of a smart

baby monitoring system based on raspberry pi and pi camera, in: 4th International Conference on Advances in Electrical Engineering, ICAEE 2017, volume 2018-January, 2017, pp. 117–122,. doi:10.1109/ICAEE.2017.8255338.

[27] W. Shalannanda, I. Zakia, E. Sutanto, F. Fahmi, Design of hardware module of iot-based infant incubator monitoring system, in: Proceedings - 2020 6th International Conference on Wireless and Telematics, ICWT, 2020. doi:10.1109/ICWT50448.2020.9243665.

[28] N. Zakaria, F. Saleh, M. Razak, Iot (internet of things) based infant body temperature monitoring, in: 2nd International Conference on BioSignal Analysis, Processing and Systems, ICBAPS, 2018, pp. 148–153,. doi:10.1109/ICBAPS.2018.8527408.

[29] L. Lamidi, A. Kholiq, M. Ali, A low cost baby incubator design equipped with vital sign parameters, Indonesian Journal of Electronics, Electromedical Engineering, and Medical Informatics 3 (2021) 53–58,. doi:10.35882/IJEEEMI.V3I2.3.

[30] S. Alduwaish, Automated humidity control system for neonatal incubator, Journal of Physics: Conference Series 2071 (2021) 012029,. doi:10.1088/1742-6596/2071/1/012029.

[31] M. Nampira, A. Kholiq, Lamidi, A modification of infant warmer with monitoring of oxygen saturation, heart rate and skin temperature, Journal of Electronics, Electromedical Engineering, and Medical Informatics 3 (2021) 19–25,. doi:10.35882/JEEEMI.V3I1.4.

[32] C. Kruse, A. Beane, Health information technology continues to show positive effect on medical outcomes: Systematic review, J Med Internet Res 2018;20(2):e41 (2018) 8793,. URL: https://www.jmir.org/2018/2/e41,. doi:10.2196/JMIR.8793.

[33] M. Javaid, A. Haleem, Industry 4.0 applications in medical field: A brief review, Current Medicine Research and Practice 9 (2019) 102–109,. doi:10.1016/J.CMRP.2019.04.001.

[34] M. Yamin, It applications in healthcare management: a survey, International Journal of Information Technology (Singapore 10 (2018) 503–509,. doi:10.1007/S41870-018-0203-3/FIGURES/3.

[35] H. Ke, Cloud-aided online eeg classification system for brain healthcare: A case study of depression evaluation with a lightweight cnn, Software: Practice and Experience 50 (2020) 596–610,. doi:10.1002/SPE.2668.

[36] L. Migliorelli, S. Moccia, R. Pietrini, V. Carnielli, E. Frontoni, The babypose dataset, Data in Brief 33 (2020) 106329,. doi:10.1016/J.DIB.2020.106329.

[37] N. Hesse, C. Bodensteiner, M. Arens, U. G. Hofmann, R. Weinberger, A. Sebastian Schroeder, Computer vision for medical infant motion analysis: State of the art and rgb-d data set, in: Proceedings of the European Conference on Computer Vision (ECCV) Workshops, 2018, pp. 0–0.

[38] O. Rihawi, D. Merad, J. Damoiseaux, 3d-ad: 3d-autism dataset for repetitive behaviours with kinect sensor, in: 2017 14th IEEE International Conference on Advanced Video and Signal Based Surveillance, AVSS 2017, 2017. doi:10.1109/AVSS.2017.8078544.

[39] C. Chambers, Computer vision to automatically assess infant neuromotor risk, IEEE Transactions on Neural Systems and Rehabilitation Engineering 28 (2020) 2431–2442,. doi:10.1109/TNSRE.2020.3029121.

[40] X. Huang, N. Fu, S. Liu, S. Ostadabbas, Invariant representation learning for infant pose estimation with small data, in: Proceedings - 2021 16th IEEE International Conference on Automatic Face and Gesture Recognition, FG 2021, 2021. doi:10.1109/FG52635.2021.

9666956.
[41] S. Rajagopalan, A. Dhall, R. Goecke, Self-stimulatory behaviours in the wild for autism diagnosis, 2013. doi:10.1109/ICCVW.2013.103.
[42] B. Priya, S. Rajendran, R. Bala, R. Gobbi, Remote wireless health monitoring systems, in: 2009 Innovative Technologies in Intelligent Systems and Industrial Applications, CITISIA 2009, 2009, pp. 383–388,. doi:10.1109/CITISIA.2009.5224177.
[43] Microcontroller based baby incubator using sensors | semantic scholar, 2022. URL: https://www.semanticscholar.org/paper/Microcontroller-Based-Baby-Incubator-Using-Sensors-Suruthi-Suma/d9ba98adde1adcfe0fff3970b58cf516efa8968e.
[44] L. Nachabe, M. Girod-Genet, B. ElHassan, J. Jammas, M-health application for neonatal incubator signals monitoring through a coap-based multi-agent system, in: 2015 International Conference on Advances in Biomedical Engineering, ICABME 2015, 2015, pp. 170–173,. doi:10.1109/ICABME.2015.7323279.
[45] A. Vyas, S. Abimannan, R. Hwang, Sensitive healthcare data: Privacy and security issues and proposed solutions, Emerging Technologies for Healthcare (2021) 93–127,. doi:10.1002/9781119792345.CH4.
[46] S. Salloum, R. Dautov, X. Chen, P. Peng, J. Huang, Big data analytics on apache spark, International Journal of Data Science and Analytics 1 (2016) 145–164,. doi:10.1007/S41060-016-0027-9/FIGURES/6.
[47] P. Merla, Y. Liang, Data analysis using hadoop mapreduce environment, in: Proceedings - 2017 IEEE International Conference on Big Data, Big Data, volume 2018-January, 2017, pp. 4783–4785,. doi:10.1109/BIGDATA.2017.8258541.
[48] Top 30 big data tools for data analysis in 2022 | octoparse, 2022. URL: https://www.octoparse.com/blog/top-30-big-data-tools-for-data-analysis-in-2021#, accessed Jul. 20, 2022).
[49] S. Tripathy, T. Swarnkar, A comparative analysis on filtering techniques used in preprocessing of mammogram image, in: Advances in Intelligent Systems and Computing, volume 1082, 2020, pp. 455–464,. doi:10.1007/978-981-15-1081-6_39.
[50] L. Courtenay, D. Herranz-Rodrigo, R. Huguet, M. Maté-González, D. González-Aguilera, J. Yravedra, Obtaining new resolutions in carnivore tooth pit morphological analyses: A methodological update for digital taphonomy 15 (2020) 0240328,.
[51] E. Gastal, M. Oliveiray, Adaptive manifolds for real-time high-dimensional filtering, ACM Transactions on Graphics (TOG 31 (2012). doi:10.1145/2185520.2185529.
[52] N. Hesse, A. Schroder, W. Muller-Felber, C. Bodensteiner, M. Arens, U. Hofmann, Body pose estimation in depth images for infant motion analysis, in: Proceedings of the Annual International Conference of the IEEE Engineering in Medicine and Biology Society, EMBS, 2017, pp. 1909–1912,. doi:10.1109/EMBC.2017.8037221.
[53] S. Moccia, L. Migliorelli, V. Carnielli, E. Frontoni, Preterm infants' pose estimation with spatio-temporal features, IEEE Transactions on Biomedical Engineering 67 (2020) 2370–2380,. doi:10.1109/TBME.2019.2961448.
[54] P. Marschik, A novel way to measure and predict development: A heuristic approach to facilitate the early detection of neurodevelopmental disorders, Current Neurology and Neuroscience Reports 17 (2017) 1–15,. doi:10.1007/S11910-017-0748-8/FIGURES/4.
[55] I. Doroniewicz, Writhing movement detection in newborns on the second and third day

of life using pose-based feature machine learning classification, Sensors 20 (2020) 5986,. doi:10.3390/S20215986.

[56] K. McCay, E. Ho, H. Shum, G. Fehringer, C. Marcroft, N. Embleton, Abnormal infant movements classification with deep learning on pose-based features, IEEE Access 8 (2020) 51582–51592,. doi:10.1109/ACCESS.2020.2980269.

[57] T. Tsuji, Markerless measurement and evaluation of general movements in infants, Scientific Reports 10 (2020) 1–13,. doi:10.1038/s41598-020-57580-z.

[58] E. Ihlen, Machine learning of infant spontaneous movements for the early prediction of cerebral palsy: A multi-site cohort study, Journal of Clinical Medicine 9 (2020) 5,. doi:10.3390/JCM9010005.

[59] S. Reich, Novel ai driven approach to classify infant motor functions, Scientific Reports 11 (2021) 1–13,. doi:10.1038/s41598-021-89347-5.

[60] W. Schmidt, M. Regan, M. Fahey, A. Paplinski, General movement assessment by machine learning: why is it so difficult?, Journal of Medical Artificial Intelligence 2 (2019). doi:10.21037/JMAI.2019.06.02.

The neurodevelopmental and mental health outcomes in children with single ventricle physiology and Fontan circulation: a state-of-the-art review and future directions

Enrico Piccinelli[1,2], Gianfranco Butera[1], Mara Pilati[1], Micol Rebonato[1], Roberto Formigari[1], Marin Verrengia[1], Alberto Testa[1], Gianluigi Perri[1], Umberto Morbiducci[2], Marco Deriu[2] and Lorenzo Galletti[1]

[1] *Paediatric Cardiology Department, Ospedale Pediatrico Bambino Gesù, Roma, Italy*
[2] *PolitoBIOMed Lab, Department of Mechanical and Aerospace Engineering, Politecnico di Torino, Italy*

Abstract
The survival of patients with single ventricle circulation undergoing Fontan operation has significantly improved in the last decades. However, the neurodevelopmental outcome of this patients is still not satisfying and far below the healthy controls. The aetiology of neurodevelopment disability and mental health disorders is multifactorial and has a cumulative and synergic trend over the years. Genetic factors, abnormal fetal circulation, peri and intra-operative care, multiple hospitalizations and socioeconomic status play a crucial role in this process. Due to the heterogeneity of anatomies and different treatment possibilities there is a need for a personalized, multidisciplinary and translational approach focused on the patient. The introduction of new technologies driven by artificial intelligence and the continuous integration of in vivo data and biomedical simulations into medicine promises significant improvements in pathologies diagnosis and treatment thus enhancing the quality of life of patients and their families.

Keywords
Neurodevelopmental outcomes, Single ventricle physiology, Fontan circulation, Future directions, Bioengineering

1. Introduction

The Fontan procedure is the final stage of three operations performed to palliate children born with single ventricle physiology. In these patients, due to the complex heart anatomy is impossible to repair the heart re-creating the physiologic biventricular circulation. The original operation was described in 1968 by Francis Fontan in patients with tricuspid atresia [1]. Various modifications have been developed in the following decades and the extracardiac total cavo-pulmonary connection (TCPC), is now the most widely used [2]. In this operation, the systemic venous blood coming from the inferior vena cava (IVC) is diverted through an extracardiac conduit connecting to the pulmonary arteries (PAs), completing the previous performed Glenn connection of the superior vena cava (SVC) to the PAs. In recent years, the survival of patients with single ventricle circulation has significantly improved due to the advancements in fetal diagnosis, perioperative management and medical care [3,4]. Therefore, all the efforts are focused on reducing the long-term morbidity and improving quality of life and neuropsychological outcomes [5,6,7,8]. The literature regarding the neurodevelopmental outcomes in children with single ventricle physiology is redundant and often controversial and no large randomized trials have been conducted. For this reason, we aim to provide a state-of-the-art review of the neurodevelopment and mental health outcomes of children with single ventricle physiology undergoing Fontan operation in the modern era and to give insight into future directions and tools for neurodevelopment impairment prediction, including artificial intelligence (AI).

DETERMINED *2022: Neurodevelopmental Impairments in Preterm Children — Computational Advancements, August 26, 2022, Ljubljana, Slovenia*
*Corresponding author.
email: dottor.piccinelli@gmail.com (E. Piccinelli); gianfranco.butera@opbg.net (G. Butera); marco.deriu@polito.it (M. Deriu); lorenzo.galletti@opbg.net (L. Galletti)
orcid: 0000-0001-6987-2745 (E. Piccinelli)
© 2022 Copyright for this paper by its authors. Use permitted under Creative Commons License Attribution 4.0 International (CC BY 4.0).
CEUR Workshop Proceedings (CEUR-WS.org)

CEUR-WS.org/Vol-3363/paper11.pdf

2. Material and methods

Relevant studies were identified by PubMed, Embase and Cochrane. No language restrictions were used. The first search from PubMed, Embase and Cochrane was performed by the first author of this review and double-checked by the other corresponding authors. The following keywords were used: (neurodevelopment outcome OR mental health OR neurodevelopment disability OR artificial intelligence OR computational models) AND (congenital heart disease OR single ventricle OR hypoplastic left heart syndrome OR Fontan circulation). We included only papers from January 2000 up to August 2022. Older papers were excluded, with the exceptions of papers explaining concepts, surgical techniques or to compare the neurodevelopment outcome early after the introduction of the Fontan operation.

3. Etiology and risk factors of neurodevelopmental disability

The aetiology of neurodevelopmental disability in patients with single ventricle physiology is multifactorial and has a cumulative and synergic trend over the years. In many patients with congenital heart disease (CHD) there is a predisposition to extracardiac and brain congenital anomalies [9]. Indeed, an exome sequencing of 1213 CHD parent-offspring trios identified shared genetic contributions to CHD and neurodevelopmental disabilities [10]. Moreover, the abnormal fetal circulation typical of univentricular physiologies is often related to brain dismaturation. Fetuses with hypoplastic left heart syndrome (HLHS) have altered cerebral perfusion and oxygenation due to intracardiac mixing and the retrograde brain perfusion through the ductus arteriosus and the hypoplastic aorta. This abnormal perfusion has a dramatic effect on brain growth and maturation. In fact, even term infants with HLHS have smaller and less mature brains than controls [11]. Fetal brain magnetic resonance imaging (MRI) of patients with CHD at 25–35 weeks of gestation demonstrated significantly lower maturation scores compared to healthy controls. In particular germinal matrix, myelination and superior temporal sulcus scores were significantly delayed in this population [12]. Moreover, a comprehensive neuropathologic evaluation of 11 electively aborted HLHS fetuses revealed chronic diffuse white matter injury (WMI) [13]. This brain dysmaturity represents the substrate for further brain injuries during and after surgery. Stegeman et al. described the pre- and post-operative spectrum of brain MRI of patients with critical CHD, including patients with HLHS. Interestingly, 348 MRI scans confirmed that the most affected area involved before and after surgery is the white matter in 25% and 30% of infants, respectively. They also noted that 6% of these patients presented with arterial ischemic stroke even before surgery. Finally, not only thrombotic lesions were reported but also hemorrhagic injuries especially intraparenchymal cerebral haemorrhage, cerebellar haemorrhage, intraventricular haemorrhage and subdural haemorrhage [14]. Interestingly, this punctate WMI typical of patients with CHD, share a similar injury pattern to preterm infants [15]. Guo et al. analysed 216 term-born CHD neonates and WMI was identified in 86 of them [16]. The comparison between WMI and preterm neonates highlighted that WMI in patients with CHD has a specific topology with a preference for anterior and posterior lesions. Indeed, the central areas are less vulnerable in comparison to the preterm neonates, reflecting the expected maturation of pre-oligodendrocytes [16]. Despite the improvements in surgical techniques and post-operative intensive care, deep hypothermic circulatory arrest (DHCA) negatively impacts on the neurologic outcome. In many centers, regional low-flow cerebral perfusion (RLFP) is used instead of DHCA to reduce the time of cerebral ischemia. A recent study comparing brain MRI before and after Norwood operation highlighted the presence of new or worsened ischemic lesions in 73% of infants, especially periventricular leukomalacia and focal ischemic lesions [17]. Furthermore, a randomized, controlled trial comparing new cerebral injuries on MRI after surgery using DHCA or antegrade cerebral perfusion in neonates with complex aortic arch obstructions including HLHS showed no significant difference between these techniques [18]. When analyzing early neurodevelopmental outcomes after cardiac surgery, these operative factors may be even less important than pre- and post-operative factors such as longer postoperative stay in intensive care, which are associated with lower psychomotor and mental development index [19]. Also socioeconomic status (SES) should be accounted for, because it emerged that children with single ventricle physiology and lower SES have reduced functional status and fine motor, problem-solving, adaptive behaviour and communication skills at the age of 6 years in comparison to patients with higher SES [20]. Finally, these children usually experience multiple

hospitalizations, catheterization and eventually further surgeries. Every additional procedure increases the risk of brain injuries due to anaesthesia, cardiac bypass and cardiac thromboembolism. These patients are naturally predisposed to thromboembolic events and stroke due to liver dysfunction or protein-losing enteropathy, which plays a role in the coagulation-fibrinolysis balance [21]. The common findings of high haematocrit and pro-inflammatory status also increase the thromboembolic risk. Finally, the blood mix and direct venous-arterial connection through interatrial communication, single ventricle and Fontan fenestration in the different stages raise the risk of stroke [22].

4. Neurodevelopmental outcomes in Childhood

In the last decades, the neurodevelopmental outcome of children with single ventricle physiology has improved. However, despite substantial progress in care, this population still presents with cognitive, motor, social and psychological deficits. In the late '80s around 64% of patients with HLHS presented major developmental disabilities at some point in their stage-palliation [23]. More recent studies and reviews bring different and controversial results [24]. Goldberg et al. assessed the neurodevelopmental outcome of 51 preschool children with HLHS and other single ventricle physiologies palliated with the Fontan procedure, reporting no significant difference in Wechsler Intelligence scale from the healthy population [25]. On the contrary, a recent nationwide Finnish prospective study of 23 patients with HLHS, 13 with other univentricular physiology, and 40 healthy controls followed until 5 years old demonstrated a significantly lower median full-scale IQ at preschool age, in the first two groups in comparison to the healthy controls. This study also confirmed a high rate of brain MRI abnormalities, mainly ischemic in 82% of the patients with HLHS and in 56% of children with other single ventricle anatomies [26]. When a broad range of neuropsychological outcome variables was extended from children to young adults with single ventricle physiology, they scored significantly lower compared to the general population. Indeed, they obtained lower intelligence test scores, decreased motor function, impaired visuospatial abilities and more marked behavioral disorders [27]. Promising data are coming from the recent introduction of hybrid approaches for initial palliation of HLHS, that has shown more favourable neurodevelopment outcomes and quality of life at 2–3 years of age, with cognitive, language and motor composite scores on the Bayley-III not significantly different from healthy peers [28].

Interestingly, when compared to preschool children with CHD undergoing biventricular repair, patients with single ventricle following the Fontan pathway presented with similar neurodevelopmental outcomes and full-scale IQ. However, the Fontan group performed worse in terms of processing speed, attention, and impulsivity [29]. Even more controversial is the sub-analysis of the HLSH group versus other functional single ventricle anatomies. According to Goldberg et al. the HLHS group had significantly lower Wechsler Intelligence scores than the non-HLHS group but no significant difference in the behavioural scores [25], while Gaynor et al. found no significant difference in the neurodevelopmental outcomes among the two groups [29].

Finally, a studies focusing on specific neurocognitive aspects,, analysing the deficits in visual-perceptive skills and executive function highlighted that the Fontan group didn't differ significantly from the control group for the Test of Visual-Perceptual Skills summary but had worse results on all scales of both the copy and immediate recall trials of the Rey–Osterrieth Complex Figure [30,31]. Regarding the executive function, patients with single ventricle physiology displayed deficits in flexibility and problem-solving [31].

5. Mental health and psychiatric disorders

Children and adolescents with CHD have a higher risk of developing mental health disorders due to multiple hospitalizations and interventions, stressful life events, social and cultural factors [32-34]. A recent large comparative cross-sectional study from the Texas Children's Hospital including 1164 patients with CHD from 4 to 17 years old highlighted that 18.2% of this population had a diagnosis or medication for anxiety or depression, significantly higher than healthy peers. In particular children with complex single ventricle hearts had around 7 times higher odds of developing anxiety and/or depression [35]. DeMaso et al. from Boston Children's Hospital confirmed that adolescents with single ventricle CHD who underwent the Fontan procedure have higher odds to receive a psychiatric diagnosis compared with healthy peers (65% *vs.* 22%). Specifically, they presented with increased risk of anxiety disorders and Attention deficit hyperactivity disorder (ADHD) [36]. The same group also highlighted that early-term-born adolescents with single

ventricle anatomy (born between 37 and 38 weeks gestation) were more likely to develop ADHD during their life when compared to full-term birth peers with the same physiology [37]. Depressive symptoms are also common in patients with single ventricle physiology, as shown by Pike et al. who correlated this condition to signs of chronic injury at MRI in specific brain areas controlling cognition, anxiety, and depression [38].

However, despite all the neurodevelopmental and psychiatric issues and the multiple operations and interventions, the quality of life (QoL) of these patients is self-perceived normal, even when compared to healthy controls [39,40]. Similar conclusions come from a more recent study highlighting that a higher level of education and full-time occupation positively influences patients' quality of life [41].

6. Biomedical technologies and future directions

Considering the anatomical inter-variability and the plethora of possible treatment strategies for patients with single ventricle physiology, the way forward to obtain better outcomes and longer life expectancy is a multidisciplinary and integrated approach tailored on the single patient: personalised surgical approach as well as ad-hoc peri and post-operative care, combined with affordable short and long-term prediction tools is the future challenge. A translational approach, combining biomedical engineering methodologies and advanced imaging technologies may address this topic, improving the surgical results and the neurodevelopmental outcomes. In this regard, Computational Fluid Dynamics (CFD) to simulate the hemodynamics in patients with single ventricle physiology models has been already applied successfully e.g. to predict the best surgical solution in the different palliation stages [42-46]. More in detail, CFD was largely adopted to assess the flow efficiency of the systemic-pulmonary shunt, at the ventricular and neo-aortic level and in the Fontan circulation quantifying energy losses and how the latter correlate with the clinical outcome. The capability of exploring different hemodynamic scenarios adopting patient-specific computational models where virtual surgical connections can be pre-operatively tested can be extremely useful for surgical and clinical decision-making. The availability of in silico but also in vitro models of possible surgical options supports the identification of the best surgical pathway, stressing the differences in the local hemodynamics, e.g. analyzing the impact that competitive flows might have in terms of energetics of the system. For instance, in Norwood I operation, a model-based approach may support the patient-specific selection between the two most commonly used shunts: the Blalock-Taussig shunt and the Sano shunt. In fact, different variables contribute to the performance of these shunts, e.g. their size, length and positions, affecting the fine balance between systemic and pulmonary blood flow [47,48]. This is an important issue among surgeons and paediatric cardiologists as there is still debate about performing one or the other shunt considering that the transplantation-free survival at 12 months is significantly better with the Sano shunt but there is no significant difference after one year between the two groups [49,50].

Moreover, biomedical simulations may predict the possibility of thrombus formation in the Fontan circulation eventually responsible for stroke in case of conduit fenestration [51]. The analysis of the different flow conditions, flow stagnation and graft size may anticipate the need for more strict anticoagulation to avoid cerebral accidents. The advantage of these technologies is not only in terms of optimization and personalization of treatment for these patients but will also allow a better resource distribution that can be invested in other aspects of their complex care.

On the other side, a strict follow-up of these patients would guarantee the prompt recognition of neurocognitive impairment and mental health disorders, allowing the early start of the neurodevelopmental interventions and psychological and educational support [52]. Numerous tools to improve executive function have been proposed for patients with ADHD and children with learning disabilities, with promising results [53,54]. Nevertheless, there is insufficient experience in the field of CHD. A preliminary experience with the Cogged intervention, consisting of home-based 45-minutes training sessions for 5-8 weeks, demonstrated to improve the self-regulatory control abilities of adolescents with CHD, but with no effects on other executive functions or behavioral outcomes [55].

Finally, AI is expanding in the medical field, and in CHD as well. From the viewpoint of the clinician, artificial intelligence can be seen as a diagnostic and therapeutic technology that enabling the analysis of very large pools of data, allows the discovery of patterns not immediately obvious [56]. Among the AI applications of specific interest here we mention its integration with fetal echocardiography for the extraction of undiscovered image features, a promising approach which can markedly improve image acquisition and optimization, automated measurements, classification of diagnoses etc [57]. This is of relevance because prenatal diagnosis of CHD is crucial in parents' decision-making regarding the

continuation of pregnancy, based on the consolidated knowledge that neonates with postnatally diagnosed CHD have increased mortality and worse neurodevelopment outcomes before and after surgery [58-60]. Within AI, machine learning models can be as important in predicting the adverse outcomes for congenital heart surgery as in improving social interaction and supportive education in patients with worse neurodevelopmental outcome after surgery [61,62].

7. Conclusion

More than 50 years after the introduction of the Fontan procedure, surgical and perioperative care developments have improved medium and long-term survival of patients with single ventricle physiology. Nevertheless, the neurodevelopmental and mental health outcome is still not satisfying, despite a clear understanding of potential risk factors. The way forward is a personalized, multidisciplinary and translational approach with the integration of imaging technologies with biomedical simulations (such as the already employed CFD models) and AI (applied e.g. for image segmentation, geometry sampling and even generation of synthetic data). It is expected that such a multidisciplinary framework will lead to a significant improvement in the objective quality of life of these patients and their families.

8. Acknowledgements

None

9. Funding

The present research work has been developed as part of the PARENT project, funded by the European Union's Horizon 2020 research and innovation program under the Marie Sklodowska-Curie-Innovative Training Network 2020, Grant Agreement N° 956394 (https://parenth2020. com/).

10. References

1. Fontan FBE. Surgical repair of tricuspid atresia. Thorax. 1971;26:240–248.
2. Marcelletti C, Corno A, Giannico S, et al. Inferior vena cava-pulmonary artery extracardiac conduit. A new form of right heart bypass. J Thorac Cardiovasc Surg. 1990;100(2):228–232.
3. Rychik J, Atz AM, Celermajer DS, et al. Evaluation and management of the child and adult with Fontan circulation: a scientific statement from the American heart association. Circulation. (2019) 140:e234–84.
4. Wernovsky G. The paradigm shift toward surgical intervention for neonates with hypoplastic left heart syndrome. Arch Pediatr Adolesc Med 2008;162:849-54.
5. Anderson PAW, Sleeper LA, Mahony L, et al. Contemporary outcomes after the Fontan procedure: a Pediatric Heart Network multicenter study. J Am Coll Cardiol. 2008;52:85–98.
6. Sood E, Jacobs JP, Marino BS. The cardiac neurodevelopmental outcome collaborative: a new community improving outcomes for individuals with congenital heart disease. Cardiol Young. (2020) 30:1595–6.
7. McCrindle BW, Williams RV, Mitchell PD, et al. Relationship of patient and medical characteristics to health status in children and adolescents after the Fontan procedure. Circulation. 2006;113:1123–1129.
8. Marshall KH, D'Udekem Y, Sholler GF, et al. Health-Related Quality of Life in Children, Adolescents, and Adults With a Fontan Circulation: A Meta-Analysis. J Am Heart Assoc. 2020 Mar 17;9(6):e014172.
9. Egbe A, Lee S, Ho D, et al. Prevalence of congenital anomalies in newborns with congenital heart disease diagnosis. Ann Pediatr Cardiol. 2014 May;7(2):86-91.
10. Homsy J, Zaidi S, Shen Y, et al. De novo mutations in congenital heart disease with neurodevelopmental and other congenital anomalies. Science. (2015) 350:1262–6.

11. Licht DJ, Shera DM, Clancy RR, et al. Brain maturation is delayed in infants with complex congenital heart defects. J Thorac Cardiovasc Surg. 2009 Mar;137(3):529-36.
12. Jaimes C, Rofeberg V, Stopp C, Ortinau CM, Gholipour A, Friedman KG, et al. Association of isolated congenital heart disease with fetal brain maturation. Am J Neuroradiol. (2020) 41:1525–31.
13. Hinton RB, Andelfinger G, Sekar P, et al. Prenatal head growth and white matter injury in hypoplastic left heart syndrome. Pediatr Res. 2008 Oct;64(4):364-9.
14. Stegeman R, Feldmann M, Claessens NHP, et al. A Uniform Description of Perioperative Brain MRI Findings in Infants with Severe Congenital Heart Disease: Results of a European Collaboration. Am J Neuroradiol. 2021 Nov;42(11):2034-2039.
15. Guo T, Duerden EG, Adams E, et al. Quantitative assessment of white matter injury in preterm neonates: Association with outcomes. Neurology. 2017 Feb 14;88(7):614-622.
16. Ting Guo T, Chau V, Peyvandi S, et al. White matter injury in term neonates with congenital heart diseases: Topology & comparison with preterm newborns.Neuroimage. 2019 Jan 15;185:742-749.
17. Dent CL, Spaeth JP, Jones BV, et al. Brain magnetic resonance imaging abnormalities after the Norwood procedure using regional cerebral perfusion. J Thorac Cardiovas Surg. (2006) 131:190–7
18. Algra SO, Jansen NJ, van der Tweel I, et al. Neurological injury after neonatal cardiac surgery: a randomized, controlled trial of 2 perfusion techniques. Circulation. (2014) 129:224– 33.
19. The International Cardiac Collaborative on Neurodevelopment (ICCON) Investigators, Impact of operative and postoperative factors on neurodevelopmental outcomes after cardiac operations. Annals Thorac Surg. (201)6 102:843–9.
20. Bucholz EM, Sleeper LA, Goldberg CS, et al. Socioeconomic Status and Long-term Outcomes in Single Ventricle Heart Disease. Pediatrics. 2020 Oct;146(4):e20201240.
21. Cromme-Dijkhuis AH, Henkes CM, Bijleveld CM, et al. Coagulation factor abnormalities as possible thrombotic risk factors after Fontan operations. Lancet. 1990;336: 1087-90.
22. Kaulitz R, Ziemer G, Rauch R, et al. Prophylaxis of thromboembolic complications after the Fontan operation (total cavopulmonary anastomosis). J Thorac Cardiovas Surg. (2005) 129:569– 75.
23. Rogers BT, Msall ME, Buck GM, et al. J Pediatr. Neurodevelopmental outcome of infants with hypoplastic left heart syndrome. 1995 Mar;126(3):496-8.
24. Calderon J, Newburger JW, Rollins CK. Neurodevelopmental and Mental Health Outcomes in Patients With Fontan Circulation: A State-of-the-Art Review. Front Pediatr. 2022 Mar 9;10:826349. doi: 10.3389/fped.2022.826349.
25. C S Goldberg 1, E M Schwartz, J A Brunberg, et al. Neurodevelopmental outcome of patients after the fontan operation: A comparison between children with hypoplastic left heart syndrome and other functional single ventricle lesions. J Pediatr. 2000 Nov;137(5):646-52.
26. Sarajuuri A, Jokinen E, Mildh L, et al. Neurodevelopmental burden at age 5 years in patients with univentricular heart. Pediatrics. 2012 Dec;130(6):e1636-46.
27. Nicole Vahsen, Arndt Bröder, Viktor Hraska, et al. Neurodevelopmental Outcome in Children With Single Ventricle After Total Cavopulmonary Connection. Klin Padiatr. 2018 Jan;230(1):24-30.
28. Reich B, Heye KN, Wetterling K, et al. Neurodevelopmental outcome in hypoplastic left heart syndrome after hybrid procedure. Transl Pediatr. 2019 Apr;8(2):94-106.
29. Gaynor JW, Ittenbach RF, Gerdes M, et al. Neurodevelopmental outcomes in preschool survivors of the Fontan procedure. J Thorac Cardiovasc Surg. 2014 Apr;147(4):1276-82.
30. Bellinger DC, Watson CG, Rivkin MJ, et al. Neuropsychological status and structural brain imaging in adolescents with single ventricle who underwent the Fontan procedure. J Am Heart Assoc. 2015;4(12):e002302
31. Cassidy AR, White MT, DeMaso DR, et al. Executive function in children and adolescents with critical cyanotic congenital heart disease. J Int Neuropsychol Soc. 2015;21(1):34–49
32. Kovacs AH, Saidi AS, Kuhl EA, et al. Depression and anxiety in adult congenital heart disease: predictors and prevalence. Int J Cardiol. 2009;137(2):158–164
33. Williamson DE, Birmaher B, AndersonBP, et al. Stressful life events in depressed adolescents: the role of dependent events during the depressive episode. J Am Acad Child Adolesc Psychiatry. 1995;34(5):591–598
34. Woolf-King SE, Anger A, Arnold EA, et al. Mental health among parents of children with critical congenital heart defects: a systematic review. J Am Heart Assoc. 2017;6(2):e004862
35. Gonzalez VJ, Kimbro RT, Cutitta KE, et al. Mental Health Disorders in Children With Congenital Heart Disease. Pediatrics. 2021 Feb;147(2):e20201693.

36. DeMaso DR, Calderon J, Taylor GA, et al. Psychiatric disorders in adolescents with single ventricle congenital heart disease. Pediatrics. (2017) 139:2241.
37. Calderon J, Stopp C, Wypij D. Early-Term Birth in Single-Ventricle Congenital Heart Disease After the Fontan Procedure: Neurodevelopmental and Psychiatric Outcomes. J Pediatr. 2016 Dec;179:96-103.
38. Pike NA, Roy B, Gupta R, et al. Brain abnormalities in cognition, anxiety, and depression regulatory regions in adolescents with single ventricle heart disease. JNeurosci Res. (2018) 96:1104– 18.
39. Pike NA, Evangelista LS, Doering LV, et al. Quality of life, health status, and depression: comparison between adolescents and adults after the Fontan procedure with healthy counterparts. J Cardiovasc Nurs. (2012) 27:539–46.
40. Saliba Z, Butera G, Bonnet D, et al. Quality of life and perceived health status in surviving adults with univentricular heart. Heart. 2001;86(1):69Y73
41. Soufi A, Gouton M, Metton O. Quality of life of adult Fontan patients. Cardiol Young. 2021 Jan;31(1):97-104.
42. Biglino G, Giardini A, Hsia T, et al. Modeling single ventricle physiol- ogy: review of engineering tools to study first stage palliation of hypoplastic left heart syndrome. Front Pediatr. 2013;1:31.
43. Qian Y, Liu JL, Itatani K, et al. Computational hemodynamic analysis in congeni- tal heart disease: simulation of the norwood proce- dure. Ann Biomed Eng. 2010;38:2302–13.
44. Grigioni M, D'Avenio G, Del Gaudio C et al. Critical issues in studies of flow through the Fontan circuit after 10 years of investigation. Cardiol Young. 2005 Dec;15 Suppl 3:68-73.
45. Marsden AL, Bernstein AJ, Reddy VM, et al. Evaluation of a novel Y-shaped extracardiac Fontan baffle using computational fluid dynamics. J Thorac Cardiovasc Surg. 2009;137(2)
46. Corsini C, Baker C, Kung E, et al. An integrated approach to patient- specific predictive modeling for single ventricle heart palliation. Comput Methods Biomech Biomed Eng. 2014;17(14):1572–89.
47. Kung E, Baretta A, Baker C, et al. Predictive modeling of the virtual hemi-Fontan operation for second stage single ventricle palliation: two patient-specific cases. J Biomech (2013) 46(2):423–9.
48. Kanter KR, Haggerty CM, Restrepo M, et al. Preliminary clinical experience with a bifurcated Y-graft Fontan procedure – a feasibility study. J Thorac Cardiovasc Surg (2012) 144(2):383–9.
49. Ohye RG, Gaynor JW, Ghanayem NS, et al. Design and rationale of a randomized trial comparing the Blalock-Taussig and right ventricle-pulmonary artery shunts in the Norwood procedure. J Thoracic Cardiovasc Surg. (2008) 136:968–75.
50. Ohye RG, Sleeper LA, Mahony L, et al. Comparison of shunt types in the Norwood procedure for single-ventricle lesions. N Engl J Med. 2010 May 27;362(21):1980-92.
51. Yang W, Chan FP, Reddy VM, et al. Flow simulations and validation for the first cohort of patients undergoing the Y-graft Fontan procedure. J Thorac Cardiovasc Surg. 2015;149:247–55.
52. Calderon J, Bellinger DC. Executive function deficits in congenital heart disease: why is intervention important? Cardiol Young. 2015 Oct;25(7):1238-46.
53. Shuai L, Daley D, Wang YF, et al. Executive Function Training for Children with Attention Deficit Hyperactivity Disorder. Chin Med J (Engl). 2017 Mar 5;130(5):549-558.
54. Shuai L, Wang Y, Li W, et al. Executive Function Training for Preschool Children With ADHD: A Randomized Controlled Trial. J Atten Disord. 2021 Dec;25(14):2037-2047.
55. Calderon J, Wypij D, Rofeberg V. Randomized Controlled Trial of Working Memory Intervention in Congenital Heart Disease. J Pediatr. 2020 Dec;227:191-198.e3.
56. Butera G, Schievano S, Biglino G, et al. Modelling Congenital Heart Disease: Engineering a Patient-specific Therapy. © Springer Nature Switzerland AG 2022. https://doi.org/10.1007/978-3-030-88892-3.
57. Reddy CD, Van den Eynde J, Kutty S.Artificial intelligence in perinatal diagnosis and management of congenital heart disease. Semin Perinatol. 2022 Jun;46(4):151588.
58. Holland BJ, Myers JA, Woods CR.Prenatal diagnosis of critical congenital heart disease reduces risk of death from cardiovascular compromise prior to planned neonatal cardiac surgery: a meta-analysis.Ultrasound Obstet Gynecol, 45 (6) (2015), pp. 631-638.
59. Peyvandi S, De Santiago V, Chakkarapani E, et al. Association of Prenatal Diagnosis of Critical Congenital Heart Disease With Postnatal Brain Development and the Risk of Brain Injury. JAMA Pediatr, 170 (4) (2016), Article e154450.
60. Mahle WT, Clancy RR, McGaurn SP, et al. Impact of prenatal diagnosis on survival and early neurologic morbidity in neonates with the hypoplastic left heart syndrome. Pediatrics, 107 (6) (2001), pp. 1277-1282.

61. Bertsimas D, Zhuo D, Dunn J, et al. Adverse Outcomes Prediction for Congenital Heart Surgery: A Machine Learning Approach. World J Pediatr Congenit Heart Surg. 2021 Jul;12(4):453-460.
62. Barua PD, Vicnesh J, Gururajan R, et al. Artificial Intelligence Enabled Personalised Assistive Tools to Enhance Education of Children with Neurodevelopmental Disorders-A Review. Int J Environ Res Public Health. 2022 Jan 21;19(3):1192.

Medical imaging and artificial intelligence to investigate neuro-cardiac pathologies and discover hidden relationships – a state of the art review

Syed Taimoor Hussain Shah[1,*,†], Veronika Calati[1,†], Alessandra Bizzarri[1,†] and Marco Agostino Deriu[1,*,†]

[1]PolitoBIOMed Lab, Department of Mechanical and Aerospace Engineering, Politecnico di Torino, Turin, Italy

Abstract

Cardiovascular and neurological diseases including their interactions are getting the attention of researchers and physicians. Both diseases often share common biomarkers, risk factors, and biological pathways. By now, researchers have confirmed that problems related to cardiovascular lead to neurological bad outcomes and vice versa. In addition, researchers have started to use machine/deep learning algorithms for better diagnosis. By now, few examples are published on little datasets consisting of computed tomography images, electrocardiograms, electroencephalograms, and so on, but most of the work is not done by artificial intelligence (AI). In this work, we reviewed a number of studies that have either used AI or manual computation with conventional techniques on different imaging modalities. From all studies, it is found that imaging modalities can support physicians in better diagnosis of neurological outcomes following cardiac events and/or diseases and vice versa. Moreover, AI driven technologies, like machine learning and deep learning, could be useful to delineate accurate models of diseases related to neuro-cardiac pathologies for predictions of consequent bad outcomes related to the different stages.

Keywords

Cardiovascular and neurological diseases, Biomarkers, Computed tomography images, Electrocardiograms, Electroencephalograms, Machine learning and deep learning

1. Introduction

In 1956, John McCarthy coined the name Artificial Intelligence (AI) for the first time at the Dartmouth conference [1]. This idea was then elaborated by Kaplan and Haenlein as "the ability to process external data systematically and learn from it to achieve specific goals and tasks" [2]. With the advancement in AI, new computer science-related studies came into life namely intelligent machines, natural language processing, machine learning (ML), pattern recognition, expert systems, and image recognition [3]. These new domains have helped the researchers to

DETERMINED 2022: Neurodevelopmental Impairments in Preterm Children — Computational Advancements, August 26, 2022, Ljubljana, Slovenia

*Corresponding author.

†These authors contributed equally.

taimoor.shah@polito.it (S. T. H. Shah); veronika.calati@studenti.polito.it (V. Calati); s272855@studenti.polito.it (A. Bizzarri); marco.deriu@polito.it (M. A. Deriu)

https://www.dimeas.polito.it/personale/scheda/(nominativo)/taimoor.shah (S. T. H. Shah); https://www.dimeas.polito.it/en/personale/scheda/(nominativo)/marco.deriu (M. A. Deriu)

0000-0002-6010-6777 (S. T. H. Shah); 0000-0003-1918-1772 (M. A. Deriu)

© 2022 Copyright for this paper by its authors. Use permitted under Creative Commons License Attribution 4.0 International (CC BY 4.0).

CEUR Workshop Proceedings (CEUR-WS.org)

CEUR-WS.org/Vol-3363/paper12.pdf

solve complex problems by taking into account different steps such as planning, reasoning, and learning [4].

In addition, in 1959, Arthur Samuel is the researcher who conveyed the concept of "machine learning" (ML) for the first time in the life cycle of AI. He directed the category of algorithms and classifiers in ML's concept [5]. These constructions of the algorithms started to learn the input data's distribution automatically and predicted new data accurately [6]. Similarly, due to the machine learning concept, different other promising breakthroughs came such as the backpropagation algorithm [7] and then neural networks [8].

After the concept of AI, in the early 1970s, a new concept came that empowered the medical-related areas by intending to improve the efficiency of the diagnosis and also the treatment against the found pathology [9]. Peleg and Combi et. al. [10] have elaborated different cycles of artificial intelligence in the history of medical-related areas such as 1) Infancy stage: Decision tree algorithm came into life; 2) Adolescence stage: Expert systems theory was proposed; 3) Coming-of-age stage: Deep learning's concept was being surfaced with machine learning; 4) the most important stage named as Maturation period: technologies related to these fields are comparably advanced and different applications of deep learning has started to prevail.

On the other hand, the advancement in medical equipment has also enhanced people's health [11]. This advancement has not just improved the survival rate but also has brought improvements in the diagnosis of disease or injury [12]. With these advancements, researchers have started their work for medical healthcare services as they came to know that it is a crucial step toward the effectiveness of clinical engineers to investigate in a better way and to ensure the patients' safety [13, 14, 15].

On the combined advancements in AI and types of equipment of the medical world, International Business Machines (IBM) has estimated that an average of 1 million gigabytes are produced from a person in his lifetime [16]. To get intuitions about medical problems, clinicians are trying to collaborate with artificial intelligence experts to use the chunks from the big data and forecast about the healthcare solutions to improve the quality of the diagnosis and cure [17, 18]. In this way, deep learning is playing a very crucial role to enhance equipment's output to support the clinicians in their decision. With this, Convolutional neural networks (CNNs) started to become popular because they learn the importance of features by themselves from the whole raw data space which saves the data scientist's time to become a domain expert in this algorithm [19, 20]. On this topic, these studies [21, 22] have compared the diagnosing capabilities of AI systems against physicians' diagnostic abilities. Results clearly highlighted that AI may support and complement physicians' diagnostic capabilities by adding a knowledge base inferred by data. In the current era of medical AI, there are several medical problems which are not yet been solved successfully and are the main focus of clinicians and medical researchers such as cardiovascular diseases (CVDs) [23], neurology [24, 25], neuro-cardiac hidden interactions [26, 27, 28, 29, 30] , cancer [31], aids [32], and so forth.

In this work, we are focusing on a detailed study of neuro-cardiac pathologies and their interrelations with the help of different imaging modalities using AI. In this essence, several researchers have proven that neuro-cardiac has a very strong relation among them. A disease, dysfunctioning, irregularity, or even surgery of cardiac can cause to other diseases or abnormalities to neuro [24, 33, 34, 35, 36], and same in vice versa like hypertension [37, 38], brain injury [39, 40], hypoxic-ischemic [41], brain tumor [42], neurogenic stress [43], and so on.

In the investigation of interrelation between Neuro-Cardiac Pathologies (NCPs), biologists have found several useful biomarkers to diagnose the influence of NCPs issues such as hs-TroponinT, hs-cTn, CK-MB and NTproBNP, galectin-3, lysophosphatidylcholine, copeptin, sST2, S100B, myeloperoxidase and GDF-15, and others [43, 44, 45]. Gopinath et. al. [43] have described that understanding the interaction between brain and heart is a very complex task and vital to keep maintaining the normal functioning of the cardiovascular system. Even sometimes, there is no cardiac disease but due to neuronal disease or injury, many cardiac diseases can be induced. The important thing is, there are different brain areas namely anterior cingulate gyrus, insular cortex, and amygdala controlling the automatic nervous system. If one of these gets damaged then many cardiac issues, interlinked with the damaged brain region, may elevate.

In the better diagnosis of the disease, nowadays radiologists and physicians are taking the support of new imaging modalities [46]. These new techniques have introduced so much improvement in revealing information with very high accuracy [47]. There are several different imaging modalities which are being used to identify the region of interest such as Perfusion Magnetic Resonance Imaging (MRI) [48], Diffusion weighted Imaging [49], Diffusion Tensor Imaging [49, 50], Proton MR Spectroscopy [51], Susceptibility-weighted Imaging [52], Cerebrospinal Fluid Flow MRI [53], etc. for neuro pathologies and Cardiac MRI with T1 and T2 Mapping [54, 55], and Dual Energy Cardiac Imaging [56] for cardiac pathologies.

In the next section, a number of states of art methodologies related to different findings about neuro-cardiac hidden interactions are being discussed in detail while the conclusion section is ending this work with final remarks.

2. State of the art methodologies related to neuro-cardiac interactions and complications

In this section, a selection of literature studies concerning methodologies employed in the field of neuro-cardiac interactions and complications will be considered. The selected studies have shown potential applications of imaging and signal analysis to unravel and investigate hidden relationships and complications between neuro-cardiac interactions. In literature, some of previous studies reported examples of imaging techniques mainly based on operator's work (clinicians' expert opinion) whereas others have taken advantage of statistical algorithms or artificial intelligence. In this review, the literature selection criteria took into account for two main factors 1) how different imaging approaches may be helpful in investigating distinctive neuro-cardiac interactions and 2) how expert opinion, statistical algorithms, and machine learning are beneficial in finding the interlinked markers. It is worth noting that, to date, only very few studies employed ML or DL to investigate neuro-cardiac relationships being medical-imaging aided investigations in the field mostly focused either on neurological or on cardiac diseases. Thus, the lack of attention indicates that this specific field of research has not yet been overburdened by studies concerning AI applications. Our comparative review may then stimulate the use of AI in this field to overcome main issues of more classical approaches in the field of neuro-cardiac pathologies.

The section is divided into four main sub-sections as also mentioned in Table 1, each referred to specific applied methodologies in the field concerning heart and brain interactions in pathology.

A first subsection concerns image analysis for heart and brain interactions, a second subsection deals with physicians' expert limitation to understand the complex neuro-cardiac interactions, a third considers signal analysis toward early diagnosis of heart and brain pathological events, and, a final subsection considers ML driven early-stage detection of heart and brain disease to support decision making. For each subsection, selected studies will be comparatively described in terms of purpose of the work, datasets, results, and then conclusive remarks at the end.

2.1. Image based analysis for heart and brain interactions in pathology

In this section, we are presenting two imaging-based clinical investigations [26, 27] employing physicians' expert opinions on CT and MRI images used to investigate neuro-cardiac pathologies through time-based checkups. More in detail, researchers have applied a conventional medical checkup approach. They gathered data from patients at first diagnosis and then at the follow-up. From this set of medical data, they tried to infer possible neuro-cardiac interactions by highlighting clinical parameter variations.

In the first study [26], authors have shown a detailed elaboration of heart and brain interactions with the pathophysiology of neuro-cardiac disorders. Mental and neurological disorders (MND) and cardiovascular diseases (CVD) are the two most prevalent disorders that lead to a large number of deaths in the world. They started their study with stress cardiomyopathy syndrome (SCS), a benign disease, in which roughly 290 patients went under observation. Different parameters like predisposing conditions/risk, physical, emotional, biological, and clinical factors were taken into account to analyze the predictions. They predicted the diagnostic score higher in females as compared to males. In addition, emotional and physical triggers, absence of ST segment depression, psychiatric and neuro disorders, and QTc prolongation were found in patients with a mortality rate of 25%.

Further, the first study has discussed another disease namely peripartum cardiomy- opathy (PPCM) which is a left ventricle (LV) systolic dysfunction. It generally affects 1 out of 1000 pregnancies but it also depends on ethnic background and most of these patients are generally diagnosed after their delivery. In the PPCM study, 740 patients were observed with different details like ethnicity, maternal age, lifestyle, history of cardiac disorders, and others. They resulted in a number of complications that appear after 6 months with mortality rate of 7% in women and mortality the rate of 6% in neonates. In the end, the first work conducted another experiment on patients with atrial fibrillation (AF) and cognitive decline diseases. AF is a very prevalent disease in aging people. For this study, 2400 patients were taken into account and all patients underwent magnetic resonance imaging (MRI) at the time of first checking, and after 2 years with cognitive tests. It was found that silent brain lesions have prevailed in the brain. Due to these detected lesions in MRI, patients started to face a reduction in cognition.

In the second study [27], they evaluated the prognostic performance of ventricular characteristics on brain computed tomography (CT) in cardiac arrest survivors based on the cerebral performance categories (CPC) score scheme. They enrolled a total of 320 survivors who faced cardiac arrest event/s (age > 18 years) and accordingly tried to calculate the score where CPC-1 is a good performance and CPC-5 is brain death or death. For each patient, they considered several features such as: age, sex, comorbidities, blood and circulation parameters, and brain CT findings to predict the neurological outcome. In addition to these features, few clinical features

such as ventricular areas (lateral, third, and fourth ventricle), distance between both anterior horns and both posterior horns of the lateral ventricle (LV), the Hounsfield units (HUs) of the putamen and corpus callosum and Grey-to-white matter ratio (GWR) were calculated.

Unfavorable outcomes were found after 6 months of cardiac arrest activity in 180 patients with the rate of 68%. Patients with favorable neurologic outcomes were younger, had a lower incidence of comorbidities (hypertension and diabetes), and had a shorter time to ROSC. They also showed significantly higher GWR, smaller LV and third ventricle areas, a significantly shorter distance between both the anterior horn of the LVs and the posterior horn of the LV, and a lower relative LV area.

At the end, ventricular characteristics were significantly different between favorable and unfavorable neurological outcomes at 6 months after cardiac arrest activity. In this regard, CT findings could be directly used to delineate accurate neurological predictions about the patients after their cardiac event.

From above-described literature studies, it emerges how neuro-cardiac interactions in pathology are investigated through physicians' opinions and score-based techniques on time-based diagnostics. Although some evidence was found, a lack of confidence characterizes results in terms of features importance related to neuro-cardiac interaction analysis. Other drawbacks are related to the choice of follow-up end point for evaluation and limitations in early diagnosis of neurological diseases and correlated to cardiac events.

2.2. Physians' opinion limitation for diagnosing neuro-cardiac pathological events using imaging modalities

This section elaborates on a study [29], based on ECGs, which has shown the physicians' opinion limitation towards understanding and predicting the complex neuro-cardiac pathological event. In the ECG work, they evaluated the cardiac alterations caused by central nervous system disorders by the observation of abnormalities on electrocardiogram (ECG) patterns. They mainly focused on different patterns namely ST segment, QT segment, QT interval prolongation, T wave, and QRS complex. The data collection was made on 161 patients as 12-lead ECGs including age of ranging from 10 to 60 years. These ECGs were having different diseases such as brain tumor (66 cases), stroke (44 cases), subarachnoid hemorrhage (11 cases), subdural hemorrhage (8 cases), brain aneurysm (25 cases), and head injury (7 cases).

The selected ECGs were then analyzed and corrected with the help of Bazett's formula. After correction, all ECGs were shown to experts, who were blinded to all data and predicted the outcomes based on different ECG components. The expert predictions showed that they put their whole attention on ST-segment's elevation or depression, inverse T-wave, non-specific ST-T abnormalities, and QT prolongation. According to them, these are the main features that are causing tumor, subarachnoid hemorrhage, or subdural hemorrhage.

This study's results are very interesting in this way that the total dataset contains different neurological diseases. In adverse, doctors' expert opinions' predictions have shown just 35.4%. It means the markers related to neuro-cardiac interactions are not observable by the naked eye. To predict the complex interactions between neuro-cardiac, it is necessary to introduce promising tools in this domain to achieve some delineate models.

2.3. Statistical analysis: signal analysis toward early diagnosis of heart and brain pathological event

This section has focused on signaling based statistical techniques that have used ECGs abnormalities to diagnose heart and brain related pathologies. In the related study [28], they have evaluated the relationship between ECGs and the outcome with mortality of 3 months after an acute stroke. On start, a total of 1070 ECGs (12-leads) were taken into account which were having three abnormalities namely acute cerebral infarction (ACI) (692 patients), intracerebral haemorrhage (ICH) (155 patients), and transient ischaemic attack (TIA) (223 patients). On these ECGs, different features were computed based on clinical parameters and CT-scans. To evaluate these features, a logistic regression classifier based on Scandinavian Stroke Scale (SSS) score, using SPSS software, has been used. After the computation of score, outcome was then rescaled on the modified Ranking Scale (mRS) algorithm for better understanding.

In results, ECG-abnormalities were predicted as 416 ECGs were containing ACI, 77 ECGs were having ICH, and 98 patients were facing TIA complications. In this multivariate analysis, they predicted that ACI strokes were detected through atrial fibrillation, atrio-ventricular block, ST-elevation, ST-depression, and inverted T-waves on ECGs. The important thing about ACI is, it is totally independent of stroke severity and age. Then, ICH was predicted by analyzing sinus tachycardia, ST-depression, and inverted T-waves. At the end, none of the ECG changes had prognostic significance in patients with TIA. In the whole experiment, they noticed that the patients with severe cerebral infarction faced high rate of heart beat for the first 12 hours. With this, at every increase in heart rate of 10/min gave another indication to the physicians that this kind of trend is directly associated to mortality at 3 months.

From the whole experiment, physicians have predicted that stroke severity SSS score decides the amount of augmentation in the frequency of ECG components. Some ECG abnormalities and increasing heart rate predict poor outcome and 3 months of mortality after an acute stroke. However, this study showed a low accuracy (only 55% of the entire dataset was correctly predicted). The reason probably lies in the ECGs feature space, which does not contain enough information to diagnose and understand this type of interaction.

2.4. ML driven early-stage detection of heart and brain disease and support to clinical decision

In this section, we have included machine learning based methodology [30] in which they have used several machine learning algorithms on cardiac arrest patients' data. At the end, they used artificial intelligence (AI) explainability and predicted the important features. In the selected ML study, researchers designed a multi-modal machine learning system to predict the survival rate of cardiac arrest patients who received cardiopulmonary resuscitation (CPR) without going to the hospital. In a greater detail, a ML model was developed to predict neurological outcome based on the scale of cerebral performance category (CPC) scores in which CPC-1 and CPC-2 were declared good neurological outcomes and CPC-3 to CPC-5 as bad outcomes.

Data to train and test the ML algorithm were taken from the Korean Cardiac Arrest Research Consortium (KoCARC) dataset [57] which is publicly available with committee approval. This dataset contains data from roughly 6000 patients who faced the return of spontaneous circulation

(ROSC). It is worth noticing that this database is highly unbalanced given that only a hundred patients had bad neurological outcomes among all the available patient data. For each patient, around 20 independent features per patient were available such as: age, sex, ECG rhythms, CPR values, defibrillation and pre-hospital intervals, etc.

Before going to ML techniques, missing value issue was faced by multiple imputation by chained equation (MICE) algorithm. MICE is basically an iterative model which imputes values step by step in all variables. Then four renowned classifiers were trained namely voting classifier (VC), XGBoost (XGB), random forest (RF), and regularized logistic regression (RLR) classifier. A five-fold cross-validation technique was applied for the training of the multimodal system. Grid search technique which helped in predicting the optimized parameters. To compute the robustness of this model, different renowned measures were used namely Brier score, log loss, area under the curve (AUC), F1-score, negative predictive value, and positive predictive value. With the help of these measures, it was found that XGB, VC, and RLR performed very well with greater than 90% AUC while RF had less than 90% AUC.

Table 1
Comparsion of different analysis techniques related to neuro-cardiac pathologies

Analysis type	*Study*	*Data Size*	*Features*	*Results*	*Drawbacks*
Imaging Modalities	[26]	3430	ECG, MRI, and so on	Mortality rate of 28% and Cognitive decline	Time taking and disease detection at appearance
	[27]	320	Age, sex, brain CT findings, and so forth	68% bad neurological outcome	
Physicians' opinion	[29]	160	Age, Gender, and ECG components	Predicted: 35%	Physicians' opinion is limited by using imaging modalities
Statistical analysis	[28]	1100	Age, 12 lead ECG, hypertension history and so on	Predicted: 55%	Features are not having promising information
Machine learning	[30]	110	Age, prehospital ECG rhythm, hospital ECG rhythm, and so forth	90% AUC	More samples to improve more

In contrast to best performances, it was found that XGB algorithm focused on predicting the true-positive and false negative samples while RLR focused on the true positive and false negative samples. In regard to predicting the poor neurological outcomes, these model were not able to predict bad neurological outcomes in a good way even though 68 patients were existed in the test set. Due to this drawback, the authors selected voting classifiers (VC) which has shown good performance in the prediction of neurological outcomes. On VC, authors applied further explainable AI technique to take out, from the whole feature space, the six most important variables for the prediction of the neurological outcome. In other words, those clinical feature, e.g., age, ECG rhythm, cardiac arrest event, and others, are mainly responsible for high scores in VC driven classification and prediction of neurological outcomes.

3. Conclusions

Advancements in imaging and signal analysis have made physicians and researchers more able to infer the structural and functional properties of the brain and heart. Continuous improvement in computational power, algorithms and finally the raise of ML and DL-driven technologies have allowed scientists to start to deepen their knowledge on hidden neuro-cardiac interactions. However, this intriguing research field is only at the beginning. In this review paper, we have collected and compared some relevant examples of research applications in the field with particular attention to neuro-cardiac imaging and signal analysis techniques aided by expert opinions (physicians), statistical algorithms, and machine learning. It is found that there are not a high number of studies reporting examples of AI techniques applied to the field. As most researchers are employing heart imaging-based models to diagnose heart diseases and brain imaging-based models for brain diseases but not in inter-related interactions. In this domain, most reported studies are based on more classical approaches, which are usually limited in quantifying feature importance and clinical variable connections given by the complexity of the investigated system. On the other side, artificial intelligence (AI) techniques has the well-known ability to surface up more hidden interactions and interlinked complications to support clinicians' decisions. In the near future, it is likely that ML/DL-driven technologies already effectively developed in other medicine areas (e.g., cancer, Cardiovascular risk, etc..) will be tailored to empower our knowledge on hidden relationships characterizing heart-brain connections.

Acknowledgment

The present research work has been developed as part of the PARENT project, funded by the European Union's Horizon 2020 research and innovation program under the Marie Sklodowska-Curie-Innovative Training Network 2020, Grant Agreement N° 956394 (https://parenth2020.com/).

Conflicts of Interest

The authors declare no conflict of interest.

References

[1] F. Puppe, Introduction to knowledge systems: Mark stefik, Artificial Intelligence in Medicine 9 (1995) 870 , 497. doi:10.1016/S0933-3657(96)00372-7, figures, hardcover,.

[2] A. Kaplan, M. Haenlein, Siri, siri, in my hand: Who's the fairest in the land? on the interpretations, illustrations, and implications of artificial intelligence, Business Horizons 62 (2019) 15–25,. doi:10.1016/J.BUSHOR.2018.08.004.

[3] A. Bundy, Clear thinking about artificial intelligence, 1992. URL: https://www.dai.ed.ac.uk/papers/documents/rp587_old.html, accessed Mar. 23, 2022).

[4] T. Shen, X. Fu, Application and prospect of artificial intelligence in cancer diagnosis and treatment, Zhonghua Zhong liu za zhi [Chinese Journal of Oncology 40 (2018) 881–884,. doi:10.3760/CMA.J.ISSN.0253-3766.2018.12.001.

[5] A. Samuel, Some studies in machine learning using the game of checkers. ii—recent progress, Computer Games I (1988) 366–400,. doi:10.1007/978-1-4613-8716-9_15.

[6] G. Kumar, R. Kalra, A survey on machine learning techniques in health care industry | semantic scholar, 2016. URL: https://www.semanticscholar.org/paper/A-survey-on-Machine-Learning-Techniques-in-Health-Kumar-Kalra/a4a63b8081e84b0e4f5533a940d9f275e7d415ac, accessed Mar. 23, 2022).

[7] J. Schmidhuber, Deep learning in neural networks: An overview, Neural Networks 61 (2015) 85–117,. doi:10.1016/J.NEUNET.2014.09.003.

[8] P. Werbos, Applications of advances in nonlinear sensitivity analysis, System Modeling and Optimization (1982) 762–770,. doi:10.1007/BFB0006203.

[9] V. Patel, The coming of age of artificial intelligence in medicine, Artificial Intelligence in Medicine 46 (2009) 5–17,. doi:10.1016/J.ARTMED.2008.07.017.

[10] M. Peleg, C. Combi, Artificial intelligence in medicine aime 2011, Artificial Intelligence in Medicine 57 (2013) 87–89,. doi:10.1016/J.ARTMED.2013.01.001.

[11] P. Chaudhary, P. Kaul, Factors affecting utilization of medical diagnostic equipment: A study at a tertiary healthcare setup of chandigarh, CHRISMED Journal of Health and Research 2 (2015) 316,. doi:10.4103/2348-3334.165741.

[12] F. Yik, J. Lai, P. Yuen, Impacts of facility service procurement methods on perceived performance of hospital engineering services, Facilities 30 (2012) 56–77,. doi:10.1108/02632771211194275/FULL/PDF.

[13] A. Badnjević, L. Gurbeta, D. Bošković, Z. Džemić, Measurement in medicine–past, present, future, Folia Medica Facultatis Medicinae Universitatis Saraeviensis 50 (2015).

[14] B. Wang, Medical equipment maintenance: Management and oversight, Synthesis Lectures on Biomedical Engineering 45 (2012) 1–83,. doi:10.2200/S00450ED1V01Y201209BME045.

[15] S. Salim, S. Mazlan, S. Salim, A conceptual framework to determine medical equipment maintenance in hospital using rcm method, in: MATEC Web of Conferences, volume 266, 2019, pp. 02011,. doi:10.1051/MATECCONF/201926602011.

[16] E. Carson, Techrepublic: Ibm watson health computes a pair of new solutions to improve healthcare data and security - sage bionetworks, 2015. URL: https://sagebionetworks.org/in-the-news/techrepublic-ibm-watson-health-computes-a-pair-of-new-solutions-to-improve-healthcare-data-and-security/, accessed Mar. 24, 2022).

[17] Artificial intelligence in healthcare market by offering, technology, application, end user and geography - global forecast to 2027, 2021. URL: https://www.reportlinker.com/p04897122/Artificial-Intelligence-in-Healthcare-Market-by-Offering-Technology-Application-End-User-Industry-and-Geography-Global-Forecast-to.html, accessed Mar. 24, 2022).

[18] E. Topol, High-performance medicine: the convergence of human and artificial intelligence, Nature Medicine 25 (2019) 44–56,. doi:10.1038/s41591-018-0300-7.

[19] A. Esteva, A guide to deep learning in healthcare, Nature Medicine 25 (2019) 24–29,. doi:10.1038/s41591-018-0316-z.

[20] G. Zaharchuk, E. Gong, M. Wintermark, D. Rubin, C. Langlotz, Deep learning in neuroradiology, American Journal of Neuroradiology 39 (2018) 1776–1784,. doi:10.3174/ajnr.A5543.

[21] H. A. Haenssle, C. Fink, R. Schneiderbauer, F. Toberer, T. Buhl, A. Blum, A. Kalloo, A. B. H. Hassen, L. Thomas, A. Enk, et al., Man against machine: diagnostic performance of a deep learning convolutional neural network for dermoscopic melanoma recognition in comparison to 58 dermatologists, Annals of oncology 29 (2018) 1836–1842. doi:10.1093/annonc/mdy166.

[22] A. Kotha, F. Prichard, Man vs machine: How will artificial intelligence and machine learning systems impact cancer diagnosis and the patient-physician relationship? (2022).

[23] B. Moore, J. Barnett, Oxford clinical psychology military psychologists ' desk reference, Case Studies in Clinical Psychological Science: Bridging the Gap from Science to Practice (2015) 1–7,. doi:10.1093/MED/9780199661756.011.0008.

[24] A. Shaban, E. Leira, Neurologic complications of heart surgery, Handbook of Clinical Neurology 177 (2021) 65–75,. doi:10.1016/B978-0-12-819814-8.00007-X.

[25] P. Landrieu, J. Baets, P. Jonghe, Hereditary motor-sensory, motor, and sensory neuropathies in childhood, Handbook of Clinical Neurology 113 (2013) 1413–1432,. doi:10.1016/B978-0-444-59565-2.00011-3.

[26] R. Schnabel, Heart and brain interactions : Pathophysiology and management of cardio-psycho-neurological disorders, Herz 46 (2021) 138–149,. doi:10.1007/S00059-021-05022-5.

[27] D. Lee, Relationship between ventricular characteristics on brain computed tomography and 6-month neurologic outcome in cardiac arrest survivors who underwent targeted temperature management, Resuscitation 129 (2018) 37–42,. doi:10.1016/J.RESUSCITATION.2018.06.008.

[28] H. Christensen, A. Christensen, G. Boysen, Abnormalities on ecg and telemetry predict stroke outcome at 3 months, Journal of the Neurological Sciences 234 (2005) 99–103,. doi:10.1016/J.JNS.2005.03.039.

[29] R. Póvoa, Póvoa et al electrocardiographic abnormalities in neurological diseases electrocardiographic abnormalities in neurological diseases, Arq Bras Cardiol 80 (2003) 355–363,.

[30] D.-W. Seo, H. Yi, H.-J. Bae, Y.-J. Kim, C.-H. Sohn, S. Ahn, K.-S. Lim, N. Kim, W.-Y. Kim, Prediction of neurologically intact survival in cardiac arrest patients without pre-hospital return of spontaneous circulation: Machine learning approach, Journal of clinical medicine 10 (2021) 1089.

[31] Cancer, 2020. URL: https://www.who.int/news-room/fact-sheets/detail/cancer, accessed

Mar. 24, 2022).
[32] B. Angell, O. Sanuade, I. M. Adetifa, I. N. Okeke, A. L. Adamu, M. H. Aliyu, E. A. Ameh, F. Kyari, M. A. Gadanya, D. A. Mabayoje, et al., Population health outcomes in nigeria compared with other west african countries, 1998–2019: a systematic analysis for the global burden of disease study, The Lancet 399 (2022) 1117–1129,. doi:10.1016/S0140-6736(21)02722-7.
[33] D. McDonagh, M. Berger, J. Mathew, C. Graffagnino, C. Milano, M. Newman, Neurologic complications of cardiac surgery, Lancet Neurol 13 (2014) 490,. doi:10.1016/S1474-4422(14)70004-3.
[34] J. Buth, Neurologic complications associated with endovascular repair of thoracic aortic pathology: Incidence and risk factors. a study from the european collaborators on stent/-graft techniques for aortic aneurysm repair (eurostar) registry, Journal of Vascular Surgery 46 (2007) 1103–1111 2,. doi:10.1016/J.JVS.2007.08.020.
[35] D. Stump, A. Rogers, J. Hammon, S. Newman, Cerebral emboli and cognitive outcome after cardiac surgery, Journal of Cardiothoracic and Vascular Anesthesia 10 (1996) 113–119,. doi:10.1016/S1053-0770(96)80186-8.
[36] P. Shaw, D. Bates, N. Cartlidge, D. Shaw, D. Heaviside, D. Julian, Early neurological complications of coronary artery bypass surgery, British Medical Journal (Clinical research ed 291 (1985) 1384–1387,. doi:10.1136/BMJ.291.6506.1384.
[37] B. Johansson, Hypertension mechanisms causing stroke, Clin Exp Pharmacol Physiol 26 (1999) 563–565,. doi:10.1046/J.1440-1681.1999.03081.X.
[38] W. Hollander, Role of hypertension in atherosclerosis and cardiovascular disease, The American Journal of Cardiology 38 (1976) 786–800,. doi:10.1016/0002-9149(76)90357-x.
[39] A. El-Menyar, A. Goyal, R. Latifi, H. Al-Thani, W. Frishman, Brain-heart interactions in traumatic brain injury, Cardiology in Review 25 (2017) 279–288,. doi:10.1097/CRD.0000000000000167.
[40] M. Kox, M. Vrouwenvelder, J. Pompe, J. Hoeven, P. Pickkers, C. Hoedemaekers, The effects of brain injury on heart rate variability and the innate immune response in critically ill patients, 2012. URL: https://home.liebertpub.com/neu,. doi:10.1089/NEU.2011.2035.
[41] M. Metzler, Pattern of brain injury and depressed heart rate variability in newborns with hypoxic ischemic encephalopathy, Pediatric Research 82 (2017) 438–443,. doi:10.1038/pr.2017.94.
[42] N. Pawar, F. Vasanwala, M. Chua, Brain tumor causing atrial fibrillation in an otherwise healthy patient, Cureus 9 (2017). doi:10.7759/CUREUS.1601.
[43] R. Gopinath, S. Ayya, Neurogenic stress cardiomyopathy: What do we need to know, Ann Card Anaesth 21 (2018) 228,. doi:10.4103/ACA.ACA_176_17.
[44] A. Ion, Biomarkers utility: At the borderline between cardiology and neurology, Journal of Cardiovascular Development and Disease 8 (2021) 139,. doi:10.3390/JCDD8110139.
[45] P. Garg, Cardiac biomarkers of acute coronary syndrome: from history to high-sensitivity cardiac troponin, Internal and Emergency Medicine 12 (2017) 147,. doi:10.1007/S11739-017-1612-1.
[46] D. Sanghvi, M. Harisinghani, Modalities in modern radiology: A synopsis, Journal of Postgraduate Medicine 56 (2010) 85,. doi:10.4103/0022-3859.65282.

[47] H. Ogul, Abdominal perfusion computed tomography, Eurasian Journal of Medicine 45 (2013) 50–57,. doi:10.5152/EAJM.2013.09.

[48] J. Provenzale, S. Mukundan, D. Barboriak, Diffusion-weighted and perfusion mr imaging for brain tumor characterization and assessment of treatment response1, 2006. URL: https://doi.org/10.1148/radiol.2393042031,. doi:10.1148/RADIOL.2393042031.

[49] C. Pierpaoli, P. Jezzard, P. Basser, A. Barnett, G. Chiro, Diffusion tensor mr imaging of the human brain, 1996. URL: https://doi.org/10.1148/radiology.201.3.8939209,. doi:10.1148/RADIOLOGY.201.3.8939209.

[50] E. Melhem, S. Mori, G. Mukundan, M. Kraut, M. Pomper, P. Zijl, Diffusion tensor mr imaging of the brain and white matter tractography, 2012. URL: http://dx.doi.org/10.2214/ajr.178.1.1780003,. doi:10.2214/AJR.178.1.1780003.

[51] N. Bulakbasi, M. Kocaoglu, F. Örs, C. Tayfun, T. Ügöz, Combination of single-voxel proton mr spectroscopy and apparent diffusion coefficient calculation in the evaluation of common brain tumors, AJNR: American Journal of Neuroradiology 24 (2003) 225,. Online]. Available: /pmc/articles/PMC7974143/.

[52] F. Schweser, A. Deistung, B. Lehr, J. Reichenbach, Differentiation between diamagnetic and paramagnetic cerebral lesions based on magnetic susceptibility mapping, Medical Physics 37 (2010) 5165–5178,. doi:10.1118/1.3481505.

[53] B. Battal, M. Kocaoglu, N. Bulakbasi, G. Husmen, H. Sanal, C. Tayfun, Cerebrospinal fluid flow imaging by using phase-contrast mr technique, 2014. URL: http://dx.doi.org/10.1259/bjr/66206791,. doi:10.1259/BJR/66206791.

[54] T. Rogers, Standardization of t1 measurements with molli in differentiation between health and disease - the consept study, Journal of Cardiovascular Magnetic Resonance 15 (2013) 1–9,. doi:10.1186/1532-429X-15-78/FIGURES/3.

[55] U. Blume, Interleaved t(1) and t(2) relaxation time mapping for cardiac applications, J Magn Reson Imag 29 (2009) 480–7,. doi:10.1002/jmri.21652.

[56] B. Ruzsics, H. Lee, P. Zwerner, M. Gebregziabher, P. Costello, U. Schoepf, Dual-energy ct of the heart for diagnosing coronary artery stenosis and myocardial ischemia-initial experience, European Radiology 18 (2008) 2414–2424,. doi:10.1007/S00330-008-1022-X/FIGURES/8.

[57] J. Y. Kim, S. O. Hwang, S. Do Shin, H. J. Yang, S. P. Chung, S. W. Lee, K. J. Song, S. S. Hwang, G. C. Cho, S. W. Moon, et al., Korean cardiac arrest research consortium (kocarc): rationale, development, and implementation, Clinical and Experimental Emergency Medicine 5 (2018) 165.

Thalamic features extraction and analysis in magnetic resonance imaging of preterm infants

Emiliano Trimarco[1,*,†], Bahram Jafrasteh[1,†], Simoń Pedro Lubiań-Lopez[2,3] and Isabel Benavente-Fernańdez[1,2,3]

[1]Biomedical Research and Innovation Institute of Cádiz (INiBICA) Research Unit, Puerta del Mar University, Cádiz, Spain
[2]Division of Neonatology, Department of Paediatrics, Puerta del Mar University Hospital, Caḍiz, Spain
[3]Area of Paediatrics, Department of Child and Mother Health and Radiology, Medical School, University of Caḍiz, Caḍiz, Spain

Abstract

Preterm birth is the primary cause of infant death and is associated with later neurodevelopmental impairments. Neuroimaging is a powerful tool to analyse neuroanatomy abnormalities in preterm infants. It allows analysing of different brain structures, such as the thalamus and their alterations. Thalamus is a crucial hub for regulating cortical connectivity. Moreover, white matter (WM) injury in preterm infants can impact thalamic growth and maturation in long-term periods. Therefore, the study of the thalamus morphology during the neonatal period using magnetic resonance imaging (MRI) can help to identify those features that predict neurodevelopmental outcomes in these vulnerable population. In this study, we automatically segmented the thalamus structure from 3D MRI scans and extracted the thalamic features from these segmentations. The gestational age at birth and post-menstrual age at the scan time is also taken into account in our study. The K-means clustering, an unsupervised machine learning algorithm, was employed to explore the hidden pattern related to thalamus features from early and term-equivalent scans. Finally, we studied the association of these features to a scoring system used in clinical settings to assess MRI scans in very preterm infants at term-equivalent age. The main results highlight that 77 percent of preterm-born infants with abnormal MRI scores share the same cluster.

Keywords

Thalamus, K-means clustering, Atlas-based segmentation, Preterm infants

1. Introduction

Preterm birth, before 37 weeks of gestation, affects fifteen million children each year in the world [1]. It remains the main cause of infant death [1]. The severity of long-term neurodevelopmental impairments increases with decreasing gestational age [2]. In particular, early exposure to extrauterine life is closely associated with deficits in cognitive, motor, visual, socio-emotional, sleep, and language domains [3]. The thalamus is a meaningful hub that shapes brain connectivity during prenatal and postnatal life. It is commonly affected in preterm infants by white

DETERMINED 2022: Neurodevelopmental Impairments in Preterm Children — Computational Advancements, August 26, 2022, Ljubljana, Slovenia

*Corresponding author.
†These authors contributed equally.
emiliano.trimarco@inibica.es (E. Trimarco); jafrasteh.bahram@uca.es (B. Jafrasteh); simonp.lubian.sspa@juntadeandalucia.es (S. P. Lubiań-Lopez); isabel.benavente@uca.es (I. Benavente-Fernańdez)

© 2022 Copyright for this paper by its authors. Use permitted under Creative Commons License Attribution 4.0 International (CC BY 4.0).
CEUR Workshop Proceedings (CEUR-WS.org)

CEUR-WS.org/Vol-3363/paper13.pdf

matter (WM) injuries, either directly or through maturational disruption [4, 5]. Preterm birth influences the growth of thalamocortical connectivity and the steps in the sensory organisation and functional specialisation of the cerebral cortex [6, 7]. Thalamo-cortical connectivity is regionally altered for preterm infants, and the thalamic volume is related to both the cortical volume and the WM tracts [8]. There is also some evidence that alterations in fronto-temporal and parieto-occipital cortical areas are related to the thalamic structural connectivity, and the volumetric measurements obtained from the thalamic region [9]. Thalamocortical connectivity abnormalities identified after preterm birth can be correlated with the future neurodevelopmental impairments [10, 11, 12].

In this study, we develop a protocol to evaluate the importance of thalamic features of preterm infants. Our hypothesis aims to relate the morphological characteristics of the thalamus to the Kidokoro score [13]. Firstly, we use an automatic method to segment Magnetic Resonance Images (MRIs) from a preterm infant cohort [14]. Then, we extract morphological features from the region of interest (ROI), i.e. the segmented thalamus area. After an exploratory analysis of the extracted features, an unsupervised machine learning algorithm is used to cluster the features. Finally, we show that it is possible to cluster the abnormal MRIs through thalamus measurements using term-equivalent scans. In addition, the results show the extracted features are sufficient to differentiate between healthy term-born infants and preterm infants at term-equivalent age.

2. Method

2.1. Atlas correction and automatic thalamus segmentation

Melbourne Children's Regional Infant Brain (M-CRIB 2.0) atlas [15] is used to segment thalamus structure from the MRI images of our cohort. In particular, the atlas contains ten scans from healthy term-born infants [15].

Preliminary visualization of the M-CRIB 2.0 atlas showed an overestimation of thalamic segmentation, including the nuclei and the hippocampal gyrus. Therefore, an expert in our group reviewed and corrected thalamic segmentation manually. We automatically segmented the thalamus from the MRI images according to the neonatal pipeline proposed by Makropoulos et al. [14, 16]. In principle, the pipeline registers the image to a neonatal atlas image at a similar gestational age [16] to separate non-cortical grey matter from the WM, grey matter and the cerebrospinal fluid (CSF). Then, the image is registered to the M-CRIB 2.0 atlas. Finally, local atlas weighting and DrawEM [16] are used to separate the thalamus from the other brain structures. This pipeline is widely used and supported by the literature studies [17, 18]. According to the changes made in the atlas, we adapted the pipeline [14] for thalamus segmentation. The clinical experts in the group have verified the quality of the automatic segmentation.

Figure 1(a)-1(c) shows an example of the original scan from the atlas, a corrected scan with a redundant part, and one of the segmentation provided by the pipeline after the correction, respectively.

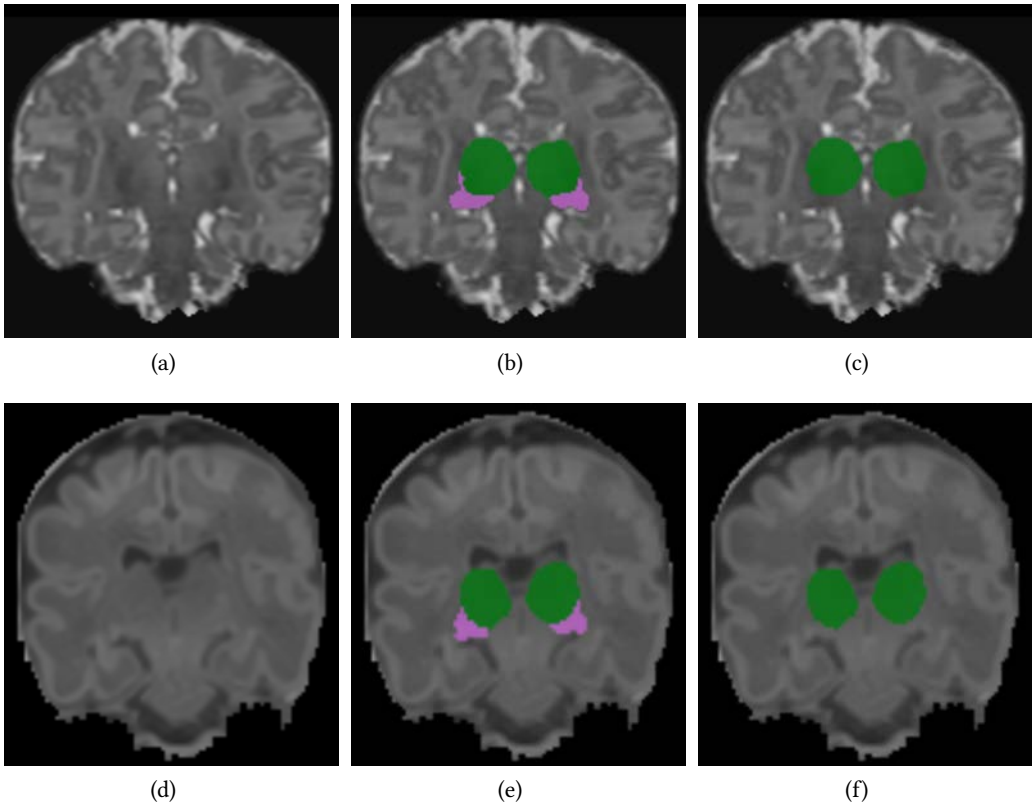

Figure 1: Atlas correction and the segmentation results. a) A slice from the coronal plane of the original atlas T2. b) A slice from the coronal plane of the correction in the atlas. c) A slice from the coronal plane of the corrected thalamus segmentation in the atlas. d) A slice from the coronal T1 plane of the preterm infant at term-equivalent age. e) A slice from the coronal plane of the automated segmentation in preterm infants at term-equivalent age. f) A slice from the coronal plane of segmented thalamus in preterm infants at term-equivalent age. The green colour indicates thalamus structure, and the purple colour refers to the corrections made by an expert on the atlas.

2.2. Thalamic feature extraction

We extracted ten features from the segmented thalamus (Table 2). All the volumetric measurements have been standardised by the Total Brain Volume (TBV). We prioritise TBV over Intra-Cranial Volume (ICV) as ICV includes extra-axial CSF. A physiological increase in extra-axial CSF in preterm infants may facilitate suboptimal brain growth in the neonatal period. Therefore, it is crucial to prioritise the TBV over the ICV to ensure measuring real brain tissue. The other measurements, like area, have been standardised by the maximum brain area at the axial plane, where the thalamus has the largest area. The following thalamus features are summarised in Figure 2 and Table 1: post-menstrual age (PMA) at the scan time, the TBV, the Standardised Left Thalamus 3D Surface (SLTS) and the Standardised Right Thalamus 3D Surface (SRTS). Furthermore, the other extracted variables are reported in Table 2. Notably, the 3D surface of the thalamus is standardised by the largest area of the brain in the axial plane. In

this way, we obtain an indirect measurement regarding the relationship between the thalamus and general brain maturation. The distributions of the four variables are shown in the diagonal boxes of Figure 2 and in Table 1. Moreover, Figure 2 shows the two-way relationships between these variables. For example, the last row of Figure 2 reveals that the volume brain increases with increasing PMA, but the standardised 3D surface of the thalamus decreases with increasing PMA. Since the brain regions grow considerably during this period, this behaviour is seen in this figure [19], and their proportion to the thalamus changes. Therefore, it affects the data standardisation and a value decrease does not concur with a natural reduction. It is relative to the growing trend of the TBV.

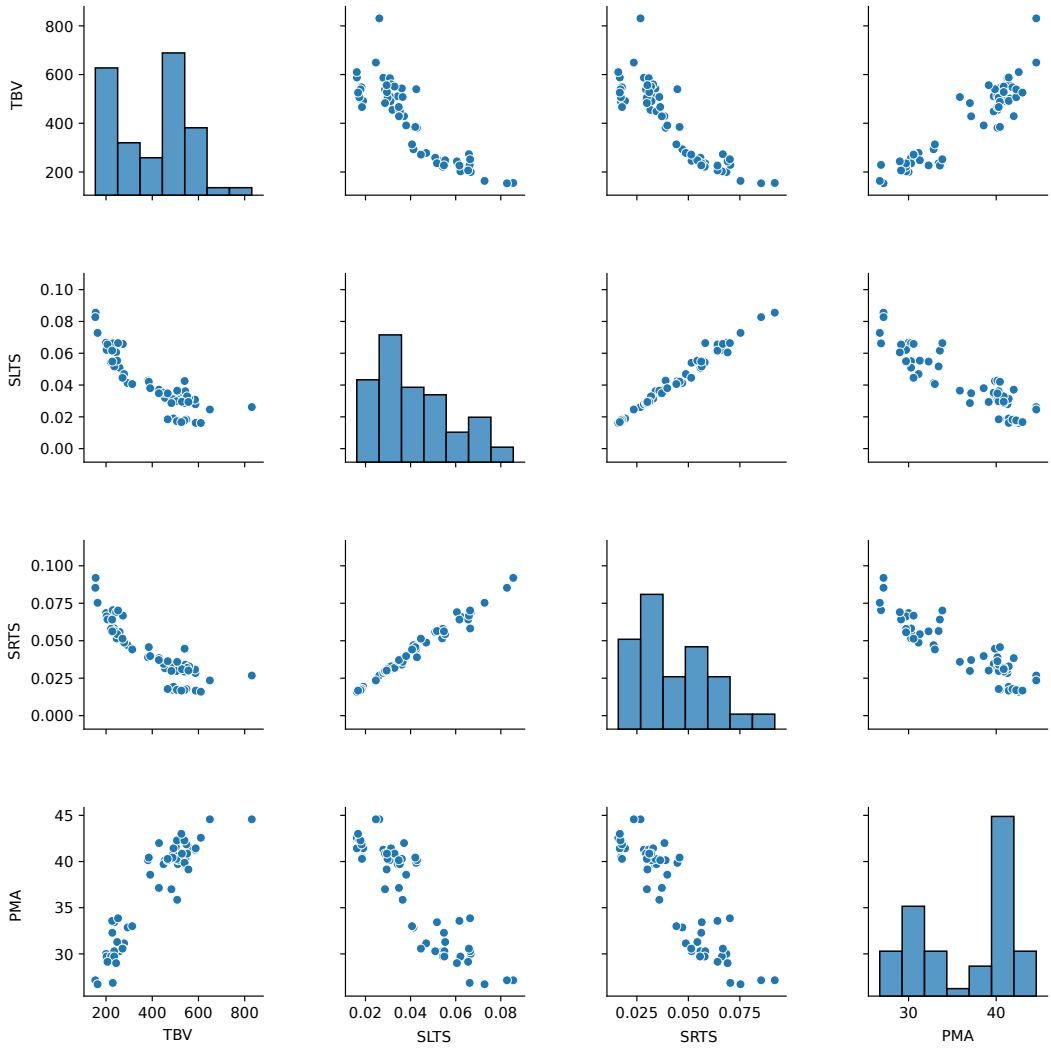

Figure 2: Distribution of Total Brain Volume in cm^3 (TBV), Standardised Left Thalamus 3D Surface (SLTS) and Standardised Right Thalamus 3D Surface (SRTS), post-menstrual age in weeks (PMA) in the diagonal boxes and the two-way relationships in the other boxes

Table 1
Statistical description of Total Brain Volume (TBV), Standardised Left Thalamus 3D Surface (SLTS) and Standardised Right Thalamus 3D Surface (SRTS), post-menstrual age (PMA)

	TBV (cm^3)	SLTS	SRTS	PMA (weeks)
Mean	402.37	0.041	0.042	36.494
S.D.	156.47	0.018	0.019	5.462
Min	153.60	0.016	0.016	26.715
25%	244.80	0.029	0.030	30.571
50%	448.93	0.036	0.037	39.715
75%	527.14	0.055	0.056	40.857
Max	830.73	0.086	0.092	44.571

2.3. MRI Score

MRI scans were acquired using a 1.5 Tesla scanner (Magneton Symphony, Siemens Health Care, Erlangen, Germany) located in the radiology unit in the University Hospital of Puerta del Mar (HUPM), Cadiz, Spain. The acquisition parameters are as follows: spacing in x, y and z direction : 0.8, 0.8, 0.8; echo time = 3.67 ms; flip angle = 15°and repetition time = 1910.0 ms. T1 weighted spin echo imaged sequences were used to collect our data. Potential risks caused by the physical properties of the MRI equipment were evaluated and minimised following the recommendations provided for preterm infants [20] and our previous experiences [21, 22]. The images obtained from the scans were evaluated through the clinicians' observation using a scoring system developed by Kidokoro et al. [13]. It provides a comprehensive and objective characterisation of the regional and global brain lesions and brain growth. In particular, it is used to confirm the clustering results and check whether patients with an abnormal score are clustered into the same group (For more details, see section 4.2). The scoring system suggested by Kidokoro et al. [13] groups the global score into four categories: (normal, mild, moderate, and severe). We then binarised the variable by considering normal versus abnormal MRI (the latter including mild, moderate and severe) as we wanted to see if the thalamic features could be associated with any degree of MRI abnormality.

2.4. K-means clustering

Given a set of observations having D dimensions, the k-means clustering as an unsupervised machine learning algorithm aims to partition the observations into k different groups by minimising within cluster sum of the squared error without having access to the outcomes.
We set K to three in our analysis because our dataset has three main groups (see section 3). It should be noted that clustering is only carried out based on the thalamic features. Table 2 shows the included attributes for K-means clustering. The K-means clustering is also performed using morphological features extracted from the atlas images. Moreover, the score proposed in Kidokoro et al. [13] was used to validate the K-means algorithm. In conclusion, according to the preliminary statistical analysis, the plots of each feature vs others (Figure 4), and other algorithms comparison, we conclude that K-means clustering as a simple algorithm can efficiently cluster our dataset (table 4).

Table 2
List of dataset variables included in the clustering. Total Brain Volume (TBV), Standardised Left Thalamus 3D Surface (SLTS), Standardised Right Thalamus 3D Surface (SRTS), post-menstrual age (PMA)

Variable	Clustering
TBV (cm^3)	included
Left Thalamus Volume (cm^3)	included
SLTS	included
Left Thalamus perimeter (cm)	included
Left Thalamus Angle (degrees)	included
Right Thalamus Volume (cm^3)	included
SRTS	included
Right Thalamus perimeter (cm)	included
Right Thalamus Angle (degrees)	included
Distance Left and Right Thalamus cm	included
Angle between Left and Right Thalamus	included
Left Centroid	not included
Left Highest Point	not included
Right Centroid	not included
Right Highest Point	not included
Kidokoro score	not included
SEX	not included
GA	not included
PMA	not included

3. Experimental configuration and cohort

We included 48 scans from 31 patients of a longitudinal cohort that involves preterm infants from the preterm cohort at Hospital Puerta del Mar (HUPM), Cadiz, Spain, with very low weight at birth, equal or <1,500 grams, and/or gestational age (GA) at birth equal or <32 weeks. The parents or legal guardians of these infants have signed the informed consent. Data were recorded prospectively from these patients as they underwent MRI as part of a cohort study of the preterm brain damage group at the Biomedical research and innovation institute of Cadiz (INIBICA). GA is calculated from the date of the last menstrual period and confirmed using data from early antenatal ultrasound scans. The weeks of postnatal life (age) are added to the weeks of GA at birth, giving the so-called post-menstrual age (PMA). Typically, two MRI scans are taken from each infant. An early scan was performed within the first ten days of life, and a late one was at the term-equivalent age (38–42 weeks of corrected age), according to PMA. Following this principle, the initial 48 MRI scans are divided into two groups, i.e. 23 early scans and 25 term-equivalent scans (17 patients have both scans).In addition, 12 patients are identified as abnormal in agreement with Kidokoro et al. [13]. Therefore, early and term-equivalent scans, plus abnormal/normal MRI scores, provide four different groups: early normal MRI score, early abnormal MRI score, term-equivalent normal MRI score, and term-equivalent abnormal MRI score. Moreover, ten scans from the M-CRIB 2.0 atlas [15] are added to the analyses. These scans are from healthy term-born neonates and are used as the control group.

4. Results

4.1. Analysis of extracted features

We extracted ten features from the segmented thalamus (see section 2.2). As visualizing all these features are not easy, we rely on the dimension reduction methods such as principal component analysis (PCA). Figure 3 shows the results of PCA on term-equivalent and M-CRIB 2.0 atlas [15] scans. Initial results demonstrate that the first five principal components can explain more than 92% of the variabilities among features. Therefore, these components are enough to explain our data. Table 3 shows the percentage of explained variance for each component. The first two components explain more than 60% of the variation among thalamic features. Moreover, Figure 3, indicates that it is possible to separate the M-CRIB 2.0 atlas scans from those of the preterm infants in our cohort according to the first two components. One of the advantages of PCA is its interpretability. For example, ID 23, highlighted in red, shows an anomaly in its first component with a value less than -0.9. This result suggests that clinicians should check this infant. In addition, according to the Kidokoro assessment score, this ID has an abnormal MRI score.

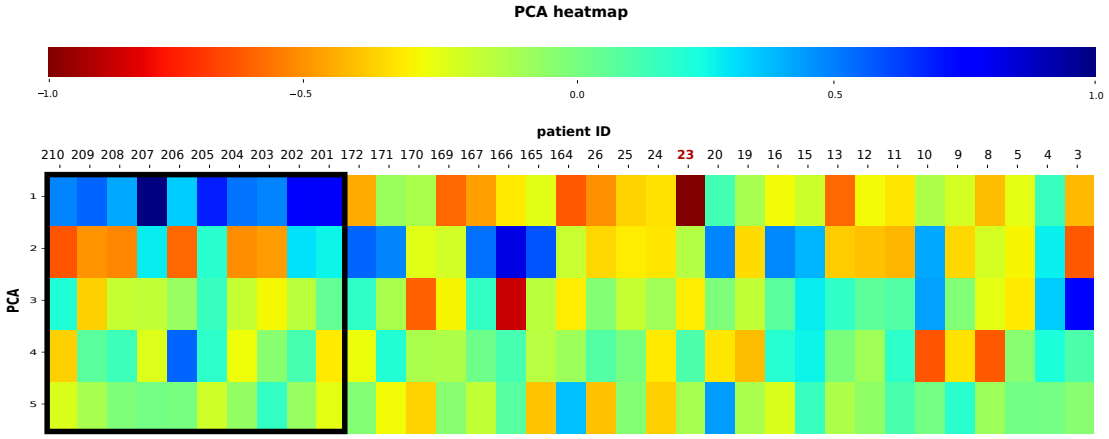

Figure 3: Visualising the PCA components of thalamic measurements in preterm infants at term-equivalent age and healthy term-born ones. The horizontal axis of the figure shows the anonymised ID of the patients, and the vertical one shows the number of principal components. The atlas scans IDs start from 201. The box in black colour separates the atlas scans from the rest. Notice that we use 5 components for PCA analysis.

PCA components	1	2	3	4	5
Explained variance	34.7	28.1	13.6	10.5	5.7

Table 3
The percentage of variance explained in measurements of thalamic features from different components of PCA.

4.2. Clustering results

After clustering, the three clusters are represented by different coloured points and also compared with MRI score [13] (abnormal = green star, normal = magenta cross) and M-CRIB 2.0 atlas [15] (yellow cross) in Figure 4. All the images in the M-CRIB 2.0 atlas [15] are correctly classified in the third cluster. These findings highlight the significant difference between healthy term-born infants and preterm infants at term-equivalent age. Furthermore, Figure 4 also shows that most premature infants with abnormal MRI scores are in the second cluster, i.e. 77%. However, the clustering of thalamic features of the early scan group does not differentiate between abnormal and normal term-equivalent MRI. The second cluster gets the highest probability values for early scans, i.e. 47%. The clustering accuracy is summarized in Table 4.

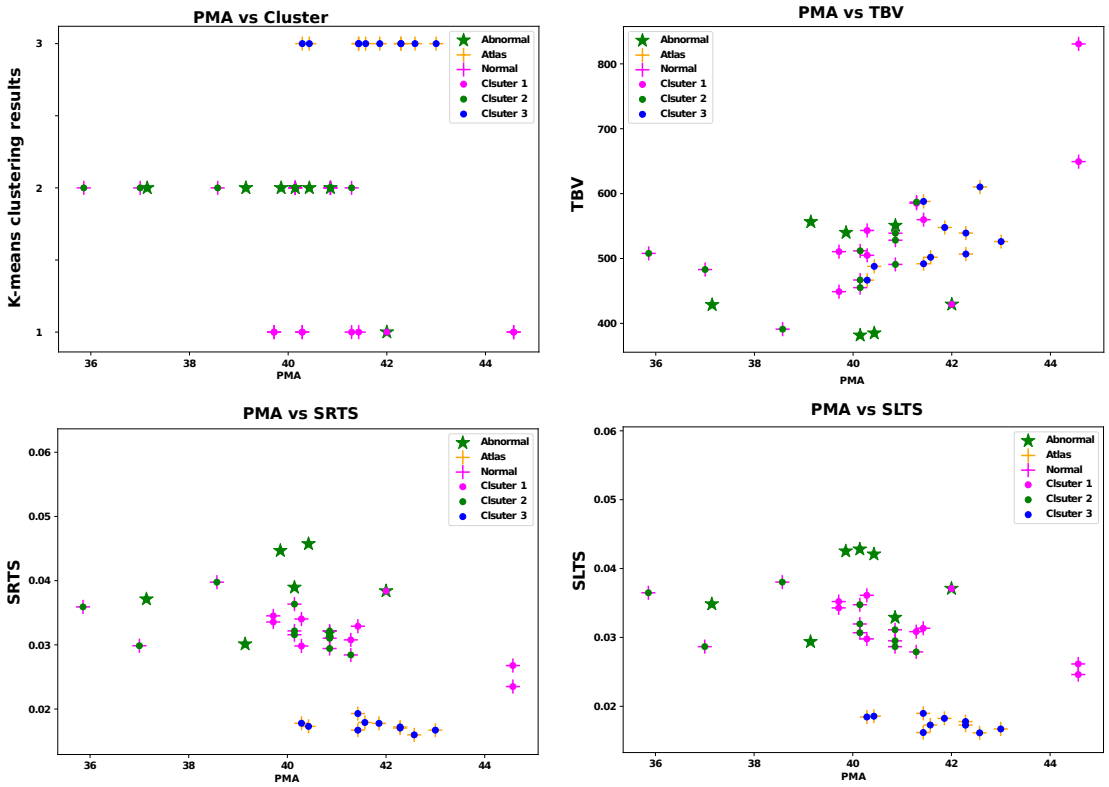

Figure 4: The plots of post-menstrual age in weeks (PMA) vs Total Brain Volume in cm^3 (TBV), Standardised Left Thalamus 3D Surface (SLTS) and Standardised Right Thalamus 3D Surface (SRTS).

Table 4
The percentage of abnormal infants in each cluster for the early and term-equivalent scans.

	Cluster 1	Cluster 2	Cluster 3
Early scans	28%	47%	25%
Term-equivalent scans	23%	77%	0%

5. Discussion

The K-means clustering correctly separated 77% of abnormal patients into the correct cluster (Table 4) and correctly distinguished all healthy neonates from the M-CRIB 2.0 atlas images, as our reference group (Figure 4). The separation of the third cluster seems easy as the first and the second component of PCA results (Figure 3) indicate the difference in the thalamic features between healthy term-born infants and preterm infants at term-equivalent age.
Nevertheless, the clustering of thalamic features of the early scans does not differentiate between the abnormal and normal MRI (Table 4). This result could be explained by postnatal brain maturation, as the MRI score system only applies to term-equivalent scans, so the patient's situation can change from one scan to the next. In particular, a patient could have a normal early MRI scan and develop clinical complications that will lead to brain injury and an abnormal term-equivalent MRI. After describing the thalamic features of a cohort of preterm and term-born infants related to GA at birth and PMA at the time of scans, we show how the thalamic features can be associated with clinical MRI scores. Furthermore, they share three clustering patterns: the first cluster can be interpreted as patients with normal MRI score, the second cluster can belong to the abnormal MRI score, and the third cluster can be associated with the M-CRIB 2.0 atlas scans.
Some other groups have done previous research on this topic. For example, Ball et al. [12], Jakab et al. [10] and Menegaux et al. [23] focused on the diffusion-weighted imaging. In contrast, we focus on the T1-weighted images in the current study. Furthermore, our work includes a detailed analysis of the thalamic features, while the work published by Wisnowski et al., [24] Lao et al. [25] and Loh et al. [26] considered only one feature, i.e. thalamic volume. Interestingly, our results align with those from Lao et al. [25], who described the standardised 3D surface as an important thalamic feature. Our study includes a more exhaustive analysis of the thalamic features and extensively extracted 2D parameters, including the thalamic perimeter where the largest thalamic area was found in the axial plane, and 3D information from the thalamus [25]. Moreover, we have normalised the thalamic volume to the TBV and studied the association between the specific morphological characteristics of the thalamus and the Kidokoro score [13] at the term-equivalent MRI.
According to Kostović et al.[19], during the beginning of the third trimester of fetal development, thalamocortical and cortico-cortical afferents migrate to the cortex and finally form their primary connections. The ontogeny of this migration process suggests that these connections grow with different starting times but from the same point. Consequently, the other brain regions grow considerably during this period, and their proportion to the thalamus significantly changes (see figure2). Conclusively, damage in the preterm brain affects thalamus features and their relation with the TBV. In some extreme cases, the atlas-based segmentation includes other structures and overestimates the thalamus and its features. Manual segmentation and the development of advanced machine learning methods can help to solve this problem.

6. Conclusion

In the current study, we associated the thalamic features with the MRI score assessment of preterm infants and explored the importance of thalamic features for the clustering of the patients. The standardised thalamic 3D surface can be suggested as a crucial morphological feature to cluster patients. Further studies, including a bigger sample size and external validation, are warranted to investigate the potential role of these thalamic features as a diagnostic and predictive tool of brain injury and long-term neurodevelopmental outcomes in preterm infants.

Acknowledgments

This study was funded by the PARENT project from the European Union's Horizon 2020 research and innovation program under the Marie Sklodowska-Curie Innovative Training Network 2020. Grant Agreement N 956394. BJ, SPLL and IBF acknowledge funding from the Cadiz integrated territorial initiative for biomedical research, European Regional Development Fund (ERDF) 2014–2020. Andalusian Ministry of Health and Families, Spain. Registration number: ITI-0019-2019.

References

[1] M. Delnord, J. Zeitlin, Epidemiology of late preterm and early term births–an international perspective, in: Seminars in Fetal and Neonatal Medicine, volume 24, Elsevier, 2019, pp. 3–10.

[2] N. Marlow, Outcomes of preterm birth and evidence synthesis, Developmental Medicine & Child Neurology 60 (2018) 330.

[3] A. Pascal, P. Govaert, A. Oostra, G. Naulaers, E. Ortibus, C. Van den Broeck, Neurodevelopmental outcome in very preterm and very-low-birthweight infants born over the past decade: a meta-analytic review, Developmental Medicine & Child Neurology 60 (2018) 342–355.

[4] W. Y. Loh, P. J. Anderson, J. L. Cheong, A. J. Spittle, J. Chen, K. J. Lee, C. Molesworth, T. E. Inder, A. Connelly, L. W. Doyle, et al., Longitudinal growth of the basal ganglia and thalamus in very preterm children, Brain imaging and behavior 14 (2020) 998–1011.

[5] J. J. Volpe, Brain injury in premature infants: a complex amalgam of destructive and developmental disturbances, The Lancet Neurology 8 (2009) 110–124.

[6] I. Kostović, M. Judaš, The development of the subplate and thalamocortical connections in the human foetal brain, Acta paediatrica 99 (2010) 1119–1127.

[7] H. Toulmin, J. O'Muircheartaigh, S. J. Counsell, S. Falconer, A. Chew, C. F. Beckmann, A. D. Edwards, Functional thalamocortical connectivity at term equivalent age and outcome at 2 years in infants born preterm, cortex 135 (2021) 17–29.

[8] R. Ceschin, J. L. Wisnowski, L. B. Paquette, M. D. Nelson, S. Blüml, A. Panigrahy, Developmental synergy between thalamic structure and interhemispheric connectivity in the visual system of preterm infants, NeuroImage: Clinical 8 (2015) 462–472.

[9] G. Ball, J. P. Boardman, P. Aljabar, A. Pandit, T. Arichi, N. Merchant, D. Rueckert, A. D.

Edwards, S. J. Counsell, The influence of preterm birth on the developing thalamocortical connectome, Cortex 49 (2013) 1711–1721.
[10] A. Jakab, G. Natalucci, B. Koller, R. Tuura, C. Rüegger, C. Hagmann, Mental development is associated with cortical connectivity of the ventral and nonspecific thalamus of preterm newborns, Brain and behavior 10 (2020) e01786.
[11] D. K. Thompson, W. Y. Loh, A. Connelly, J. L. Cheong, A. J. Spittle, J. Chen, C. E. Kelly, T. E. Inder, L. W. Doyle, P. J. Anderson, Basal ganglia and thalamic tract connectivity in very preterm and full-term children; associations with 7-year neurodevelopment, Pediatric Research 87 (2020) 48–56.
[12] G. Ball, J. P. Boardman, D. Rueckert, P. Aljabar, T. Arichi, N. Merchant, I. S. Gousias, A. D. Edwards, S. J. Counsell, The effect of preterm birth on thalamic and cortical development, Cerebral cortex 22 (2012) 1016–1024.
[13] H. Kidokoro, J. J. Neil, T. E. Inder, New mr imaging assessment tool to define brain abnormalities in very preterm infants at term, American Journal of Neuroradiology 34 (2013) 2208–2214.
[14] A. Makropoulos, E. C. Robinson, A. Schuh, R. Wright, S. Fitzgibbon, J. Bozek, S. J. Counsell, J. Steinweg, K. Vecchiato, J. Passerat-Palmbach, et al., The developing human connectome project: A minimal processing pipeline for neonatal cortical surface reconstruction, Neuroimage 173 (2018) 88–112.
[15] B. Alexander, W. Y. Loh, L. G. Matthews, A. L. Murray, C. Adamson, R. Beare, J. Chen, C. E. Kelly, P. J. Anderson, L. W. Doyle, et al., Desikan-killiany-tourville atlas compatible version of m-crib neonatal parcellated whole brain atlas: the m-crib 2.0, Frontiers in Neuroscience 13 (2019) 34.
[16] A. Makropoulos, I. S. Gousias, C. Ledig, P. Aljabar, A. Serag, J. V. Hajnal, A. D. Edwards, S. J. Counsell, D. Rueckert, Automatic whole brain mri segmentation of the developing neonatal brain, IEEE transactions on medical imaging 33 (2014) 1818–1831.
[17] G. Li, L. Wang, P.-T. Yap, F. Wang, Z. Wu, Y. Meng, P. Dong, J. Kim, F. Shi, I. Rekik, et al., Computational neuroanatomy of baby brains: A review, NeuroImage 185 (2019) 906–925.
[18] I. Grigorescu, L. Vanes, A. Uus, D. Batalle, L. Cordero-Grande, C. Nosarti, A. D. Edwards, J. V. Hajnal, M. Modat, M. Deprez, Harmonized segmentation of neonatal brain mri, Frontiers in Neuroscience 15 (2021) 662005.
[19] I. Kostović, N. Jovanov-Milošević, The development of cerebral connections during the first 20–45 weeks' gestation, in: seminars in fetal and neonatal medicine, volume 11, Elsevier, 2006, pp. 415–422.
[20] I. Benavente-Fernández, P. Lubián-López, M. Zuazo-Ojeda, G. Jiménez-Gómez, A. Lechuga-Sancho, Safety of magnetic resonance imaging in preterm infants, Acta Paediatrica 99 (2010) 850–853.
[21] M. L. Gutiérrez, I. B. Fernández, A. Z. Ojeda, S. L. López, Alteraciones en resonancia magnética asociadas a tratamiento con vigabatrina, Anales de Pediatría: Publicación Oficial de la Asociación Española de Pediatría (AEP) 96 (2022) 165–166.
[22] I. Benavente-Fernández, A. García-Cazorla, Y. Jordán-García, A. Capdevila-Cirera, J. Campistol, Diffusion-weighted imaging in pediatric central nervous system infections, Revista de Neurologia 50 (2010) 133–138.
[23] A. Menegaux, C. Meng, J. G. Bäuml, M. T. Berndt, D. M. Hedderich, B. Schmitz-Koep,

S. Schneider, R. Nuttall, J. Zimmermann, M. Daamen, et al., Aberrant cortico-thalamic structural connectivity in premature-born adults, Cortex 141 (2021) 347–362.

[24] J. L. Wisnowski, R. C. Ceschin, S. Y. Choi, V. J. Schmithorst, M. J. Painter, M. D. Nelson, S. Blüml, A. Panigrahy, Reduced thalamic volume in preterm infants is associated with abnormal white matter metabolism independent of injury, Neuroradiology 57 (2015) 515–525.

[25] Y. Lao, Y. Wang, J. Shi, R. Ceschin, M. D. Nelson, A. Panigrahy, N. Leporé, Thalamic alterations in preterm neonates and their relation to ventral striatum disturbances revealed by a combined shape and pose analysis, Brain Structure and Function 221 (2016) 487–506.

[26] W. Y. Loh, P. J. Anderson, J. L. Cheong, A. J. Spittle, J. Chen, K. J. Lee, C. Molesworth, T. E. Inder, A. Connelly, L. W. Doyle, et al., Neonatal basal ganglia and thalamic volumes: very preterm birth and 7-year neurodevelopmental outcomes, Pediatric research 82 (2017) 970–978.